Neural Plasticity

Neural Circuits, Synaptic Plasticity, and Epigenetics in Non-Drug Treatment of Neurodegenerative Diseases

Lead Guest Editor: Wei-Lin Liu
Guest Editors: Guangpu Li, Binbin Nie, and Feng Zhang

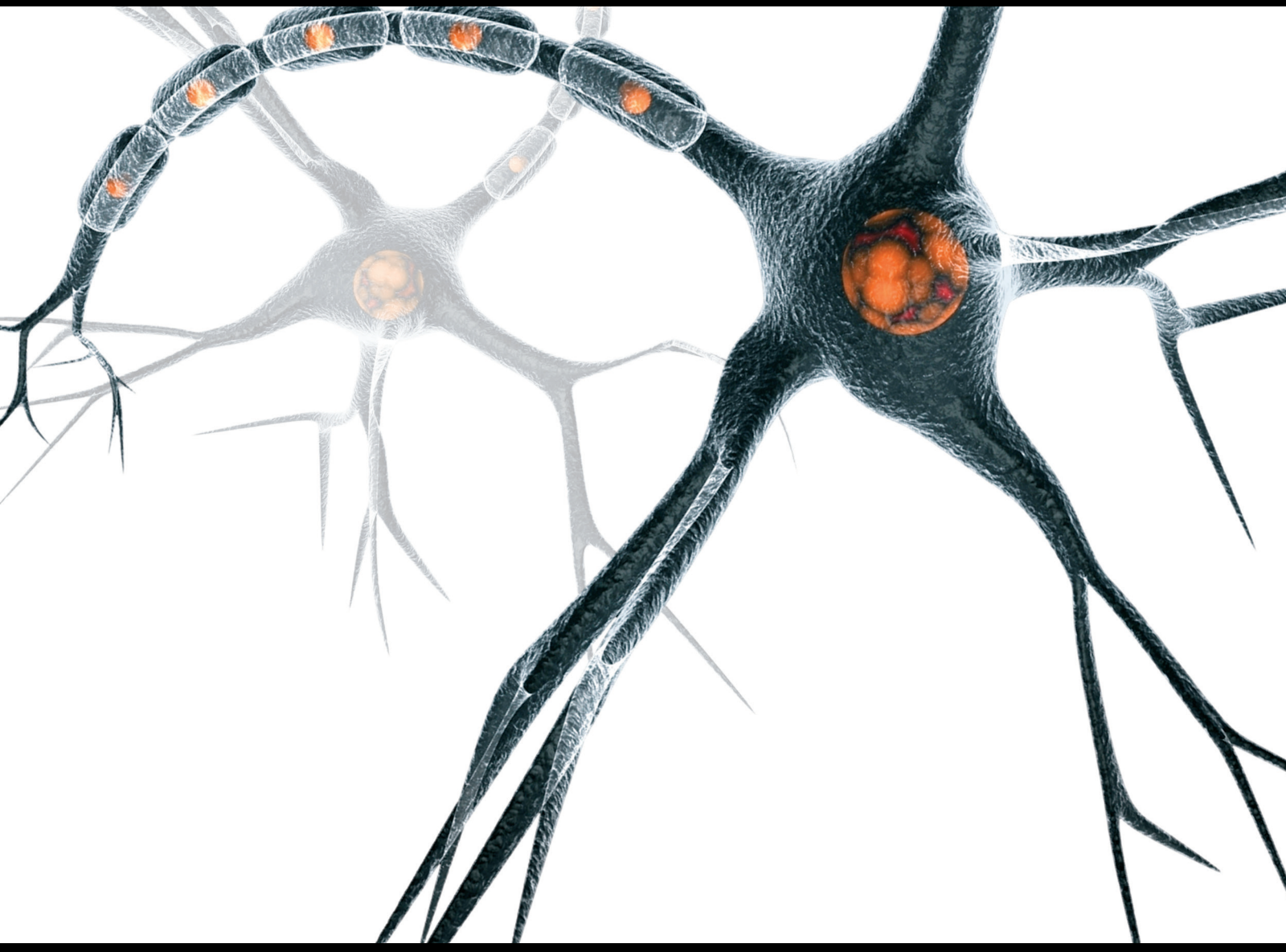

Neural Circuits, Synaptic Plasticity, and Epigenetics in Non-Drug Treatment of Neurodegenerative Diseases

Neural Plasticity

Neural Circuits, Synaptic Plasticity, and Epigenetics in Non-Drug Treatment of Neurodegenerative Diseases

Lead Guest Editor: Wei-Lin Liu
Guest Editors: Guangpu Li, Binbin Nie, and Feng Zhang

Contents

Hindawi
Neural Plasticity
Volume 2021, Article ID 9960304, 11 pages
https://doi.org/10.1155/2021/9960304

Research Article

Electroacupuncture Improves Clearance of Amyloid-β through the Glymphatic System in the SAMP8 Mouse Model of Alzheimer's Disease

Pei-zhe Liang,[1,2] **Li Li**,[1,2,3] **Ya-nan Zhang**,[1,2,4] **Yan Shen**,[1,2,4] **Li-li Zhang**,[1,2,3] **Jie Zhou**,[1,2] **Zhi-jie Wang**,[1,2] **Shu Wang**,[2,5] **and Sha Yang**[1,2,6]

[1]*First Teaching Hospital of Tianjin University of Traditional Chinese Medicine, Tianjin, China*
[2]*National Clinical Research Center for Chinese Medicine Acupuncture and Moxibustion, Tianjin, China*
[3]*Academy for Advanced Interdisciplinary Studies Peking University, Beijing, China*
[4]*Tianjin Key Laboratory of Acupuncture and Moxibustion, Tianjin, China*
[5]*Tianjin Academy of Traditional Chinese Medicine Affiliated Hospital, Tianjin, China*
[6]*Key Laboratory of Cerebropathy Acupuncture Therapy of State Administration of Traditional Chinese Medicine, Tianjin, China*

Correspondence should be addressed to Shu Wang; wangs2008@163.com and Sha Yang; yangsha2008@foxmail.com

Received 23 March 2021; Accepted 12 August 2021; Published 27 August 2021

Academic Editor: Feng Zhang

Background. Memory loss and cognitive impairment characterize the neurodegenerative disorder, Alzheimer's disease (AD). Amyloid-β (Aβ) is the key factor that triggers the course of AD, and reducing the deposition of Aβ in the brain has been considered as a potential target for the treatment of AD. In clinical and animal studies, electroacupuncture (EA) has been shown to be an effective treatment for AD. In recent years, substantial evidence has accumulated suggesting the important role of the glymphatic system in Aβ clearance. *Objective*. The purpose of this study was to explore whether EA modifies the accumulation of Aβ through the glymphatic system and may thus be applied to alleviate cognitive impairments. *Methods*. Seven-month-old SAMP8 mice were randomized into a control group (Pc) and an electroacupuncture group (Pe). Age-matched SAMR1 mice were used as normal controls (Rc). Mice in the Pe group were stimulated on Baihui (GV20) and Yintang (GV29) for 10 min and then pricked at Shuigou (GV26) for ten times. EA treatment lasted for 8 weeks. In each week, EA would be applied once a day for the first five consecutive days and ceased at the remaining two days. After EA treatment, Morris water maze (MWM) test was used to evaluate the cognitive function; HE and Nissl staining was performed to observe the brain histomorphology; ELISA, contrast-enhanced MRI, and immunofluorescence were applied to explore the mechanisms underlying EA effects from Aβ accumulation, glymphatic system function, reactivity of astrocytes, and AQP4 polarization, respectively. *Results*. This EA regime could improve cognition and alleviate neuropathological damage to brain tissue. And EA treatment might reduce Aβ accumulation, enhance paravascular influx in the glymphatic system, inhibit the reactivity of astrocytes, and improve AQP4 polarity. *Conclusion*. EA treatment might reduce Aβ accumulation from the brain via improving clearance performance of the glymphatic system and thereby alleviating cognitive impairment.

1. Introduction

Alzheimer's disease (AD), a common degenerative disease of the central nervous system (CNS), is characterized by progressive memory impairment, aphasia, agnosia, and executive dysfunction, accompanied with a varying degree of changes in personality and behavior [1]. Amyloid β (Aβ) accumulation is a histopathological hallmark of AD [2–5]. In recent years, there is substantial evidence suggesting that the astrocyte-mediated brain-wide paravascular pathway may contribute to Aβ clearance [6, 7]. Such pathway is also referred as "glymphatic system" since the draining space resembles the peripheral lymphatic system. The glymphatic system enables cerebrospinal fluid (CSF) to enter the brain

via periarterial spaces and move into the interstitium via aquaporin-4 (AQP4) located in the endfeet of perivascular astrocytes; it also drives the perivenous drainage of interstitial fluid (ISF) and its solutes, thereby clearing the brain of metabolic waste [8–12]. AQP4 is an important factor affecting the glymphatic system's functionality [6]. The increasing reactivity of astrocytes in the aging brain causes the loss of AQP4 polarization, and thus, Aβ clearance by the glymphatic system is reduced [7].

Electroacupuncture (EA), a combination of electrical stimulation and traditional acupuncture, is an important nondrug treatment for AD and is widely used in clinical practice [13]. EA has been shown to improve cognitive performance, neuropsychiatric symptoms, and the ability to perform daily activities in Alzheimer's patients [14, 15]. Previous experimental studies have shown that EA can improve cognitive deficits in animal models of AD [16, 17], and such benefit might contribute to reducing Aβ deposition and thereby delaying the pathological progression of AD from multiple pathways. For instance, EA intervention might upregulate the content of Aβ-degrading enzymes such as neprilysin (NEP) and insulin-degrading enzyme (IDE) in the brain, enhance the phagocytosis of Aβ by microglia, and improve the expression of Aβ-related transporters on the blood-brain barrier [18–21]. The glymphatic system is also an important clearance pathway of Aβ. However, no existing study demonstrates whether the glymphatic system might participant in the EA's effect on regulating Aβ deposition in AD.

Here, we investigated the effect of EA on the clearance of Aβ via the glymphatic system in AD model mice, to provide more scientific experimental support for the treatment of AD with electroacupuncture. In the light of a previous study [16, 20, 22, 23], senescence-accelerated mouse prone 8 (SAMP8) mice were used for the animal model of AD and the age-matched senescence accelerated mouse resistant 1 (SAMR1) mice as the control with normal aging phenotype. After EA treatment, the Morris water maze (MWM) test was applied to evaluate cognition, HE and Nissl staining to determine brain histomorphology, ELISA to ascertain the expression of Aβ, contrast-enhanced MRI for the assessment of glymphatic system function, and immunofluorescence to assess the reactivity of astrocytes and AQP4 polarization. The process of this study is described in Figure 1.

2. Material and Methods

2.1. Animals. 7-month-old male SAMP8 and SAMR1 mice (30 ± 5 g) were provided by the SAM Breeding Center of the First Teaching Hospital of Tianjin University of Traditional Chinese Medicine (license number: SCXK (Jing) 2015-0003). All mice were housed under standard conditions at 23 ± 2°C and a 12 h light/dark cycle with free access to food and water. The Animal Ethics and Welfare Committee of Tianjin University of Traditional Chinese Medicine approved all procedures (TCM-LAEC2020028).

2.2. Animal Grouping and Electroacupuncture Treatment. Before the experiment began, all mice were initially screened through a water maze to remove those that were too sensitive or stupid. The remaining thirty SAMP8 mice were randomly divided into a SAMP8 control group (Pc) and SAMP8 electroacupuncture group (Pe). Fifteen SAMR1 mice were assigned to a SAMR1 normal control group (Rc).

Based on our previous preliminary experiment, GV20, GV29, and GV26 were selected for EA regime. During EA stimulation, the mice were immobilized in self-made fixators (Figure 2). Location of these acupoints in mice was determined as follows [17]. GV20 is located halfway between the auricular apices; GV29 is located halfway between the medial ends of the two eyebrows; and GV26 is below the apex nasi, at one-third from the top of the midline of the cleft lip. Two sterile acupuncture needles were separately inserted downward horizontally at GV20 and upward horizontally at GV29, to a depth of 0.5 cm. Continuous-wave stimulation for 10 min at a frequency of 2 Hz (intensity 1 mA) was applied by a programmed apparatus (HANS-100A, Nanjing Jisheng Medical Technology, China) to which the needles were connected. Then, GV26 acupoint was pricked quick for 10 times with the needle at the end of EA treatment. The treatment lasted for a total of 8 weeks. In each week, EA would be applied once a day for the first five consecutive days and ceased at the remaining two days. The Pc group and Rc group did not receive EA stimulation, only the same fixation as the Pe group.

2.3. Morris Water Maze Test. Morris water maze (MWM) is a well-validated test for cognitive function. For the whole test period, the lab was maintained as a sound-insulated and low-light environment, while the objects in the room were kept at their original locations and other experimental conditions remained unchanged. After EA treatment, a circular water tank (80 cm in diameter and 50 cm in depth) divided into four equal quadrants (I, II, III, and IV) was used for MWM test; a circular escape platform (9 cm in diameter and 28 cm in height) was placed at the center of quadrant I. The tank was filled with warm water (23 ± 1°C) to a depth of 30 cm and edible melanin to dye the water black. Visual cues of various shapes were located on the side of each quadrant of the tank, in plain sight of the mice. A digital camera connected with an image acquisition system was used to automatically track all trials. The MWM test was performed as two stages. (1) To evaluate changes in learning ability, each animal was subjected to a trial with a hidden platform. In order to familiarize mice with the test environment, the mice used in the experiment were separately allowed to swim freely in the water tank (without platform) for 60 seconds on the day before being subjected to the hidden platform trial. Throughout the trail, mice in each group were placed in the water at a fixed position in quadrant III while the submerged platform remained fixed in location in quadrant I. If the tested animal found the hidden platform within 60 seconds and stayed on it for at least 5 seconds, we recorded the escape latency time (expressed as the time spent swimming to find the platform). If the animal failed to find the platform within 60 seconds, it was placed on the platform for 10 seconds, allowing it to observe and memorize the location, and the escape latency time was recorded as 60 seconds. The trial with a hidden platform was repeated daily for five consecutive days. (2) We conducted a probe trial on day

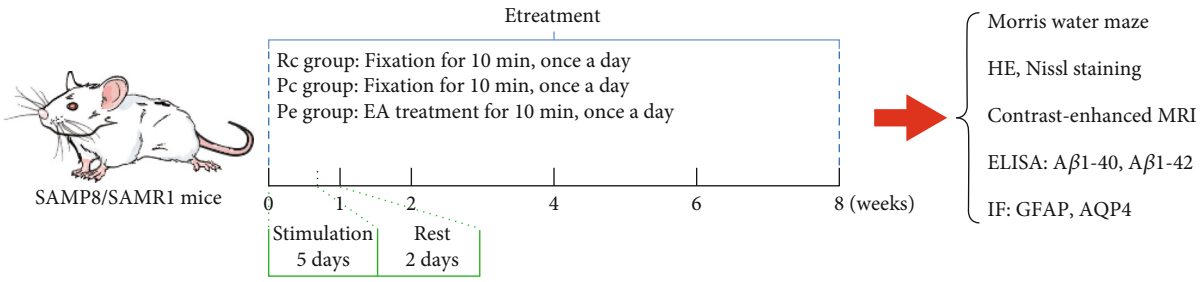

Figure 1: The process of this study.

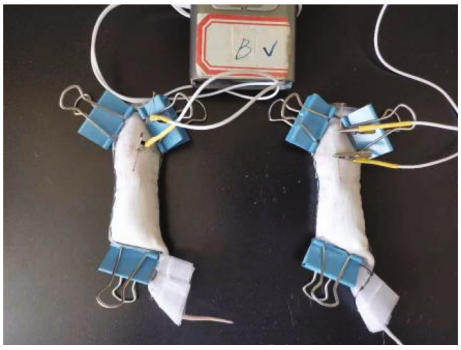

Figure 2: EA stimulation.

six to measure the ability of the mice to maintain long-term memories with the hidden platform removed. The frequency with which the platform's former location was crossed was recorded together with the time spent in the target quadrant (I) during the trial.

2.4. HE Staining. The mice were perfused with 0.01 M phosphate-buffered saline (PBS) and 4% paraformaldehyde successively under isoflurane gas anesthesia (isoflurane, RWD Life Science Co., Ltd., China), and then, the brains were dissected and postfixed for 24 hours in 4% paraformaldehyde. To observe pathologic morphological changes with HE staining, standard paraffin tissue sections of the brain tissue were prepared (LEiCA RM2245, China). The section thickness was 5 μm.

2.5. Nissl Staining. Brains were immersed in 4% paraformaldehyde, embedded in paraffin, and then cut into coronal sections for Nissl staining. Briefly, the sections were deparaffinized in xylene, gradually rehydrated using alcohol, and treated with Nissl staining solution (Bioss, Beijing, China) for 5 min. Then, sections were mounted in neutral balsam and examined by light microscopy (Olympus, DP26). The number of Nissl bodies observed in three fields of the hippocampus and cortex was recorded. The IPP6.0 software was used for analyzation and quantification.

2.6. ELISA. The mice were euthanized by cervical dislocation under isoflurane gas anesthesia. The brains were removed immediately, followed by isolation of the hippocampus and cortex. Using mouse Aβ1-40 and Aβ1-42 ELISA kits (Meimian, Jiangshu, China), the Aβ levels were measured following the manufacturer's instructions.

2.7. Contrast-Enhanced MRI. To measure the dynamic cerebrospinal-interstitial fluid (CSF-ISF) exchange, 3D T1-weighted MR images (T1WIs) with Gd-DTPA contrast agent were used following a protocol for contrast-enhanced MRI (CE-MRI) [9]. The mice were anesthetized and fixed in a stereotaxic apparatus, then dissected to expose the cisterna magna. A total of 7 μl Gd-DTPA was delivered to the cisterna magna at an infusion rate of 2 μl per minute for each mouse. MRI (Bruker, Germany) measurements were performed 10, 20, 30, 40, and 50 min after injection; anesthesia was maintained using isoflurane gas. The signal intensity of regions of interest (ROIs), including the pituitary recess, olfactory arterial complex, and olfactory bulb, was recorded.

2.8. Immunofluorescence. Paraffin sections were treated with 1% BSA for 30 min. Subsequently, sections were incubated overnight in the dark using rabbit anti-GFAP (Bioss, Beijing, China) and mouse anti-AQP4 (Bioss, Beijing, China) primary antibodies at the temperature of 4°C. They were then incubated with the corresponding secondary antibodies. The nuclei were stained using DAPI (Bioss, Beijing, China). The slides were examined using a fluorescence microscope (Olympus, BX51).

2.9. Quantitative Analysis of AQP4 Water Channel Polarization. Polarization of the astrocytic AQP4 was analyzed using immunofluorescence images, with reference to a previous study [24]. Histological sections labeled for GFAP and AQP4 were subjected to color channel separation. The overall area of AQP4 immunoreactivity was defined by the low-stringency threshold, whereas the high-stringency threshold demarcated the area of intense AQP4 immunoreactivity found in the endfeet of the astrocytes. "AQP4 polarity" was defined as the ratio of low-stringency area to high-stringency area. Higher AQP4 polarity means that a greater proportion of immunoreactivity is restricted to perivascular regions, whereas a lower proportion shows that the distributed immunoreactivity is restricted to the astrocytes' soma.

2.10. Statistical Methods. All results are reported using their mean and SD. Between-group differences were assessed by one-way analyses of variance (ANOVA), followed by tests of least-significant difference (LSD; equal variances assumed) or Dunnett's T3 (equal variances not assumed). For all

comparisons, a significance level of $P < 0.05$ was assumed. All analyses were done with SPSS version 23.0.

3. Results

3.1. EA Improves Learning Ability and Memory in SAMP8 Mice. The escape latency time in the hidden platform trial displayed a downward trend in each group as the number of training days increased. Compared with the Rc group, the Pc group revealed a longer escape latency time ($P < 0.001$), and the seven-month SAMP8 mice exhibited an obvious learning disability. On days 1 and 2 of the hidden platform trial, the Pc group and the Pe group did not differ statistically. After days 3, 4, and 5, the escape latency time in the Pe group decreased significantly compared to that in the Pc groups ($P < 0.001$ or $P < 0.05$), demonstrating that EA improved the learning ability of SAMP8 mice (Figure 3(a)). Typical swimming traces of each group reflected the search strategies in the hidden platform trial (Figure 3(b)). After training the trial for five days, the probe trial was utilized to test whether the memory was maintained. As more time was spent in the quadrant where the platform used to be and the more times the platform was crossed, the higher the level of memory retention was assumed to be. In this trial, the time spent in the target quadrant and the number of times that the platform was crossed were found to be significantly less in the Pc group than in the Rc group ($P < 0.001$), and the number is greater in the Pe group than in the Pc group ($P < 0.05$). These data suggest that memory was obviously disabled in the seven-month SAMP8 mice and that EA improved memory preservation capability (Figures 3(c) and 3(d)).

3.2. EA Alleviates Neuropathological Injury of Brain Tissue in SAMP8 Mice. Among all pathological changes of AD, neuron injury should be the basic one [25]. As shown by HE staining, no abnormalities were observed on in the hippocampus and cortex of SAMR1 mice in the Rc group since the structures of neurons were complete, dense, and orderly. Obvious pathological changes were observed in brain tissue of the Pc group in morphological and structural: neuron arrangement was loose, the nuclei had shrunk and were deeply stained, and fibrous tangles were visible (black arrow; Figure 4(a)). To a certain degree, pathological changes in neurons at the hippocampus and cortex area of the Pe groups were alleviated compared with those of the Pc group, where the neuron arrangement was orderly, with a small number of abnormalities in the morphology and structure of neurons. Nissl bodies are a characteristic structure of neurons, and its number is a gold index to reflect the functional state of neurons [26]. Compared with the Rc control group, Nissl bodies in the Pc group were arranged sparsely, and there were significantly fewer Nissl bodies in the hippocampus and cortex ($P < 0.001$). After EA treatment, the number of Nissl bodies was higher in the Pe group than in the Pc group ($P < 0.05$; Figures 4(b) and 4(c)). These results indicate that neuropathological injury had been observed in the brains of seven-month SAMP8 mice and that EA could alleviate this injury in the brain tissue of SAMP8 mice.

3.3. EA Reduces Aβ Accumulation in SAMP8 Mice. ELISA was applied to investigate the effects of EA on Aβ production (Aβ1-40 and Aβ1-42) in the brain of SAMP8 mice. The results showed that the contents of Aβ1-40 and Aβ1-42 in both the hippocampus and cortex of the Pc group were significantly higher than those of the Rc group ($P < 0.001$ and $P < 0.01$, respectively). Compared with the Pc group, the contents of both Aβ1-40 and Aβ1-42 were reduced significantly in the Pe group ($P < 0.01$ and $P < 0.05$, respectively; Figures 5(a) and 5(b)). These data suggest that accumulation of Aβ in the brain was increased in SAMP8 mice at seven months, and EA might reduce Aβ accumulation in the brain.

3.4. EA Improves Clearance Function of the Glymphatic System in SAMP8 Mice. Contrast-enhanced MRI allows the assessment of the brain-wide CSF-ISF exchange in glymphatic system. After contrast agent was injected into the subarachnoid space of the cisterna magna, it would pass through specific paravascular pathways before entering the brain parenchyma along with CSF, where contrast agent and CSF were intermingled with fluid in the interstitial compartments. Dynamic time series of T1-weighted MRIs could clearly reveal the different anatomical paths followed over time by the paravascular influx in the glymphatic system; thus, paramagnetic contrast agent injected into the cisterna magna was transported along the basilar artery and appears in the pituitary recess, from where it was conveyed along the olfactory arterial complex and into the olfactory bulb (Figure 6(a)). Compared with the Rc group, the signal intensity of all ROIs in the Pc group showed a higher trend, indicating that the retention concentration of Gd-DTPA was higher. Starting from the time of Gd-DTPA injection, the signal intensity in the pituitary recess was significantly higher in the Pc group than in the Rc group after 30 min, while that in the Pe group was significantly lower than in the Pc group. The signal intensity at the olfactory arterial complex and olfactory bulb was significantly higher in the Pc group than in the Rc group for 40 min after Gd-DTPA injection, while in the Pe group, it was significantly lower than in the Pc group ($P < 0.05$; Figure 6(b)). The overall effects in the Pc group versus the Rc group reflects that reduced clearance of Gd-DTPA during CSF–ISF exchange caused the higher residual concentrations, the suppressed glymphatic system, and the reduction in its ability to clear and that EA could accelerate the CSF-ISF exchange, improve the function of the glymphatic system in SAMP8 mice, and promote the clearance of material from the brain's parenchyma.

3.5. EA Inhibits the Reactivity of Astrocytes and Improves AQP4 Polarity. In the brain, impairment of the glymphatic system and the depolarization of AQP4 in reactive astrocytes are closely associated [7]. Astrocyte activation in the brain's parenchyma and AQP4 polarization were evaluated to clarify how EA treatment restores the glymphatic system's function. As shown by immunofluorescence, GFAP-positive astrocytes were present in the cortex and hippocampus of SAMR1 and SAMP8 mice. In the Pc group, the mean fluorescence intensity of GFAP-positive cells in the hippocampus and

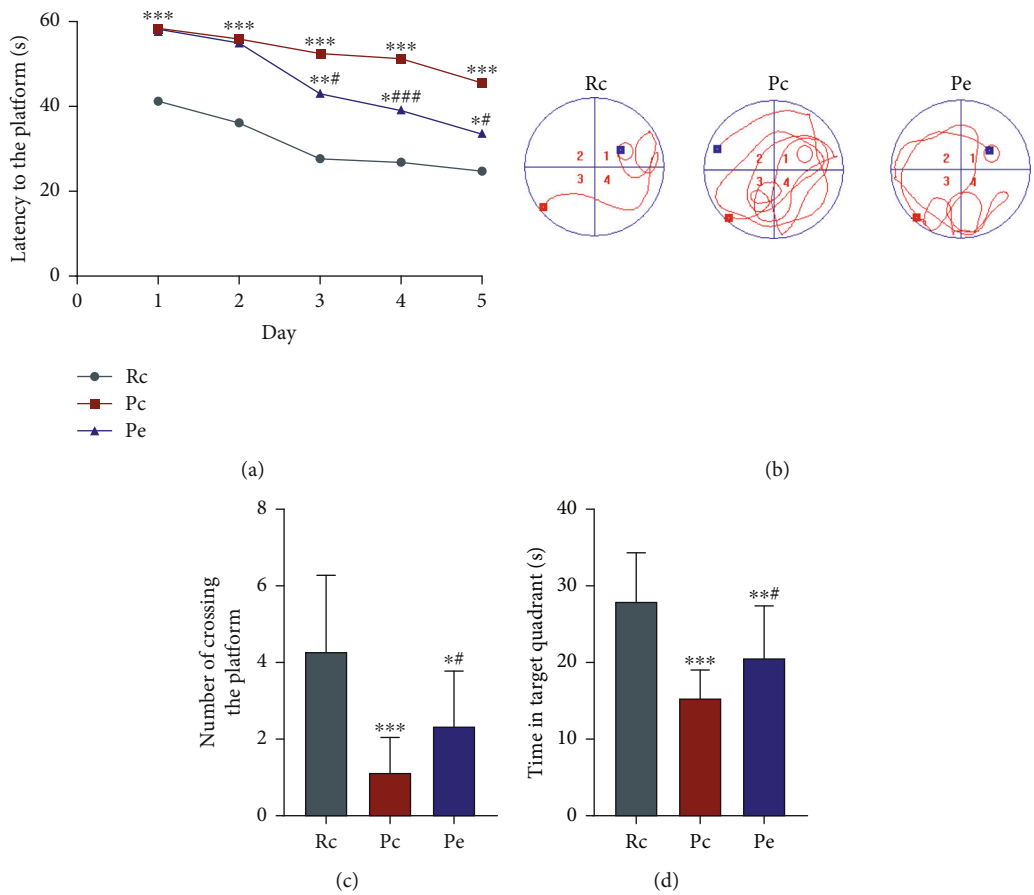

Figure 3: EA improved the ability of learning and memory of SAMP8 mice: (a) the escape latency time; (b) representative swim paths of each group in the hidden platform trial; (c) number of crossing the platform; (d) time in target quadrant. Data are expressed as the mean ± SD ($n = 15$ in each group). $^{*}P < 0.05$ and $^{***}P < 0.001$ versus the Rc group; $^{\#}P < 0.05$ and $^{\#\#\#}P < 0.001$ versus the Pc group.

cortex was significantly higher than that in the Rc group ($P < 0.001$), and the mean fluorescence intensity of GFAP-positive cells in the hippocampus and cortex was significantly lower in the Pe group than in the Pc group ($P < 0.01$ and $P < 0.05$, respectively; Figures 7(a) and 7(b)).

AQP4, the main component of water channel proteins expressed by astrocytes, is polarized in the perivascular astrocytic endfeet of the healthy brain, but not of the aging brain. The displacement of AQP4 from the endfeet of astrocytes to their soma is, in part, associated with failure of the glymphatic system-paravascular pathway [7]. We therefore explored the polarization of AQP4 in the brain of SAMR1 and SAMP8 mice. In the Rc group, AQP4 was expressed well all over the perivascular region, where it sheathed the astrocytic endfeet, whereas in the Pc group, it was located wrongly in the soma of astrocytes. In the Pe group, AQP4 was less widespread in the astrocytic soma, being mostly distributed around endfeet. The value of AQP4 polarity was analyzed following a previous study [24] and was assessed in SAMR1 and SAMP8 mice by the ratio between low-stringency area (total area of AQP4 immunoreactivity) and high-stringency area (area of intense AQP4 immunoreactivty around the perivascular endfeet) in an image. As a result, astrocytic AQP4 polarity was shown to be significantly lower in the Pc group than in the Rc group ($P < 0.001$) and higher in the Pe group than in the Pc group ($P < 0.05$; Figures 7(c) and 7(d)). The above result suggests that EA inhibited the reactivity of astrocytes and improved AQP4 polarity, triggering an improvement of the glymphatic system's function in the SAMP8 brain.

4. Discussion

At present, the treatment of AD is mainly based on antipsychotic drug therapy, but more and more studies have shown that antipsychotic drug therapy can increase the risk of death in Alzheimer's patients [27]. Therefore, nonpharmaceutical intervention for Alzheimer's disease has attracted more and more attention, including cognitive behavioral therapy (CBT), music therapy, transcranial magnetic stimulation (TMS), and acupuncture therapy. CBT and music therapy can reduce psychological and emotional problems such as depression and anxiety, but there are few reports on whether these two therapies can improve the cognition of AD patients [28, 29]. TMS mainly improves cognitive function by changing the excitability of local cerebral cortices [30]. However, TMS devices may cause side effects such as headache and even epilepsy during treatment due to the

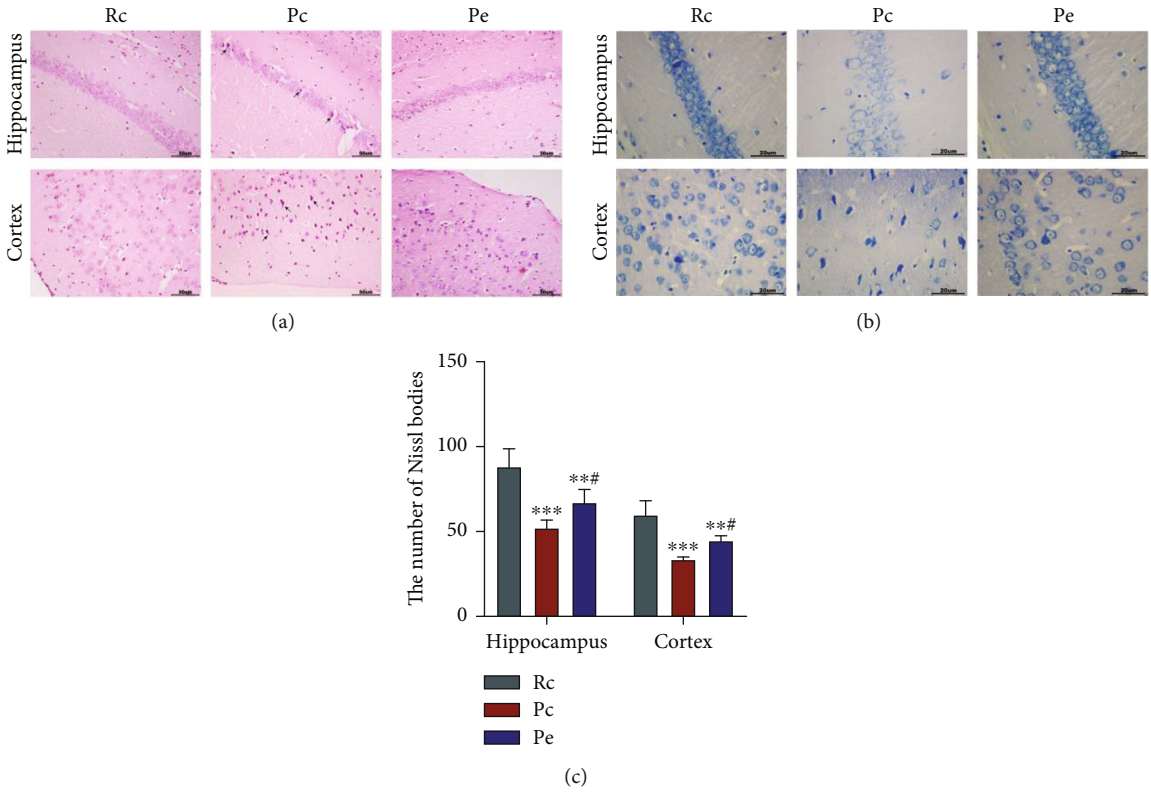

Figure 4: EA alleviated neuropathological injury of brain tissue in SAMP8 mice: (a) HE staining, scale bars = 50 μm; (b) Nissl staining, scale bars = 20 μm; (c) the number of Nissl bodies in the hippocampus and cortex. Data are expressed as the mean ± SD ($n = 4$ in each group). $^{**}P < 0.01$ and $^{***}P < 0.001$ versus the Rc group; $^{\#}P < 0.05$ versus the Pc group.

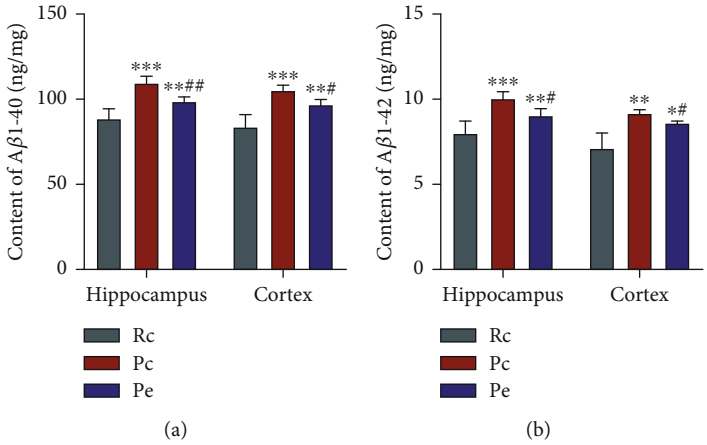

Figure 5: EA reduced Aβ accumulation in SAMP8 mice: (a) content of Aβ1-40 in the hippocampus and cortex; (b) content of Aβ1-42 in the hippocampus and cortex. Data are expressed as the mean ± SD ($n = 6$ in each group). $^{**}P < 0.01$ and $^{***}P < 0.001$ versus the Rc group; $^{\#}P < 0.05$ and $^{\#\#}P < 0.01$ versus the Pc group.

electrical characteristics of high voltage, high current, and strong magnetic field [31, 32]. Acupuncture, one of the most important nonpharmaceutical treatments that originated from traditional Chinese medicine, has a long history in the treatment of dementia in China. EA, a combination of traditional acupuncture and electrical stimulation [13], is safe and highly accessible. Clinical studies have shown that EA is one of the effective techniques for treating AD [33]. EA can effectively improve the overall intelligence and cognitive function of patients and alleviate various emotional symptoms of AD for a long time, with few negative side effects [14, 15]. In conclusion, EA has a wide range of action and is relatively safe among various nondrug treatments, so EA was selected as an intervention method in this study. In

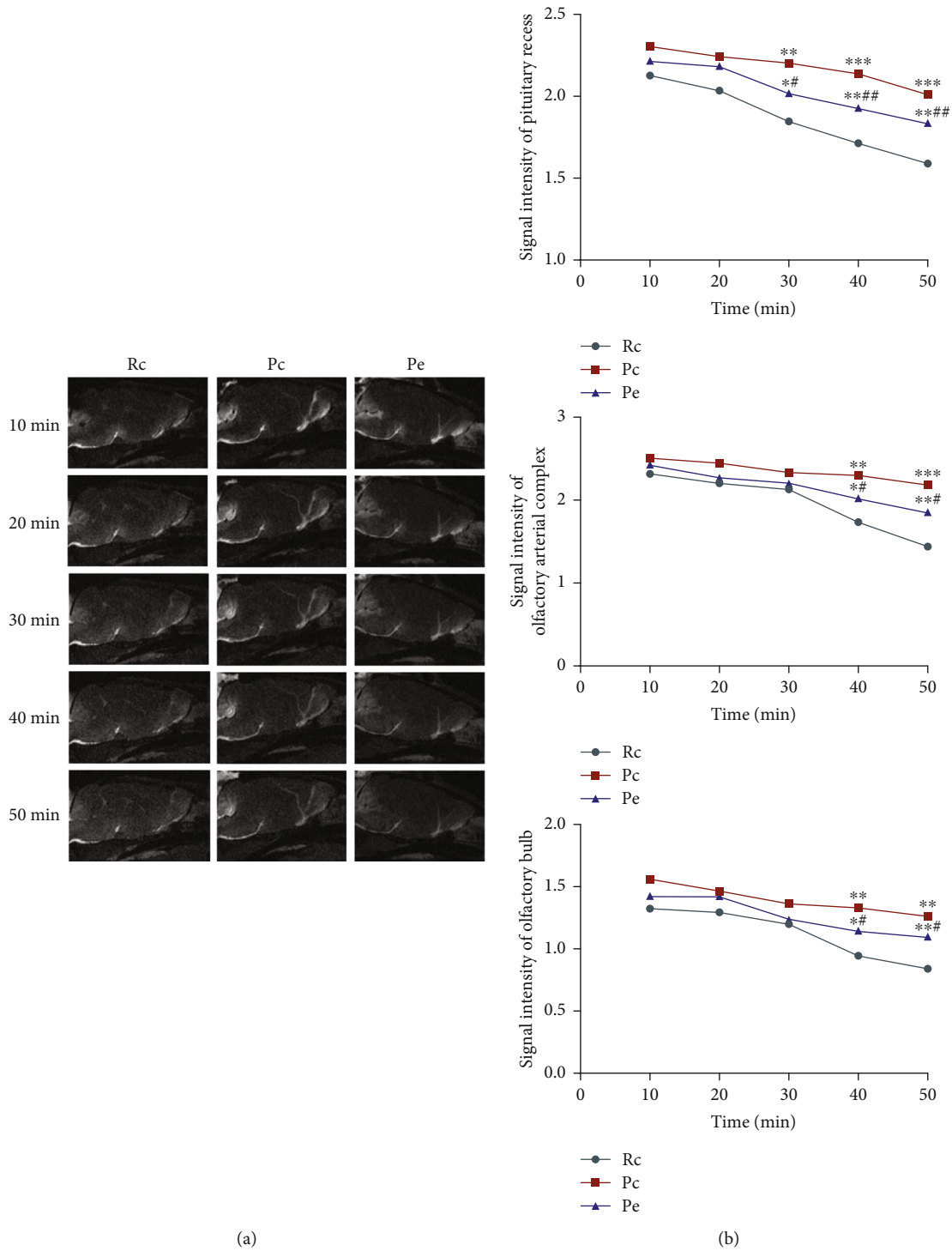

Figure 6: EA improved glymphatic system function in SAMP8 mice: (a) time-dependent anatomical routes of paravascular influx in the glymphatic system; (b) signal intensity of ROIs. Data are expressed as the mean ± SD ($n = 3$ in each group). $^{*}P < 0.05$, $^{**}P < 0.01$, and $^{***}P < 0.001$ versus the Rc group; $^{\#}P < 0.05$ and $^{\#\#}P < 0.01$ versus the Pc group.

previous studies, mechanisms of EA for cognitive function have been explored from different aspects in animal models of AD. The experiments have demonstrated that EA can effectively improve memory function and learning by inhibiting Aβ deposition, tau phosphorylation, and neuron loss [20, 21, 34–36].. Besides, a previous study also has shown that EA can promote Aβ clearance through Aβ-degrading enzymes, microglia phagocytosis, and blood-brain barrier transport, thereby delaying cognitive impairment in animal models of AD [18, 19, 37, 38]. The glymphatic system is closely related to the clearance of Aβ, but the research on the mechanism of EA regulating Aβ targeting the

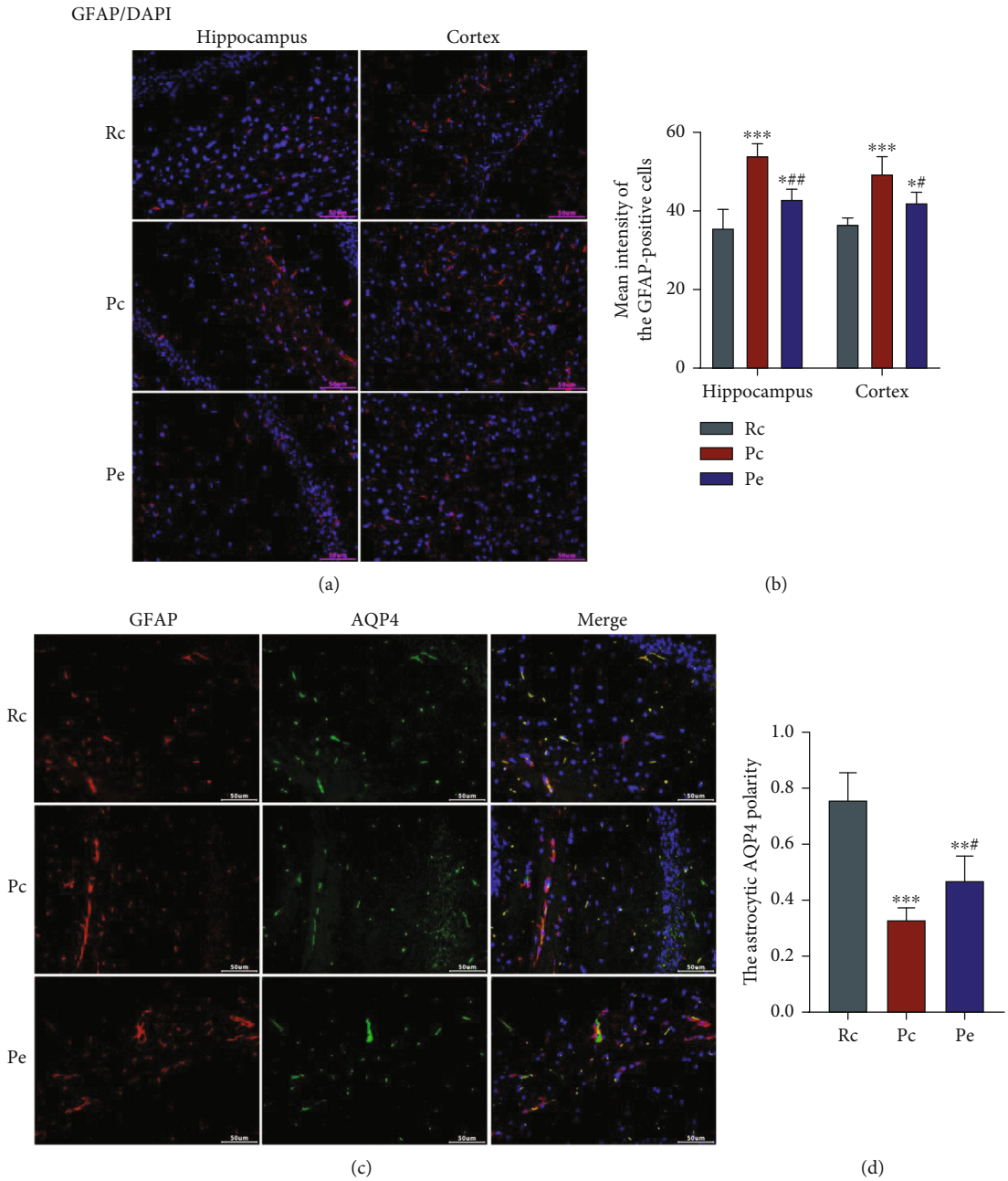

Figure 7: EA inhibited the reactivity of astrocytes and improved AQP4 polarity. (a) GFAP-positive cells were spread in each group, scale bars = 50 μm. (b) The mean fluorescence intensity of GFAP-positive cells in the hippocampus and cortex. (c) Immunofluorescence: double-labeling of GFAP and AQP4, scale bars = 50 μm. (d) Astrocytic AQP4 polarity. Data are expressed as the mean ± SD ($n = 4$ in each group). $^{*}P < 0.05$, $^{**}P < 0.01$, and $^{***}P < 0.001$ versus the Rc group; $^{\#}P < 0.05$ and $^{\#\#}P < 0.01$ versus the Pc group.

glymphatic system is still insufficient. Therefore, our study was designed to fill that gap for better understanding the mechanism of EA in treating AD.

According to the theory of traditional Chinese medicine, the trunk and branches of Governor Vessel (GV) are all closely correlated with the brain and if lesions occur in the brain, the GV is recommended as a preferred treatment option, and therefore, the acupoints in GV are frequently used in the treatment of CNS diseases. In our study, GV20, GV29, and GV26 were selected for the treatment since these three acupoints of GV could supplementarily combine to regulate the spirit, activate local collaterals, calm the frightened and awaking mind, awake the brain, and open orifices, respectively, therefore enhancing cognitive function and benefiting intelligence. The efficacy of such combination has been confirmed experimentally by many previous studies [17, 35, 39, 40]. Progressive cognitive impairment is the most common symptom of AD patients [41], and the progressively low cognitive ability of AD patients is closely linked to neuron loss in the brain [42]. Consistent with previous studies, our results of MWM test and HE and Nissl staining all demonstrated that EA could improve the

cognitive ability to learn, memorize, and explore the target platform and has a protective effect on neurons. Our data supported that such EA regime is effective in the treatment of AD animal models.

The hypothesis of "amyloid cascade for Alzheimer's disease" proposes that excessive accumulation of Aβ is the initiator and core link of the AD progression. In AD patients, the excessive accumulation of Aβ in the brain parenchyma forms senile plaque (SP), which can stimulate hyperphosphorylated tau aggregation, form NFTs, increase free radical release, and enhance oxidative stress response, which leads to synaptic degeneration and neuron death and ultimately triggers AD [43]. A variety of previous evidences have shown that EA can improve cognitive impairment in animal models of AD by reducing Aβ accumulation [20, 21]. Consistent with previous studies, our results of ELISA demonstrated that Aβ accumulation in the brain decreased significantly after EA treatment. Furthermore, how EA decreases Aβ accumulation of AD model was also explored.

In vivo, Aβ is mainly cleared from the brain by related degrading enzymes, glial cell phagocytosis, and blood-brain barrier transport [44]. In recent years, it is suggested that metabolites closely related to AD such as Aβ, Apolipoprotein E (ApoE), and tau protein [45, 46] can be cleared through the paravascular pathway in addition to the classical way of clearance [6]. This is the emerging concept of "glymphatic system." Dysfunction of the glymphatic system has been linked experimentally to Aβ accumulation [47]. Previous studies have shown that EA could reduce Aβ accumulation in the brain by upregulating the expression of Aβ-degrading enzymes such as neprilysin (NEP) and insulin-degraded enzyme (IDE) [18, 37], enhancing the Aβ uptake by microglia [38], and improving the expression of Aβ-related transporters such as low-density lipoprotein receptor-related protein-1 (LRP1) under the blood–brain barrier (BBB) [19]. However, evidence on the clearance of glymphatic system is lacking.

Iliff et al. found that glymphatic pathway function could be measured using dynamic contrast-enhanced MRI following intrathecal contrast agent administration. Dynamic contrast-enhanced MRI provides an intuitive approach to characterize both the kinetics and spatial distribution of paravascular CSF-ISF exchange throughout the whole brain [6]. The method has been widely used in research on the mechanism of the glymphatic system [48–51]. We used contrast-enhanced MRI to show the paravascular pathway and found that EA accelerated paravascular CSF-ISF exchange and significantly improved the function of glymphatic system. Reactive astrogliosis is a conspicuous feature of aging and the injured brain [7, 46, 52], and reactive astrocytes lead directly to withdrawal of AQP4 from the endfeet to the soma of astroglia, thus affecting the clearance function of the glymphatic system [7]. Here, EA was found to inhibit the reactivity of astrocytes and maintain the preferential location of AQP4 in the endfeet. Similar to our results, previous studies have demonstrated that the paravascular pathway's function is improved, and Aβ accumulation and impaired spatial memory cognition reduced by overexpression of Slit2 in the aging brain [53]. Based on these data, we propose that EA inhibits the reactivity of astrocytes and maintains AQP4 polarity, which improves the glymphatic system's function, thereby promoting Aβ clearance and consequently improving learning and the memory ability in SAMP8 mice.

There are some limitations in this study. In our study, dynamic contrast-enhanced MRI was used to demonstrate the EA could improve the overall clearance function of the glymphatic pathway, and it is suggested that when the overall clearance efficiency is improved, the clearance rate of Aβ could also be improved. However, direct evaluation of Aβ clearance from paravascular pathways is lacking. Previous studies have found that the neuroinflammation involved by activated astrocytes plays an important role in the pathogenesis of AD [54]. The results of this study showed that the injury of the glymphatic system in the animal model of AD is closely related to the increasing reactivity of astrocytes. Therefore, in the later stage, in-depth studies can be carried out based on the relationship between the function of the glymphatic system and neuroinflammation, as well as the reasons for the increasing reactivity of astrocytes and the effects on the brain tissue. Meanwhile, this study was conducted in order to further explore the regulation mechanism of EA on the glymphatic system and inflammatory response.

5. Conclusion

In summary, EA treatment can improve cognitive impairment in AD animal models, and its mechanism may involve the reduction of Aβ accumulation and improvement of the glymphatic system. This may provide new direction for further exploration of the mechanism of EA for the treatment of AD.

Data Availability

The data used to support the findings of this study are available from the corresponding author upon request.

Conflicts of Interest

The authors declare that they have no competing interests.

Authors' Contributions

Pei-zhe Liang, Li Li, Shu Wang, and Sha Yang had full access to all data in the study and took responsibility for the integrity of the data and the accuracy of the data analysis. Shu Wang, Sha Yang, Ya-nan Zhang, Yan Shen, and Li-li Zhang designed the study. Pei-zhe Liang conducted the experiments and drafted the manuscript. Li Li revised the manuscript and gave the valuable advice about data analysis and interpretation. Jie Zhou and Zhi-jie Wang provided technical assistance for this experiment. All authors approved the final version of the paper. Pei-zhe Liang and Li Li contribute equally to this article. Pei-zhe Liang and Li Li are regarded as co-first authors.

Acknowledgments

This work was supported by the Program of Tianjin Municipal Commission of Education (2017KJ144), the National Natural Science Foundation of China (81804189), the Program of Tianjin Science and Technology Project (18PTLCSY00040, 20ZYJDSY00020), and the Developmental Program for Changjiang Scholars and Innovative Research Team Program (IRT1167).

References

[1] D. S. Knopman and W. J. Jagust, "Alzheimer disease spectrum: syndrome and etiology from clinical and PET imaging perspectives," *Neurology*, vol. 96, no. 7, pp. 299-300, 2021.

[2] C. A. Ross and M. A. Poirier, "Protein aggregation and neurodegenerative disease," *Nature Medicine*, vol. 10, no. 7, pp. S10–S17, 2004.

[3] B. Penke, F. Bogár, and L. Fülöp, "β-Amyloid and the pathomechanisms of Alzheimer's disease: a comprehensive view," *Molecules*, vol. 22, no. 10, p. 1692, 2017.

[4] B. Regland and C. G. Gottfries, "The role of amyloid β-protein in Alzheimer's disease," *Lancet*, vol. 340, no. 8817, pp. 467–469, 1992.

[5] J. Wang, B. J. Gu, C. L. Masters, and Y. J. Wang, "A systemic view of Alzheimer disease – insights from amyloid-β metabolism beyond the brain," *Nature Reviews. Neurology*, vol. 13, no. 10, pp. 612–623, 2017.

[6] J. J. Iliff, M. Wang, Y. Liao et al., "A Paravascular Pathway Facilitates CSF Flow Through the Brain Parenchyma and the Clearance of Interstitial Solutes, Including Amyloid β," *Science Translational Medicine*, vol. 4, no. 147, article 147ra111, 2012.

[7] B. T. Kress, J. J. Iliff, M. Xia et al., "Impairment of paravascular clearance pathways in the aging brain," *Annals of Neurology*, vol. 76, no. 6, pp. 845–861, 2014.

[8] J. J. Iliff, M. Wang, D. M. Zeppenfeld et al., "Cerebral arterial pulsation drives paravascular CSF-interstitial fluid exchange in the murine brain," *The Journal of Neuroscience*, vol. 33, no. 46, pp. 18190–18199, 2013.

[9] J. J. Iliff, H. Lee, M. Yu et al., "Brain-wide pathway for waste clearance captured by contrast-enhanced MRI," *The Journal of Clinical Investigation*, vol. 123, no. 3, pp. 1299–1309, 2013.

[10] B. A. Plog and M. Nedergaard, "The glymphatic system in central nervous system health and disease: past, present, and future," *Annual Review of Pathology: Mechanisms of Disease*, vol. 13, no. 1, pp. 379–394, 2018.

[11] A. Arighi, A. di Cristofori, C. Fenoglio et al., "Cerebrospinal fluid level of aquaporin4: a new window on glymphatic system involvement in neurodegenerative disease?," *Journal of Alzheimer's Disease*, vol. 69, no. 3, pp. 663–669, 2019.

[12] S. B. Hladky and M. A. Barrand, "Mechanisms of fluid movement into, through and out of the brain: evaluation of the evidence," *Fluids and Barriers of the CNS*, vol. 11, no. 1, p. 26, 2014.

[13] Y.-y. Song, W.-t. Xu, X.-c. Zhang, and G.-x. Ni, "Mechanisms of electroacupuncture on Alzheimer's disease: a review of animal studies," *Chinese Journal of Integrative Medicine*, vol. 26, no. 6, pp. 473–480, 2020.

[14] K. P. Xia, J. Pang, S. L. Li, M. Zhang, H. L. Li, and Y. J. Wang, "Effect of electroacupuncture at governor vessel on learning-memory ability and serum level of APP, A$\beta_{1\text{-}42}$ in patients with Alzheimer's disease," *Zhongguo Zhen Jiu*, vol. 40, no. 4, pp. 375–378, 2020.

[15] Q. Feng, L. L. Bin, Y. B. Zhai, M. Xu, Z. S. Liu, and W. N. Peng, "Long-term efficacy and safety of electroacupuncture on improving MMSE in patients with Alzheimer's disease," *Zhongguo Zhen Jiu*, vol. 39, no. 1, pp. 3–8, 2019.

[16] Z. Hou, R. Qiu, Q. Wei et al., "Electroacupuncture improves cognitive function in senescence-accelerated P8 (SAMP8) mice via the NLRP3/caspase-1 pathway," *Neural Plasticity*, vol. 2020, Article ID 8853720, 14 pages, 2020.

[17] A. Xu, Y. Tang, Q. Zeng et al., "Electroacupuncture enhances cognition by promoting brain glucose metabolism and inhibiting inflammation in the APP/PS1 mouse model of Alzheimer's disease: a pilot study," *Journal of Alzheimer's Disease*, vol. 77, no. 1, pp. 387–400, 2020.

[18] Q. Yang, S. Zhu, J. Xu et al., "Effect of the electro-acupuncture on senile plaques and its formation in $APP^+/PS1^+$ double transgenic mice," *Genes & Diseases*, vol. 6, no. 3, pp. 282–289, 2019.

[19] X. Wang, Y. Miao, J. Abulizi et al., "Improvement of Electroacupuncture on APP/PS1 Transgenic Mice in Spatial Learning and Memory Probably due to Expression of Aβ and LRP1 in Hippocampus," *Evidence-Based Complementary and Alternative Medicine*, vol. 2016, Article ID 7603975, 10 pages, 2016.

[20] W. G. Dong, F. Wang, Y. Chen et al., "Electroacupuncture reduces Aβ production and BACE1 expression in SAMP8 mice," *Frontiers in Aging Neuroscience*, vol. 7, 2015.

[21] C. C. Yu, Y. Wang, F. Shen et al., "High-frequency (50 Hz) electroacupuncture ameliorates cognitive impairment in rats with amyloid beta 1-42-induced Alzheimer's disease," *Neural Regeneration Research*, vol. 13, no. 10, pp. 1833–1841, 2018.

[22] S. Chang, X. Guo, G. Li et al., "Acupuncture promotes expression of Hsp84/86 and delays brain ageing in SAMP8 mice," *Acupuncture in Medicine*, vol. 37, no. 6, pp. 340–347, 2019.

[23] W. Dong, W. Quo, F. Wang et al., "Electroacupuncture upregulates SIRT1-dependent PGC-1α expression in SAMP8 mice," *Medical Science Monitor*, vol. 21, pp. 3356–3362, 2015.

[24] M. Wang, J. J. Iliff, Y. Liao et al., "Cognitive deficits and delayed neuronal loss in a mouse model of multiple microinfarcts," *The Journal of Neuroscience*, vol. 32, no. 50, pp. 17948–17960, 2012.

[25] B. Dubois, H. Hampel, H. H. Feldman et al., "Preclinical Alzheimer's disease: definition, natural history, and diagnostic criteria," *Alzheimer's & Dementia*, vol. 12, no. 3, pp. 292–323, 2016.

[26] J. Li, P.-y. Wen, W.-w. Li, and J. Zhou, "Upregulation effects of Tanshinone IIA on the expressions of NeuN, Nissl body, and IκB and downregulation effects on the expressions of GFAP and NF-κB in the brain tissues of rat models of Alzheimer's disease," *NeuroReport*, vol. 26, no. 13, pp. 758–766, 2015.

[27] D. T. Maust, H. M. Kim, L. S. Seyfried et al., "Antipsychotics, other psychotropics, and the risk of death in patients with dementia," *JAMA Psychiatry*, vol. 72, no. 5, pp. 438–445, 2015.

[28] A. Spector, G. Charlesworth, M. King et al., "Cognitive-behavioural therapy for anxiety in dementia: pilot randomised controlled trial," *The British Journal of Psychiatry*, vol. 206, no. 6, pp. 509–516, 2015.

[29] A. C. Vink, M. Zuidersma, F. Boersma, P. de Jonge, S. U. Zuidema, and J. P. Slaets, "Effect of music therapy versus recreational activities on neuropsychiatric symptoms in elderly adults with dementia: an exploratory randomized controlled trial," *Journal*

of the American Geriatrics Society, vol. 62, no. 2, pp. 392-393, 2014.

[30] M. Wegrzyn, S. J. Teipel, I. Oltmann et al., "Structural and functional cortical disconnection in Alzheimer's disease: a combined study using diffusion tensor imaging and transcranial magnetic stimulation," *Psychiatry Research*, vol. 212, no. 3, pp. 192–200, 2013.

[31] R. Taylor, V. Galvez, and C. Loo, "Transcranial magnetic stimulation (TMS) safety: a practical guide for psychiatrists," *Australasian Psychiatry*, vol. 26, no. 2, pp. 189–192, 2018.

[32] V. BRUNO, C. Fossataro, and F. Garbarini, "Report of seizure induced by 10 Hz rTMS over M1," *Brain Stimulation*, vol. 11, no. 2, pp. 454-455, 2018.

[33] W. Peng, J. Zhou, M. Xu, Q. Feng, L. Bin, and Z. Liu, "The effect of electroacupuncture combined with donepezil on cognitive function in Alzheimer's disease patients: study protocol for a randomized controlled trial," *Trials*, vol. 18, no. 1, p. 301, 2017.

[34] Y. Yang, S. Hu, H. Lin, J. He, and C. Tang, "Electroacupuncture at GV24 and bilateral GB13 improves cognitive ability via influences the levels of Aβ, p-tau (s396) and p-tau (s404) in the hippocampus of Alzheimer's disease model rats," *NeuroReport*, vol. 31, no. 15, pp. 1072–1083, 2020.

[35] A. Xu, Q. Zeng, Y. Tang et al., "Electroacupuncture Protects Cognition by Regulating Tau Phosphorylation and Glucose Metabolism via the AKT/GSK3β Signaling Pathway in Alzheimer's Disease Model Mice," *Frontiers in Neuroscience*, vol. 14, article 585476, 2020.

[36] H.-d. Guo, J. Zhu, J.-x. Tian et al., "Electroacupuncture Improves Memory and Protects Neurons by Regulation of the Autophagy Pathway in a Rat Model of Alzheimer—s Disease," *Acupuncture in Medicine*, vol. 34, no. 6, pp. 449–456, 2016.

[37] X. Wang, Y. Wang, S. Yu, and L. Ren, "Effect of Electroacupuncture on Levels of β-amyloid and Neprilysin Proteins in the Cerebral Cortex of Alzheimer's Disease Mice Based on "Mutual Assistance of Kidney and Brain" Theory," *Zhen ci yan jiu = Acupuncture research*, vol. 43, no. 1, pp. 20–24, 2018.

[38] L. Li, L. Li, J. Zhang et al., "Disease Stage-Associated Alterations in Learning and Memory through the Electroacupuncture Modulation of the Cortical Microglial M1/M2 Polarization in Mice with Alzheimer's Disease," *Neural Plasticity*, vol. 2020, Article ID 8836173, 14 pages, 2020.

[39] J. Cao, Y. Tang, Y. Li, K. Gao, X. Shi, and Z. Li, "Behavioral changes and hippocampus glucose metabolism in APP/PS1 transgenic mice via electro-acupuncture at governor vessel acupoints," *Frontiers in Aging Neuroscience*, vol. 9, 2017.

[40] Y. Tang, A. Xu, S. Shao, Y. Zhou, B. Xiong, and Z. Li, "Electroacupuncture Ameliorates Cognitive Impairment by Inhibiting the JNK Signaling Pathway in a Mouse Model of Alzheimer's Disease," *Frontiers in Aging Neuroscience*, vol. 12, 2020.

[41] Y. Duan, L. Lu, J. Chen et al., "Psychosocial interventions for Alzheimer's disease cognitive symptoms: a Bayesian network meta-analysis," *BMC Geriatrics*, vol. 18, no. 1, p. 175, 2018.

[42] O. Wirths and S. Zampar, "Neuron loss in Alzheimer's disease: translation in transgenic mouse models," *International Journal of Molecular Sciences*, vol. 21, no. 21, p. 8144, 2020.

[43] E. Karran, M. Mercken, and B. D. Strooper, "The amyloid cascade hypothesis for Alzheimer's disease: an appraisal for the development of therapeutics," *Nature Reviews. Drug Discovery*, vol. 10, no. 9, pp. 698–712, 2011.

[44] P. Gallina, A. Scollato, R. Conti, N. di Lorenzo, and B. Porfirio, "Aβ Clearance, "hub" of multiple deficiencies leading to Alzheimer disease," *Frontiers in Aging Neuroscience*, vol. 7, 2015.

[45] T. M. Achariyar, B. Li, W. Peng et al., "Glymphatic distribution of CSF-derived apoE into brain is isoform specific and suppressed during sleep deprivation," *Molecular Neurodegeneration*, vol. 11, no. 1, 2016.

[46] J. J. Iliff, M. J. Chen, B. A. Plog et al., "Impairment of Glymphatic Pathway Function Promotes Tau Pathology after Traumatic Brain Injury," *The Journal of Neuroscience*, vol. 34, no. 49, pp. 16180–16193, 2014.

[47] E. N. T. P. Bakker, B. J. Bacskai, M. Arbel-Ornath et al., "Lymphatic Clearance of the Brain: Perivascular, Paravascular and Significance for Neurodegenerative Diseases," *Cellular and Molecular Neurobiology*, vol. 36, no. 2, pp. 181–194, 2016.

[48] K. N. Mortensen, S. Sanggaard, H. Mestre et al., "Impaired glymphatic transport in spontaneously hypertensive rats," *The Journal of Neuroscience*, vol. 39, no. 32, pp. 6365–6377, 2019.

[49] H. Lee, L. Xie, M. Yu et al., "The effect of body posture on brain glymphatic transport," *The Journal of Neuroscience*, vol. 35, no. 31, pp. 11034–11044, 2015.

[50] L. Li, M. Chopp, G. Ding et al., "MRI detection of impairment of glymphatic function in rat after mild traumatic brain injury," *Brain Research*, vol. 1747, article 147062, 2020.

[51] Q. Jiang, L. Zhang, G. Ding et al., "Impairment of the glymphatic system after diabetes," *Journal of Cerebral Blood Flow and Metabolism*, vol. 37, no. 4, pp. 1326–1337, 2017.

[52] C. Luo, X. Yao, J. Li et al., "Paravascular pathways contribute to vasculitis and neuroinflammation after subarachnoid hemorrhage independently of glymphatic control," *Cell Death & Disease*, vol. 7, no. 3, article e2160, 2016.

[53] G. Li, X. He, H. Li et al., "Overexpression of Slit2 improves function of the paravascular pathway in the aging mouse brain," *International Journal of Molecular Medicine*, vol. 42, no. 4, pp. 1935–1944, 2018.

[54] D. Kaur, V. Sharma, and R. Deshmukh, "Activation of microglia and astrocytes: a roadway to neuroinflammation and Alzheimer's disease," *Inflammopharmacology*, vol. 27, no. 4, pp. 663–677, 2019.

Hindawi
Neural Plasticity
Volume 2021, Article ID 9926445, 23 pages
https://doi.org/10.1155/2021/9926445

Review Article

Acupuncture for Parkinson's Disease: Efficacy Evaluation and Mechanisms in the Dopaminergic Neural Circuit

Yadan Zhao,[1] Zichen Zhang,[1] Siru Qin,[1] Wen Fan,[2] Wei Li,[1] Jingyi Liu,[1] Songtao Wang,[1] Zhifang Xu,[1,3] and Meidan Zhao[1,3]

[1]*Research Center of Experimental Acupuncture Science, Tianjin University of Traditional Chinese Medicine, Tianjin 301617, China*
[2]*Suzuka University of Medical Science, Suzuka 5100293, Japan*
[3]*School of Acupuncture & Moxibustion and Tuina, Tianjin University of Traditional Chinese Medicine, Tianjin 301617, China*

Correspondence should be addressed to Zhifang Xu; xuzhifangmsn@hotmail.com and Meidan Zhao; zhaomeidan2012@163.com

Received 25 March 2021; Revised 10 May 2021; Accepted 27 May 2021; Published 16 June 2021

Academic Editor: Feng Zhang

Parkinson's disease (PD) is a chronic and progressive neurodegenerative disease caused by degeneration of dopaminergic neurons in the substantia nigra. Existing pharmaceutical treatments offer alleviation of symptoms but cannot delay disease progression and are often associated with significant side effects. Clinical studies have demonstrated that acupuncture may be beneficial for PD treatment, particularly in terms of ameliorating PD symptoms when combined with anti-PD medication, reducing the required dose of medication and associated side effects. During early stages of PD, acupuncture may even be used to replace medication. It has also been found that acupuncture can protect dopaminergic neurons from degeneration via antioxidative stress, anti-inflammatory, and antiapoptotic pathways as well as modulating the neurotransmitter balance in the basal ganglia circuit. Here, we review current studies and reflect on the potential of acupuncture as a novel and effective treatment strategy for PD. We found that particularly during the early stages, acupuncture may reduce neurodegeneration of dopaminergic neurons and regulate the balance of the dopaminergic circuit, thus delaying the progression of the disease. The benefits of acupuncture will need to be further verified through basic and clinical studies.

1. Introduction

Parkinson's disease (PD) is a chronic and progressive neurodegenerative disease typically affecting middle-aged and elderly people. The key clinical manifestation is the dysfunction of voluntary motor regulation, including bradykinesia, resting tremor, myotonia, and postural instability [1]. In addition to motor dysfunction, nonmotor symptoms may arise during progression of PD, including cognitive dysfunction, emotional disorders such as apathy, depression, anxiety, and hallucinations, and autonomic nervous dysfunction, such as constipation, hyposmia, and sleep disorders [2]. PD has a prevalence of 0.3% and is thus the second most common neurodegenerative disease after Alzheimer's disease [3]. Tragically, the physical status of PD patients declines even when treated, often deteriorating to severe disability and death. Treatment costs impose enormous financial demands on patients and their families, incurring over US$14 billion annually [4].

Pathologically, PD is characterized by the loss and degeneration of dopaminergic neurons in the substantia nigra (SN), α-synuclein (α-syn) deposition, and Lewy body formation [5]. Current treatment options for PD include medication, surgery, and exercise therapy, although medication is the first choice for PD, with the most commonly prescribed drugs being dopaminergic and anticholinergic agents [2]. These have been shown to control the initial symptoms of patients rapidly and effectively [6], but after a so-called "honeymoon period" of treatment, the effectiveness often decreases and medication may no longer be beneficial for patients with advanced PD. The fundamental reason for this phenomenon is that existing anti-PD drugs offer only symptomatic treatment but cannot delay disease progression. Moreover, anti-PD drugs can also lead to considerable side

effects which can aggravate PD symptoms, and some of which still lack effective treatment [7]. Many patients with PD have therefore turned to complementary and alternative therapies which may be used in the early stages of PD or prior to the use of levodopa (L-DOPA) to relieve symptoms and delay PD progression, with the potential expectation that these therapies may also reverse or delay neuronal degeneration [8].

Acupuncture is an economical therapy in traditional Chinese medicine originating from China where it has been developed for more than 4,000 years. It can promote health or treat diseases via various different techniques such as manual acupuncture (MA), electroacupuncture (EA), moxibustion, and acupressure on specific anatomical locations (i.e., acupoints) [9]. Numerous clinical trials have shown that acupuncture exhibits significant therapeutic benefits for PD patients, reducing both motor and nonmotor symptoms. Moreover, acupuncture may help to reduce the dose and frequency of anti-PD drugs as well as alleviate their side effects [10]. The therapeutic mechanisms of acupuncture have also been shown to involve a reduction of mitochondrial dysfunction, oxidative stress, protein aggregation, impaired autophagy, and neuroinflammation [11]. In the present review, we aim to address the clinical efficacy and potential mechanisms of acupuncture in PD treatment, providing novel insights for the clinical application of acupuncture for the reversal the degeneration of dopaminergic neurons and delay of PD progression.

2. Methods

2.1. Search Strategy. We searched the PubMed database for studies published between January 2000 and December 2020 containing the keywords "Acupuncture" and "Parkinson's disease". Only studies in English language were included. This search identified relevant 183 articles.

2.2. Study Selection. Following the search engine selection of 183 articles, a manual search was performed by screening the reference list for articles that met our inclusion criteria based on the titles and abstracts. We excluded 43 articles due to absence of an abstract, unavailability of the full text, or irrelevance to the subject, leaving 140 articles, including 43 basic research articles, 38 clinical research articles, and 59 review articles or meta-analyses. The full texts of the 43 basic research and 38 clinical research articles were obtained and assessed carefully. Out of the 38 clinical studies, 17 were excluded as they described single case reports, editorials, and uncompleted or uncontrolled trials, resulting in 21 clinical articles meeting our inclusion criteria. All 43 basic research articles met our inclusion criteria. Thus, a total of 64 articles were included in our review. A flow chart of this search process is illustrated in Figure 1.

2.3. Data Extraction. Two authors independently assessed the titles and abstracts of the retrieved articles and evaluated the full-text articles. The data from finally included articles were validated and extracted according to the predefined criteria. Any disagreement was resolved by discussion between the authors.

3. Clinical Efficacy of Acupuncture in Parkinson's Disease Patients

Acupuncture is commonly and globally used as both an adjuvant therapy and monotherapy for PD treatment [8]. Comprehensive evidence for the efficacy and safety of acupuncture in PD has been provided by a total of twelve systematic reviews (SRs) or meta-analyses (MAs) assessing this topic, involving 179 randomized controlled trials (RCTs) with a total of 11,717 participants [12]. These SRs/MAs have compared the effects of acupuncture combined with medication versus medication alone, demonstrating better efficacy at symptom alleviation with the combination of acupuncture with medication compared to medication alone [13]. The Unified Parkinson's Disease Rating Scale (UPDRS) provides a comprehensive, efficient, and flexible means of monitoring PD-related disabilities and impairments as well as treatment evaluation, assessing behavior and mood, activities of daily living, motor functions, and therapeutic complications [14]. Acupuncture combined with dopaminergic drugs was superior to medication only for improving the UPDRS score [15]. Interestingly, when comparing acupuncture only with medication only, there is no significant difference in the scores. Moreover, evidence-based medicine (EBM) studies have analyzed 13 parallel RCTs and found no difference in the efficacy of acupuncture compared with medication for PD treatment [10], suggesting that acupuncture may achieve an efficacy close to that of medication. The Webster Scale is applied to assess the clinical severity of PD, rating levels of akinesia, rigidity, upper limb swing, gait, tremor, facial appearance, speech, and self-care [16]. Compared with medication only, acupuncture and medication combined have been shown to result in a greater Webster score reduction, indicating an alleviation of clinical severity [12], and compared with medication only, acupuncture alone similarly exhibited a positive effect for decreasing the Webster score [10], suggesting that acupuncture alone may be able to effectively reduce the severity of PD. EBM reviews reveal that even with an optimized oral dose of L-DOPA, there is a risk for a worsening of movement disorders, and a variety of anti-PD drugs may also induce or exacerbate nonmotor symptoms [17]. Hence, treatment with L-DOPA and other anti-PD drugs should be delayed as much as possible in patients with early-stage PD. If acupuncture achieves a similar therapeutic effect to currently available medication, it may represent a new therapeutic option for PD, especially for early stages. There is no evidence for any serious adverse reactions associated with acupuncture, suggesting that it is a relatively safe choice for PD patients. Therefore, the current evidence indicates that acupuncture may enhance the therapeutic efficacy of drugs and reduce the required dose of medication, thus also alleviating adverse effects.

Besides UPDRS and Webster scales, there are more targeted evaluation criteria corresponding to different PD symptoms [18]. The characteristics of the 15 clinical studies included in our analysis are summarized in Table 1. Using

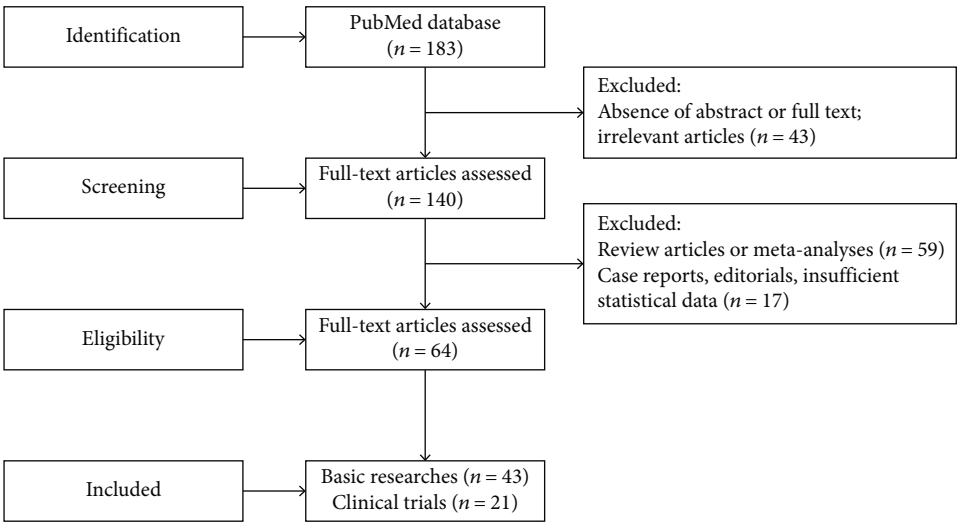

Figure 1: Flow chart of the review processes.

wearable sensors, Lei et al. [19] found that EA had overall beneficial impact on different temporal and spatial parameters of gait (gait speed and stride length) as well as dynamic posture control (increase of midswing angular velocity and decrease of double support). Kong et al. [20] evaluated changes in the General Fatigue score of the Multidimensional Fatigue Inventory after acupuncture treatment and found that 5-week acupuncture treatment effectively alleviated moderate and severe fatigue of PD patients. These results are similar to reports of an RCT by Kluger et al. assessing the relief of PD with fatigue by acupuncture [21]. Using functional magnetic resonance imaging (fMRI), Yu et al. [22] found enhanced connectivity in four junctions via fMRI after acupuncture. There was a significant correlation between changes in functional connectivity and the King's Parkinson's Disease Pain Scale, indicating that acupuncture relieves pain in PD patients via modulation of brain regions related to both sensory-discriminative and emotional aspects. In an unblinded trial including 20 PD patients, no adverse reactions were reported with an improvement of individual symptoms including tremor, walking, writing, bradykinesia, pain, sleep, depression, and anxiety in 85% of patients [23]. An RCT by Cristian et al. [24] showed a trend toward an improvement in the Parkinson's Disease Questionnaire, daily living activities, and UPDRS motor score following acupuncture, suggesting that acupuncture has a potential effect for alleviation of both movement and nonmotor symptoms including pain, depression, and autonomic symptoms. Using the Parkinson Disease Sleep Scale, Aroxa et al. [25] found that acupuncture was beneficial for the alleviation of sleep disorders in PD patients. Furthermore, acupuncture may be beneficial for improving oral cavity function as observed by increased mean tongue pressure and decreased average saliva swallowing reflex latency in PD patients after acupuncture [26].

Taken together, the clinical studies above have concluded that acupuncture exhibits a comprehensive beneficial effect on symptoms associated with dyskinesia, psychology, behavior, emotion, and cognition of PD patients. Additionally, there are various types of acupuncture methods, such as MA, EA, and bee venom acupuncture (BVA). A combination of body and scalp acupoints is typically used in PD patients, with scalp acupoints located in the occipital, frontal, and parietal lobes as well as in motor and chorea-tremor controlled areas [33]. It has been shown that scalp acupoints cannot only directly activate and adjust functional areas of the corresponding cerebral cortex but also convey certain therapeutic advantages for movement disorders [34]: EA at scalp acupoints has been found to reduce the loss of dopaminergic neurons in the SN and delay the degeneration of dopaminergic neurons, thereby alleviating clinical symptoms and postponing the progression of PD [35]. Therefore, scalp acupoints are an indispensable part of PD acupuncture treatment. In clinical PD acupuncture trials, the acupoints LR3 (*Taichong*), GB34 (*Yanglingquan*), and ST36 (*Zusanli*) were the primary body acupoints used, followed by LI4 (*Hegu*), LI11 (*Quchi*), and SI3 (*Houxi*) [2]. Previous reports showed that GB34 significantly improves PD symptoms, in particular motor dysfunction, and attenuates dopaminergic neuronal loss in animal models of PD [36]. Other acupoints such as ST36 [37] and LR3 [38] displayed the same effects. Several preclinical randomized studies have demonstrated that acupuncture stimulation at GB34, GV20, and LR3 modulates PD-associated brain regions and results in an amelioration of locomotor function closely associated with a reduction of neuronal apoptosis in the striatum (ST) and SN [39]. Thereby, these three acupoints have been recommended as the basic setting of acupuncture in clinical treatment of PD according to the World Health Organization standards [40].

In the clinical application of acupuncture, acupoints are also selected according to different PD symptoms and complications [26, 27]. For instance, acupoints LR3, KI6 (*Zhaohai*), and KI7 (*Fuliu*) located in the lower leg are expected to relieve pain; acupoints HT3 (*Shaohai*), LI7 (*Wenliu*), and SI3 are stimulated in severe tremor; moxibustion at acupoints SP21 (*Dabao*) and LR14 (*Qimen*) or acupuncture at acupoints DU16 (*Fengfu*), DU14 (*Dazhui*), and Extra (*Baliao*) is used for obvious neck stiffness; acupoints DU4 (*Mingmen*)

Table 1: The clinical efficacy of acupuncture in the patients with Parkinson's disease.

Study	Clinical trial design	Clinical condition	Intervention	Comparison	Acupoints	Acupuncture parameters	Outcomes
Lei et al. (2016) [19]	RCT	PD patients	EA ($n = 10$)	Sham EA ($n = 5$)	GV20, GV14; bilateral foot motor, sensory area, balance area, LI4, ST36, GB34, BL40, SP6, KI3, LR3	Asymmetric biphasic square wave pulse, 100 μS pulse width, "*deqi*", 100 Hz or 4 Hz, three times a week, 3 weeks	Primary outcome: STHW↑, STFW↑, DTFW↑, and DTHW↑ Secondary outcome: UPRDS scores↓
Kong et al. (2017) [20]	RCT	PD patients with moderately severe fatigue	Acupuncture ($n = 20$)	Sham acupuncture ($n = 20$)	CV6; bilateral PC6, ST36, LI4, SP6, KI3	5-30 inches, no flicking or rotation of needles after insertion, 20 minutes, twice a week, at least 3 days apart, 5 weeks, 10 sessions	Primary outcome: MFI-GF↓ Secondary outcome: MFI-total score↓, UPDRS-motor↓
Kluger et al. (2016) [21]	RCT	PD patients with moderate or severe fatigue	EA ($n = 47$)	Sham acupuncture ($n = 47$)	GV20, GV24; bilateral LI10, HT7, ST36, SP6	0.5-1 cm, twisted three times to the right, 30 minutes, every two weeks, 6weeks	Primary outcome: MFIS (total, physical, cognitive, psychosocial)↓ Secondary outcomes: PDQ-39↓, HADS (depression)↓, ESS↓, AES↓
Yu et al. (2019) [22]	Comparison trials	PD patients with pain	Acupuncture +medication ($n = 9$)	Medication ($n = 7$)	GV20; bilateral 77.18, GB34	5-10 mm, "*deqi*" for 20 s, 30 minutes, 1-3 sessions per week, separated by at least 1 day, 8 weeks	Primary outcome: KPPS↓, UPDRS (total)↓, enhanced connectivity at the four areas, a significant correlation between functional connectivity changes and KPPS
Shulman et al. (2002) [23]	Controlled trial	Idiopathic PD patients (stages I-III)	EA ($n = 20$)	Self-control	Bilateral LI4, GB34, ST36, K3, KI7, SP6, SI3, TB5	Intensity knob: 0; electric exciter switch: 1; wave form: intermittent; twice a week, 10/16 treatments	Sleep and rest category: SIP (sleep and rest)↓
Cristian et al. (2005) [24]	RCT	PD patients (stages II-III)	EA ($n = 7$)	Sham acupuncture group ($n = 7$)	GV20; bilateral K3, K10, BL60, L3, ST41, ST36, GB34, *bafeng* points, MH6, LI4	4 Hz, 20 minutes, 5 sessions, 2 weeks	NS
Aroxa et al. (2016) [25]	RCT	Idiopathic PD patients (stages I-III)	Acupuncture+ medication ($n = 11$)	Medication ($n = 11$)	Bilateral LR3, SP6, LI4, TE5, HT7, PC6, LI11, GB20	30 minutes, once a week, 8 weeks	Sleep disorders evaluation: PDSS↑
Fukuda et al. (2016) [26]	Controlled trial	PD patients (stages I-III)	Acupuncture ($n = 13$)	Self-control	Bilateral ST36, SP6, LR3, LI4, LI11, GB20, BL18, BL23	Inserted perpendicularly, 10-20 mm, 10-15 minutes, only once	Tongue function: mean tongue pressure↑, mean swallowing reflex latency↓, saliva swallow↓
Chen et al. (2015) [2]	Comparison clinical trial	PD patients	Acupuncture+ medication ($n = 20$)	Medication ($n = 20$)	DU20; bilateral GB20, LI11, LI10, LI4, GB31, ST32, GB34, GB38	MA, 5-30 mm, 15 minutes, twice a week, 18 (short-term)/36 (long-term) weeks	Short-term: UPDRS (total scores and subscores I, II, III, and IV)↓, BDI-II score↓, WHO-QOL score↓ Long-term: UPDRS (total scores and subscores I, II,

Table 1: Continued.

Study	Clinical trial design	Clinical condition	Intervention	Comparison	Acupoints	Acupuncture parameters	Outcomes
							III, and IV)↓, BDI-II score↓
Wang et al. (2002) [27]	Controlled trial	PD patients (stages I-III)	Acupuncture ($n = 29$)	Blank control ($n = 14$)	Group 1: DU20; bilateral GB20, LI4, SP6, LR3; group 2: Extra6; bilateral LI11, SJ5, GB34, ST36, ST40, Extra21	MA at Extra6, GB13, and GB20, then electric stimulator with continuous wave for 15 minutes; the rest acupoints: uniform reinforcing-reducing method, 40 minutes; once every other day, 3 months	The Webster's cumulative scores↓, correlation analysis of ABP indices and the cumulative scores in Webster's scale↓, the latent period of V wave and the intermittent periods of III-V peak and I-V peak↓
Yeo et al. (2018) [28]	Controlled trial	Idiopathic PD patients	EA+MA ($n = 10$)	Self-control	Right GB34, LR3 (EA) Bilateral LR3, LI11, ST36, GB20, SP6, LI4, GB34 (MA)	EA: 15 minutes, 120 Hz, twice a week, 8 weeks; MA: 3 to 15 mm, 15 minutes; twice a week, 8 weeks	UPDRS (total, 1, 2, 3, and4) score↓, BDI-II scores↓, neural responses (thalamus, cingulate gyrus, anterior cingulate, lingual gyrus, parahippocampal gyrus, lateral globus pallidus, mammillary body, middle temporal gyrus, cuneus, and fusiform gyrus)↑
Cho et al. (2017) [29]	RCT	Idiopathic PD patients (stages I-IV)	Acupuncture+ BVA ($n = 29$)	Sham treatment ($n = 29$)/ conventional treatment ($n = 15$)	Bilateral GB20, LI11, GB34, ST36, LR3	BVA: injected diluted bee venom 0.1 ml; EA: 1-1.5 cm, rotated at 2 Hz for 10 seconds to achieve "*deqi*", 15 minutes; twice a week, 12 weeks	Primary outcome: UPDRS (part II+III) scores↓ Secondary outcomes: UPDRS (part II and III) scores↓, gait speed↓, gait number↑, PIGD↓
Eng et al. (2006) [30]	Controlled trial	Idiopathic PD patients	Acupuncture+ Yin Tui Na ($n = 25$)	Self-control	Bilateral ST42, SP3, LI11, LI15, LI20, ST7, ST36	7-10 minutes, 8-14 Hz, once a week, 6 months, 24 sessions	UPDRS (I and II) scores↓, UPDRS (III) scores↑, PDQ-39 total score↓, BDI↓
Doo et al. (2015) [31]	Controlled trial	Idiopathic PD patients	Acupuncture and BVA+conventional treatment ($n = 11$)	Self-control	Bilateral GB20, LI4, GB34, ST36, LR3	BVA: injected diluted bee venom 0.1 ml; EA: 1-1.5 cm, rotated at 2 Hz for 10 seconds to achieve "*deqi*", 15 minutes; twice per week, 12 weeks	Primary outcome: UPDRS (part II+III) scores↓ Secondary outcomes: UPDRS (part II and III) scores↓, gait speed ↓, PDQL score↑
Ren (2008) [32]	Controlled trial	PD patients	Acupuncture+ Madopar ($n = 50$)	Madopar ($n = 30$)	From TE14 to TE2, from PC2 to PC7 (areas being tapped) Bilateral TE4, LI5, PC7,	Tap: with a plum-blossom needle, until skin turns red; MA: uniform reinforcing and reducing method,	Total effective rate↑, the minimum dose of Madopar needed↓

Table 1: Continued.

Study	Clinical trial design	Clinical condition	Intervention	Comparison	Acupoints	Acupuncture parameters	Outcomes
					SI6, LI11, LU5, PC3, HT3, TE14, LI15, SI9, LR4, KI3, ST41, SP9, GB34, BL40, GB30, BL36 (MA)	30 minutes; once a day, 10 sessions a course, 3-5 days between courses, 2 courses	

RCT: randomized controlled trial; PD: Parkinson's disease; EA: electroacupuncture; GV20: *Baihui*; GV14: *Dazhui*; LI4: *Hegu*; ST36: *Zusanli*; GB34: *Yanglingquan*; BL40: *Weizhong*; SP6: *Sanyinjiao*; KI3: *Taixi*; LR3: *Taichong*; STHW: single-task habitual walking; STFW: single-task fast walking; DTFW: dual-task fast walking; DTHW: dual-task habitual walking; UPDRS: Unified Parkinson's Disease Rating Scale; PC6: *Neiguan*; CV6: *Qihai*; MFI-GF: General Fatigue score of the Multidimensional Fatigue Inventory; GV24: *Shenting*; LI10: *Shousanli*; HT7: *Shenmen*; MFIS: Modified Fatigue Impact Scale; PDQ-39: 39-item Parkinson's Disease Questionnaire; HADS: Hospital Anxiety and Depression Scale; ESS: Epworth Sleepiness Scale; AES: Apathy Evaluation Scale; 77.18: *Shenguan*; KPPS: King's Parkinson's Disease Pain Scale; KI7: *Fuliu*; SI3: *Houxi*; TB5: *Waiguan*; SIP: Sickness Impact Profile; KI10: *Yingu*; BL60: *Kunlun*; NS: no significance; ST41: *Jiexi*; MH6: *Yinwei*; TE5: *Waiguan*; LI11: *Quchi*; GB20: *Fengchi*; PDSS: Parkinson's Disease Sleep Scale; BL18: *Ganshu*; BL23: *Shenshu*; DU20: *Baihui*; GB31: *Fengshi*; ST32: *Futu*; GB38: *Juegu*; MA: manual acupuncture; BDI-II: Beck Depression Inventory-Version 2; WHO-QOL: WHO quality of life; Extra6: *Sishencong*; SJ5: *Waiguan*; ST40: *Fenglong*; Extra21: *Huatuojiaji*; GB13: *Benshen*; ABP: auditory evoked brain stem potential; TE14: *Jianliao*; TE2: *Yemen*; PC2: *Tianquan*; PC7: *Daling*; TE4: *Yangchi*; LI5: *Yangxi*; SI6: *Yanglao*; LU5: *Chize*; PC3: *Quze*; HT3: *Shaohai*; LI15: *Jianyu*; SI9: *Jianzhen*; LR4: *Zhongfeng*; SP9: *Yinlingquan*; GB30: *Huantiao*; BL36: *Chengfu*; BVA: bee venom acupuncture; PIGD: postural instability and gait disturbance; PDQL: Parkinson's Disease Quality of Life Questionnaire; ST42: *Chongyang*; SP3: *Taibai*; LI20: *Yingxiang*; ST7: *Xiaguan*.

Table 2: The neuroprotective mechanisms of acupuncture in the treatment of Parkinson's disease.

Study	PD model	Intervention	Acupoints	Acupuncture parameters	Behavioral measurements	Biochemical measurements
Hong et al. (2010) [49]	MPTP mice	MA	GB34	Turned at a rate of two spins per second for 15 s	—	Grm5↓, Itpr1↓, Itpr2↓, Pde1c↓, Prkcb1↓, Plcb4↓, Atp2b3↓, Slc8a3↑, Htr5a↑, Adcy1↑, Drd5↓, Npy1r↓, Gpr156↓, Cxcl10↓, Rxfp2↑, Agtrl1↑, Inhbb↓, Cxcl5↓, IL21↓, Cox6a1↓, Uqcrq↓, Ndufc1↓, Atp5e↓, Mapt↓, Ngfr↓, Nefh↓
Choi et al. (2011) [50]	MPTP mice	MA	GB34, LR3	Turned at a rate of two spins per second for 15 s	—	TH levels in the ST and the SNpc↑, DAT↑, Ctla2a↓, EG383229↓, Ppbp↓, Ube2l6↓, EG665033↑, ENSMUSG00000055323↑, Obox6↑, Pbp2↑, Tmem150↑
Yeo et al. (2013) [51]	MPTP mice	MA	GB34, LR3	Turned at a rate of two spins per second for 15 s	—	TH in the ST, SNpc, and thalamus↑, Dusp4↑, Mafg↑, Pgm5↑, Ndph↑, Dnase1l2↑, Ucp2↓, Sp2↓, Serinc2↓
Yeo et al. (2015) [39]	MPTP mice	MA	GB34, LR3	Turned at a rate of two spins per second for 15 s	—	TH in the ST and SNpc↑, Cdh1↓, Slc6a13↓, Tph2↓, Mpzl2↓, Serping1↓, Itih2↓, Slc6a20a↓, Slc6a4↓, Ucma↓, Rdh9↓, 4921530L21Rik↑, Gm13931↑
Jeon et al. (2008) [52]	MPTP mice	EA	GB34	2/100 Hz, 1 mA for 20 minutes	Pole test: time on the pole↓	TH-positive cells in the SN↑, CyPA in the SN↑, MBP↑, Ube2N↑, LMP6↑, LMP2↑, lipocalin/cytosolic fatty acid-binding protein↑, eIF5A↑, CLP↑, ATPase, H1-transporting V1 subunit F↑, NSF↑
Wang et al. (2013) [53]	MPTP mice	EA	ST36, SP6	0/100 Hz, 1-1.25-1.5 mA for 30 minutes	Open-field test: total movement time↓, movement velocity↓, total movement distance↓	—
Kim et al. (2005) [54]	6-OHDA rats	MA	ST36	Left in acupoint for 20 minutes	Rotational behavior test: the average net number of turns/min↓	The survival rate of TH-positive neurons↑, the density of TH-positive fibers↑
Yang et al. (2011) [55]	MPTP mice	RA/EA	PC7	Left in acupoint for 15 minutes/2 and 15 Hz, alternatively, 1 mA for 15 minutes	Pole test: descending time↓	TH-positive neurons (RA)↑, DA in the SN↓, the intensity of radionuclide or radiopharmaceutical uptake (RA)↑, the peak time of [^{123}I]IBZM uptake (RA)↓, HVA concentration in the SN (EA)↓
Yeo and Lim (2019) [56]	MPTP mice	MA	GB34, LR3	Turned at a rate of two spins per second for 15 s	—	TH in the ST and SNpc↑, α-syn in the SN↓, SGK1↑
Yeo et al. (2020) [57]	MPTP mice	MA	GB34, LR3	Turned at a rate of two spins per second for 15 s	—	TH in the ST and SNpc↑, α-syn in the ST and SN↓, p-α-syn 32↓, p-α-syn 16↓, p-α-syn 32/total α-syn values↑
Tian et al. (2016) [58]	MPTP mice	MA	GB34	Turned at a rate of two spins per second for 15 s, retained for 10 minutes	Rotarod test: the ORP scores↑	α-syn in the SNpc↓, autophagosome accumulation↓, LC3-II↓, LAMP1↓, the number and function of DA neurons↑,

Table 2: Continued.

Study	PD model	Intervention	Acupoints	Acupuncture parameters	Behavioral measurements	Biochemical measurements
						density of TH-positive neurons in the SNpc and ST↑, DA concentration↑, synaptophysin protein↑
Wang et al. (2018) [59]	Rotenone rats	Moxibustion	ST36, CV4, GV16	Placed 2-3 cm above each acupoint, retained for 10 minutes	Behavioral scoring [60]↓	TH-immunoreactive neurons↑, α-syn-positive aggregates↓, p-mTOR and p-p70S6K in the SNpc↓, LC3-II in the SNpc↑
Song et al. (2020) [37]	MPTP mice	Acupoint injection	ST36	Choroid plexus cells were injected into ST36, a depth of 3 mm, maintained for 1 week	Pole test: exercise capacity↑	TH in the SNpc↑, Bax↓, cytochrome C↓, BCL-2↑, COX-2↓, iNOS↓
Park et al. (2015) [61]	MPTP mice	MA	GB34	Turned at a rate of two spins, per second for 15 s	Rotarod test: latency time↑; cylinder test: the number of wall touches↑	TH-positive neurons in the SN↑, TH-positive fibers↑, 40 of 76 differentially expressed genes are involved in the p53 signaling network
	MPTP +P53 knockout mice	MA	GB34	Turned at a rate of two spins, per second for 15 s	—	TH-positive cells and fibers slightly↑
Doo et al. (2010) [62]	MPTP mice	BVA	GB34	—	—	TH-positive neurons in the SN↑, DA fibers in the ST↑, p-c-Jun-positive cells in the SN↓
Liang et al. (2002) [63]	MFB rats	EA	GV14, GV20	2/100 Hz, 1-2-3 mA for 30 minutes	—	TH-positive neurons on the lesion side↑, BDNF mRNA expression on the lesioned side of the VTA (100 Hz)↑, BDNF mRNA in the SNpc (100 Hz)↑
Wang et al. (2013) [64]	Rotenone rats	EA	GV16, LR3	100 Hz, 1-1.25-1.5 mA for 30 minutes	—	BDNF mRNA expression in the SN↑, GDNF mRNA expression in the SN↑
Liang et al. (2003) [48]	MFB rats	EA	GV14, GV20	2/100 Hz, 1-2-3 mA for 30 minutes	Rotational behavior test: day 14 the average net number of turns/min↓, day 28 the average net number of turns/min (100 Hz)↓	GDNF mRNA-positive cells in the SNpr (100 Hz)↑, GDNF mRNA expression in the GP of the unlesioned side (2 Hz)↑, GDNF mRNA level in both the lesioned and unlesioned side of GP (100 Hz)↑
Jang et al. (2020) [65]	MPTP mice	MA	GB34, ST36	Turned at a rate of two spins per second for 30 s	Cylinder test: the number of wall touches↑; rotarod test: latency time↑; akinesia test: latency time↓; open-field test: the total distance↑, central distance↑, the ratio of central/total distance↑, the number of crossings in the central zone↑	Dopaminergic fibers and neurons in the ST and SN↑, TH-positive neurons in the ST and SN↑, TH in the ST and SN↑, Bax↓, Bcl-2↑, GFAP↓, Iba-1↓, NF-κB↓, TNF-α↓, the Chao1 index↑, the number of observed OTUs↑, the Shannon index↑, Rikenellaceae↑, Vallitaleaceae↑, Alistipes↑, Vallitalea↑, Lachnoclostridium↑, Pseudoclostridium↑, Bacteroides xylanolyticus↑, Vallitalea pronyensis↑, Clostridium aerotolerans↑, Pseudoclostridium

Table 2: Continued.

Study	PD model	Intervention	Acupoints	Acupuncture parameters	Behavioral measurements	Biochemical measurements
						thermosuccinogenes↑, Roseburia faecis↑, holdemania↓, frisingicoccus↓, aestuariispira↓, sporobacter↓, rhodospirillum↓, Bifidobacterium↓, turicibacter↓, marvinbryantia↓, desulfovibrio↓, phascolarctobacterium↓, erysipelatoclostridium↓, butyricimonas↑, gracilibacter↑, phocea↑, desulfitobacterium↑, oscillibacter↑, acutalibacter↑, flintibacter↑, photosynthesis↑, glutathione metabolism↑, tetracycline biosynthesis↑, photosynthetic proteins↑, methane metabolism↓, drug metabolism↓
Park et al. (2003) [66]	6-OHDA rats	MA	Acu1: GB34, LR3; Acu2: LI4, LI11	Turned at a rate of two spins per second for 15 s, retained for 60 s	Rotational behavior test: the average net number of turns/min (Acu1)↓	TH-immunoreactive neurons in the ipsilateral SN (Acu1)↑, TH-immunoreactive terminals in the dorsolateral ST ipsilateral to the lesion (Acu1)↑, TrkB-positive cells in the SN (Acu1)↑
Lin et al. (2017) [67]	MPTP rats	EA	GB34, LR3	0/50 Hz, 1 mA for 20 minutes	Rotarod test: day 9 latency time↑; rotational behavior test: the average net number of turns/min↓	DA content in the ST↑, TH-positive neurons in the SN↑, degeneration in the ST↓, DA depletion in the ipsilateral side↓, mature BDNF, Bcl-2 and TH levels in the ipsilateral side↑, pAkt↑
Zhao et al. (2019) [68]	MFB rats	EA	GV20, GV29	2 Hz, 1.5 mA for 10 minutes	Rotarod test: latency time↑; tail suspension test: the immobility time↓	TH in the midbrain↑, BDNF$^+$ cells↑, pAkt↑, pERK↑, functional TrkB FL↑, the ratio of TrkB FL/TrkB T1↑
	MFB rats	EA+K252a injection	GV20, GV29	2 Hz, 1.5 mA for 10 minutes	Rotarod test: latency time↓; tail suspension test: the immobility time↑	TH in the midbrain↓, BDNF$^+$ cells↓, pAkt↓, pERK1/2↓
Kim et al. (2011) [69]	MPTP mice	MA	GB34	Turned at a rate of two spins per second for 15 s	Rotarod test: latency time↑, the ORP scores↑	pAkt↑
	MPTP mice	MA +LY294002	GB34	Turned at a rate of two spins per second for 15 s	Rotarod test: latency time↓, the ORP scores↓	pAkt↓, TH-positive dopaminergic neurons in SN↓, TH-positive dopaminergic fibers in ST↓
Hwang et al. (2019) [70]	MPTP mice	MA +Chunggan formula	GB34	Turned at a rate of two spins per second for 30s	Rotarod test: latency time↑; cylinder test: the number of wall touches↑; pole test: descending times↓	TH-positive dopaminergic neurons in the SNpc↑, TH protein in the SNpc and ST↑, pIκBα↓, pAkt↑, pGSK3β↑, pERK↑, pCREB↑, BDNF↑
Jeon et al. (2017) [71]	MPTP mice	MA	Acu1: GB34; Acu2: HT7	Turned at a rate of two spins per second for 30 s	Pole test: day 5 descending times (GB34)↓, day 12 descending times↓	TH-positive cells in the SN (GB34)↑, TH immunoreactivity in the ST (GB34)↑, BrdU-positive cells in the SVZ (GB34)↑,

Table 2: Continued.

Study	PD model	Intervention	Acupoints	Acupuncture parameters	Behavioral measurements	Biochemical measurements
						BrdU/DCX-double stained cells in the SVZ↓, BrdU/GFAP-double stained cells in the SVZ (GB34)↑, GFAP-positive cells in the ST↑
Yu et al. (2010) [38]	6-OHDA rats	MA	GB34, LR3, ST36, SP10	Left in acupoints for 20 minutes	Rotational behavior test: the average net number of turns/min↓	SOD↑, GSH-Px↑, GSH↑, MDA↓
Wang et al. (2011) [47]	MPTP mice	EA	ST36, SP6	0/100 Hz, 1-1.25-1.5 mA for 30 minutes	—	TH immunoreactivity↑, day 3 DA, DOPAC, and HVA in the ST↑, H_2O_2 content in the ST↓, day 3 GSH content↑, days 3 and 7 GSH-Px↓, days 7 and 14 SOD activity↑, day 7 MDA content in the ST↓
Lee et al. (2018) [72]	MPTP mice	MA	Acu1: GB34; Acu2: SI3	Turned at a rate of two spins per second for 30 s	Pole test: descending times (GB34)↓	TH-positive neurons in the SN (GB34)↑, caspase-3 in the ST (GB34)↓, DJ-1 in the ST (GB34)↑, SOD activity (GB34)↑, CAT activity (GB34)↑
Kang et al. (2007) [73]	MPTP mice	MA	GB34, LR3	Turned at a rate of two spins per second for 15 s	—	TH-immunoreactive in the ST↑, TH-positive neurons in the SN↑, MAC-1↓, COX-2↓, iNOS↓, DA, DOPAC, and HVA in the ST↑
Li et al. (2019) [74]	6-OHDA rats	MA	CV12, ST25, CV4	Left in acupoints for 15 minutes	Rotational behavior test: the average net number of turns/min↓	TH-positive neurons in the SN↑, TNF-α↓, IL-1β↓, Fe levels↓, ratio of Fpn1/DMT1 mRNA↓, α-syn in the duodenum↓
Yang et al. (2017) [75]	MPTP mice	MA	GB34	Turned at 2 Hz for 15 s	—	NS
Kim et al. (2019) [76]	Pitx3-deficient ak/ak mice	MA+L-DOPA	GB34	Turned at a rate of two spins per second for 15 s	Three-paw dyskinesia test, abnormal three-paw movements↓; AIM scores↓	Pmch↑, Tac2 mRNA↑, Lcn2 mRNA↑
	Pitx3-deficient ak/ak mice	MA+L-DOPA+TC-MCH7c	GB34	Turned at a rate of two spins per second for 15 s	Three-paw dyskinesia test: abnormal three-paw movements↑	—
	6-OHDA mice	MA+L-DOPA	GB34	Turned at a rate of two spins per second for 15 s	AIM scores↓	Pmch↑
Wattanathorn and Sutalangka (2014) [77]	6-OHDA rats	Laser acupuncture	HT7	Continuous blue laser beam, wavelength of 405 nm, output power 100 mW, a spot diameter of 500 μm for 10 minutes	Morris water maze: escape latency (days 7 and 14)↓, retention time (day 14)↑	Neuron density in CA3 and dentate gyrus↑, AChE in the hippocampus↓, MAO-B activity in the hippocampus↓, GSH-Px activity in the right SN↑, MDA in the right SN↓
Park et al. (2017) [78]	MPTP mice	MA	GB34	Turned at a rate of two spins per second for 15 s	Rotarod test: latency time↑; cylinder test: the number of wall touches↑	TH-positive neurons in the SN↑, dopaminergic fibers in the ST↑, Pmch in the hypothalamus↑, double-labeled c-Fos^+/MCH^+ cells↑, MCH concentration in the SN↑, the expression levels of

Table 2: Continued.

Study	PD model	Intervention	Acupoints	Acupuncture parameters	Behavioral measurements	Biochemical measurements
	MPTP mice	MA+TC-MCH7c	GB34	Turned at a rate of two spins per second for 15 s	Rotarod test: latency time↓; cylinder test: the number of wall touches↓	TH and synaptophysin in the SN↑, pAkt↑, and pCREB↑ TH-positive neurons in the SN↓, dopaminergic fibers in the ST↓
	Pitx3$^{-/+}$ mice	MA	GB34	Turned at a rate of two spins per second for 15 s	Rotarod test: latency time↑	—
	Pitx3$^{-/+}$ mice	MA+TC-MCH7c	GB34	Turned at a rate of two spins per second for 15 s	Rotarod test: latency time↓	—
	A53T Tg mice	MA	GB34	Turned at a rate of two spins per second for 15 s	Rotarod test: latency time↑; cylinder test: the number of wall touches↑	pGSK-3β and pAMPK in the SN↑, BDNF expression in the SN↑, synuclein expression in the SN↓

MPTP: 1-methyl-4-phenyl-1,2,3,6-tetrahydropyridine; MA: manual acupuncture; GB34: *Yanglingquan*; Grm5: glutamate receptor metabotropic 5; Itpr1: inositol 1,4,5-triphosphate receptor 1; Itpr2: inositol 1,4,5-triphosphate receptor 2; Pde1c: phospho-diesterase 1C; Prkcb1: protein kinase beta 1; Plcb4: phospholipase C beta 4; Atp2b3: ATPase calcium-transporting plasma membrane 3; Slc8a3: solute carrier family 8, sodium/calcium exchange member 3; Htr5a: 5-hydroxytryptamine (serotonin) receptor 5A; Adcy1: adenylate cyclase 1; Drd5: dopamine receptor 5; Npy1r: neuropeptide Y receptor Y1; Gpr156: G protein-coupled receptor 156; Cxcl10: chemokine (C–X–C motif) ligand 10; Rxfp2: relaxin/insulin-like family peptide receptor 2; Agtrl1: angiotensin receptor-like 1; Inhbb: inhibin beta-B; Cxcl5: chemokine (C–X–C motif) ligand 5; IL21: interleukin 21; Cox6a1: cytochrome c oxidase, subunit VI a, polypeptide 1; Uqcrq: ubiquinol-cytochrome c reductase, complex III subunit VII; Ndufc1: NADH dehydrogenase (ubiquinone) 1, subcomplex unknown, 1; Atp5e: ATP synthase, epsilon subunit; Mapt: microtubule-associated protein tau; Ngfr: nerve growth factor receptor (TNFR superfamily, member 16); Nefh: neurofilament, heavy polypeptide; LR3: *Taichong*; TH: tyrosine hydroxylase; ST: striatum; SNpc: substantia nigra pars compacta; DAT: dopamine transporter; Ctla2a: cytotoxic T lymphocyte-associated protein 2 alpha; EG383229: predicted gene EG383229; Ppbp: proplatelet basic protein; Ube2l6: ubiquitin-conjugating enzyme E2L 6; EG665033: predicted gene EG665033; ENSMUSG00000055323: predicted gene ENSMUSG00000055323; Obox6: oocyte-specific homeobox 6; Pbp2: phosphatidylethanolamine-binding protein 2; Tmem150: transmembrane protein 150; Dusp4: dual specificity phosphatase 4; Mafg: v-maf musculoaponeurotic fibrosarcoma oncogene family, protein G; Pgm5: phosphoglucomutase 5; Ndph: Norrie disease homolog; Dnase1l2: deoxyribonuclease 1-like 2; Ucp2: uncoupling protein 2; Sp2: Sp2 transcription factor; Serinc2: serine incorporator 2; Cdh1: cadherin 1; Slc6a13: solute carrier family 6 (neurotransmitter transporter, GABA), member 13; Tph2: tryptophan hydroxylase 2; Mpzl2: myelin protein zero-like 2; Serping1: the serine (or cysteine) peptidase inhibitor, clade G, member 1; Itih2: interalpha trypsin inhibitor, heavy chain 2; Slc6a20a: SLC6 (neurotransmitter transporter), member 20A; Slc6a4: SLC6 (neurotransmitter transporter, serotonin), member 4; Ucma: upper zone of growth plate and cartilage matrix associated; Rdh9: retinol dehydrogenase 9; 4921530L21Rik: RIKEN cDNA 4921530L21 gene; Gm13931: predicted gene 13931; EA: electroacupuncture; CyPA: cyclophilin A; MBP: myelin basic protein; Ube2N: ubiquitin-conjugating enzyme E2N; LMP6: proteasome subunit C7-I; LMP2: 20S proteasome subunit; eIF5A: eukaryotic translation initiation factor 5A; CLP: coactosin-like protein; NSF: N-ethylmaleimidesensitive fusion protein; ST36: *Zusanli*; SP6: *Sanyinjiao*; 6-OHDA: 6-hydroxydopamine; LI4: *Hegu*; RA: retained acupuncture; PC7: *Daling*; DA: dopamine; [^{123}I] IBZM: [^{123}I] iodobenzamide; HVA: homovanillic acid; α-syn: α-synuclein; SGK1: serum/glucocorticoid-regulated kinase 1; p-α-syn: phosphorylated α-synuclein; ORP: overall rod performance; LC3-II: microtubule-associated protein 1 light chain 3 II; LAMP1: lysosome-associated membrane protein 1; CV4: *Guanyuan*; GV16: *Fengfu*; p-mTOR: phosphorylated mammalian target of rapamycin; p-p70S6k: phosphorylated ribosomal protein S6 kinase; BVA: bee venom acupuncture; Bax: Bcl-2-associated X protein; MDA: malondialdehyde; GSH: glutathione; TNF-α: tumor necrosis factor-α; IL-1β: interleukin-1β; Bcl-2: B cell lymphoma-2; GFAP: glial fibrillary acidic protein; Iba-1: ionized calcium-binding adaptor molecule-1; NF-κB: nuclear factor kappa-B; OTUs: operational taxonomic units; COX-2: cyclooxygenase; iNOS: inducible NO synthase; p-c-Jun: phosphorylated c-Jun kinase; MFB: medial forebrain bundle; GV14: *Dazhui*; GV20: *Baihui*; BDNF: brain-derived neurotrophic factor; VTA: ventral tegmental area; GDNF: glial cell-derived neurotrophic factor; SNpr: substantia nigra pars reticulata; GP: globus pallidus; LI11: *Quchi*; TrkB: tyrosine kinase receptor B; GV29: *Yintang*; PKB/Akt: protein kinase B; p-Akt: phosphorylated Akt; pERK: phosphorylated extracellular-regulated protein kinase; TrkB FL: full-length TrkB; TrkB T1: splicing truncated isoforms TrkB; pIκBα: phosphorylated inhibitor kappa B alpha; pGSK3β: phosphorylated glycogen synthase kinase 3β; pCREB: phosphorylated cAMP-response element-binding protein; HT7: *Shenmen*; BrdU: 5-bromo-2′-deoxyuridine; SVZ: subventricular zone; DCX: doublecortin; SP10: *Xuehai*; SOD: superoxide dismutase; GSH-Px: glutathione peroxidase; DOPAC: dihydroxyphenylacetic acid; SI3: *Houxi*; CAT: catalase; MAC-1: macrophage antigen complex-1; CV12: *Zhongwan*; ST25: *Tianshu*; Fpn1: ferroportin1; DMT1: recombinant divalent metal transporter 1; NS: no significance; L-DOPA: levodopa; AIM: abnormal involuntary movement; Pmch: pro-melanin-concentrating hormone; Tac2: tachykinin 2; Lcn2: lipocalin 2; CA3: the CA3 region of the hippocampus; AChE: acetyl cholinesterase; MAO-B: monoamine oxidase-B; MCH: melanin-concentrating hormone; pAMPK: phosphorylated cAMP-response phosphorylated adenosine 5-monophosphate-activated protein kinase.

and UB23 (*Shenshu*) are stimulated for low back pain; BL15 (*Xinshu*), LR3, and SP6 (*Sanyinjiao*) points for depression and anxiety; acupoints CV23 (*Lianquan*) and ST4 (*Dicang*) for dysphagia; acupoints SP15 (*Daheng*), ST25 (*Tianshu*), CV6 (*Qihai*), and SJ6 (*Zhigou*) for constipation; acupoints CV11 (*Jianli*) and P6 (*Neiguan*) for fullness in the chest and epigastrium; and LR3, KI7, and BL18 (*Ganshu*), BL15, GB34, and UB13 (*Feishu*), UB20 (*Pishu*), and CV6 for hot flashes and paroxysmal sweating.

Taken together, a host of clinical studies have shown that acupuncture is beneficial for PD patients, especially for reducing the required dose of medication and related side effects [41]. However, there are several limitations in current acupuncture studies. First, outcome measures of most studies are subjective and vulnerable to potential biases, potentially reducing the credibility of the efficacy of acupuncture. Second, only few articles have defined acupoints according to different pathological stages or symptoms. Appropriate acupoints should be added according to different symptoms of patients. Third, the acupuncture protocol and stimulating parameters differ between trials. In the future, research on acupuncture treatment for PD should be carried out with higher methodological quality, optimized acupoint selection, frequency, duration, and study of long-term effects.

4. Mechanism of Acupuncture Protecting from Dopaminergic Neurodegeneration

Extensive studies have shown that genetic predisposition [42], environmental factors [43], and a variety of intracellular and extracellular pathogenic factors contribute to the development of PD, which is characterized by selective loss of dopaminergic neurons in the SN, depletion of dopamine (DA) in the ST, and the formation of Lewy bodies that are mainly composed of α-syn [44]. The reduction of striatal DA levels disrupts the neurotransmitter balance in the basal ganglia and thalamus, resulting in motor symptoms such as paralysis agitans, bradykinesia, and rigidity [45]. Loss of DA and changes in neurotransmitters such as serotonin (5-HT), norepinephrine (NE), γ-aminobutyric acid (GABA), and glutamate (Glu) in different brain regions and the peripheral nervous system lead to the occurrence of nonmotor symptoms, such as autonomic nervous dysfunction, neuropsychiatric disorders, sleep disorders, and gastrointestinal symptoms [46].

After reviewing 31 basic studies on acupuncture treatment of PD models (Table 2), we found that MA and EA were most commonly utilized, although BVA, moxibustion, acupoint injection, and laser acupuncture were also reported. It is worth mentioning that EA at high frequencies shows better efficacy than low frequencies in some animal models of PD [47, 48]. The most commonly selected acupoint was GB34 followed by LR3. Thirty studies showed that acupuncture improves motor function in PD models as assessed by the rotarod test, the cylinder test, and the pole test. Basic studies suggest that acupuncture may achieve its effectiveness for PD treatment by preventing the DA neurons from α-syn aggregation, apoptosis, oxidative stress, and modulating neuroinflammation and the basal ganglia circuit around DA neurons, which we have outlined in detail below.

4.1. α-Synuclein Aggregation. During the pathogenesis of PD, soluble α-syn monomers are thought to progressively aggregate to large insoluble α-syn fibrils, called Lewy bodies [79]. Overproduction and aggregation of α-syn furthermore induces mitochondrial dysfunction, oxidative stress, and neuroinflammation, leading to damage of dopaminergic neurons in the SN and ST.

It is suggested that acupuncture may inhibit increased levels of α-syn for its neuroprotective effects. Serum/glucocorticoid-regulated kinase 1 (SGK1) is a serine threonine-specific protein kinase which may regulate α-syn. Yeo and Lim [56] found that acupuncture at GB34 and LR3 upregulated SGK1 and inhibited an α-syn increase. In SGK1 siRNA knockdown SH-SY5Y cells, the authors observed a downregulation of SGK1 in dopaminergic neurons along with an increase in α-syn expression, suggesting that acupuncture may inhibit the increase of α-syn expression by downregulation of SGK1. Other research shows that overexpression of SGK1 exerts neuroprotective functions by reducing the production of reactive oxygen species (ROS) and mitochondrial dysfunction [80]. It has been reported that in the process of α-syn aggregation, phosphorylation at serine 129 increases the neurotoxicity of α-syn. A previous study has shown that acupuncture suppressed α-syn levels in the SN and ST and inhibits increased levels of p-α-syn 32 and p-α-syn 16 at serine 129 in the nigral dopaminergic neurons, providing evidence that acupuncture may reduce neurotoxicity via inhibiting the level of α-syn and p-α-syn, thereby protecting dopaminergic neurons [57].

Acupuncture has also been demonstrated to promote the degradation of α-syn by restoring autophagy. Autophagy is essential for the removal of toxic α-syn aggregates in order to maintain intracellular homeostasis [81]. Mammalian target of rapamycin (mTOR) is a negative regulator of cellular autophagy and it has been shown that 1-methyl-4-phenyl-1,2,3,6-tetrahydropyridine (MPTP) upregulates microtubule-associated protein 1 light chain 3 II (LC3-II) in a PD model, while downregulation lysosomal-associated membrane protein 1 (LAMP1, lysosomal structural protein) indicates that an impairment of lysosomes and the interruption of autophagosome-lysosome fusion may lead to an accumulation of autophagosomes in the substantia nigra pars compacta (SNpc) of MPTP mice [58]. Tian et al. observed that after acupuncture treatment for 4 days, LC3-II was reduced by approximately 40% and LAMP1 by approximately 20%, and more than 50% of α-syn in the SNpc was cleared, suggesting that acupuncture at GB34 restores lysosomal structures and reduces the accumulation of autophagosomes, enhancing the clearance of autophagosomes and degradation of α-syn. This group further found that acupuncture did not change levels of upstream proteins of lysosomal autophagy system (LAS), p-mTOR, p-p70s6k, and ULK1, which indicated that acupuncture activates the independent mTOR pathway to enhance the autophagic clearance of α-syn. After activation of mTOR, p70S6K and 4E-binding protein 1 (4E-BP1) are activated to form p-p70S6K and p-4E-BP1, which then inhibit autophagy. Wang et al. [59] found that moxibustion at ST36, CV4 (*Guanyuan*), and GV16 (*Fengfu*) decreased p-mTOR, p-p70s6k and α-syn levels while increasing LC3-II levels, suggesting moxibustion exerts neuroprotective effects by promoting clearance of α-syn and enhancing autophagy via the mTOR pathway. As rapamycin (mTOR antagonist) treatment results in considerable side effects in PD patients such as dyslipidemia, antiproliferative toxicity, and renal dysfunction [82], acupuncture may represent as the alternative strategy to target mTOR.

4.2. Apoptosis. It is established that nigral dopaminergic neurons in PD patients undergo apoptosis and the formation of apoptotic bodies [83]. Acupuncture may possess antiapoptosis properties via blocking apoptosis pathways of dopaminergic neurons. BVA has been found to decrease caspase-3 activity and downregulate caspase-3 and Bax gene expression, suggesting that it may inhibit the mitochondrion-dependent apoptotic pathway of dopaminergic neurons [84]. MA and acupoint injection exhibited similar effects: MA or acupoint injection at ST36 has been shown to downregulate Bax, cytochrome C, and upregulate Bcl-2 [65]. Park et al. [61] found that p53 may be involved in the neuroprotective effect of acupuncture: 40 of 76 differentially expressed genes following acupuncture were involved in the p53 signaling network, and conditionally knocking down p53 pathway genes in midbrain dopaminergic neurons attenuated the neuroprotective effect of acupuncture. The c-Jun N-terminal

kinase (JNK) signaling may mediate apoptosis through phosphorylation of c-Jun [85]. Doo et al. [62] observed that BVA at GB34 can rescue dopaminergic neurons from apoptosis by inhibiting c-Jun activation in MPTP mouse, while another study suggested that MA at GB34 does not change p-c-Jun levels [69]. Therefore, the effects of different acupuncture stimulation methods on JNK need to be further clarified.

Several reports have established neurotrophic factors (NTFs) as a major player in the neuroprotective effects of acupuncture in PD treatment. Liang et al. [63] found that long-term high-frequency EA at GV14 and GV20 effectively prevented the degeneration of ventral dopaminergic neurons and upregulated the levels of brain-derived neurotrophic factor (BDNF) in the ventral subregions of the midbrain, which induced the regeneration of injured dopaminergic neurons. Subsequently, the authors also reported that EA at 2 Hz increased glial cell-derived neurotrophic factor (GDNF) mRNA in both sides of the globus pallidus, and 100 Hz EA increased GDNF mRNA in both sides of the globus pallidus and unlesioned side of SN pars reticulata, speculating that EA could regulate the retrograde transport of GDNF from ganglion to SN and restore the balance of different nuclei in the basal ganglia circuit which contributes to the behavioral improvement of medial forebrain bundle- (MFB-) lesioned rats [48]. Another study confirmed that EA upregulated BDNF and GDNF mRNA in the SN of PD models [64]. Tyrosine kinase receptor B (TrkB) is a high-affinity BDNF receptor whose activation results in the maintenance of neuronal differentiation and survival [86]. Acupuncture at GB34 and LR3 increases the TrkB expression in the damaged SN of 6-hydroxydopamine- (6-OHDA-) induced PD rats [66]. TrkB consists of different subtypes, including full-length (TrkB FL) and truncated (TrkB T1 or T2) TrkB. TrkB T1 is regarded as a dominant negative form of TrkB, which may suppress the neurotrophic activity of the BDNF/TrkB signaling pathway [87]. Hence, balancing TrkB FL and TrkB T1 is essential for neuroprotection [88]. It has been reported that the TrkB inhibitor (K252A) eliminates the neuroprotective effect of EA, and another study revealed that EA may reverse the imbalance between TrkB FL and TrkB T1 to upregulate p-Akt, p-ERK1/2, and BDNF [68]. 50 Hz EA at GB34 and LR3 has been shown to increase BDNF and downstream p-Akt levels [67], improving rotational behavior in a rat model of unilateral MPP injury, and another study revealed that inhibition of the PI3K/Akt signaling pathway blocked the protective effect of acupuncture on DA neurons [69]. Acupuncture at GB34 combined with KD5040 downregulated pIκBα and upregulated pAkt, pGSK3β, pERK, pCREB, and BDNF, which significantly improve motor function [70]. Therefore, the results presented above suggest that BDNF/TrkB and their downstream signaling pathways may mediate the neuroprotective effects of acupuncture in PD treatment. Besides, acupuncture has been found to increase the number of 5-bromo-2′-deoxyuridine- (BrdU) positive cells and to restore neurogenesis in the subventricular zone [71], which provides a new pathway for studying the molecular mechanisms of acupuncture treatment for PD.

4.3. Oxidative Stress. Aggregation of free radicals causes lipid peroxidation, which leads to excessive oxidation during the process of protein synthesis in DA neurons, destroying the structure of the cellular membrane and ultimately resulting in the death of DA neurons. The neuroprotective effects of acupuncture treatment may be mediated through the regulation of antioxidant systems, as a study reported that MA at GB34, LR3, ST36, and SP10 increases levels of superoxide dismutase (SOD), glutathione (GSH), and glutathione peroxidase (GSH-Px), and decreases levels of malondialdehyde (MDA), along with improved rotarod behavior [38], and similar results were also observed in EA and BVA treatment. For example, high-frequency EA at ST36 and SP6 increases levels of GSH and SOD and decreases striatal H_2O_2 and MDA levels [47]. BVA at GB34 increases GSH and paraoxonase-1 activities and decreases MDA levels [84]. In addition to increased SOD and catalase (CAT) activities, Lee et al. also observed upregulated DJ-1, which exists widely in peripheral tissues, neurons, and glial cells, playing an essential role in antioxidation via regulating the activity of SOD and CAT [72]. It is therefore speculated that the elevation of DJ-1 caused by acupuncture at GB34 may exert antioxidant effects by enhancing the activity of striatal SOD and CAT. These results indicate that acupuncture protects DA neurons from oxidative stress by restoring the balance between oxides and antioxidants.

4.4. Neuroinflammation. Microglia, the primary immune cells of the central nervous system, play a vital role in the neuroinflammation in PD [89]. Injury signaling in degenerated DA neurons can shift microglia to a pro-inflammatory "M1" phenotype, resulting in the release of ROS and cytokines such as tumor necrosis factor-α (TNF-α), interleukin-1β (IL-1β), interleukin-6, and interleukin-12, which exacerbate oxidative stress and inflammation, ultimately leading to DA neuron apoptosis [90]. Inducible nitric oxide synthase (iNOS) expressed in glial cells causes nitric oxide production, which in turn activates microglia in conjunction with various proinflammatory "M1" phenotype cytokines. Acupuncture at GB34 and LR3 has been shown to attenuate the expression of macrophage antigen complex-1, a marker of microglial activation, and mitigate increases in cyclooxygenase-2 (COX-2) and iNOS expression in an MPTP-induced PD models [73]. Similarly, striatal DA levels were shown to increase from 46% to 78% within 7 days, suggesting that acupuncture exerts neuroprotective effects by attenuating MPTP-induced glial activation and neuroinflammation. Injecting choroid plexus cells at ST36 likewise decreased iNOS and COX-2 expression and enhanced exercise capacity of MPTP-induced mice [37], while BVA at GB34 has been suggested to protect dopaminergic neurons by downregulating inflammatory factors such as TNF-α and IL-1β [84].

Acupuncture can also inhibit neuroinflammation by regulating the brain-gut axis, thus alleviating movement dysfunction in PD. An altered gut microbiota has been reported to induce microglial activation and neuroinflammation, which may promote α-syn overexpression and contribute to motor dysfunction in PD models [91]. Jang et al. [65] observed that acupuncture changed the relative abundance of *Butyricimonas*, *Holdemania*, *Frisingicoccus*, *Gracilibacter*, *Phocea*, and *Aestuariispira*, which showed significant

correlations with anxiety as well as motor functions. The authors proposed that acupuncture blocks inflammatory responses and apoptosis as acupuncture increased the levels of DA fibers and neurons in the SN and ST, downregulated glial fibrillary acidic protein, ionized calcium-binding adaptor molecule 1, and nuclear factor kappa B and TNF-α, and restored the conversion of Bax and Bcl-2 expression in the SN and ST. In addition, the PICRUSt-predicted functional analyses based on 16S rRNA taxonomic profiles showed that acupuncture restored physiological functions such as the glutathione and methane metabolism and other PD related pathways. Collectively, the authors postulated that modulation of the gut microbial dysbiosis and inhibition of neuroinflammation may serve as the mechanisms by which acupuncture mitigates dyskinesia and protects dopaminergic neurons in PD. Moreover, acupuncture can promote anti-inflammation by regulating inflammatory factors and the iron homeostasis in the intestine, so as to improve PD motor symptoms. Iron aggregation in the SN is an early feature of PD. Activated microglial cells regulate the import of DMT1 from microglia and downregulate the export of ferritin via FPN1, leading to accumulation of iron in microglia and ultimately damaging neurons [92]. Acupuncture at CV12 (*Zhongwan*), ST25, and CV4 not only reduced α-syn expression in the duodenum and inflammatory factors such as IL-1β and TNF-α in the serum and duodenum but also balanced ferritin import through DMT1 and ferritin export via FPN1 and ultimately reducing iron accumulation in the duodenum and SN [74]. It is worth mentioning that CV12, ST25, and CV4 are acupoints for the treatment of gastrointestinal symptoms, which are thought to inhibit neuroinflammation by influencing the intestinal canal to relieve movement disorders. Acupuncture has been shown to provide additional potential benefits for the brain-gut axis [93], highlighting the brain-gut-neuroinflammation-PD axis as a novel area for research.

5. Neural Circuit Alterations Underlying the Efficacy of Acupuncture Treatment for Parkinson's Disease

The measurement of neural activity provides more direct experimental evidence for the study of the mechanisms involved in the development and treatments of PD. Functional magnetic resonance imaging (fMRI), positron emission tomography (PET), and single-photon emission computed tomography (SPECT) have been used to measure alterations in neural signals caused by acupuncture [94]. The pathological hallmark of PD is the loss of dopaminergic neurons in the SNpc, which leads to insufficient DA projecting to the ST and cerebral cortex and results in abnormal regulation of the neural circuitry of the basal ganglia [95]. Therefore, the functional connectivity of the SN, caudate nucleus, and thalamus, which are all part of the basal ganglia circuit, is impaired in PD patients [96]. Dopaminergic neural pathways, including the basal nuclei, thalamus, and limbic system, are also impaired in animal models of PD [97]. Consequently, Tables 3 and 4 summarize the characteristics of 6 clinical studies and 12 preclinical studies assessing the neural circuit.

5.1. Evidence for Neural Circuit Regulation by Acupuncture Based on Clinical Imaging Studies. Using fMRI imaging, Chae et al. [98] found that acupuncture stimulation of GB34 activated regions associated with intensified motor function as evidenced by increased BOLD signals (the index of brain activation), illustrating that acupuncture may promote the improvement of motor functions in PD patients via the basal ganglia-thalamic-cortical circuit. Furthermore, neural responses of PD patients at resting state were lower than in healthy controls in extensive brain regions including the putamen, thalamus, and supplementary motor area. This variation is secondary to DA deficiency and is related to PD severity [110]. Yeo et al. performed acupuncture stimulation in 12 PD patients and 12 healthy volunteers and compared whole-brain fMRI images of the two groups before and after acupuncture treatment. The authors found that acupuncture at GB34 increased brain activation in regions impaired by PD, such as the SN, caudate, thalamus, and putamen [99], and moreover activated the prefrontal cortex, precentral gyrus, and putamen in PD patients [100]. These results support the hypothesis that PD rehabilitation may be related to modulation of areas associated with PD by GB34 acupuncture stimulation. Besides, the dyskinesia represented by tremor may also be closely related to the activity of the compensatory circuit, in particular the cerebello-thalamo-cortical (CTC) circuit, after the basal ganglia circuit is damaged [111]. Li et al. [101] demonstrated that acupuncture alleviated PD tremor by stimulation and modulation of the cerebellum, thalamus, and motor cortex, in connection with the CTC circuit. Meanwhile, by adjusting neural activity within cognitive brain regions which connect with the CTC circuit, acupuncture may contribute to enhancing movement and improving the daily life activities. The thalamus, originally thought to be a passive transmissive structure for sensory information, plays an indispensable role in the CTC pathway along with the cerebellum and is hypothesized to be involved in movement and balance. Thalamic dysfunction may result in dyspnea with stiffness and tremor as well as nonmotor symptoms [112]. Modulation of the tremor site in the ventral thalamus may help to explain the effectiveness of acupuncture for controlling tremor symptoms [113]. Pathological changes of the basal ganglia are the basis of tremor in PD; however, the direct cause of tremor is the abnormal regulation of the CTC circuit, and the contact points of these two circuits may be located in the motor cortex or other brain locations [114]. Hence, we speculate that the tremor-related neural network may include several brain regions such as the sensorimotor cortex, cerebellum, thalamus, and basal ganglia. Within this network, the neural circuit represented by the basal ganglia and the CTC plays different roles in tremor. The restoration of function of PD patients by acupuncture may involve activation of compensatory brain regions to increase the survival rate of dopaminergic neurons or the activity of DA receptors, and to correct the network imbalance caused by the loss of the dopaminergic neurons in SN [41]. Huang et al. conducted two RCTs using PET

Table 3: The neural circuit mechanisms of acupuncture for Parkinson's disease in clinical researches.

Study	Clinical trial design	Clinical condition	Intervention	Comparison	Acupoints	Acupuncture parameters	Outcomes
Chae et al. (2009) [98]	Controlled trial	PD patients (mild)	Verum acupuncture ($n = 10$)	Covert placebo/overt placebo ($n = 10$)	Left GB34	10 mm, manually rotated clockwise and counterclockwise once per second (1 Hz), 60 seconds, then withdrawn for 120 seconds, only once	The putamen and the primary motor cortex↑, motor function↑ (VA vs. CP)
Yeo et al. (2012) [99]	RCT	Idiopathic PD patients	Acupuncture ($n = 12$)	Acupuncture on healthy participants ($n = 12$)	Right GB34	1 cm, remained in the skin for 1 min and rotated bidirectionally for 1 min, needle remained in the skin without rotation for 1 min and then the pattern of 1 min rotation and 1 min rest was repeated, only once	Neural responses in the SN, caudate, thalamus, and putamen (impaired caused by PD)↑
Yeo et al. (2014) [100]	RCT	Idiopathic PD patients	Acupuncture ($n = 12$)	Acupuncture on healthy participants ($n = 12$)	Right GB34	1 cm, for "stimulated" blocks: rotated bidirectionally at 1 Hz; for "not stimulated" blocks: the needle was only inserted into the skin and then left in place, only once	Neural responses in the prefrontal cortex, precentral gyrus, and putamen in PD patients↑
Li et al. (2018) [101]	Controlled trial	PD patients with tremor	Acupuncture +L-DOPA ($n = 14$)	Sham acupuncture +L-DOPA ($n = 14$)	DU20, bilateral GB20, and the chorea-tremor controlled zone	2-3 cm, reinforcing-reducing method, twirling every 10 minutes, 30 minutes, twice weekly, 12 weeks	Clinical evaluation: UPDRS (II and III) scores↓, neural responses (SN, caudate, thalamus, and putamen)↑
Huang et al. (2010) [102]	RCT	PD patients	Acupuncture +L-DOPA ($n = 5$)	L-DOPA ($n = 5$)	Bilateral MS6, MS4, MS8, MS9, MS14	Continuous wave, 50 Hz, 2-4 mA, 30 minutes, six times a week, 5 weeks	rCBF (the frontal lobe, the occipital lobe, the basal ganglion, and the cerebellum in the most affected hemisphere)↑
Huang et al. (2009) [103]	RCT	PD patients	Acupuncture +Madopar ($n = 5$)	Madopar ($n = 5$)	Bilateral MS6, MS4, MS8, MS9, MS14	Continuous wave, 50 Hz, 2–4 mA, 30 minutes, six times a week, 5 weeks	The glucose metabolisms (parietal, temporal, occipital lobes, the thalamus, and the cerebellum in the light-diseased hemisphere, and in parietal and occipital lobes of the severe-diseased hemisphere)↑

PD: Parkinson's disease; GB34: *Yanglingquan*; VA: verum acupuncture; CP: covert placebo; RCT: randomized controlled trial; SN: substantia nigra; L-DOPA: levodopa; DU20: *Baihui*; GB20: *Fengchi*; UPDRS: Unified Parkinson's Disease Rating Scale; MS6: the anterior oblique line of the vertex to temple; MS4: the lateral line III on forehead; MS8: the lateral line I of the vertex; MS9: the lateral line II of the vertex; MS14: the lower-lateral line of the occipital scalp; rCBF: regional cerebral blood flow.

Table 4: The neural circuit mechanisms of acupuncture for Parkinson's disease in basic researches.

Study	PD model	Intervention	Acupoints	Acupuncture parameters	Behavioral measurements	Biochemical measurements
Zhang et al. (2018) [104]	MPTP rhesus monkeys	EA	ST36, LI4	100 Hz, 3-4-5 mA for 30 minutes	The speed of movement↑, longer performance time of the affected hand↑	The BOLD activations of the caudate nucleus, putamen, M1, cingulate gyrus, and GPe↓
Lee et al. (2013) [97]	MPTP beagle dogs	RA	ST36	Rotated clockwise and counterclockwise to generate *Deqi*	—	The BOLD signal intensity in the ipsilateral parietal lobe, contralateral temporal lobe, basal ganglia, pons, and cerebellum↓
Khalil et al. (2015) [84]	Rotenone rats	BVA	GB34	—	Suspension test: latency time↑; cylinder test: the number of wall touches↑	Caspase-3 activity↓, caspase-3 genes↓, Bax genes↓, DNA damage↓, MDA↓, PON1 activity↑, GSH↑, TNF-α↓, IL-1β↓, DA↑, 5-HT↑, noradrenaline↑
Kim et al. (2011) [36]	MPTP mice	MA	GB34	Turned at a rate of two spins per second for 15 s	Rotarod test: the ORP scores↑	TH-positive neurons in the SN↑, Nissl-positive cells in the SNpc↑, dopaminergic fibers in the ST↑, HVA in the ST↑, dopamine turnover ratios (DOPAC/DA, HVA/DA, and DOPAC +HVA/DA)↑, dopamine efflux in the ST↑, pDARPP-32 at Thr34↓, FosB in the ST↓
Rui et al. (2013) [105]	6-OHDA rats	EA	SP6, GB34, ST36	0/2/100 Hz, 1-3 mA for 30 minutes	Rotational behavior test: the average net number of turns/min (100 Hz)↓	TH-positive neurons on the lesion side (100 Hz)↑, TH-positive dendritic fibers in the ST↑, DAT in the ST and SN (100 Hz)↑, D1R mRNA and protein in the ST (100 Hz)↑, D2R protein (100 Hz) in the ST↓
Jia et al. (2009) [106]	MFB rats	EA	GV14, GV20	0/2/100 Hz, 1-2-3 mA for 30 minutes	Rotational behavior test: the average net number of turns/min (100 Hz)↓	TH-positive neurons in the SN (100 Hz)↑, TH-positive dendritic fibers in the ipsilateral SNpr (100 Hz)↑, substance P content in the SN (100 Hz)↑, GAD67 mRNA↓
Jia et al. (2010) [107]	MFB rats	EA	GV14, GV20	0/2/100 Hz, 1-2-3 mA for 30 minutes	Rotarod test: week 2 treadmill occupancy time (100 Hz)↑	GABA levels in midbrain (100 Hz)↓
Kim et al. (2014) [108]	6-OHDA mice	MA+L-DOPA	GB34	Turned at a rate of two spins per second for 15 s	Cylinder test: the number of wall touches↑; AIM scores↓	FosB in the ST↓, GABA contents in the SNpr↓, Glu levels in the SN↓
Sun et al. (2012) [109]	MFB rats	EA	GV14, GV20	100 Hz, 1-2-3 mA for 30 minutes	Rotarod test: treadmill occupancy time↑; rotational behavior test: the average net number of turns/min↓	TH-positive neurons↑, ACh, Glu in the ST↓

PD: Parkinson's disease; MPTP: 1-methyl-4-phenyl-1,2,3,6-tetrahydropyridine; EA: electroacupuncture; ST36: *Zusanli*; LI4: *Hegu*; M1: primary motor cortex; GPe: globus pallidus externa; RA: retained acupuncture; BVA: bee venom acupuncture; GB34: *Yanglingquan*; Bax: Bcl-2-associated X protein; MDA: malondialdehyde; PON1: paraoxonase-1; GSH: glutathione; TNF-α: tumor necrosis factor-α; IL-1β: interleukin-1β; DA: dopamine; 5-HT: serotonin; MA: manual acupuncture; ORP: overall rod performance; SNpc: substantia nigra pars compacta; ST: striatum; HVA: homovanillic acid; DOPAC: dihydroxyphenylacetic acid; pDARPP-32: phosphorylated dopamine and adenosine 35-monophosphate-regulated phospho-protein; SP6: *Sanyinjiao*; DAT: dopamine transporter dopamine; D1R: D1 receptor; D2R: dopamine D2 receptor; MFB: medial forebrain bundle; GV14: Dazhui; GV20: Baihui; GAD67: glutamate decarboxylase-67; GABA: γ-aminobutyric acid; ACh: acetylcholine; Glu: glutamate.

[103] and SPECT scans [102] to compare the efficacy of EA combined with medication versus medication alone. After 5 weeks of acupuncture, PET scans of the EA+medication group showed an increased glucose metabolism in the temporal lobes, cerebellum, and thalamus of the less-affected hemisphere and in the parietal and occipital lobes of the severe-diseased hemisphere, while these changes were not observed in the medication-only group. The study

highlighted that more brain regions exhibited increased metabolism in the less-affected hemisphere than in the diseased hemisphere and the survival rate of dopaminergic neurons and DA receptor activity were increased, indicating that acupuncture may also affect the number and activity of nigral cells in the less-affected hemisphere [103]. The SPECT study highlighted that regional cerebral blood flow (rCBF) of the frontal and occipital lobes, basal ganglia, and cerebellum in the more severely affected cerebral hemispheres increased, yet DAT levels in the basal ganglia remained unchanged after acupuncture treatment in PD patients, while L-DOPA treatment alone did not affect rCBF, but increased DAT activity in the basal ganglia of the most severely affected cerebral hemispheres [102].

These neuroimaging results illustrate that acupuncture enhances local brain activity and glucose metabolism and improves rCBF, which in turn reactivates both the dysfunctional motor and nonmotor neural circuits, ameliorating symptoms and improving overall quality of life. These neuroimaging quantifications rather than subjective findings helped to further objectively evaluate the effectiveness of acupuncture in PD.

5.2. Experimental Animal Model Studies Investigating the Regulation of the Basal Ganglia Circuit in Parkinson's Disease by Acupuncture. The basal ganglia circuit consists of the ST (caudate and putamen), the globus pallidus (internal and external parts), the subthalamic nucleus, and the SN, which are responsible for motor control, motor learning, emotions, and executive functions [115]. Several neurotransmitters are involved in regulating the function of the basal ganglia circuit. Once DA levels are reduced, the imbalance of DA and acetylcholine (ACh) and disorders of the neurotransmitter system contribute to the development of dyskinesia in PD [116]. GABA is the most predominant inhibitory neurotransmitter in the ST and its downstream nucleus projections are regulated by DA either via dopamine D1 receptor (D1R) or dopamine D2 receptor (D2R). SPECT imaging in PD models revealed that retained acupuncture may attenuate MPTP-induced neuronal injury [55]. Besides, fMRI studies have demonstrated that acupuncture activates the caudate nucleus, putamen, M1, cingulate gyrus, and globus pallidus externa [104], and modulates the ipsilateral parietal lobe, contralateral temporal lobe, basal ganglia, pons, and cerebellum [97], which are closely linked to the basal ganglia circuit.

Acupuncture can improve the motor function in PD models by regulation of neurotransmitters and restoration of the homeostasis of the basal ganglia circuit: first, acupuncture mediates improvements of motor function by directly affecting the dopaminergic system. Kim et al. [36] found that acupuncture improves motor function and protects dopaminergic neurons via increasing DA release, which in turn enhances the availability of DA in the synaptic cleft. Moreover, the authors observed that acupuncture reduces the expression of FosB, a marker of striatal postsynaptic dopamine depletion, and the phosphorylation of DARPP-32, which can affect postsynaptic medium spiny neurons by activating the cAMP signaling pathway. These results raised the possibility that the effects of acupuncture for the amelioration of MPTP-induced dyskinesia are mediated by upregulation of neurotransmission of postsynaptic DA and rebalanced basal ganglia circuit. EA at SP6, GB34, and ST36 with 100 Hz increased the survival of nigral DA neurons and increased the expression of striatal DAT by 253.78%, as well as elevating the levels of D1R mRNA and protein by 81.88% and 62.62%, respectively, while inhibiting increases in the D2R. These results suggested that high-frequency EA may act on both presynaptic DAT and postsynaptic DA receptors, contributing to the balance of basal ganglia output to the thalamus [105].

In terms of the regulation of other neurotransmitters, Jia et al. [106] observed that 100 Hz EA at GV14 and GV20 increased the content of nigral substance P, protected damaged DA neurons from degeneration, and reversed the abnormal elevation of GAD67 mRNA in the midbrain induced by MFB axotomy. Subsequently, the authors further found that EA at high frequency reversed increases in GABA content in the midbrain and alleviated motor coordination in MFB-lesioned rats [107]. These findings suggest that the amelioration of dyskinesia in MFB-lesioned rats may occur via restoration of the homeostasis of dopaminergic transmission and inhibition of the overoutput of GABA in the basal ganglia circuit. Sun et al. [109] reported that high-frequency EA at GV14 and GV20 reduced abnormally elevated levels of Glu and ACh on the lesioned side in the ST, improved motor coordination in MFB-lesioned rats, and protected the nigral DA neurons from degeneration. Furthermore, Glu levels were significantly correlated with the survival ratios of DA neurons in SNpc and rotational behavior, suggesting that alleviation of dyskinesia by EA may involve the downregulation of Glu and ACh in the ST. Another study found that BVA at GB34 may increase the levels of DA, NE, and 5-HT, proposing that the improvement of motor function induced by BVA may be related to increased levels of DA and NE [84].

In addition, acupuncture can also reduce L-DOPA-induced dyskinesia (LID) by regulating neurotransmitters to restore the balance of the basal ganglia circuit. As a precursor of DA, L-DOPA is used to increase DA levels and enhance synaptic DA transmission. However, after approximately 10 years of treatment with L-DOPA, most patients develop side effects, including nonmotor complications such as hallucinations, insomnia, nausea [117], and motor complications including dystonia, chorea, and athetosis, known as LID [118]. Kim et al. [108] observed that L-DOPA at half the typical dose combined with acupuncture can improve motor function. Combination therapy can also restore the levels of GABA and Glu, which are elevated by high-dose L-DOPA. Moreover, FosB expression, an early indicator of LID, is also reduced by combination therapy. These results not only suggest that acupuncture may relieve LID by balancing neurochemicals in the basal ganglia but also demonstrated a possible synergistic effect of acupuncture and L-DOPA.

In a nutshell, it is widely believed that the dysfunction of the basal ganglia circuit induced by the apoptosis of dopaminergic neurons is an essential mechanism in the development and progression of PD. The basal ganglia circuit is regulated

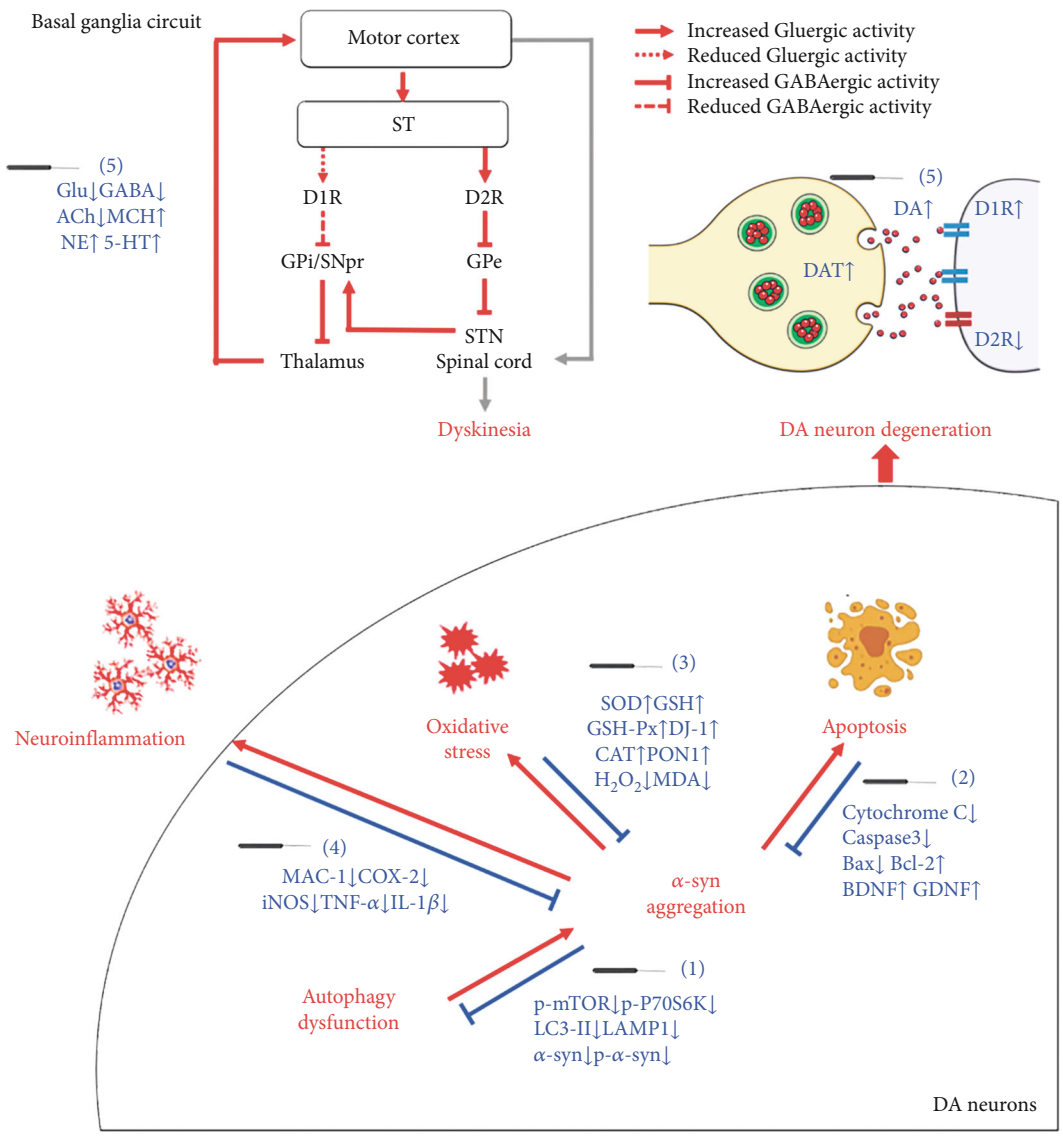

Figure 2: The neuroprotective mechanisms of acupuncture in the treatment of Parkinson's disease. The pathological activities associated with PD include α-syn aggregation, oxidative stress, apoptosis, neuroinflammation, and the disbalance of basal ganglia circuit (red). The key molecules (blue) in the above events are regulated by acupuncture to display neuroprotective effect in PD brain. ACh: acetylcholine; α-syn: α-synuclein; Bax: Bcl-2-associated X protein; Bcl-2: B cell lymphoma-2; BDNF: brain-derived neurotrophic factor; caspase-3: cysteinyl aspartate-specific proteinase-3; CAT: catalase; COX-2: cyclooxygenase-2; DA: dopamine; DAT: dopamine transporter; D1R: dopamine D1 receptor; D2R: dopamine D2 receptor; GABA: γ-aminobutyric acid; GDNF: glial cell-derived neurotrophic factor; Glu: glutamate; GPe: globus pallidus externus; GPi: globus pallidus internus; GSH: glutathione; GSH-Px: glutathione peroxidase; 5-HT: serotonin; IL-1β: interleukin-1β; iNOS: inducible nitric oxide synthase; LAMP1: lysosomal-associated membrane protein 1; LC3-II: microtubule-associated protein 1 light chain 3 II; MAC-1: macrophage antigen complex-1; MCH: melanin concentration hormone; MDA: malondialdehyde; NE: norepinephrine; p-α-syn: phosphorylated α-synuclein; p-mTOR: phosphorylated mammalian target of rapamycin; PON1: paraoxonase-1; p-p70S6k: phosphorylated ribosomal protein S6 kinase; SNpr: substantia nigra pars reticulate; SOD: superoxide dismutase; ST: striatum; STN: subthalamic nucleus; TNF-α: tumor necrosis factor-α.

by various neurotransmitters, and if a part in the circuit is abnormal, the function of the whole circuitry may thus be abnormal. However, since the mechanism of acupuncture for the regulation of the basal ganglia circuit which mediates improvements of PD dyskinesia has not been fully clarified so far, this paper only reviewed the published research so far. Further studies on neuropathology in this field will be beneficial to further increase the objectivity of the evaluation of the efficacy of acupuncture in PD treatment.

6. Conclusion

The effectiveness of acupuncture for PD treatment has been demonstrated by several clinical, preclinical, and basic research studies. Benefits predominantly manifested via the amelioration PD symptoms and the reversal of dopaminergic neurodegeneration in the early stages of PD. The combined application of acupuncture and anti-PD drugs may enhance the therapeutic efficacy of drugs while reducing the required

dose and associated side effects. Acupuncture may protect dopaminergic neurons from degeneration via antioxidative stress, anti-inflammatory, and antiapoptotic pathways, and modulating the neurotransmitter balance in the basal ganglia circuit. As shown in Figure 2, acupuncture can exert protective effects on dopaminergic neurons through multiple pathways: (1) acupuncture reduces the abnormal aggregation of α-syn by inhibiting the production of α-syn and reinstating the autophagic clearance of α-syn; (2) acupuncture inhibits the apoptotic pathways and upregulates the expression of NTFs to activate the downstream PI3K/AKT and MEK/ERK pathways, thus promoting the survival of dopaminergic neurons; (3) acupuncture increases the level of intracellular antioxidants to reduce the oxidative stress response after PD; (4) acupuncture inhibits the activation of microglia and the release of inflammatory factors, and reverses neuroinflammation by regulating intestinal microorganisms; (5) acupuncture regulates DA and other neurotransmitters to reinstate the balance of basal ganglia circuit and exerts a synergistic effect with L-DOPA and other anti-PD drugs. Therefore, acupuncture may represent a novel and effective strategy for the treatment of PD, particularly for halting the degeneration of DA neurons at the early stages of PD to delay PD progression, although this hypothesis needs to be further verified by high-quality basic and clinical research.

Abbreviations

Ach: Acetylcholine
AChE: Acetylcholinesterase
α-syn: α-Synuclein
Bcl-2: B cell lymphoma-2
BDNF: Brain-derived neurotrophic factor
BrdU: 5-Bromo-2′-deoxyuridine
BVA: Bee venom acupuncture
Caspase: Cysteinyl aspartate-specific proteinase
CAT: Catalase
COX-2: Cyclooxygenase-2
CTC: Cerebello-thalamo-cortical
DA: Dopamine
DAT: Dopamine transporter
D1R: Dopamine D1 receptor
D2R: Dopamine D2 receptor
EA: Electroacupuncture
EBM: Evidence-based medicine
4E-BP1: 4E-binding protein 1
fMRI: Functional magnetic resonance imaging
GABA: γ-Aminobutyric acid
GDNF: Glial cell-derived neurotrophic factor
Glu: Glutamate
GSH: Glutathione
GSH-Px: Glutathione peroxidase
5-HT: Serotonin
IL-1β: Interleukin-1β
iNOS: Inducible nitric oxide synthase
JNK: c-Jun N-terminal kinase
LAMP1: Lysosomal-associated membrane protein 1
LAS: Lysosomal autophagy system
LC3-II: Microtubule-associated protein 1 light chain 3 II
L-DOPA: Levodopa
LID: L-DOPA-induced dyskinesia
MA: Manual acupuncture
MAO-B: Monoamine oxidase B
MAs: Meta-analyses
MCH: Melanin concentration hormone
MDA: Malondialdehyde
MFB: Medial forebrain bundle
mTOR: Mammalian target of rapamycin
MPTP: 1-Methyl-4-phenyl-1,2,3,6-tetrahydropyridine
NE: Norepinephrine
NTFs: Neurotrophic factors
6-OHDA: 6-Hydroxydopamine
PD: Parkinson's disease
PET: Positron emission tomography
rCBF: Regional cerebral blood flow
RCTs: Randomized controlled trials
ROS: Reactive oxygen species
SGK1: Serum/glucocorticoid-regulated kinase 1
SN: Substantia nigra
SNpc: Substantia nigra pars compacta
SOD: Superoxide dismutase
SPECT: Single-photon emission computed tomography
SRs: Systematic reviews
ST: Striatum
TNF-α: Tumor necrosis factor-α
TrkB: Tyrosine kinase receptor B
UPDRS: Unified Parkinson's Disease Rating Scale.

Conflicts of Interest

The authors have no competing interests to declare.

Authors' Contributions

Yadan Zhao and Zichen Zhang contributed equally to this work.

Acknowledgments

This work was financially supported by the National Natural Science Foundation of China (NSFC) (No. 82074534, No. 81804186, and No. 81904295) and the Scientific Research Projects of Tianjin Education Commission (2017KJ150).

References

[1] J. Jankovic, "Parkinson's disease: clinical features and diagnosis," *Journal of Neurology, Neurosurgery, and Psychiatry*, vol. 79, no. 4, pp. 368–376, 2008.

[2] F. P. Chen, C. M. Chang, J. H. Shiu et al., "A clinical study of integrating acupuncture and Western medicine in treating patients with Parkinson's disease," *The American Journal of Chinese Medicine*, vol. 43, no. 3, pp. 407–423, 2015.

[3] F. K. Cheng, "The use of acupuncture in patients with Parkinson's disease," *Geriatric Nursing*, vol. 38, no. 4, pp. 302–314, 2017.

[4] S. L. Kowal, T. M. Dall, R. Chakrabarti, M. V. Storm, and A. Jain, "The current and projected economic burden of Parkinson's disease in the United States," *Movement Disorders:*

official journal of the Movement Disorder Society, vol. 28, no. 3, pp. 311–318, 2013.

[5] D. K. Simon, C. M. Tanner, and P. Brundin, "Parkinson disease epidemiology, pathology, genetics, and pathophysiology," *Clinics in Geriatric Medicine*, vol. 36, no. 1, pp. 1–12, 2020.

[6] L. V. Kalia and A. E. Lang, "Parkinson's disease," *The Lancet*, vol. 386, no. 9996, pp. 896–912, 2015.

[7] A. C. Catherine and H. Fox Susan, "Clinical spectrum of levodopa-induced complications," *Movement Disorders*, vol. 30, no. 1, 2015.

[8] H. Noh, S. Kwon, S. Y. Cho et al., "Effectiveness and safety of acupuncture in the treatment of Parkinson's disease: a systematic review and meta-analysis of randomized controlled trials," *Complementary Therapies in Medicine*, vol. 34, pp. 86–103, 2017.

[9] H. J. Kim and B. S. Jeon, "Is acupuncture efficacious therapy in Parkinson's disease?," *Journal of the Neurological Sciences*, vol. 341, no. 1-2, pp. 1–7, 2014.

[10] J. Huang, X. Qin, X. Cai, and Y. Huang, "Effectiveness of acupuncture in the treatment of Parkinson's disease: an overview of systematic reviews," *Frontiers in Neurology*, vol. 11, p. 917, 2020.

[11] J. H. Ko, H. Lee, S. N. Kim, and H. J. Park, "Does acupuncture protect dopamine neurons in Parkinson's disease rodent model?: a systematic review and meta-analysis," *Frontiers in Aging Neuroscience*, vol. 11, p. 102, 2019.

[12] L. Cao, X. Li, M. Li et al., "The effectiveness of acupuncture for Parkinson's disease: an overview of systematic reviews," *Complementary Therapies in Medicine*, vol. 50, p. 102383, 2020.

[13] T. Qiang, C. Gai, Y. Chai et al., "Combination therapy of scalp electro-acupuncture and medication for the treatment of Parkinson's disease: a systematic review and meta-analysis," *Journal of Traditional Chinese Medical Sciences*, vol. 6, no. 1, pp. 26–34, 2019.

[14] Movement Disorder Society Task Force on Rating Scales for Parkinson's Disease, "The Unified Parkinson's Disease Rating Scale (UPDRS): status and recommendations," *Movement Disorders*, vol. 18, no. 7, pp. 738–750, 2003.

[15] M. S. Lee, B. C. Shin, J. C. Kong, and E. Ernst, "Effectiveness of acupuncture for Parkinson's disease: a systematic review," *Movement Disorders: official journal of the Movement Disorder Society*, vol. 23, no. 11, pp. 1505–1515, 2008.

[16] D. D. Webster, "Critical analysis of the disability in Parkinson's disease," *Modern Treatment*, vol. 5, no. 2, pp. 257–282, 1968.

[17] K. Seppi, K. Ray Chaudhuri, M. Coelho et al., "Update on treatments for nonmotor symptoms of Parkinson's disease-an evidence-based medicine review," *Movement Disorders: official journal of the Movement Disorder Society*, vol. 34, no. 2, pp. 180–198, 2019.

[18] I. Subramanian, "Complementary and alternative medicine and exercise in nonmotor symptoms of Parkinson's disease," *International Review of Neurobiology*, vol. 134, pp. 1163–1188, 2017.

[19] H. Lei, N. Toosizadeh, M. Schwenk et al., "A pilot clinical trial to objectively assess the efficacy of electroacupuncture on gait in patients with Parkinson's disease using body worn sensors," *PloS One*, vol. 11, no. 5, article e0155613, 2016.

[20] K. H. Kong, H. L. Ng, W. Li et al., "Acupuncture in the treatment of fatigue in Parkinson's disease: a pilot, randomized, controlled, study," *Brain and Behavior*, vol. 8, no. 1, article e00897, 2018.

[21] B. M. Kluger, D. Rakowski, M. Christian et al., "Randomized, controlled trial of acupuncture for fatigue in Parkinson's disease," *Movement Disorders: official journal of the Movement Disorder Society*, vol. 31, no. 7, pp. 1027–1032, 2016.

[22] S. W. Yu, S. H. Lin, C. C. Tsai et al., "Acupuncture effect and mechanism for treating pain in patients with Parkinson's disease," *Frontiers in Neurology*, vol. 10, p. 1114, 2019.

[23] L. M. Shulman, X. Wen, W. J. Weiner et al., "Acupuncture therapy for the symptoms of Parkinson's disease," *Movement Disorders: official journal of the Movement Disorder Society*, vol. 17, no. 4, pp. 799–802, 2002.

[24] A. Cristian, M. Katz, E. Cutrone, and R. H. Walker, "Evaluation of acupuncture in the treatment of Parkinson's disease: a double-blind pilot study," *Movement Disorders: official journal of the Movement Disorder Society*, vol. 20, no. 9, pp. 1185–1188, 2005.

[25] F. H. Aroxa, I. T. Gondim, E. L. Santos, M. D. Coriolano, A. G. Asano, and N. M. Asano, "Acupuncture as adjuvant therapy for sleep disorders in Parkinson's disease," *Journal of Acupuncture and Meridian Studies*, vol. 10, no. 1, pp. 33–38, 2017.

[26] S. Fukuda, N. Kuriyama, H. Tsuru, and M. Egawa, "Immediate effects of acupuncture on tongue pressure including swallowing reflex latency in Parkinson's disease," *Acupuncture in Medicine: journal of the British Medical Acupuncture Society*, vol. 34, no. 1, pp. 59–61, 2016.

[27] L. Wang, C. He, Y. Liu, and L. Zhu, "Effect of acupuncture on the auditory evoked brain stem potential in Parkinson's disease," *Journal of Traditional Chinese Medicine*, vol. 22, no. 1, pp. 15–17, 2002.

[28] S. Yeo, M. van den Noort, P. Bosch, and S. Lim, "A study of the effects of 8-week acupuncture treatment on patients with Parkinson's disease," *Medicine*, vol. 97, no. 50, article e13434, 2018.

[29] S. Y. Cho, Y. E. Lee, K. H. Doo et al., "Efficacy of combined treatment with acupuncture and bee venom acupuncture as an adjunctive treatment for Parkinson's disease," *The Journal of Alternative and Complementary Medicine: Research on Paradigm, Practice, and Policy*, vol. 24, no. 1, pp. 25–32, 2018.

[30] M. L. Eng, K. E. Lyons, M. S. Greene, and R. Pahwa, "Open-label trial regarding the use of acupuncture and yin tui na in Parkinson's disease outpatients: a pilot study on efficacy, tolerability, and quality of life," *The Journal of Alternative and Complementary Medicine: Research on Paradigm, Practice, and Policy*, vol. 12, no. 4, pp. 395–399, 2006.

[31] K. H. Doo, J. H. Lee, S. Y. Cho et al., "A prospective open-label study of combined treatment for idiopathic Parkinson's disease using acupuncture and bee venom acupuncture as an adjunctive treatment," *The Journal of Alternative and Complementary Medicine: Research on Paradigm, Practice, and Policy*, vol. 21, no. 10, pp. 598–603, 2015.

[32] X. M. Ren, "Fifty cases of Parkinson's disease treated by acupuncture combined with Madopar," *Journal of Traditional Chinese Medicine = Chung i tsa chih ying wen pan*, vol. 28, no. 4, pp. 255–257, 2008.

[33] H. S. Lee, H. L. Park, S. J. Lee, B. C. Shin, J. Y. Choi, and M. S. Lee, "Scalp acupuncture for Parkinson's disease: a systematic review of randomized controlled trials," *Chinese Journal of Integrative Medicine*, vol. 19, no. 4, pp. 297–306, 2013.

[34] P. P. Tang, Q. Xu, D. Chen, L. L. Zhu, Q. H. Wu, and C. Bao, "Effect of scalp acupuncture stimulation on cerebral cortex function and related mechanism," *Zhen ci yan jiu = Acupuncture Research*, vol. 45, no. 6, pp. 504–507, 2020.

[35] T. Wichmann and M. R. DeLong, "Pathophysiology of Parkinson's disease: the MPTP primate model of the human disorder," *Annals of the New York Academy of Sciences*, vol. 991, pp. 199–213, 2003.

[36] S. N. Kim, A. R. Doo, J. Y. Park et al., "Acupuncture enhances the synaptic dopamine availability to improve motor function in a mouse model of Parkinson's disease," *PloS One*, vol. 6, no. 11, article e27566, 2011.

[37] J. Song, S. S. Lee, S. Lim, and S. Yeo, "Mechanism of the neuroprotective effect of injecting brain cells on ST36 in an animal model of Parkinson's disease," *Neuroscience Letters*, vol. 717, p. 134698, 2020.

[38] Y. P. Yu, W. P. Ju, Z. G. Li, D. Z. Wang, Y. C. Wang, and A. M. Xie, "Acupuncture inhibits oxidative stress and rotational behavior in 6-hydroxydopamine lesioned rat," *Brain Research*, vol. 1336, pp. 58–65, 2010.

[39] S. Yeo, K. S. An, Y. M. Hong et al., "Neuroprotective changes in degeneration-related gene expression in the substantia nigra following acupuncture in an MPTP mouse model of parkinsonism: microarray analysis," *Genetics and Molecular Biology*, vol. 38, no. 1, pp. 115–127, 2015.

[40] S. H. Lee and S. Lim, "Clinical effectiveness of acupuncture on Parkinson disease: a PRISMA-compliant systematic review and meta-analysis," *Medicine*, vol. 96, no. 3, article e5836, 2017.

[41] D. Xiao, "Acupuncture for Parkinson's disease: a review of clinical, animal, and functional magnetic resonance imaging studies," *Journal of Traditional Chinese Medicine = Chung i tsa chih ying wen pan*, vol. 35, no. 6, pp. 709–717, 2015.

[42] X. S. Zeng, W. S. Geng, J. J. Jia, L. Chen, and P. P. Zhang, "Cellular and molecular basis of neurodegeneration in Parkinson disease," *Frontiers in Aging Neuroscience*, vol. 10, p. 109, 2018.

[43] X. S. Zeng, W. S. Geng, and J. J. Jia, "Neurotoxin-induced animal models of Parkinson disease: pathogenic mechanism and assessment," *ASN Neuro*, vol. 10, 2018.

[44] V. M. Lee and J. Q. Trojanowski, "Mechanisms of Parkinson's disease linked to pathological α-synuclein: new targets for drug discovery," *Neuron*, vol. 52, no. 1, pp. 33–38, 2006.

[45] F. Blandini, G. Nappi, C. Tassorelli, and E. Martignoni, "Functional changes of the basal ganglia circuitry in Parkinson's disease," *Progress in Neurobiology*, vol. 62, no. 1, pp. 63–88, 2000.

[46] I. Ferrer, "Neuropathology and neurochemistry of nonmotor symptoms in Parkinson's disease," *Parkinson's Disease*, vol. 2011, Article ID 708404, 13 pages, 2011.

[47] H. Wang, Y. Pan, B. Xue et al., "The antioxidative effect of electro-acupuncture in a mouse model of Parkinson's disease," *PloS One*, vol. 6, no. 5, article e19790, 2011.

[48] X. B. Liang, Y. Luo, X. Y. Liu et al., "Electro-acupuncture improves behavior and upregulates GDNF mRNA in MFB transected rats," *Neuroreport*, vol. 14, no. 8, pp. 1177–1181, 2003.

[49] M. S. Hong, H. K. Park, J. S. Yang et al., "Gene expression profile of acupuncture treatment in 1-methyl-4-phenyl-1,2,3,6-tetrahydropyridine-induced Parkinson's disease model," *Neurological Research*, vol. 32, Supplement 1, pp. 74–78, 2010.

[50] Y. G. Choi, S. Yeo, Y. M. Hong, S. H. Kim, and S. Lim, "Changes of gene expression profiles in the cervical spinal cord by acupuncture in an MPTP-intoxicated mouse model: microarray analysis," *Gene*, vol. 481, no. 1, pp. 7–16, 2011.

[51] S. Yeo, Y. G. Choi, Y. M. Hong, and S. Lim, "Neuroprotective changes of thalamic degeneration-related gene expression by acupuncture in an MPTP mouse model of parkinsonism: microarray analysis," *Gene*, vol. 515, no. 2, pp. 329–338, 2013.

[52] S. Jeon, Y. J. Kim, S. T. Kim et al., "Proteomic analysis of the neuroprotective mechanisms of acupuncture treatment in a Parkinson's disease mouse model," *Proteomics*, vol. 8, no. 22, pp. 4822–4832, 2008.

[53] H. Wang, X. Liang, X. Wang, D. Luo, J. Jia, and X. Wang, "Electro-acupuncture stimulation improves spontaneous locomotor hyperactivity in MPTP intoxicated mice," *PloS One*, vol. 8, no. 5, article e64403, 2013.

[54] Y. K. Kim, H. H. Lim, Y. K. Song et al., "Effect of acupuncture on 6-hydroxydopamine-induced nigrostratal dopaminergic neuronal cell death in rats," *Neuroscience Letters*, vol. 384, no. 1-2, pp. 133–138, 2005.

[55] J. L. Yang, J. S. Chen, Y. F. Yang et al., "Neuroprotection effects of retained acupuncture in neurotoxin-induced Parkinson's disease mice," *Brain, Behavior, and Immunity*, vol. 25, no. 7, pp. 1452–1459, 2011.

[56] S. Yeo and S. Lim, "Acupuncture inhibits the increase in alpha-synuclein by modulating SGK1 in an MPTP induced parkinsonism mouse model," *The American Journal of Chinese Medicine*, vol. 47, no. 3, pp. 527–539, 2019.

[57] S. Yeo, J. Song, and S. Lim, "Acupuncture inhibits the increase in alpha-synuclein in substantia nigra in an MPTP-induced parkinsonism mouse model," *Advances in Experimental Medicine and Biology*, vol. 1232, pp. 401–408, 2020.

[58] T. Tian, Y. Sun, H. Wu et al., "Acupuncture promotes mTOR-independent autophagic clearance of aggregation-prone proteins in mouse brain," *Scientific Reports*, vol. 6, no. 1, p. 19714, 2016.

[59] S. J. Wang, Q. Wang, J. Ma, P. H. Yu, Z. M. Wang, and B. Wang, "Effect of moxibustion on mTOR-mediated autophagy in rotenone-induced Parkinson's disease model rats," *Neural Regeneration Research*, vol. 13, no. 1, pp. 112–118, 2018.

[60] X. Chen, N. Zhang, H. Zhao et al., "The protect effect of baicalin on the substantial nigra dopaminergic neuron in Parkinson's rats induced by rotenone," *Zhongfeng yu Shenjing Jibing Zazhi*, vol. 2, pp. 174–177, 2008.

[61] J. Y. Park, H. Choi, S. Baek et al., "p53 signalling mediates acupuncture-induced neuroprotection in Parkinson's disease," *Biochemical and Biophysical Research Communications*, vol. 460, no. 3, pp. 772–779, 2015.

[62] A. R. Doo, S. T. Kim, S. N. Kim et al., "Neuroprotective effects of bee venom pharmaceutical acupuncture in acute 1-methyl-4-phenyl-1,2,3,6-tetrahydropyridine-induced mouse model of Parkinson's disease," *Neurological Research*, vol. 32, Supplement 1, pp. 88–91, 2010.

[63] X. B. Liang, X. Y. Liu, F. Q. Li et al., "Long-term high-frequency electro-acupuncture stimulation prevents neuronal degeneration and up-regulates BDNF mRNA in the substantia nigra and ventral tegmental area following medial forebrain bundle axotomy," *Brain Research. Molecular Brain Research*, vol. 108, no. 1-2, pp. 51–59, 2002.

[64] S. Wang, J. Fang, J. Ma et al., "Electroacupuncture-regulated neurotrophic factor mRNA expression in the substantia nigra

of Parkinson's disease rats," *Neural Regeneration Research*, vol. 8, no. 6, pp. 540–549, 2013.

[65] J. H. Jang, M. J. Yeom, S. Ahn et al., "Acupuncture inhibits neuroinflammation and gut microbial dysbiosis in a mouse model of Parkinson's disease," *Brain, Behavior, and Immunity*, vol. 89, pp. 641–655, 2020.

[66] H. J. Park, S. Lim, W. S. Joo et al., "Acupuncture prevents 6-hydroxydopamine-induced neuronal death in the nigrostriatal dopaminergic system in the rat Parkinson's disease model," *Experimental Neurology*, vol. 180, no. 1, pp. 93–98, 2003.

[67] J. G. Lin, C. J. Chen, H. B. Yang, Y. H. Chen, and S. Y. Hung, "Electroacupuncture promotes recovery of motor function and reduces dopaminergic neuron degeneration in rodent models of Parkinson's disease," *International Journal of Molecular Sciences*, vol. 18, no. 9, p. 1846, 2017.

[68] Y. Zhao, D. Luo, Z. Ning, J. Rong, and L. Lao, "Electro-acupuncture ameliorated MPTP-induced parkinsonism in mice via TrkB neurotrophic signaling," *Frontiers in Neuroscience*, vol. 13, p. 496, 2019.

[69] S. N. Kim, S. T. Kim, A. R. Doo et al., "Phosphatidylinositol 3-kinase/Akt signaling pathway mediates acupuncture-induced dopaminergic neuron protection and motor function improvement in a mouse model of Parkinson's disease," *The International Journal of Neuroscience*, vol. 121, no. 10, pp. 562–569, 2011.

[70] T. Y. Hwang, M. A. Song, S. Ahn et al., "Effects of combined treatment with acupuncture and Chunggan formula in a mouse model of Parkinson's disease," *Evidence-Based Complementary and Alternative Medicine: ECAM*, vol. 2019, article 3612587, 14 pages, 2019.

[71] H. Jeon, S. Ryu, D. Kim, S. Koo, K. T. Ha, and S. Kim, "Acupuncture stimulation at GB34 restores MPTP-induced neurogenesis impairment in the subventricular zone of mice," *Evidence-Based Complementary and Alternative Medicine: ECAM*, vol. 2017, article 3971675, 9 pages, 2017.

[72] Y. Lee, G. Choi, H. Jeon et al., "Acupuncture stimulation at GB34 suppresses 1-methyl-4-phenyl-1,2,3,6-tetrahydropyridine-induced oxidative stress in the striatum of mice," *The Journal of Physiological Sciences: JPS*, vol. 68, no. 4, pp. 455–462, 2018.

[73] J. M. Kang, H. J. Park, Y. G. Choi et al., "Acupuncture inhibits microglial activation and inflammatory events in the MPTP-induced mouse model," *Brain Research*, vol. 1131, no. 1, pp. 211–219, 2007.

[74] L. Li, J. Lu, Y. Sun, and X. Jin, "Acupuncture protects from 6-OHDA-induced neuronal damage by balancing the ratio of DMT1/Fpn1," *Saudi Journal of Biological Sciences*, vol. 26, no. 8, pp. 1948–1955, 2019.

[75] H. J. Yang, Y. Gao, J. Y. Yun et al., "Acupuncture does not protect against 1-methyl-4-phenyl-1,2,3,6-tetrahydropyridine-induced damage of dopaminergic neurons in a preclinical mouse model of Parkinson's disease," *Neuroreport*, vol. 28, no. 1, pp. 50–55, 2017.

[76] Y. K. Kim, A. R. Lee, H. Park et al., "Acupuncture alleviates levodopa-induced dyskinesia via melanin-concentrating hormone in Pitx3-deficient aphakia and 6-hydroxydopamine-lesioned mice," *Molecular Neurobiology*, vol. 56, no. 4, pp. 2408–2423, 2019.

[77] J. Wattanathorn and C. Sutalangka, "Laser acupuncture at HT7 acupoint improves cognitive deficit, neuronal loss, oxidative stress, and functions of cholinergic and dopaminergic systems in animal model of Parkinson's disease," *Evidence-Based Complementary and Alternative Medicine: ECAM*, vol. 2014, article 937601, 8 pages, 2014.

[78] J. Y. Park, S. N. Kim, J. Yoo et al., "Novel neuroprotective effects of melanin-concentrating hormone in Parkinson's disease," *Molecular Neurobiology*, vol. 54, no. 10, pp. 7706–7721, 2017.

[79] W. Poewe, K. Seppi, C. M. Tanner et al., "Parkinson disease," *Nature Reviews. Disease Primers*, vol. 3, no. 1, p. 17013, 2017.

[80] S. Yeo, B. Sung, Y. M. Hong et al., "Decreased expression of serum- and glucocorticoid-inducible kinase 1 (SGK1) promotes alpha-synuclein increase related with down-regulation of dopaminergic cell in the substantia nigra of chronic MPTP-induced parkinsonism mice and in SH-SY5Y cells," *Gene*, vol. 661, pp. 189–195, 2018.

[81] D. Ebrahimi-Fakhari, I. Cantuti-Castelvetri, Z. Fan et al., "Distinct roles in vivo for the ubiquitin-proteasome system and the autophagy-lysosomal pathway in the degradation of α-synuclein," *The Journal of Neuroscience: The Official Journal of the Society for Neuroscience*, vol. 31, no. 41, pp. 14508–14520, 2011.

[82] B. Kahan, "Toxicity spectrum of inhibitors of mammalian target of rapamycin in organ transplantation: etiology, pathogenesis and treatment," *Expert Opinion on Drug Safety*, vol. 10, no. 5, pp. 727–749, 2011.

[83] S. Ruchaud, N. Korfali, P. Villa et al., "Caspase-6 gene disruption reveals a requirement for lamin A cleavage in apoptotic chromatin condensation," *The EMBO Journal*, vol. 21, no. 8, pp. 1967–1977, 2002.

[84] W. K. Khalil, N. Assaf, S. A. ElShebiney, and N. A. Salem, "Neuroprotective effects of bee venom acupuncture therapy against rotenone-induced oxidative stress and apoptosis," *Neurochemistry International*, vol. 80, pp. 79–86, 2015.

[85] M. G. Willesen, S. Gammeltoft, and E. Vaudano, "Activation of the c-Jun N terminal kinase pathway in an animal model of Parkinson's disease," *Annals of the New York Academy of Sciences*, vol. 973, no. 1, pp. 237–240, 2002.

[86] E. J. Huang and L. F. Reichardt, "Trk receptors: roles in neuronal signal transduction," *Annual Review of Biochemistry*, vol. 72, no. 1, pp. 609–642, 2003.

[87] V. K. Gupta, Y. You, V. B. Gupta, A. Klistorner, and S. L. Graham, "TrkB receptor signalling: implications in neurodegenerative, psychiatric and proliferative disorders," *International Journal of Molecular Sciences*, vol. 14, no. 5, pp. 10122–10142, 2013.

[88] R. Andero, D. C. Choi, and K. J. Ressler, "BDNF-TrkB receptor regulation of distributed adult neural plasticity, memory formation, and psychiatric disorders," *Progress in Molecular Biology and Translational Science*, vol. 122, pp. 169–192, 2014.

[89] W. J. Streit, "Microglia as neuroprotective, immunocompetent cells of the CNS," *Glia*, vol. 40, no. 2, pp. 133–139, 2002.

[90] F. Blandini, "Neural and immune mechanisms in the pathogenesis of Parkinson's disease," *Journal of Neuroimmune Pharmacology: the official journal of the Society on NeuroImmune Pharmacology*, vol. 8, no. 1, pp. 189–201, 2013.

[91] T. R. Sampson, J. W. Debelius, T. Thron et al., "Gut Microbiota Regulate Motor Deficits and Neuroinflammation in a Model of Parkinson's Disease," *Cell*, vol. 167, no. 6, pp. 1469–1480.e12, 2016.

[92] K. I. Rathore, A. Redensek, and S. David, "Iron homeostasis in astrocytes and microglia is differentially regulated by TNF-α and TGF-β1," *Glia*, vol. 60, no. 5, pp. 738–750, 2012.

[93] H. Li, T. He, Q. Xu et al., "Acupuncture and regulation of gastrointestinal function," *World Journal of Gastroenterology*, vol. 21, no. 27, pp. 8304–8313, 2015.

[94] R. P. Dhond, N. Kettner, and V. Napadow, "Neuroimaging acupuncture effects in the human brain," *The Journal of Alternative and Complementary Medicine: Research on Paradigm, Practice, and Policy*, vol. 13, no. 6, pp. 603–616, 2007.

[95] G. Deuschl, J. Raethjen, R. Baron, M. Lindemann, H. Wilms, and P. Krack, "The pathophysiology of parkinsonian tremor: a review," *Journal of Neurology*, vol. 247, Supplement 5, pp. V33–V48, 2000.

[96] T. Wu, J. Wang, C. Wang et al., "Basal ganglia circuits changes in Parkinson's disease patients," *Neuroscience Letters*, vol. 524, no. 1, pp. 55–59, 2012.

[97] S. H. Lee, G. H. Jahng, I. H. Choe, C. B. Choi, D. H. Kim, and H. Y. Kim, "Neural pathway interference by retained acupuncture: a functional MRI study of a dog model of Parkinson's disease," *CNS Neuroscience & Therapeutics*, vol. 19, no. 8, pp. 585–595, 2013.

[98] Y. Chae, H. Lee, H. Kim et al., "Parsing brain activity associated with acupuncture treatment in Parkinson's diseases," *Movement Disorders: official journal of the Movement Disorder Society*, vol. 24, no. 12, pp. 1794–1802, 2009.

[99] S. Yeo, S. Lim, I. H. Choe et al., "Acupuncture stimulation on GB34 activates neural responses associated with Parkinson's disease," *CNS Neuroscience & Therapeutics*, vol. 18, no. 9, pp. 781–790, 2012.

[100] S. Yeo, I. H. Choe, M. van den Noort et al., "Acupuncture on GB34 activates the precentral gyrus and prefrontal cortex in Parkinson's disease," *BMC Complementary and Alternative Medicine*, vol. 14, no. 1, p. 336, 2014.

[101] Z. Li, J. Chen, J. Cheng et al., "Acupuncture modulates the cerebello-thalamo-cortical circuit and cognitive brain regions in patients of Parkinson's disease with tremor," *Frontiers in Aging Neuroscience*, vol. 10, p. 206, 2018.

[102] Y. Huang, X. Jiang, Y. Zhuo, and G. Wik, "Complementary acupuncture in Parkinson's disease: a SPECT study," *The International Journal of Neuroscience*, vol. 120, no. 2, pp. 150–154, 2010.

[103] Y. Huang, X. Jiang, Y. Zhuo, A. Tang, and G. Wik, "Complementary acupuncture treatment increases cerebral metabolism in patients with Parkinson's disease," *The International Journal of Neuroscience*, vol. 119, no. 8, pp. 1190–1197, 2009.

[104] R. Zhang, A. H. Andersen, P. A. Hardy et al., "Objectively measuring effects of electro-acupuncture in parkinsonian rhesus monkeys," *Brain Research*, vol. 1678, pp. 12–19, 2018.

[105] G. Rui, Z. Guangjian, W. Yong et al., "High frequency electro-acupuncture enhances striatum DAT and D1 receptor expression, but decreases D2 receptor level in 6-OHDA lesioned rats," *Behavioural Brain Research*, vol. 237, pp. 263–269, 2013.

[106] J. Jia, Z. Sun, B. Li et al., "Electro-acupuncture stimulation improves motor disorders in parkinsonian rats," *Behavioural Brain Research*, vol. 205, no. 1, pp. 214–218, 2009.

[107] J. Jia, B. Li, Z. L. Sun, F. Yu, X. Wang, and X. M. Wang, "Electro-acupuncture stimulation acts on the basal ganglia output pathway to ameliorate motor impairment in parkinsonian model rats," *Behavioral Neuroscience*, vol. 124, no. 2, pp. 305–310, 2010.

[108] S. N. Kim, A. R. Doo, J. Y. Park et al., "Combined treatment with acupuncture reduces effective dose and alleviates adverse effect of L-dopa by normalizing Parkinson's disease-induced neurochemical imbalance," *Brain Research*, vol. 1544, pp. 33–44, 2014.

[109] Z. Sun, J. Jia, X. Gong et al., "Inhibition of glutamate and acetylcholine release in behavioral improvement induced by electroacupuncture in parkinsonian rats," *Neuroscience Letters*, vol. 520, no. 1, pp. 32–37, 2012.

[110] T. Wu, X. Long, Y. Zang et al., "Regional homogeneity changes in patients with Parkinson's disease," *Human Brain Mapping*, vol. 30, no. 5, pp. 1502–1510, 2009.

[111] M. M. Lewis, G. du, S. Sen et al., "Differential involvement of striato- and cerebello-thalamo-cortical pathways in tremor- and akinetic/rigid-predominant Parkinson's disease," *Neuroscience*, vol. 177, pp. 230–239, 2011.

[112] A. C. Bostan, R. P. Dum, and P. L. Strick, "Cerebellar networks with the cerebral cortex and basal ganglia," *Trends in Cognitive Sciences*, vol. 17, no. 5, pp. 241–254, 2013.

[113] M. K. Lyons, "Deep brain stimulation: current and future clinical applications," *Mayo Clinic Proceedings*, vol. 86, no. 7, pp. 662–672, 2011.

[114] A. C. Bostan and P. L. Strick, "The basal ganglia and the cerebellum: nodes in an integrated network," *Nature Reviews. Neuroscience*, vol. 19, no. 6, pp. 338–350, 2018.

[115] J. L. Lanciego, N. Luquin, and J. A. Obeso, "Functional neuroanatomy of the basal ganglia," *Cold Spring Harbor Perspectives in Medicine*, vol. 2, no. 12, article a009621, 2012.

[116] T. Aosaki, M. Miura, T. Suzuki, K. Nishimura, and M. Masuda, "Acetylcholine-dopamine balance hypothesis in the striatum: an update," *Geriatrics & Gerontology International*, vol. 10, Supplement 1, pp. S148–S157, 2010.

[117] S. Fahn, D. Oakes, I. Shoulson et al., "Levodopa and the progression of Parkinson's disease," *The New England Journal of Medicine*, vol. 351, no. 24, pp. 2498–2508, 2004.

[118] A. Manson, P. Stirpe, and A. Schrag, "Levodopa-induced-dyskinesias clinical features, incidence, risk factors, management and impact on quality of life," *Journal of Parkinson's Disease*, vol. 2, no. 3, pp. 189–198, 2012.

Hindawi
Neural Plasticity
Volume 2021, Article ID 6641506, 10 pages
https://doi.org/10.1155/2021/6641506

Research Article

Weakened Effective Connectivity Related to Electroacupuncture in Stroke Patients with Prolonged Flaccid Paralysis: An EEG Pilot Study

Yi-Fang Lin,[1] Xin-Hua Liu,[1] Zheng-Yu Cui,[1] Zuo-Ting Song,[2] Fei Zou,[1] Shu-Geng Chen,[1] Xiao-Yang Kang,[2] Bin Ye,[3] Qiang Wang,[4] Jing Tian,[1] and Jie Jia[1]

[1]*Department of Rehabilitation Medicine, Huashan Hospital, Fudan University, Shanghai, China*
[2]*Engineering Research Center of AI & Robotics, Ministry of Education, Shanghai Engineering Research Center of AI & Robotics, MOE Frontiers Center for Brain Science, Institute of AI and Robotics, Academy for Engineering & Technology, Fudan University, Shanghai, China*
[3]*Department of Rehabilitation Medicine, The Shanghai Third Rehabilitation Hospital, Shanghai, China*
[4]*Department of Rehabilitation Medicine, Shanghai Jing'an District Central Hospital, Shanghai, China*

Correspondence should be addressed to Jing Tian; karentianjing@126.com and Jie Jia; shannonjj@126.com

Received 18 December 2020; Revised 3 February 2021; Accepted 18 February 2021; Published 10 March 2021

Academic Editor: Feng Zhang

Flaccid paralysis in the upper extremity is a severe motor impairment after stroke, which exists for weeks, months, or even years. Electroacupuncture treatment is one of the most widely used TCM therapeutic interventions for poststroke flaccid paralysis. However, the response to electroacupuncture in different durations of flaccid stage poststroke as well as in the topological configuration of the cortical network remains unclear. The objectives of this study are to explore the disruption of the cortical network in patients in different durations of flaccid stage and observe dynamic network reorganization during and after electroacupuncture. Resting-state networks were constructed from 18 subjects with flaccid upper extremity by partial directed coherence (PDC) analysis of multichannel EEG. They were allocated to three groups according to time after flaccid paralysis: the short-duration group (those with flaccidity for less than two months), the medium-duration group (those with flaccidity between two months and six months), and the long-duration group (those with flaccidity over six months). Compared with short-duration flaccid subjects, weakened effective connectivity was presented in medium-duration and long-duration groups before electroacupuncture. The long-duration group has no response in the cortical network during electroacupuncture. The global network measures of EEG data (sPDC, mPDC, and N) indicated that there was no significant difference among the three groups. These results suggested that the network connectivity reduced and weakly responded to electroacupuncture in patients with flaccid paralysis for over six months. These findings may help us to modulate the formulation of electroacupuncture treatment according to different durations of the flaccid upper extremity.

1. Introduction

Flaccid paralysis is the most severe motor impairment following stroke, characterized by weakness and reduced muscle tone [1]. According to the Brunnstrom recovery stage, stroke survivors go through from initial flaccid paralysis to a number of stages characterized by spasticity, to the development of selective control of movement, and finally to the restoration of normal movement [2]. The time required for patients to go through from one stage to the next varies. The time required from flaccid phase to spasticity occurrence in stroke patients is one to three weeks in general [3]. Previous research has suggested that the prevalence of spasticity at 2-10 days, 2 weeks, and 4 weeks since stroke onset is 4%,

20.2%-24.5%, and 27%, respectively [4]. However, the duration of flaccid stage lasted for months, or even for years in some individuals with stroke. As we know, independence by activities of daily living (ADL) relies to a great extent on the motor function recovery of the upper extremity [5]. Prolonged flaccid upper extremity impacts independence and accelerates disability. Prolonged flaccidity has been defined as muscle hypotonia lasting for more than 2 months after stroke [6]. If a patient has flaccid paralysis for more than one year since stroke onset, his motor recovery occurs later or proceeds more slowly and he may not be able to regain any function from treatment [6, 7].

As an effective nondrug treatment, electroacupuncture has been widely used poststroke for upper extremity recovery. Several studies have reported that Quchi (LI11), Shousanli (LI10), and Hegu (LI4) are the frequently used and effective acupoints of motor recovery in patients with stroke [8–10]. These acupoints belong to the large intestine meridians. Stimulating them can promote the restoration of free flow of essence and blood according to the TCM theory [11]. A large number of studies published in recent years showed that electroacupuncture used for poststroke upper extremity rehabilitation was a growing field of interest. However, these researches paid little attention to flaccid upper extremity. Little attention was paid to the cortical impact (e.g., neuroplasticity, functional connectivity, cortical network) aroused by electroacupuncture in this population. Neuroplasticity refers to the capacity of the nervous system to modify its structure and function in response to environmental changes, which is strongly related to brain remodeling [12]. Promotion and modulation of neuroplasticity through therapeutic techniques (e.g., noninvasive brain stimulation, acupuncture/electroacupuncture, task-oriented training) are the keys to facilitate motor recovery [13, 14]. Thus, investigating the electroacupuncture-related brain activity among patients with different durations of flaccid stage is essential. It may have important implications for adjusting the electroacupuncture prescription in clinical practice.

EEG is convenient to detect real-time cortical activity as a high-time-resolution electrophysiological technique [15]. It is used widely to detect the brain oscillations, cortex excitability, cortical network, and electrophysiological biomarker in multiple disciplines through various EEG signal processing and feature extraction (e.g., spectral analysis, time-frequency analysis, connectivity analysis) [16–21]. Given that brain activity is a dynamic and complex network with each area's communication and coordination, effective connectivity is selected to investigate the different brain area connectivity and plasticity in this study. Granger causality-based effective connectivity is regarded as an important dimension of functional connectivity under specific conditions, which estimated the causal influence from one neural region to another [22]. A convenient measure of effective cortical connectivity is partial directed coherence (PDC) which is often used to deduce the intensity of information flow over the brain from EEG data [23, 24].

Brain oscillations of twenty-three flaccid stroke patients have been investigated by spectral analysis in our preliminary study [25]. We found that beta-band oscillations increased and delta-band oscillations decreased in the motor cortex in patients with flaccid upper extremity during electroacupuncture [25]. However, neural oscillations based on spectral analysis are not enough to reveal the electroacupuncture-related brain activity in patients with flaccidity. Different durations of flaccid stage were ignored in our previous research. Hence, it is necessary to implement further investigation and in-depth cortical network analyses.

With these considerations, based on our preliminary study, we continuously enrolled patients with flaccid upper extremity after stroke and constructed effective cortical networks using PDC analysis of 32-channel EEG signals. Connective deviation of patients was uncovered by comparing with three different durations of flaccid stage groups from peculiarities of global network connectivity and individual connection. We hypothesize that the cortical connectivity descended and the response to electroacupuncture weakened along with the prolonged duration of flaccid stage.

2. Methods

2.1. Study Design and Participants. Eighteen patients with flaccid upper extremity after stroke were recruited from the Department of Rehabilitation Medicine, Huashan Hospital, and Shanghai Third Rehabilitation Hospital. The types of stroke and lesions were confirmed by a clinical CT or MRI scanner. The inclusion criteria were (1) adult patients with first-time stroke; (2) Mini-Mental State Examination ≥ 23; (3) unilateral upper limb and hand hemiplegia with weakness and reduced muscle tone; and (4) right-handedness assessed by the Edinburgh Handedness Inventory [26]. Patients were excluded if they had (1) spasticity (Modified Ashworth Spasticity Scale ≥ 1) of the affected arm; (2) severe osteoarthrosis comorbidities; (3) allergy to EEG electrode cream; and (4) participating in other rehabilitation or drug clinical trials. Eighteen patients were allocated to three groups according to their duration of flaccid stage: the short-duration group (SDG, $n = 6$, 4 males and 2 female), in which patients' flaccid stage was less than for two months; the medium-duration group (MDG, $n = 6$, 5 males and 1 female), in which patients' flaccid stage was between two months and six months; and the long-duration group (LDG, $n = 6$, 4 males and 2 female), in which patients' flaccid stage was over six months. All patients received the electroacupuncture treatment once and EEG recording. The flowchart of participants through the study is shown in Figure 1. All patients signed informed consent forms before the participation in accordance with the Declaration of Helsinki. Demographic and clinical characteristics of participants are shown in Table 1. This trial was registered on the Chinese Clinical Trial Registry (ChiCTR2000036959).

2.2. Electroacupuncture Stimulation. The current study is based on our previous research [25]. The methods have been published in our previous study. An acupuncturist with more than 5 years of clinical experience inserted the sterile disposable acupuncture needles (Jiajian, 0.30 × 40 mm; Wuxi Jiajian Medical Instruments, Wuxi, China) in three acupoints (Hegu (LI4), Shousanli (LI10), Quchi (LI11)) [25]. These

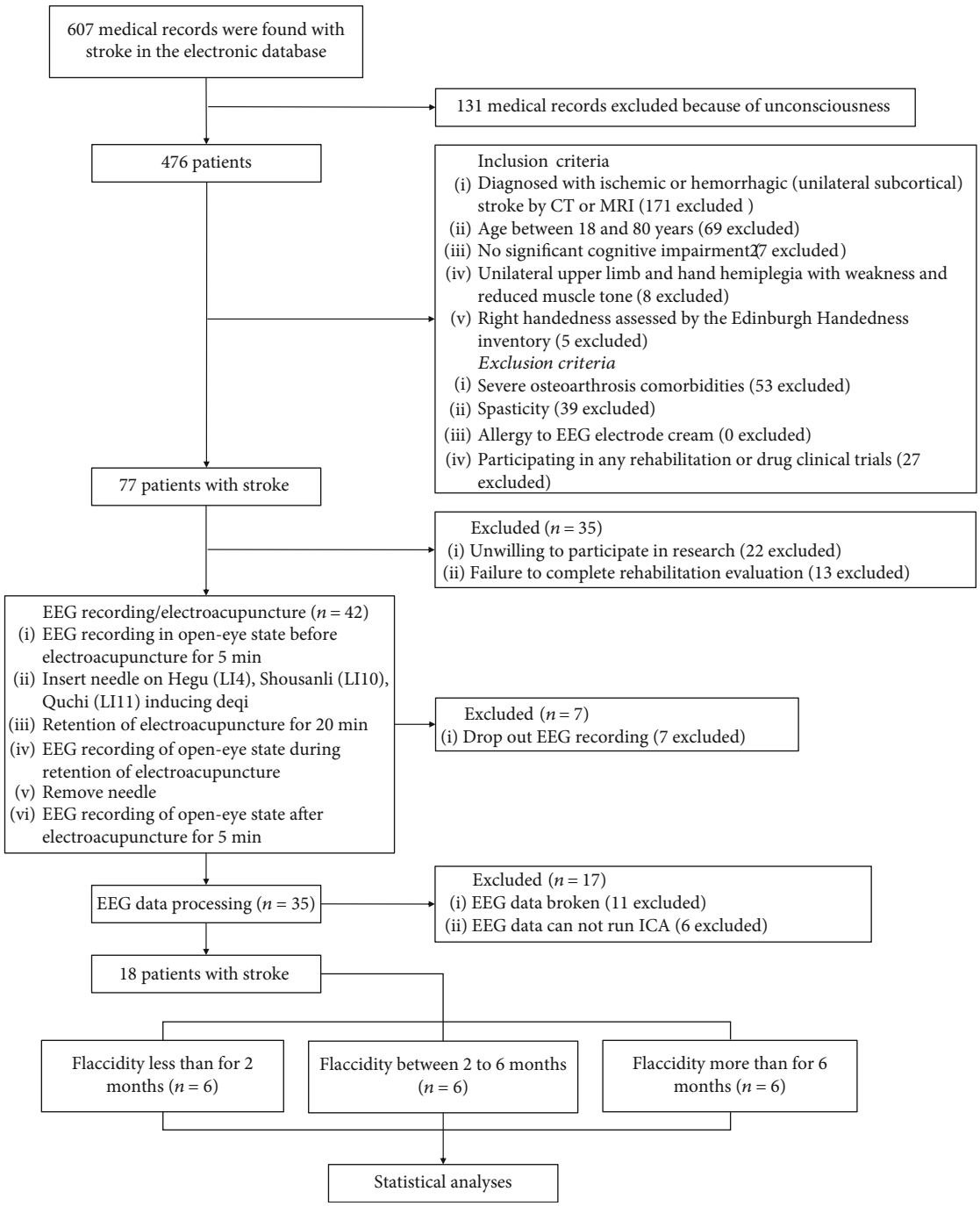

Figure 1: Flow chart of the study participant.

acupoints will be needled perpendicularly, with a depth of 10-15 mm approximately [25]. Following insertion, electrical stimulation parameters applied to the needles are intermittent wave, pulse signal with 250 μs, sharp waveform, and frequency with 2 Hz [27, 28]. This electroacupuncture recipe is effective in activating the nerves and muscles. The current intensity was adjusted according to the patients' tolerance. After 20 minutes of retention of electroacupuncture, the needles were removed. Details of experiment setup and three acupoints in the procedure of electroacupuncture are shown in Figure 2.

2.3. EEG Recording. All patients' cortical activities were recorded by EEG in a sitting position with eyes opened before, during, and after electroacupuncture. EEG signals were recorded with BrainCap (Brain Products, Gilching, Germany) from 32-channel electrodes positioned according to the international 10-20 system at a sampling rate of 1000 Hz. The ground electrode and reference electrode were placed in the midsagittal line. All electrode impedances were maintained below 5 kΩ. The details of recording brain wave data were described in previous research [25].

Table 1: Demographic and clinical data of participants.

Group-ID	Gender	Age (years)	Site of lesion	Ischemia/hemorrhage	Days since stroke	Side of lesion	Side of hemiparesis	Handedness	NIHSS	BI
SDG-1	M	70	BG, FL PL, pons	I	55	R	L	R	11	40
SDG-2	M	60	BG, CR	I	15	R	L	R	11	60
SDG-3	M	56	BG	H	22	L	R	R	13	40
SDG-4	M	64	BG, CR, FL	I	17	L	R	R	12	25
SDG-5	F	71	BG, CO, FL, PL, pons	I	11	R	L	R	7	20
SDG-6	F	77	BG, CR, FL, PL	I	25	R	L	R	8	40
Mean (±SD)		66.33 (±7.09)			24.17 (±14.52)				10.33 (±2.13)	37.50 (±12.83)
MDG-1	M	77	BG, FL, PL	I	98	R	L	R	9	50
MDG-2	M	60	BG	H	108	R	L	R	4	55
MDG-3	M	60	BG, CO, FL, OL, TL	I	62	L	R	R	14	30
MDG-4	M	61	Th, OL, TL	I	111	L	R	R	9	65
MDG-5	M	60	BG, IC	I	146	L	R	R	8	40
MDG-6	F	59	TL	I	118	L	R	R	15	30
Mean (±SD)		62.83 (±6.36)			107.17 (±25.05)				9.83 (±3.72)	45.00 (±12.91)
LDG-1	M	66	BG	I	938	R	L	R	5	50
LDG-2	M	62	BG, FL, PL	I	198	L	R	R	10	70
LDG-3	M	48	BG, FL, PL, TL	I	407	L	R	R	10	65
LDG-4	M	44	BG	H	185	L	R	R	7	70
LDG-5	F	68	BG	H	1184	R	L	R	29	10
LDG-6	F	75	BG, Th	I	370	L	R	R	24	10
Mean (±SD)		60.50 (±11.01)			547.00 (±379.13)				14.17 (±9.01)	45.83 (±26.21)

Abbreviations: BI: Barthel Index; BG: basal ganglia; CO: centrum ovale; CR: corona radiate; F: female; FL: frontal lobe; H: hemorrhage; I: ischemia; IC: internal capsule; L: left; M: male; NIHSS: National Institutes of Health Stroke Scale; OL: occipital lobe; PL: parietal lobe; R: right; Th: thalamus; TL: temporal lobe.

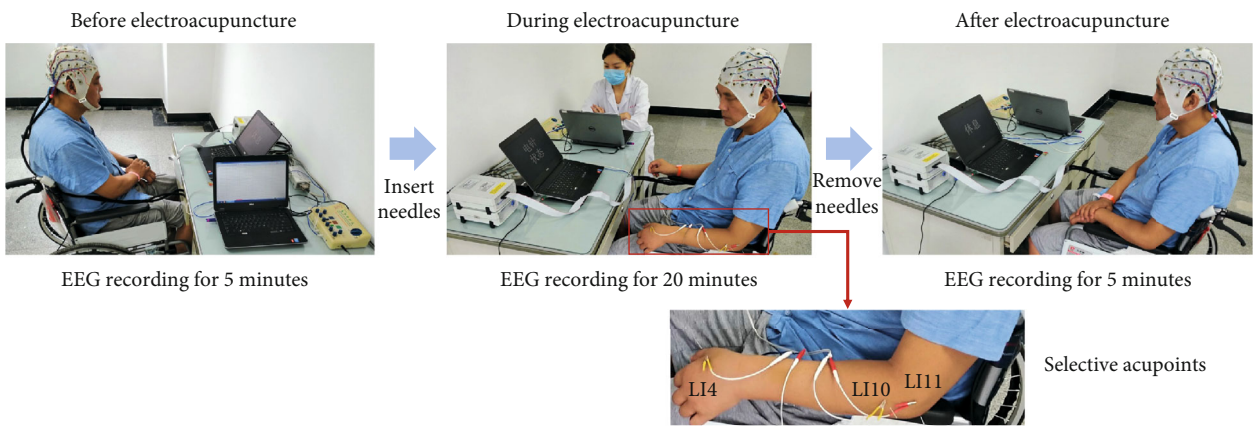

Figure 2: Details of experiment setup and three acupoints in the procedure of electroacupuncture.

2.4. EEG Processing. Data were performed with Matlab R2020a software (MathWorks, MA, USA) and using scripts based on the EEGLAB 2019 toolbox (http://sccn.ucsd.edu/eeglab/). To begin this process, raw data of the IO electrode was removed. Then, there were 31 channels (C3, C4, CP1, CP2, CP5, CP6, Cz, F3, F4, F7, F8, FC1, FC2, FC5, FC6, Fp1, Fp2, FT9, FT10, Fz, O1, O2, P3, P4, P7, P8, Pz, T7, T8, TP10, TP9) left for subsequent cortical network analysis. EEG signals were band-pass filtered into the beta-band (14–30 Hz), which play an important role in motor recovery [17, 29, 30]. Alpha-band- and beta-band-related brain functional indexes (e.g., coherence, multiscale permutation transfer entropy, oscillations) are most concerned in motor impairment and recovery after stroke. However, recent researches suggested that alpha-band is probably more associated with motor learning mechanisms and beta-band is associated with upper extremity motor recovery and neural networks that propagate activity between primary motor cortex and muscles [31, 32]. In this study, upper extremity motor recovery and the time since stroke onset are the main research purposes. Thus, beta-band was selected for EEG signal analysis. Then, EOG, ECG, and electroacupuncture-related artifacts were identified and eliminated through independent component analysis (ICA). ICA is a blind source separation algorithm that can be enabled to effectively separate eye movements and blink artifacts from EEG data. For each participant, 5 minutes before electroacupuncture, 20 minutes during electroacupuncture, and 5 minutes after needles were removed, artifact-free EEG signals were chosen for further PDC analysis.

Partial directed coherence (PDC) was used for effective connectivity calculation, which is a Granger causality-based measure in the frequency domain [23]. PDC is different from other undirected functional cortical networks based on phase synchronization (i.e., phase locking value and phase lag index). PDC measure the causal effects between channel signals, with direction. Briefly, the 31-channel EEG signals at a time point are defined as a vector

$$X(n) = [X_1(n), X_2(n), X_3(n), \cdots, X_N(n)]^T, \quad (1)$$

where $X_N(n)(N = 1, 21, 2, \cdots, N)$ denote EEG signal from the Nth channel. The EEG series can be modeled with a multivariate autoregressive (MVAR) model.

$$X(n) = \sum_{r=1}^{p} A_r X(n-r) + \mathrm{W(n)}, \quad (2)$$

where p is the model order of MVAR, $A_r(r = 1, 2, \cdots, p)$ are the coefficient matrixes, and W(n) is a vector of multivariate uncorrelated white Gaussian noise. The model order p is defined by the Akaike Information Criterion (AIC) [33], and A_r are calculated by the Yule-Walker equation. Once A_r is estimated, $A(f)$ could be calculated as

$$A(f) = I - \sum_{r=1}^{p} A_r e^{-2jfr\pi}, \quad (3)$$

where I is the identity matrix. Then, the directed information flow from channel j to i at the frequency (PDC values) could be calculated as [23].

$$\mathrm{PDC}(i, j, f) = \frac{|A_{ij}(f)|}{\sqrt{\sum_k A_{kj}^*(f) A_{kj}(f)}}, \quad (4)$$

where $A_{ij}(f)$ is the element of $A(f)$ matrix and $*$ denotes the matrix transpose and complex conjugate. The PDC values range from 0 to 1; a higher value indicated a stronger information flow from channel j to i.

In this study, the PDC value that exceeded a threshold of 0.1 denotes significant causality, according to the spectral causality criterion (SCC) proposed by Schnider et al. [34]. PDC values for patients with infarct in the damaged left hemisphere (10 out of 18 in this study) were flipped along the midsagittal plane so that the right hemisphere corresponded to the ipsilesional hemisphere for all patients [35].

2.5. Network Analyses. In this study, the nodes of the network were 31-channel electrodes; 961 PDCs were estimated for all nodes in pair to build up the cortical network. The significant connection value (SCV) was considered to more than 0.1

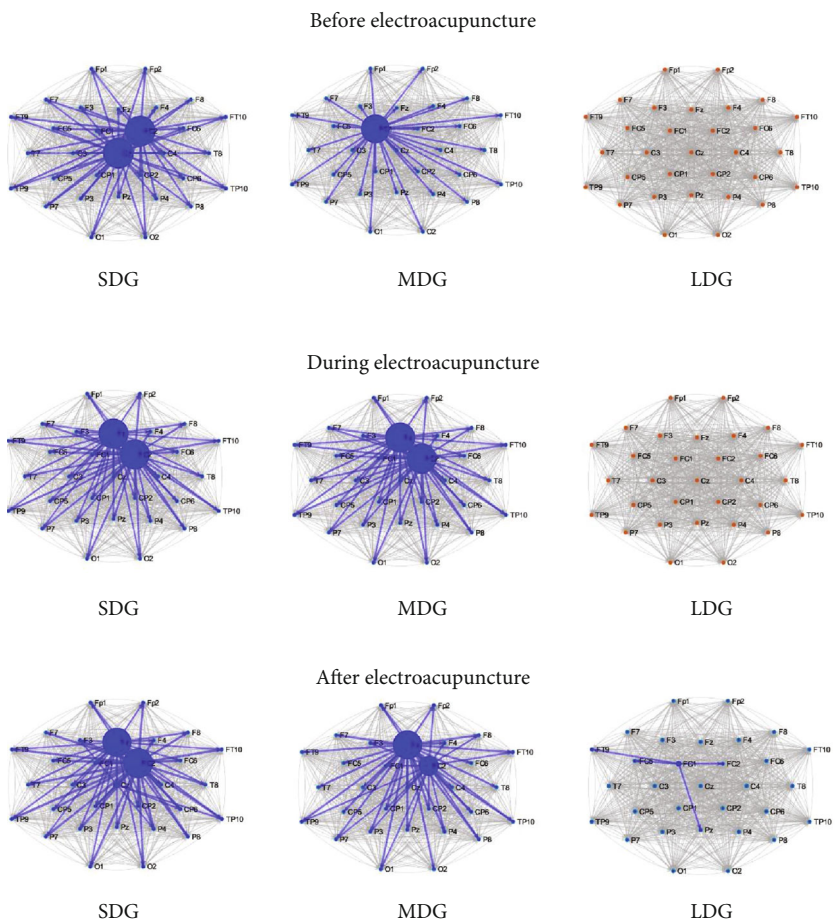

Figure 3: Grand averages of cortical networks at beta-band in patients with short duration, medium duration, and long duration of flaccid stage following stroke. Arrows indicate the significant connections. The size of the nodes is proportional to the degree.

according to SCC [23, 34]. The sum of PDCs (sPDC) of all SCV, the mean PDC (mPDC), and the number (N) of SCV were calculated to estimate the global connectivity of the cortical network [36].

2.6. Statistics. Statistical analyses were carried out using SPSS version 25.0 (IBM Inc., Chicago, IL, USA). Group differences of sPDC, mPDC, N, and the PDC value of each connection were tested with one-way ANOVA test. Two-tailed t-tests with Bonferroni adjustment were performed for all pairwise comparisons to reveal the changes before, during, and after electroacupuncture in each group. Significant level was set at 0.05 with a two-sided test.

3. Results

The grand averages of cortical networks of three groups (SDG, MDG, and LDG) were representatively visualized with the Matlab R2020a software (Figure 3). Generally, the network of LDG presented a global less connectivity compared with SDG and MDG. Before electroacupuncture, two nodes were observed in the SDG patients' network, one node was observed in the MDG patients' network, and no nodes were observed in the LDG patients' network. During electroacupuncture, two nodes were observed in SDG and MDG patients' networks, and no nodes were observed in LDG patients' networks. After electroacupuncture, two nodes were observed in SDG and MDG patients' networks, and one node was observed in LDG patients' networks. The size of the nodes denotes the number of average SCV for patients. After electroacupuncture, larger nodes were observed in the SDG patients' network, and less node was observed in the LDG patients' network. That means patients with a duration of flaccid stage less than two months have more effective connectivity.

Figure 4 presents the global network connectivity among the three groups before, during, and after electroacupuncture. There is no significant difference of sPDC, mPDC, and N among the three groups, indicating that the overall strength of the cortical connections and mean strength of SCV were not significantly different, no matter before, during, and after electroacupuncture.

Figure 5 shows the detailed differences in each connection between groups. Six among 961 connections were significantly stronger for MDG compared with SDG (i.e., C4⟶O2, CP6⟶O2, F3⟶O2, F8⟶O2, Fp1⟶O2, T8⟶O2) before electroacupuncture (see details in Figure 5(a)). These results indicate that the direction information flow from channels C4, CP6, F3, F8, Fp1, and T8 to channel O2 is stronger in MDG than SDG before

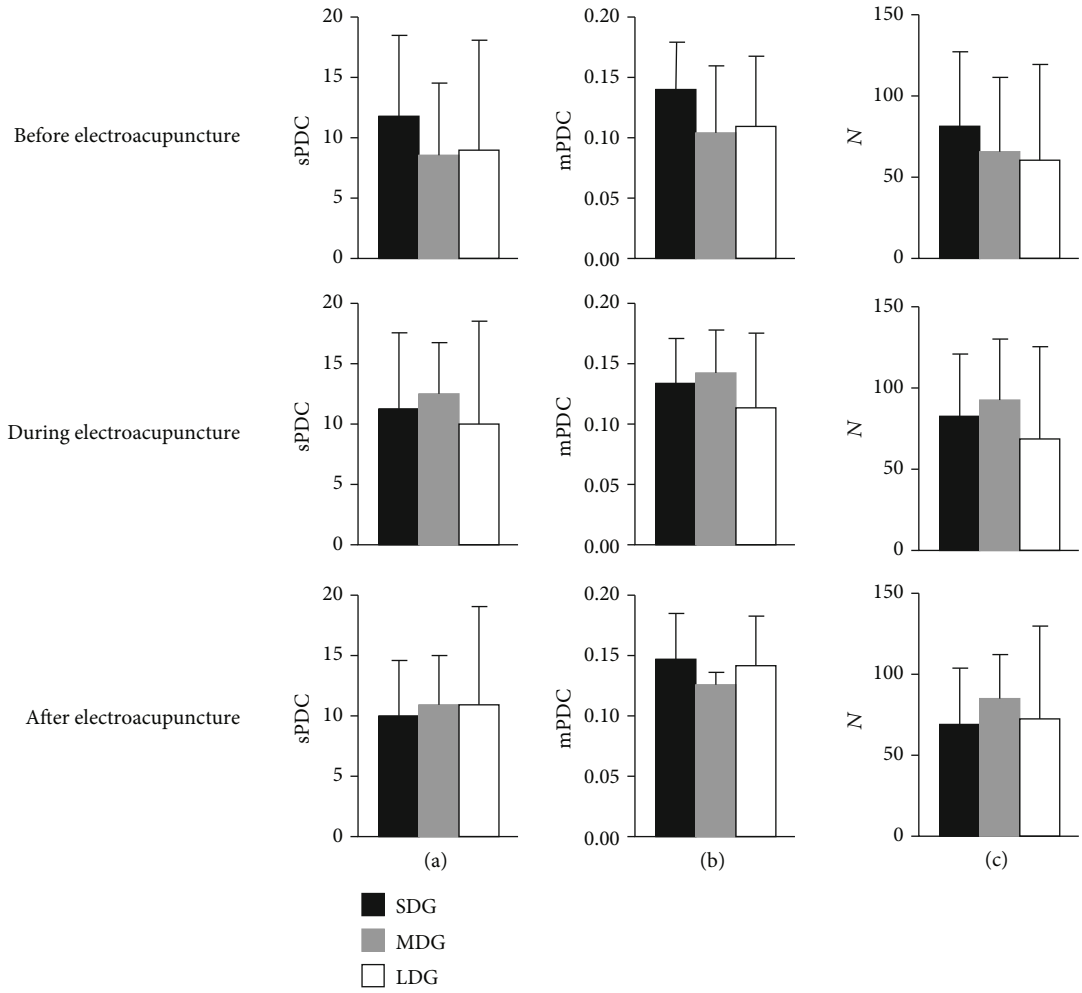

Figure 4: Global network connectivity at beta-band in patients with short duration, medium duration, and long duration of flaccid stage following stroke: (a) sum of PDCs (sPDC) of all significant connection values; (b) mean PDC (mPDC) of significant connections value; (c) number (N) of significant connection value.

electroacupuncture. Twenty among 961 connections were significantly stronger for LDG compared with MDG (i.e., C4⟶CP1, CP2⟶CP1, CP5⟶CP1, Cz⟶CP1, F3⟶CP1, F4⟶CP1, F8⟶CP1, FC1⟶CP1, FC2⟶CP1, FC5⟶CP1, FC6⟶CP1, Fp1⟶CP1, FT10⟶CP1, FT9⟶CP1, O1⟶CP1, O2⟶CP1, P3⟶CP1, P4⟶CP1, P8⟶CP1, Pz⟶CP1) after electroacupuncture treatment (see details in Figure 5(b)). These results suggest that the direction information flow from channels C4, CP2, CP5, Cz, F3, F4, F8, FC1, FC2, FC5, FC6, Fp1, FT10, FT9, O1, O2, P3, P4, P8, and Pz to channel CP1 is stronger in LDG than MDG after electroacupuncture.

4. Discussion

The current study provides tentative cortical network evidence that the effective connectivity decreased at beta-band in patients with prolonged flaccid paralysis compared to those with short-duration and medium-duration flaccid stage. Patients with prolonged flaccidity seem to have no response to electroacupuncture treatment in topological configuration of the cortical network.

Disruption of cortical structural or functional networks after stroke has been broadly studied by neuroimaging or neural electrophysiological techniques [37, 38]. Prior study suggested an imbalance of intracortical inhibition between the affected and unaffected motor cortex and greater cortical density in the motor areas in patients with prolonged flaccidity [39]. Flaccidity has been verified associating with disruption of basal ganglia, internal and external capsule, and parietal lobe [7, 40]. In this study, 17 out of 18 stroke subjects were basal ganglia destruction subjects and 6 out of 18 subjects were parietal lobe destruction subjects, which is consistent with previous research findings.

Before electroacupuncture, we found that the effective connectivity is reduced at beta-band in patients with flaccidity for over six months compared to those with flaccidity for less than two months and those with flaccidity between two and six months. Effective connectivity of the medium-duration group is weak compared to that of the short-duration group. These findings suggested that functional connectivity turns into abnormalities or even disappearance along with the increasing duration of flaccid stage, which is in accordance with a major pattern of stroke patients:

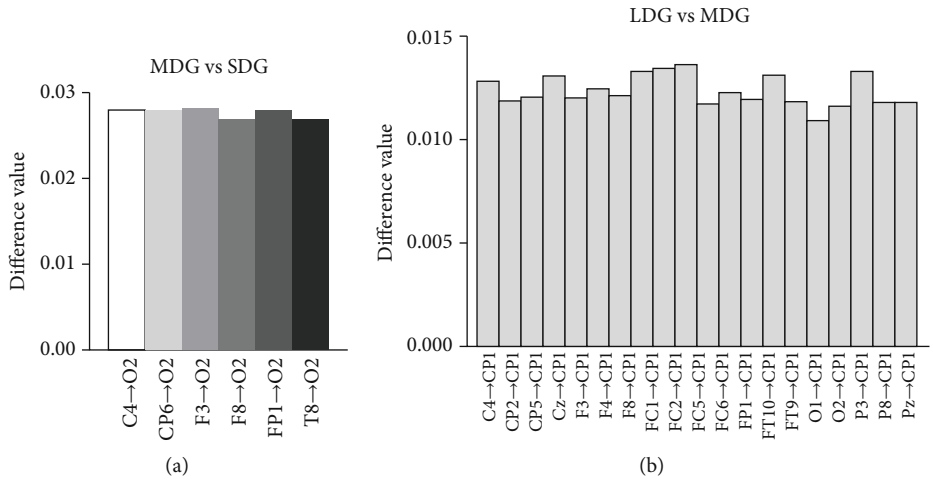

Figure 5: Significant difference of each connection between groups: (a) significant difference connections between medium duration and short duration of flaccid stage before electroacupuncture; (b) significant connections between long duration and medium duration of flaccid stage after electroacupuncture.

reduced cortical connectivity was correlated with clinical deficits [36].

During electroacupuncture, three interesting findings are (1) cortical network presented dynamic changes in topological configuration (the node goes from Cz to Fz) in SDG; (2) functional connectivity increased in MDG, and the connectivity transferred from contralesional into ipsilesional; and (3) network connectivity has no response to electroacupuncture in LDG. For SDG, the possible interpretation might be a reorganization occurred in the interhemispheres due to electroacupuncture. Recent studies have verified that cortical reorganization may contribute to the recovery of motor function after stroke [41]. For MDG, electroacupuncture may reduce inhibition of the affected hemisphere by the unaffected hemisphere, resulting in increased connectivity of the affected hemisphere. As we know, the major model of functional recovery is the interhemispheric competition model. The model hypothesized that a mutual, balanced inhibition between the hemispheres was disrupted following stroke, resulting in decreased inhibition of the unaffected hemisphere by the affected hemisphere and increased inhibition of the affected hemisphere by the unaffected hemisphere [14]. For LDG, electroacupuncture may not arouse the changes of the cortical network. This finding is consistent with that of Daly et al. who found that the patient will probably not regain any function in response to treatment if he had flaccid paralysis for more than one year after stroke [6].

After electroacupuncture, we found that the size of nodes reduced in MDG, suggesting that the dynamic changes of the cortical network due to electroacupuncture maintain for a while after treatment. The size of node is unchanged in SDG, indicating that the neuroplasticity in patients with different durations of flaccid stage is different.

The sPDC, mPDC, and N of SCV are the global network connectivity measurements. There is no significant difference among the three groups before, during, and after electroacupuncture. A possible interpretation is that the disruptions of global network connectivity are similar among the three groups. The PDC value of each connection was also calculated in this study. Comparing to SDG, the stronger information flow from six channels (i.e., C4, CP6, F3, F8, Fp1, and T8) to channel O2 was observed in MDG before electroacupuncture. After electroacupuncture, the stronger information flow from twenty channels (e.g., C4, CP2, CP5, Cz, F3) to channel CP1 was observed in LDG comparing to MDG. However, these connections were uninvolved in the significant connection value (see Figure 2). Thus, we speculated that these connections are not important for global network connectivity analysis in this study.

Our study suggested that patients with different durations of flaccid stage have various responses to electroacupuncture in the topological configuration of the cortical network. These findings.

may help us to understand that the same electroacupuncture prescriptions are not applicable to all stroke patients with flaccid paralysis. The customization of electroacupuncture therapeutic regimen according to flaccid stage is needed. However, which electroacupuncture regimens are more beneficial to patients is unclear and needs to be explored in future research. There are several limitations in this study. Firstly, electroacupuncture was performed only once on each stroke patient; the clinical significance of electroacupuncture therapy for stroke patients is hardly explained in this study. Secondly, we did not set up a control group with three randomized acupoints or three nonacupoints so that the results are not that convincing. Thirdly, the repeatability of these results may be affected due to the cross-sectional trail design. Therefore, the long-term electroacupuncture therapy with a large sample size would be designed and implemented to explore the time window and the prescription of electroacupuncture on stroke patients in the future.

5. Conclusions

This study investigated the cortical network changes from different durations of flaccid stage in stroke patients during electroacupuncture. Our results revealed that the cortical connectivity weakened and less responded to

electroacupuncture in patients with prolonged flaccid stage. These findings may be helpful for modulating the formulation of electroacupuncture treatment in motor recovery after stroke.

Data Availability

The data used to support the findings of this research are available from the corresponding author.

Conflicts of Interest

The authors declare that they have no conflicts of interest.

Authors' Contributions

Jie Jia and Jing Tian conceived the study design. Yi-Fang Lin, Xin-Hua Liu, and Zheng-Yu Cui collected the data and wrote the manuscript. Yi-Fang Lin and Fei Zou conducted the experiments. Zuo-Ting Song did with the EEG data processing. Shu-Geng Chen, Xiao-Yang Kang, Bin Ye, and Qiang Wang reviewed and edited the manuscript. All the authors have reviewed the manuscript and agreed to its submission. All authors read and approved the final manuscript. Xin-Hua Liu and Zheng-Yu Cui are the co-first authors.

Acknowledgments

We would like to thank all volunteers for their participation in the study. This study was supported by the National Key Research & Development Program of Ministry of Science and Technology of the People's Republic of China under Grants 2018YFC2002300 and 2018YFC2002301.

References

[1] P. Pantano, R. Formisano, M. Ricci et al., "Prolonged muscular flaccidity after stroke. Morphological and functional brain alterations," *Brain*, vol. 118, no. 5, pp. 1329–1338, 1995.

[2] S. Brunnstrom, "Motor testing procedures in hemiplegia: based on sequential recovery stages," *Physical Therapy*, vol. 46, no. 4, pp. 357–375, 1966.

[3] K. E. Nam, S. H. Lim, J. S. Kim et al., "When does spasticity in the upper limb develop after a first stroke? A nationwide observational study on 861 stroke patients," *Journal of Clinical Neuroscience*, vol. 66, pp. 144–148, 2019.

[4] J. Wissel, A. Manack, and M. Brainin, "Toward an epidemiology of poststroke spasticity," *Neurology*, vol. 80, no. 3, Supplement 2, pp. S13–S19, 2013.

[5] J. M. Veerbeek, G. Kwakkel, E. E. van Wegen, J. C. Ket, and M. W. Heymans, "Early prediction of outcome of activities of daily living after stroke: a systematic review," *Stroke*, vol. 42, no. 5, pp. 1482–1488, 2011.

[6] J. J. Daly, R. L. Ruff, S. Osman, and J. J. Hull, "Response of prolonged flaccid paralysis to FNS rehabilitation techniques," *Disability and Rehabilitation*, vol. 22, no. 12, pp. 565–573, 2000.

[7] R. Formisano, P. Pantano, M. G. Buzzi et al., "Late motor recovery is influenced by muscle tone changes after stroke," *Archives of Physical Medicine and Rehabilitation*, vol. 86, no. 2, p. 308, 2005.

[8] Y. Xu, S. Lin, C. Jiang et al., "Synergistic effect of acupuncture and mirror therapy on post-stroke upper limb dysfunction: a study protocol for a randomized controlled trial," *Trials*, vol. 19, no. 1, p. 303, 2018.

[9] W.-S. Kim, I. S. Kim, S. J. Kim, P. X. Wei, D. H. Choi, and T. R. Han, "Effect of electroacupuncture on motor recovery in a rat stroke model during the early recovery stage," *Brain Research*, vol. 1248, pp. 176–183, 2008.

[10] J. S. Yang, X. Gao, R. Sun et al., "Effect of electroacupuncture intervention on rehabilitation of upper limb motor function in patients with ischemic stroke," *Zhen Ci Yan Jiu*, vol. 40, no. 6, pp. 489–492, 2015.

[11] F. K. Sze, E. Wong, X. Yi, and J. Woo, "Does acupuncture have additional value to standard poststroke motor rehabilitation?," *Stroke*, vol. 33, no. 1, pp. 186–194, 2002.

[12] R. von Bernhardi, L. E. Bernhardi, and J. Eugenin, "What is neural plasticity?," *Advances in Experimental Medicine and Biology*, vol. 1015, pp. 1–15, 2017.

[13] D. M. Hermann and M. Chopp, "Promoting brain remodelling and plasticity for stroke recovery: therapeutic promise and potential pitfalls of clinical translation," *The Lancet Neurology*, vol. 11, no. 4, pp. 369–380, 2012.

[14] G. Di Pino, G. Pellegrino, G. Assenza et al., "Modulation of brain plasticity in stroke: a novel model for neurorehabilitation," *Nature Reviews Neurology*, vol. 10, no. 10, pp. 597–608, 2014.

[15] S. Comani, L. Velluto, L. Schinaia et al., "Monitoring neuromotor recovery from stroke with high-resolution EEG, robotics and virtual reality: a proof of concept," *IEEE Transactions on Neural Systems and Rehabilitation Engineering*, vol. 23, no. 6, pp. 1106–1116, 2015.

[16] L. Hu and Z. Zhiguo, *EEG Signal Processing and Feature Extraction*, Springer, 2019.

[17] C.-W. Tang, F.-J. Hsiao, P.-L. Lee et al., "*B*-Oscillations reflect recovery of the paretic upper limb in subacute stroke," *Neurorehabilitation and Neural Repair*, vol. 34, no. 5, pp. 450–462, 2020.

[18] T. Hoshino, K. Oguchi, K. Inoue, A. Hoshino, and M. Hoshiyama, "Relationship between upper limb function and functional neural connectivity among motor related-areas during recovery stage after stroke," *Topics in Stroke Rehabilitation*, vol. 27, no. 1, pp. 57–66, 2020.

[19] D. Reckziegel, E. Vachon-Presseau, B. Petre, T. J. Schnitzer, M. N. Baliki, and A. V. Apkarian, "Deconstructing biomarkers for chronic pain: context- and hypothesis-dependent biomarker types in relation to chronic pain," *Pain*, vol. 160, no. 1, pp. S37–S48, 2019.

[20] L.-r. Weitzel, D. Sampath, K. Shimizu, A. M. White, P. S. Herson, and Y. H. Raol, "EEG power as a biomarker to predict the outcome after cardiac arrest and cardiopulmonary resuscitation induced global ischemia," *Life Sciences*, vol. 165, pp. 21–25, 2016.

[21] J. M. Cassidy, A. Wodeyar, J. Wu et al., "Low-frequency oscillations are a biomarker of injury and recovery after stroke," *Stroke*, vol. 51, no. 5, pp. 1442–1450, 2020.

[22] K. J. Blinowska, S. Supek, and R. Magjarevic, "Review of the methods of determination of directed connectivity from multichannel data," *Medical & Biological Engineering & Computing*, vol. 49, no. 5, pp. 521–529, 2011.

[23] K. Sameshima and L. A. Baccalá, "Using partial directed coherence to describe neuronal ensemble interactions," *Journal of Neuroscience Methods*, vol. 94, no. 1, pp. 93–103, 1999.

[24] B. Schelter, M. Winterhalder, M. Eichler et al., "Testing for directed influences among neural signals using partial directed coherence," *Journal of Neuroscience Methods*, vol. 152, no. 1, pp. 210–219, 2006.

[25] F. Zou, Y.-F. Lin, S.-G. Chen et al., "The impact of electroacupuncture at Hegu, Shousanli, and Quchi based on the theory "treating flaccid paralysis by Yangming alone" on stroke patients' EEG: a pilot study," *Evidence-based Complementary and Alternative Medicine*, vol. 2020, Article ID 8839491, 9 pages, 2020.

[26] R. C. Oldfield, "The assessment and analysis of handedness: the Edinburgh inventory," *Neuropsychologia*, vol. 9, no. 1, pp. 97–113, 1971.

[27] J. Zhan, R. Pan, M. Zhou et al., "Electroacupuncture as an adjunctive therapy for motor dysfunction in acute stroke survivors: a systematic review and meta-analyses," *BMJ Open*, vol. 8, no. 1, article e17153, 2018.

[28] Y. S. Kim, J. W. Hong, B. J. Na et al., "The effect of low versus high frequency electrical acupoint stimulation on motor recovery after ischemic stroke by motor evoked potentials study," *The American Journal of Chinese Medicine*, vol. 36, no. 1, pp. 45–54, 2008.

[29] J. Wagner, S. Makeig, M. Gola, C. Neuper, and G. Müller-Putz, "Distinct *B* band oscillatory networks subserving motor and cognitive control during gait adaptation," *The Journal of Neuroscience*, vol. 36, no. 7, pp. 2212–2226, 2016.

[30] G. Rabiller, J. W. He, Y. Nishijima, A. Wong, and J. Liu, "Perturbation of brain oscillations after ischemic stroke: a potential biomarker for post-stroke function and therapy," *International Journal of Molecular Sciences*, vol. 16, no. 10, pp. 25605–25640, 2015.

[31] R. I. Carino-Escobar, P. Carrillo-Mora, R. Valdes-Cristerna et al., "Longitudinal analysis of stroke patients' brain rhythms during an intervention with a brain-computer interface," *Neural Plasticity*, vol. 2019, Article ID 7084618, 11 pages, 2019.

[32] T. D. Aumann and Y. Prut, "Do sensorimotor *B*-oscillations maintain muscle synergy representations in primary motor cortex?," *Trends in Neurosciences*, vol. 38, no. 2, pp. 77–85, 2015.

[33] H. Akaike, "A new look at the statistical model identification," *IEEE Transactions on Automatic Control*, vol. 19, no. 6, pp. 716–723, 1974.

[34] S. M. Schnider, R. H. Kwong, F. A. Lenz, and H. C. Kwan, "Detection of feedback in the central nervous system using system identification techniques," *Biological Cybernetics*, vol. 60, no. 3, pp. 203–212, 1989.

[35] F. Pichiorri, M. Petti, S. Caschera, L. Astolfi, F. Cincotti, and D. Mattia, "An EEG index of sensorimotor Interhemispheric coupling after unilateral stroke: clinical and neurophysiological study," *European Journal of Neuroscience*, vol. 47, no. 2, pp. 158–163, 2018.

[36] X. Guo, Z. Jin, X. Feng, and S. Tong, "Enhanced effective connectivity in mild occipital stroke patients with hemianopia," *IEEE Transactions on Neural Systems and Rehabilitation Engineering*, vol. 22, no. 6, pp. 1210–1217, 2014.

[37] L. Cheng, Z. Wu, J. Sun et al., "Reorganization of motor execution networks during sub-acute phase after stroke," *IEEE Transactions on Neural Systems and Rehabilitation Engineering*, vol. 23, no. 4, pp. 713–723, 2015.

[38] Y. Li, T. Wang, T. Zhang et al., "Fast high-resolution metabolic imaging of acute stroke with 3D magnetic resonance spectroscopy," *Brain*, vol. 143, no. 11, pp. 3225–3233, 2020.

[39] A. Benussi, E. Premi, V. Cantoni et al., "Cortical inhibitory imbalance in functional paralysis," *Frontiers in Human Neuroscience*, vol. 14, 2020.

[40] I. Miyai, A. D. Blau, M. J. Reding, and B. T. Volpe, "Patients with stroke confined to basal ganglia have diminished response to rehabilitation efforts," *Neurology*, vol. 48, no. 1, pp. 95–101, 1997.

[41] L. Wang, C. Yu, H. Chen et al., "Dynamic functional reorganization of the motor execution network after stroke," *Brain*, vol. 133, no. 4, pp. 1224–1238, 2010.

Hindawi
Neural Plasticity
Volume 2021, Article ID 6690523, 7 pages
https://doi.org/10.1155/2021/6690523

Review Article

The Histone Modifications of Neuronal Plasticity

Huixia Geng,[1] **Hongyang Chen**,[2] **Haiying Wang**,[2] **and Lai Wang**[1,2]

[1]*Institute of Chronic Disease Risks Assessment, School of Nursing and Health Sciences, Henan University, Kaifeng, 475004 Henan Province, China*
[2]*College of Life Science, Henan University, Kaifeng, 475004 Henan Province, China*

Correspondence should be addressed to Lai Wang; wanglai@henu.edu.cn

Received 17 December 2020; Revised 21 January 2021; Accepted 30 January 2021; Published 11 February 2021

Academic Editor: Wei-Lin Liu

Nucleosomes composed of histone octamer and DNA are the basic structural unit in the eukaryote chromosome. Under the stimulation of various factors, histones will undergo posttranslational modifications such as methylation, phosphorylation, acetylation, and ubiquitination, which change the three-dimensional structure of chromosomes and affect gene expression. Therefore, the combination of different states of histone modifications modulates gene expression is called histone code. The formation of learning and memory is one of the most important mechanisms for animals to adapt to environmental changes. A large number of studies have shown that histone codes are involved in the formation and consolidation of learning and memory. Here, we review the most recent literature of histone modification in regulating neurogenesis, dendritic spine dynamic, synapse formation, and synaptic plasticity.

1. Introduction

Histone modification, as a precise regulation of gene expression to make cells adapt to changes in the environment, plays an important role in neuronal development, plasticity, and behavioral memory. Histone posttranslational modifications affect the spatial structure of chromatin, modulate the transcript and expression of genes, and change biological functions. Therefore, the combination of these histone modification patterns is called "histone codes" [1]. Accumulated evidence has shown that histone modification-mediated chromatin structure remodeling promotes the formation of excitatory synapses and hippocampal-dependent long-term memory. The most important forms of synaptic plasticity are long-term potentiation (LTP) or long-term depression (LTD). These two distinct types of synaptic plasticity reflect the increase and decrease of synaptic transmission efficiency, respectively, and extensive research has been conducted in the field of learning and memory.

2. Histone Modification

The genome of eukaryotes exists in the nucleus in the form of chromosome, which is composed of nucleosomes, which are the basic structure unit of chromatin, and packed with DNA. Two copies of histones H2A, H2B, H3, and H4 form an octamer core, and the approximately 147 base pair DNA is wrapped around the octamer core. Each nucleosome is linked by histone H1 to form higher-order chromatin fibre with a diameter of 30 nm [2, 3]. Increasing evidence has confirmed that at least 12 types of specific modifications occur to the N-terminal amino acid residues of histones, which affect the nucleosomes bind to DNA and the three-dimensional structure of chromosomes, and regulate gene expression. The patterns of histone modification are the following way: acetylation (lysine), methylation (lysine and arginine), phosphorylation (serine and threonine), sumoylation (lysine), ubiquitylation (lysine), ADP ribosylation, butyrylation, citrullination, crotonylation, formylation,

proline isomerization, propionylation, serotonylation, and dopaminylation (glutamine) [4, 5]. The nomenclature of histone modification is as follows, such as H3K9me3, H3 refers to the core histone protein, K refers to the amino acid, the number 9 indicates the position of lysine residue from the N-terminal end of the amino acid tail of histone protein, and me3 refers to the type of modification on the lysine residue [6]. These different combinations and patterns of histone modifications are known as histone code [7].

The different amino acid residues at the N-terminal and C-terminal of these histones will undergo various posttranslational modifications, such as acetylation and methylation at lysine (K) or arginine (R) residues and phosphorylation at serine (S) or threonine (T) residues [8]. The histone acetylation modification is an important histone modification type, which means an increase in gene transcription activity and an epigenetic mark associated with dynamic chromatin. Histone acetyltransferases (HATs) catalyze the transfer of the acetyl group of acetyl-CoA molecule to lysine residues within the histone tails, while histone deacetylases (HDACs) remove these modifications. H3K27ac is related to active gene enhancers, and H4 acetylation is often found in the promoter region and bodies of activated genes. Therefore, histone acetylation can be used to compare gene transcript activity, especially H3 acetylation (H3ac) [9].

A number of amino acid residues in histones can be methylated, and the different methylation types show multiple valence states such as monomethylation (me 1), dimethylation (me 2), and trimethylation (me 3) forms. Therefore, histone methylation pattern changes may either promote gene expression or inhibit gene expression. Methylation of lysine 4 on histone 3 (H3K4) is one of the most studied modifications, with its trimethylated form (H3K4me3) enriched at transcriptional start sites (TSSs) of actively transcribed genes [10]. Histone methyltransferases (HMTs) and demethylases (HDM) are involved in the methylation modification process of histones. Histone methylation modification always occurs on both lysine (K) and arginine (R) side-chain groups of H3 and H4 histone tails. Trimethylaton of lysine 9 on histone 3 (H3K9me3) is often associated with chromatin superaggregation and heterochromatin, and the state of H3K27me3 affects the conversion from heterochromatin to euchromatin [11, 12]. Different modification types of histones also influence each other and together regulate the expression of specific genes. For example, the increase in H3K4me3 increases H3K9Ac, which indicates the mutual regulation function between histone modification and the complexity of gene expression regulation [13].

3. The Effect of Histone Modifications in Neuroplasticity

The brain makes higher animals more adaptable to environmental changes through the process of learning and memory. The formation of learning and memory is inseparable from the synaptic connections between neurons. Histone acetylation and deacetylation modification modulate the chromatin structure to regulate the synaptic connectivity and memory storage-related gene expression. On the other hand, the histone methylation modification states of the promoter region of the gene that controls the synaptic function have also changed, such as the increase of H3K4me3 [14]. More importantly, histone deacetylases 2 (HDAC 2) are enriched at the promoter regions or gene bodies of several neuroplasticity-associated genes, such as BDNF IV, activity-regulated cytoskeleton-associated protein (Arc), Cdk5, Egr1, Homer1, Gria1 and 2, neurofilament light protein (Nfl), N-methyl-D-aspartate receptor subunit 2B (NR2B), synaptophysin (Syn), and synaptotagmin (Syt) [15]. It can be seen that histone modification is involved in the formation of neuronal plasticity and memory formation and consolidation (Table 1 and Figure 1).

In cell nucleus, the histones at gene promoters related to neuroplasticity are modified by acetylation, phosphorylation, methylation, and other modifications, which alter the affinity of histones with these gene promoters. Thereby, it would activate or inhibit the transcriptional activity of these genes and regulate neuroplasticity.

3.1. Neurogenesis. The marks of histone methylation affect the pluripotency of neural progenitor cell (NPC) and determine their neural lineage specification and neuronal differentiation [16]. Polycomb group proteins (PcGs) and trithorax group proteins (TrxGs) antagonistically affect gene expression by histone methylation and demethylation to regulate neuronal differentiation and development. The PcGs are mainly divided into two types of multiprotein complexes, polycomb repressive complexes 1 (PRC1) and 2 (PRC2) [17]. In the central nervous system, the H3K27me3 repressive marks are removed by the histone demethylase Jmjd3 during the differentiation of embryonic stem cells (ESCs) into neural progenitor cell (NPCs) [18]. However, PcGs can prevent the differentiation of ESCs into NPCs by increasing the level of H3K27me3 at neuronal-specific genes such as *Ngns*, *Pax6*, and *Sox1*. In NPCs, the deletion of the subunit Ezh2 of PRC2 signally promotes neurogenesis and neuronal differentiation. In addition, Ezh2 gene silencing is also related to nerve migration [19–21].

RING1B, the core catalytic subunit of PRC1, catalyze H2AK119 monoubiquitination modification at promoters of neuronal-specific genes, such as *Tuj1*, *Ncan*, and *Nestin* to induce human embryonic stem cells (hESCs) and human pluripotent stem cells (hiPSCs) towards neural progenitor differentiation [22]. A maternal low choline diet significantly decreases H3K27me3 levels at the Toll-like receptor 4 (Tlr4) and increases Tlr4 expression, which mediate neuronal differentiation in fetal mouse neural progenitor cells [23]. During neurogenesis, the methylation of H3K4 and H3K36 is often used to indicate increased gene transcription activity, and the removal of H3K4me3 inhibits the expression of neurogenesis-related genes [24].

3.2. Axon Formation. The next-generation sequencing method has confirmed that there are multiple mutations in genes that encode chromatin structure regulators in the neurodevelopmental and psychiatric disorders, such as members of the lysine methyltransferase 2 (KMT2A/C/D) and lysine demethylase 5 (KDM5A/B/C) families. KMT2

Table 1: The histone modification in neuronal plasticity.

Histone	Amino acid	Modification	Method	Impact in neuronal plasticity	References
H2A	K119	Monoubiquitination	The human embryonic stem cells and human pluripotent stem cells	Induce neural progenitor differentiation	Desai et al., 2020 [22]
H3	K9	Deacetylation	Rats	Decreased dendritic spine density	Moonat et al., 2013 [37]
	S10	Phosphorylation	The cortical neuron from Sprague-Dawley rat	Remodel dendritic spine morphology	VanLeeuwen et al., 2014 [36]
	K9, K14	Deacetylation	The hippocampal slices of rat	Increase dendritic spine density and excitatory quantal transmitter release	Calfa et al., 2012 [44]
	K9	Trimethylation	Female Sprague-Dawley rat	Impact the expression of genes with synaptic plasticity	Prini et al., 2017 [57]
	K9	Acetylation	SY5Y cell	Increase dendritic spine density	Al Sayed et al., 2019 [41]
	K4	Monomethylation and trimethylation	SY5Y cell	Increase dendritic spine density	Al Sayed et al., 2019 [41]
H4	K14	Acetylation	Aplysia cell culture	Induce synapse-specific long-term facilitation	Guan et al., 2002 [51]
	K8	Acetylation	Aplysia cell culture	Induce synapse-specific long-term facilitation	Guan et al., 2002 [51]

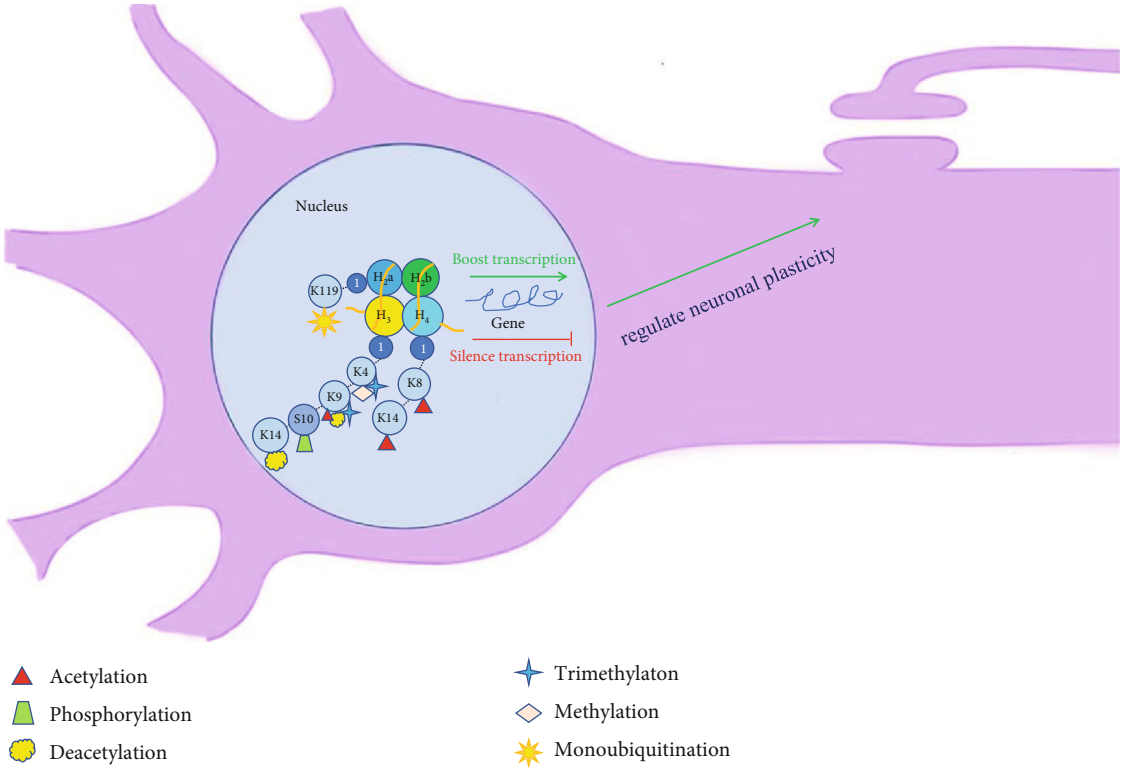

Figure 1: Histone modification mediates neuronal plasticity.

catalyzes the di- and trimethylation of H3K4, while KDM5 executes H3K4 demethylation [25–27]. These results suggest that the methylation of H3K4 is very important for the neuronal development and function in the central nervous system [28, 29]. RBR-2, the sole homolog of the KDM5 family of H3K4me3/2 demethylases in *Caenorhabditis elegans*, controls the axon guidance and growth by regulating the expression of the actin regulator *wsp-1*. Knockout of the *rbp-2* gene increases the level of H3K4me3 at the transcription promoter site of the *wsp-1* gene, resulting in the abnormal transcription and high expression of *wsp-1*, leading to abnormal formation of axon guidance, and similar

results as mutations in H3K4 methyltransferase KMT2F/G (SETD1A/B) genes [30, 31].

In addition to histone methylation regulating axon growth, histone acetylation also regulates axon regeneration and growth. Some research results in the lamprey spinal cord injury model showed that the expression of HDAC1 was upregulated in regenerated neurons, while the expression of HDAC1 did not change in nonregenerating neurons. These results suggest that HDAC1 is involved in neuron regeneration and axon growth [32].

3.3. Density and Morphology of Dendritic Spines. Many years of research has shown that the phosphorylation of the histone H3 protein induces the transformation of chromatin from a heterochromatin state to a euchromatin state, increases the transcriptional activity of genes, regulates the formation and maintenance of dendritic spines, and participates in the process of environmental learning and cognitive formation [33, 34].

The p90 ribosomal S6 kinase (p90RSK) was a protein shuttling from the cytosol to the nucleus, which has multiple functions. In quiescent cells, p90RSK forms a complex with the upstream regulatory molecule ERK1/2 in the cytoplasm. Once the cell is activated by growth factors and ROS, p90RSK would translocate to the nucleus and regulate gene expression through prompting Iκ-B, c-Fos, Nur77, and cAMP-response element-binding protein and other downstream molecule phosphorylation [35]. NMDA receptor activation is crucial for long-term memory. Glycine activates the NMDA receptor of cortical neurons *in vitro*, and p90RSK accumulates in the nucleus in a time-dependent manner, phosphorylate histone H3 at serine 10 (H3S10p), changes the structure of dendritic spines, and regulates the remodeling of dendritic spines [36].

Histone acetylation and methylation modifications also regulate dendritic spine morphogenesis and increase in density. Acute ethanol exposure reduced the activity of HDAC and the expression level of HDAC2 protein in the central nucleus of the amygdala of rat, increased the histone acetylation status of brain-derived neurotrophic factor (BDNF), and activity-regulated cytoskeleton-associated protein (Arc) genes, which attenuated anxiety-like behaviors [37]. ANP32A is one of the most important members of histone acetyltransferase inhibitor, which is abnormally highly expressed in the brains of Alzheimer's disease (AD) patients and model mice. The hippocampal infusion of lenti-siANP32A reduces the ANP32A expression in AD model mice with human tau transgenic, which increases the acetylation of histones in the neuron, promotes the formation of dendritic spines, and restores the learning and memory ability of mice [38]. Histone deacetylase inhibitors increase the number of dendritic spines, enhance synaptic plasticity, and improve memory in young mice [39].

Inhibition of methyltransferase SUV39H1 activity decreases the level of H3K9me3 in the hippocampus of aged mice, which increases BDNF expression levels, and the spine density of thin and stubby. Furthermore, the inhibition of SUV39H1 reversed the deficits in hippocampal memory through enhancing surface GluR1 levels in hippocampal synaptosomes and facilitating synaptic plasticity [40]. The inhibition of H3K4 histone methyltransferase (HMT) activity decreased the level of H3K4me1, H3K4me3, and H3K9Ac, which increased the density of dendritic spine densities in SY5Y cells [41]. UTX, a histone demethylase, could remove the repressive trimethylation of histone H3 lysine 27 (H3K27me3). UTX regulate the expression of a subset of genes that are involved in the regulation of dendritic morphology, synaptic transmission through modulating expression of neurotransmitter 5-hydroxytryptamine receptor 5B (Htr5b) in mouse hippocampal neurons [42].

3.4. Synaptic Plasticity. The BDNF is an important neurotrophin in neuronal survival and growth, which is involved in synaptogenesis, synaptic plasticity, and memory consolidation. Under the different environmental stimuli, the expression of the BDNF gene is regulated by epigenetic mechanisms such as histone modification, DNA methylation, and microRNA machineries [43]. HDAC inhibitors increase the acetylation of the RNA polymerase II at the promoter 3 BDNF gene and histone H4, which enhance BDNF transcription and expression [44]. Cultured rat hippocampal slices in vitro, BDNF treatment increases the density of mature spines (type-I stubby and type-II mushroom) and immature type-III thin spines, enhancing the release of excitatory neurotransmitters and excitatory postsynaptic current (EPSC) in hippocampal slice cultures, while the HDAC inhibitor TSA (trichostatin-A, TSA) reverses this process. Mechanism studies have shown that H3 at lysines 9 and 14 acetylation states participate in this process [45]. The treatment of TSA promotes the BDNF and activity-regulated cytoskeleton-associated protein (Arc) gene expression in the amygdala of rats, increases the dendritic spine density, facilitates synaptic plasticity, and attenuates anxiety-like behaviors of rats [46].

Proper histone acetylation level at the promoter region of the BDNF gene affects LTP and long-term memory. The acetylation of histones H3 and H4 at the activity-dependent BDNF promoters I and IV upregulates the transcription and expression of BDNF in the hippocampus, then enhances the consolidation of fear memory in rats [47]. The expression level of BDNF is decreased in AD patients and mouse model [48, 49]. The sulforaphane, a universal inhibitor of HDAC, is extracted from the hydrolysis product of glucoraphanin present in Brassica vegetables. Sulforaphane inhibited HDAC activity and increased global acetylation states of histone 3 (H3) and H4 in primary cortical neurons. Additional analyses show that sulforaphane enhanced BDNF expression and increased levels of neuronal and synaptic molecules such as microtubule-associated protein 2 (MAP2), synaptophysin, and PSD-95, as well as elevated levels of synaptic TrkB signaling pathway components in primary cortical neurons and $3\times$Tg-AD mice [50]. Microglia is the main form of immune defense in the central nervous system and also has been shown to play a significant role in the synaptic plasticity in neurons. The histone sumoylation modification regulates the expression of phosphatidylinositol 3-kinase (PI3K), the phosphorylation of AKT and CREB, and the expression of BDNF. The ablation or disruption of microglial function

abolishes long-term potentiation (LTP) and reduces synaptic plasticity in rat hippocampal slices [51].

In addition to affecting BDNF gene expression to modulate synaptic plasticity, histone modification also facilitates synaptic plasticity by affecting the expression of other genes, which affects cognition and memory functions. The CAAT box enhancer binding protein (CBP), a histone acetylase, could induce gene expression for the growth of new synapses and for increasing synaptic strength through acetylating lysine residues on core histones. CREB1 recruits CBP into the gene promoter region, and acetylase lysine 8 (K8) of histone H4 and lysine 14 (K14) of histone H3, which form long-term synaptic plasticity with increased synapse strength called long-term facilitation. On the contrary, FMRFamide, an inhibitory transmitter, promotes recruitment HDAD5 and reduces the acetylation of K8 of histone H4 and C/EBP gene expression, which switch the synaptic plasticity to long-term depression [52]. Tip 60, a multifunctional HAT, could modulate the expression of neurogenesis-related genes through epigenetic methods. Targeted loss of Tip60 HAT activity causes thinner and shorter axonal lobes in mushroom body (MB) in the central nervous system of *Drosophila* and defects in immediate-recall memory, while increasing Tip60 HAT levels reverse these process and facilitate immediate-recall memory and cognitive function [53]. K-Acetyltransferase 2a (Kat2a) is a multifunctional histone acetyltransferases (HATs) that has the highest level expression in the hippocampal CA1 region. Kat2a regulates the expression of genes related to the hippocampal gene network linked to the neuroactive receptor by activating the NF-κB signaling pathway, thereby participating in hippocampal synaptic plasticity and long-term memory consolidation [54]. The neuron-specific overexpression of HDAC2 but not that of HDAC1 would reduce dendritic spine density, number of synapses, synaptic plasticity, and memory formation [55].

G9a/G9a-like protein (G9a/GLP), a lysine dimethyltransferase, is an essential role for the formation of the histone H3 lysine 9 dimethylation (H3K9me2). The inhibition of G9a/GLP activity in the entorhinal cortex (EC) enhances H3K9me2 in the area CA1, leading to the silencing of nonmemory permissive gene COMT in the hippocampus, promoting synaptic plasticity, and is conducive to the formation and consolidation of long-term memory. However, the mechanism by which G9a/GLP activity mediates the formation and consolidation of long-term memory (LTM) is different in the hippocampus and entorhinal cortex of SD rats [56]. α-Synuclein (αS) is mostly localized within synapses and linked to Parkinson's disease (PD). The expression level of euchromatic histone lysine N-methyltransferase 2 (EHMT2) was increased in αS-induced SH-SY5Y cells, which enhanced H3K9 methylation (H3K9me2) and the synaptosomal-associated protein SNAP25 expression. Thus, αS overexpression enhances synaptic vesicle fusion events and synaptic plasticity through increasing *EHMT*2 expression to elevate H3K9me2 at the SNAP25 promoter [57]. The cannabis consumption leads to a large number of mental illnesses among adolescents. The Δ9-tetrahydrocannabinol (THC) exposure significantly induce the expression of histone methyltransferase (Suv39H1) and enhance 3K9me3 in the prefrontal cortex of female rats after adolescent. Moreover, the Δ9-tetrahydrocannabinol (THC) exposure downregulates the expression of synaptic plasticity genes, reduces the time for rats to recognize new objects in object recognition experiment (NOR), and destroys cognitive function [58].

4. Summary and Outlook

A large number of research studies have shown that the synaptic plasticity-associated gene expression by neuroepigenetic regulation is essential for the formation and consolidation of learning and memory, and histone modification is one of the most important ways of neuroepigenetic regulation. Under the stimulation of different factors, histones in neurons will undergo various types of chemical modification, such as methylation/demethylation, acetylation/deacetylation, and phosphorylation/dephosphorylation, which could change the three-dimensional structure of chromosomes in the promoter region of synaptic plasticity-related genes and regulate the transcriptional activity of these genes. In the process of neurological disorder, the degradation of dendrites and axons and the reduction of synaptic plasticity are the early morphological pathological changes of the disease. At present, numerous studies on the effect of histone modification inhibitors on synaptic plasticity have been extensively carried out in neurological disorder animal models and achieved meaningful research results. However, in the process of applying histone modification inhibitors to affect synaptic plasticity, how to ensure that the inhibitor can accurately enter the nervous system instead of spreading to the whole body is a problem that must be considered. Secondly, many types of histone modifications are involved in the regulation of synaptic plasticity, but how to determine a certain type of modification is the dominant factor in the regulation of synaptic plasticity in a specific condition, which is also a consideration important factor for the application of histone inhibitors to the prevention and treatment of neurological diseases.

Abbreviations

LTP: Long-term potentiation
LTD: Long-term depression
HATs: Histone acetyltransferases
HDACs: Histone deacetylases
HMT: Histone methyltransferases
Syn: Synaptophysin
Syt: Synaptotagmin
p90RSK: p90 ribosomal S6 kinase
ROS: Reactive oxygen species
NMDA: N-Methyl-D-aspartate
BDNF: Brain-derived neurotrophic factor
AD: Alzheimer's disease
EPSC: Excitatory postsynaptic current
MAP2: Microtubule-associated protein 2
CBP: CAAT box enhancer binding protein
PD: Parkinson's disease
NOR: Object recognition experiment
ESC: Embryonic stem cells
NPC: Neural progenitor cell.

Conflicts of Interest

The authors declare that they have no conflict of interest.

Authors' Contributions

All authors read and approved the final version of the manuscript. H.X.G, H.Y.C, H.Y.W., and L.W. drafted the manuscript. H.X.G. and L.W. conceived and designed the research. H.X.G. and L.W. contributed to writing the manuscript.

Acknowledgments

This work was supported by the National Natural Science Foundation of China (NSFC) grants (81871856), Foundation for University Key from the Ministry of Education of Henan Province (20B180003), and Henan Province Science and Technology Research and Development (212102310695).

References

[1] B. M. Turner, "Cellular memory and the histone code," *Cell*, vol. 111, no. 3, pp. 285–291, 2002.

[2] T. Jenuwein and C. D. Allis, "Translating the histone code," *Science*, vol. 293, no. 5532, pp. 1074–1080, 2001.

[3] J. Wong, D. Patterton, A. Imhof, D. Guschin, Y. B. Shi, and A. P. Wolffe, "Distinct requirements for chromatin assembly in transcriptional repression by thyroid hormone receptor and histone deacetylase," *The EMBO Journal*, vol. 17, no. 2, pp. 520–534, 1998.

[4] M. Tan, H. Luo, S. Lee et al., "Identification of 67 histone marks and histone lysine crotonylation as a new type of histone modification," *Cell*, vol. 146, no. 6, pp. 1016–1028, 2011.

[5] R. D. Shepard and F. S. Nugent, "Early life stress- and drug-induced histone modifications within the ventral tegmental area," *Frontiers in Cell and Development Biology*, vol. 8, p. 588476, 2020.

[6] K. Prakash and D. Fournier, "Evidence for the implication of the histone code in building the genome structure," *Bio Systems*, vol. 164, pp. 49–59, 2018.

[7] J. A. Latham and S. Y. Dent, "Cross-regulation of histone modifications," *Nature Structural & Molecular Biology*, vol. 14, no. 11, pp. 1017–1024, 2007.

[8] B. Ding, "Gene expression in maturing neurons: regulatory mechanisms and related neurodevelopmental disorders," *Sheng Li Xue Bao*, vol. 67, no. 2, pp. 113–133, 2015.

[9] H. He, Z. Hu, H. Xiao, F. Zhou, and B. Yang, "The tale of histone modifications and its role in multiple sclerosis," *Human Genomics*, vol. 12, no. 1, p. 31, 2018.

[10] A. Barski, S. Cuddapah, K. Cui et al., "High-resolution profiling of histone methylations in the human genome," *Cell*, vol. 129, no. 4, pp. 823–837, 2007.

[11] W. Fischle, B. S. Tseng, H. L. Dormann et al., "Regulation of HP1-chromatin binding by histone H3 methylation and phosphorylation," *Nature*, vol. 438, no. 7071, pp. 1116–1122, 2005.

[12] T. Chandra, K. Kirschner, J. Y. Thuret et al., "Independence of repressive histone marks and chromatin compaction during senescent heterochromatic layer formation," *Molecular Cell*, vol. 47, no. 2, pp. 203–214, 2012.

[13] L. A. Gates, J. Shi, A. D. Rohira et al., "Acetylation on histone H3 lysine 9 mediates a switch from transcription initiation to elongation," *The Journal of Biological Chemistry*, vol. 292, no. 35, pp. 14456–14472, 2017.

[14] I. Cheung, H. P. Shulha, Y. Jiang et al., "Developmental regulation and individual differences of neuronal H3K4me3 epigenomes in the prefrontal cortex," *Proceedings of the National Academy of Sciences of the United States of America*, vol. 107, no. 19, pp. 8824–8829, 2010.

[15] C. Schmauss, "The roles of class I histone deacetylases (HDACs) in memory, learning, and executive cognitive functions: a review," *Neuroscience and Biobehavioral Reviews*, vol. 83, pp. 63–71, 2017.

[16] E. Cacci, R. Negri, S. Biagioni, and G. Lupo, "Histone methylation and microRNA-dependent regulation of epigenetic activities in neural progenitor self-renewal and differentiation," *Current Topics in Medicinal Chemistry*, vol. 17, no. 7, pp. 794–807, 2017.

[17] D. Desai and P. Pethe, "Polycomb repressive complex 1: regulators of neurogenesis from embryonic to adult stage," *Journal of Cellular Physiology*, vol. 235, no. 5, pp. 4031–4045, 2020.

[18] T. Burgold, F. Spreafico, F. De Santa et al., "The histone H3 lysine 27-specific demethylase Jmjd3 is required for neural commitment," *PLoS One*, vol. 3, no. 8, article e3034, 2008.

[19] B. E. Bernstein, T. S. Mikkelsen, X. Xie et al., "A bivalent chromatin structure marks key developmental genes in embryonic stem cells," *Cell*, vol. 125, no. 2, pp. 315–326, 2006.

[20] T. S. Mikkelsen, M. Ku, D. B. Jaffe et al., "Genome-wide maps of chromatin state in pluripotent and lineage-committed cells," *Nature*, vol. 448, no. 7153, pp. 553–560, 2007.

[21] T. Di Meglio, C. F. Kratochwil, N. Vilain et al., "Ezh2 orchestrates topographic migration and connectivity of mouse precerebellar neurons," *Science*, vol. 339, no. 6116, pp. 204–207, 2013.

[22] D. Desai, A. Khanna, and P. Pethe, "PRC1 catalytic unit RING1B regulates early neural differentiation of human pluripotent stem cells," *Experimental Cell Research*, vol. 396, no. 1, article 112294, 2020.

[23] X. Guan, X. Chen, L. Dai et al., "Low maternal dietary intake of choline regulates toll-like receptor 4 expression via histone H3K27me3 in fetal mouse neural progenitor cells," *Molecular Nutrition & Food Research*, vol. 3, article e2000769, 2020.

[24] M. Zhang, J. Zhao, Y. Lv et al., "Histone variants and histone modifications in neurogenesis," *Trends in Cell Biology*, vol. 30, no. 11, pp. 869–880, 2020.

[25] J. C. Eissenberg and A. Shilatifard, "Histone H3 lysine 4 (H3K4) methylation in development and differentiation," *Developmental Biology*, vol. 339, no. 2, pp. 240–249, 2010.

[26] M. T. Pedersen and K. Helin, "Histone demethylases in development and disease," *Trends in Cell Biology*, vol. 20, no. 11, pp. 662–671, 2010.

[27] S. M. Kooistra and K. Helin, "Molecular mechanisms and potential functions of histone demethylases," *Nature Reviews Molecular Cell Biology*, vol. 13, no. 5, pp. 297–311, 2012.

[28] J. L. Ronan, W. Wu, and G. R. Crabtree, "From neural development to cognition: unexpected roles for chromatin," *Nature Reviews Genetics*, vol. 14, no. 5, pp. 347–359, 2013.

[29] C. N. Vallianatos and S. Iwase, "Disrupted intricacy of histone H3K4 methylation in neurodevelopmental disorders," *Epigenomics*, vol. 7, no. 3, pp. 503–519, 2015.

[30] L. Mariani, Y. C. Lussi, J. Vandamme, A. Riveiro, and A. E. Salcini, "The H3K4me3/2 histone demethylase RBR-2 controls axon guidance by repressing the actin-remodeling gene wsp-1," *Development*, vol. 143, no. 5, pp. 851–863, 2016.

[31] S. Abay-Nørgaard, B. Attianese, L. Boreggio, and A. E. Salcini, "Regulators of H3K4 methylation mutated in neurodevelopmental disorders control axon guidance in *Caenorhabditis elegans*," *Development*, vol. 147, no. 15, article dev190637, 2020.

[32] J. Chen, C. Laramore, and M. I. Shifman, "Differential expression of HDACs and KATs in high and low regeneration capacity neurons during spinal cord regeneration," *Experimental Neurology*, vol. 280, pp. 50–59, 2016.

[33] S. L. Berger, "The complex language of chromatin regulation during transcription," *Nature*, vol. 447, no. 7143, pp. 407–412, 2007.

[34] F. D. Lubin and J. D. Sweatt, "The IkappaB kinase regulates chromatin structure during reconsolidation of conditioned fear memories," *Neuron*, vol. 55, no. 6, pp. 942–957, 2007.

[35] S. Itoh, B. Ding, C. P. Bains et al., "Role of p90 ribosomal S6 kinase (p90RSK) in reactive oxygen species and protein kinase C β (PKC-β)-mediated cardiac troponin I phosphorylation," *The Journal of Biological Chemistry*, vol. 280, no. 25, pp. 24135–24142, 2005.

[36] J. E. VanLeeuwen, I. Rafalovich, K. Sellers et al., "Coordinated nuclear and synaptic shuttling of afadin promotes spine plasticity and histone modifications," *The Journal of Biological Chemistry*, vol. 289, no. 15, pp. 10831–10842, 2014.

[37] S. Moonat, A. J. Sakharkar, H. Zhang, L. Tang, and S. C. Pandey, "Aberrant histone deacetylase2-mediated histone modifications and synaptic plasticity in the amygdala predisposes to anxiety and alcoholism," *Biological Psychiatry*, vol. 73, no. 8, pp. 763–773, 2013.

[38] G. S. Chai, Q. Feng, Z. H. Wang et al., "Downregulating ANP32A rescues synapse and memory loss via chromatin remodeling in Alzheimer model," *Molecular Neurodegeneration*, vol. 12, no. 1, p. 34, 2017.

[39] L. Peixoto and T. Abel, "The role of histone acetylation in memory formation and cognitive impairments," *Neuropsychopharmacology*, vol. 38, no. 1, pp. 62–76, 2013.

[40] S. Snigdha, G. A. Prieto, A. Petrosyan et al., "H3K9me3 inhibition improves memory, promotes spine formation, and increases BDNF levels in the aged hippocampus," *The Journal of Neuroscience*, vol. 36, no. 12, pp. 3611–3622, 2016.

[41] R. Al Sayed, W. Smith, N. Rogers et al., "A 2x folic acid treatment affects epigenetics and dendritic spine densities in SHSY5Y cells," *Biochemistry and Biophysics Reports*, vol. 20, article 100681, 2019.

[42] G. B. Tang, Y. Q. Zeng, P. P. Liu et al., "The histone H3K27 demethylase UTX regulates synaptic plasticity and cognitive behaviors in mice," *Frontiers in Molecular Neuroscience*, vol. 10, p. 267, 2017.

[43] N. N. Karpova, "Role of BDNF epigenetics in activity-dependent neuronal plasticity," *Neuropharmacology*, vol. 76, pp. 709–718, 2014.

[44] G. Calfa, C. A. Chapleau, S. Campbell et al., "HDAC activity is required for BDNF to increase quantal neurotransmitter release and dendritic spine density in CA1 pyramidal neurons," *Hippocampus*, vol. 22, no. 7, pp. 1493–1500, 2012.

[45] C. You, H. Zhang, A. J. Sakharkar, T. Teppen, and S. C. Pandey, "Reversal of deficits in dendritic spines, BDNF and Arc expression in the amygdala during alcohol dependence by HDAC inhibitor treatment," *The International Journal of Neuropsychopharmacology*, vol. 17, no. 2, pp. 313–322, 2014.

[46] S. Takei, S. Morinobu, S. Yamamoto, M. Fuchikami, T. Matsumoto, and S. Yamawaki, "Enhanced hippocampal BDNF/TrkB signaling in response to fear conditioning in an animal model of posttraumatic stress disorder," *Journal of Psychiatric Research*, vol. 45, no. 4, pp. 460–468, 2011.

[47] J. W. Hao, Y. G. Li, L. Wang, and H. X. Geng, "Effect of BDNF expression in cerebral cortex and hippocampus on ability of learning and memory in APP/PS1 transgenic mice," *Chinese Journal of Pathophysiology*, vol. 35, no. 5, pp. 858–864, 2019.

[48] B. Michalski and M. Fahnestock, "Pro-brain-derived neurotrophic factor is decreased in parietal cortex in Alzheimer's disease," *Brain Research Molecular Brain Research*, vol. 111, no. 1-2, pp. 148–154, 2003.

[49] J. Kim, S. Lee, B. R. Choi et al., "Sulforaphane epigenetically enhances neuronal BDNF expression and TrkB signaling pathways," *Molecular Nutrition & Food Research*, vol. 61, no. 2, 2017.

[50] G. Saw, K. Krishna, N. Gupta et al., "Epigenetic regulation of microglial phosphatidylinositol 3-kinase pathway involved in long-term potentiation and synaptic plasticity in rats," *Glia*, vol. 68, no. 3, pp. 656–669, 2020.

[51] Z. Guan, M. Giustetto, S. Lomvardas et al., "Integration of long-term-memory-related synaptic plasticity involves bidirectional regulation of gene expression and chromatin structure," *Cell*, vol. 111, no. 4, pp. 483–493, 2002.

[52] S. Xu, R. Wilf, T. Menon, P. Panikker, J. Sarthi, and F. Elefant, "Epigenetic control of learning and memory in Drosophila by Tip60 HAT action," *Genetics*, vol. 198, no. 4, pp. 1571–1586, 2014.

[53] R. M. Stilling, R. Rönicke, E. Benito et al., "K-Lysine acetyltransferase 2a regulates a hippocampal gene expression network linked to memory formation," *The EMBO Journal*, vol. 33, no. 17, pp. 1912–1927, 2014.

[54] J. S. Guan, S. J. Haggarty, E. Giacometti et al., "HDAC2 negatively regulates memory formation and synaptic plasticity," *Nature*, vol. 459, no. 7243, pp. 55–60, 2009.

[55] S. Gupta-Agarwal, A. V. Franklin, T. Deramus et al., "G9a/GLP histone lysine dimethyltransferase complex activity in the hippocampus and the entorhinal cortex is required for gene activation and silencing during memory consolidation," *The Journal of Neuroscience*, vol. 32, no. 16, pp. 5440–5453, 2012.

[56] N. Sugeno, S. Jäckel, A. Voigt, Z. Wassouf, J. Schulze-Hentrich, and P. J. Kahle, "α-Synuclein enhances histone H3 lysine-9 dimethylation and H3K9me2-dependent transcriptional responses," *Scientific Reports*, vol. 6, article 36328, 2016.

[57] P. Prini, F. Rusconi, E. Zamberletti et al., "Adolescent THC exposure in female rats leads to cognitive deficits through a mechanism involving chromatin modifications in the prefrontal cortex," *Journal of Psychiatry & Neuroscience*, vol. 43, no. 2, pp. 87–101, 2018.

[58] C. Schmauss, "An HDAC-dependent epigenetic mechanism that enhances the efficacy of the antidepressant drug fluoxetine," *Scientific Reports*, vol. 5, no. 1, article 8171, 2015.

Hindawi
Neural Plasticity
Volume 2021, Article ID 6636999, 6 pages
https://doi.org/10.1155/2021/6636999

Research Article

Effect of Cognitive Function on Balance and Posture Control after Stroke

Hui-xian Yu,[1,2] Zhao-xia Wang,[1,2] Chang-bin Liu,[1,2] Pei Dai,[1,2] Yue Lan,[3] and Guang-qing Xu[4]

[1]*Department of Rehabilitation Medicine, Beijing Tiantan Hospital, Capital Medical University, Beijing 100060, China*
[2]*China National Clinical Research Center for Neurological Diseases, Beijing 100060, China*
[3]*Department of Rehabilitation Medicine, Guangzhou First People's Hospital, School of Medicine, South China University of Technology, Guangzhou 510050, China*
[4]*Department of Rehabilitation Medicine, Guangdong General Hospital, Guangdong Academy of Medical Sciences, 510080, China*

Correspondence should be addressed to Yue Lan; bluemooning@163.com and Guang-qing Xu; guangchingx@163.com

Received 13 November 2020; Revised 1 January 2021; Accepted 13 January 2021; Published 28 January 2021

Academic Editor: Wei-Lin Liu

Hemiplegic gait is the most common sequela of stroke. Patients with hemiplegic gait are at a risk of falling because of poor balance. The theory of cognitive-motor networks paved the way for a new field of research. However, the mechanism of the relationship of cognition with gait or posture control networks is unclear because of the dynamic characteristics of walking and changing postures. To explore differences in the balance function and fall risk between patients with and without cognitive impairment after stroke, we utilized the Berg balance scale, Timed "Up and Go" test, and 10 m walking test. Patients were divided into two groups: the observation group (16 patients, female 6 and male 10), comprising patients with cognitive impairment after stroke, and the control group (16 patients, female 7 and male 9), comprising patients without cognitive impairment after stroke. We found that patients with cognitive impairment had worse balance function and a higher risk of falls. They needed a longer time to turn around or sit down. Our findings indicated that posture control in turning around and sitting down required more cognitive resources in daily life.

1. Introduction

Approximately 60% to 80% of patients after stroke cannot ambulate independently after completion of rehabilitation, and many of them have hemiplegic gait, which limits motor function [1]. Decreased balance and gait after stroke are the most common factors of decreased activities of daily living (ADL). Falls are a major adverse event in daily care. Approximately 60% of patients fall at least once during hospitalization, while 73% of them fall in the first 6 months after stroke [2]. Falling can increase the patient's fear of falling, restrict activity, and increase dependency [3]. A fall can enhance social dependence, cause serious anxiety and depression [4], and prolong hospitalization. It can also cause hip fractures, necessitating long-term wheelchair use after stroke [5].

In earlier reports, most researchers thought that our actions were controlled by the motor system alone. However, recently, many researchers have found that a sensory-cognitive-motor network system is necessary to ascertain the accuracy of an action [6–8]. The sensory-cognitive-motor neural circuits involve the frontal cortex, subcortex, basal ganglia (caudate nucleus, globus pallidus, and thalamus), brainstem, and cerebellum [9]. They can ensure safe and effective posture changing for adaptation to complex environments at home or in a community. Cognition is associated with gait velocity [10]. Evidence has been increasing on the associations between cognitive function and balance in the elderly patients with Alzheimer's or Parkinson's disease [11, 12]. However, limited research has focused on this relationship after stroke. Elucidating the relationship between the brain areas for motor function and cognition is

important for establishing rehabilitation strategies. Our assumptions on balance and posture control guide how we assess and treat balance and posture control disorders. Therefore, understanding the mechanisms of cognitive function in posture control and coordination could help us improve balance and reduce the incidence of falls. This study was aimed at observing the effects of cognitive function on balance and fall during complex motor skills for ADL performed by patients after stroke.

2. Methods

2.1. Patients. A retrospective case-control study design was used. We collected the data of 32 patients with hemiplegic gait after stroke. Patients were divided into two groups: the observation group, comprising patients with cognitive impairment (CI), and the control group, comprising patients without CI. From the department of rehabilitation from May 2019 to January 2020, we randomly selected 16 patients, including ten men and six women, with a Montreal Cognitive Assessment (MoCA) score of 15–25, and 16 patients, including nine men and seven women, with an MoCA score ≥ 26. Inclusion criteria were (1) the definitive diagnosis of first-ever stroke, (2) localization of stroke in the basal ganglia region of the right or left hemisphere, (3) age of 40–60 years, (4) ≤3 months poststroke, (5) junior high school education, (6) lower-limb Fugl-Meyer motor assessment score of 20–30, and (7) independent walking for several meters. Exclusion criteria were (1) prestroke vascular dementia, (2) aphasia, (3) traumatic hemorrhage, (4) sensory impairment, (5) medical instability hindering participation, and (6) visual or hearing impairment.

2.2. Screening Measures. MoCA was first developed by Nasreddine et al. [13]. It is a brief screening tool to evaluate cognitive and attentive/executive functions and has also been used in studies on executive function assessment [14]. The scale includes eight cognitive domains with a best potential score of 30 points. Each correct answer accounts for 1 point, while a wrong answer or no answer accounts for 0 point.

2.3. Outcome Measurement. The Berg balance scale (BBS) was used to assess balance function for activity limitations [15]. It is a consensus measurement of the International Classification Functioning (ICF) activity on a five-point scale, ranging from 0 to 4, where "0" indicates the lowest level of function and "4" the highest, with a total score of 56.

The fall risk was assessed with the Timed "Up and Go" test (TUGT) [16], constituting five steps: getting up, walking, turning around, walking, and sitting down (Figure 1). Patients were asked to stand up from a standardized armchair, walk 3 m (marked by two tapes: one, 0.5 m from the chair; another, 0.5 m from the cone), turn around the cone, and sit down on the chair safely. To clarify the difference in each posture condition between the two groups, we divided the process into four periods: getting up, walking straight, turning around, and sitting down. Before testing, participants sat in the chair. The tester recorded the time taken to complete the four processes with a stopwatch. Getting-up time (GT) was the time between the patient's back leaving the chair and the patient reaching the line drawn 0.5 m from the chair. Walking-straight time (WT) was the time between the patient reaching the line 0.5 m from the chair and the patient reaching the line 0.5 m from the cone. Turning-around time (TT) was the time between the patient reaching the line 0.5 m from the cone and the patient finishing the turning and crossing the line 0.5 m from the cone. Sitting time (ST) was the time between the patient reaching 0.5 m from the chair and the patient sitting down again with their back to the chair. The total time of "get up and go" is TGUG.

The 10 m walking test (10MWT) was used to assess the walking function. Patients walked from the taped line on the floor to an invisible line drawn 10 m away, which they were unaware of. Testers recorded the time with a stopwatch between the patient's first step crossing the line and the patient's first leg crossing the invisible line [17].

2.4. Data Analysis. The statistical analysis and graphing were performed using GraphPad Prism 8.0 (GraphPad Software, Inc., San Diego, California, USA). Continuous variables are expressed as the mean ± standard deviation. The unpaired t-test was performed to evaluate between- and within-group differences before and after the treatment of patients in the observation and control groups. A P value < 0.05 was considered statistically significant.

3. Results

Age, sex, onset time, lesions, or scores of the lower-limb Fugl-Meyer motor assessment did not differ from baseline in either group, and there was no difference in baseline data between the groups (Table 1). BBS scores were significantly lower in the observation group than in the control group ($P = 0.039$; Figure 2). As for TUGT, the overall time was significantly longer in the observation group than in the control group ($P = 0.005$; Figure 3). GT or WT did not significantly differ between the groups (GT, $P = 0.18$; WT, $P = 0.19$). TGUG, TT, and ST were significantly longer in the observation group than in the control group (TGUG, $P = 0.005$; TT, $P = 0.003$; and ST, $P = 0.002$). The 10MWT scores did not differ between the two groups ($P = 0.48$; Figure 4).

4. Discussion

This study showed that patients with poor cognitive function had worse balance and posture control. Compared to walking straight, turning around and sitting down required more cognitive resources. Patients with hemiplegia with CI had a greater risk of fall during turning around or sitting down. These results suggested that we should pay more attention to the training of turning around or sitting down in the balance training of patients with CI after stroke.

The BBS is commonly used to evaluate balance function after stroke. Patients with CI had significantly poorer balance function than those without CI. This may be associated with decreased executive function, which is subsumed by frontal regions and is the most common type of impairment in cognitive function. Pahlman et al. reported that differences in

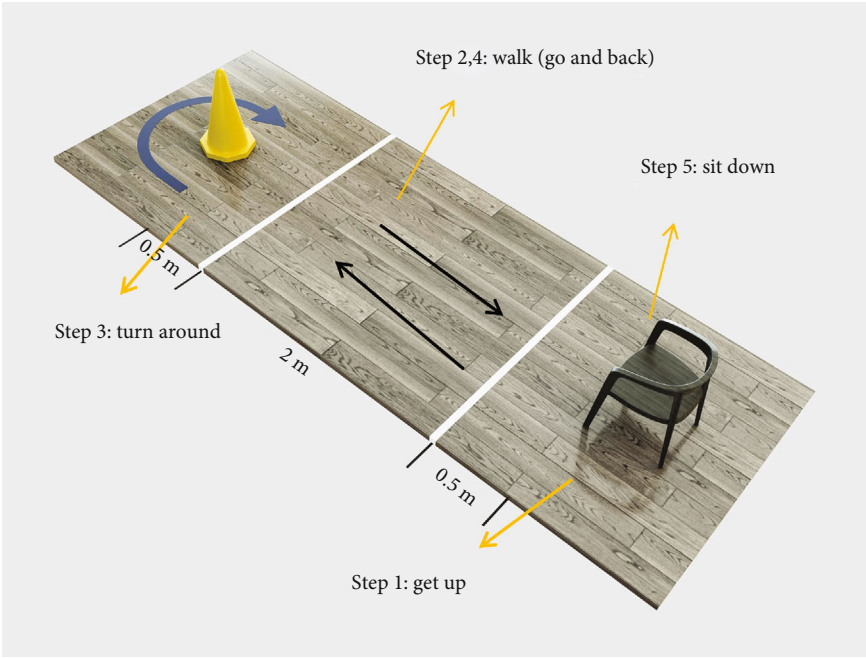

Figure 1: Timed "Up and Go" test was divided into four periods based on the posture: steps 1, 2+4, 3, and 5. The times in the four periods are shown.

Table 1: The baseline data.

Group	Age (years)	Sex (number)	Hemiplegic limb (number)	Onset time (month)	Fugl-Meyer (lower-limb)
Control group	52.31 ± 8.56	Female 7 Male 9	Left 8 Right 8	2.33 ± 0.24	23.21 ± 7.34
Observation group	51.56 ± 11.03	Female 6 Male 10	Left 9 Right 7	3.12 ± 0.98	20.97 ± 9.56

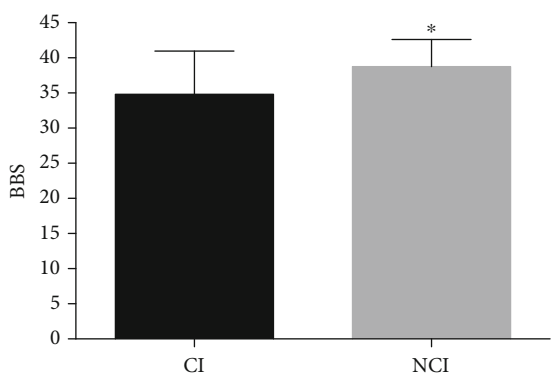

Figure 2: Differences in Berg balance scale scores between the observation and control groups. A P value < 0.05 was considered to indicate statistical significance.

BBS scores between patients with and without executive dysfunction were significant in the first year poststroke [18].

Although some studies reported that cognition has a mediating effect on some associations between gait velocity and volumes [6, 19, 20], the present study showed no significant difference in 10MWT results between the two groups. It is currently unclear if cognition directly affects gait velocity and if impairments in both gait and cognition result from changes within the brain. Our understanding of the interactions among gait, cognition, and brain, and whether or not it applies to gait characteristics other than velocity, is limited because of the scarcity of studies assessing cognition in addition to gait with neuroimaging parameters [21]. Walking in the community can be more challenging for stroke survivors. Our results suggested that declined cognitive function would increase the risk of falling during turning around and sitting down after stroke. It is unclear if there is a direct relationship between gait and cognition, if CI directly impacts gait velocity, or if CI and hemiplegic gait are concurrent sequelae due to damaged cognitive-gait neural circuits after stroke. Our understanding is limited on the interactions among gait, cognition, and cognitive-gait neural circuits and on which gait characteristics would manifest with CI after stroke.

Unlike walking in a straight line, the control of balance during gait and changing postures (getting up, walking, stopping, turning around, and sitting down) requires a complex control of the center of body weight. The TUGT, which detects the risk of falls in individuals with stroke, includes several parts of autonomous posture control, such as the movement from sitting to standing (which requires the

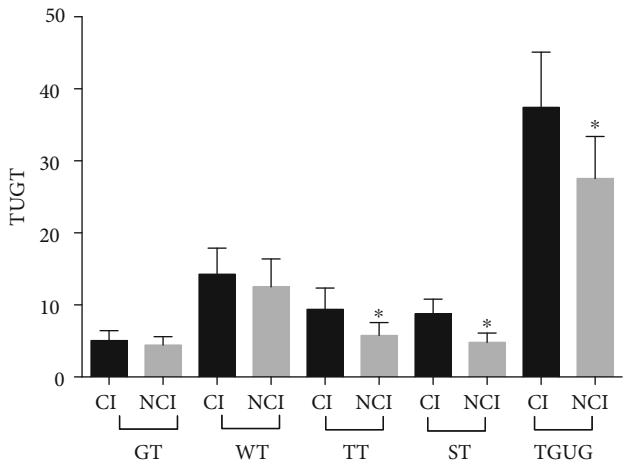

Figure 3: Differences in the overall time in the Timed "Up and Go" test and the times of the four periods of getting up, walking straight, turning around, and sitting down between the observation and control groups. *A P value < 0.05 was considered to indicate statistical significance. GT: getting-up time; WT: walking-straight time; TT: turning-around time; ST: sitting time; TGUG: the total time of "get up and go."

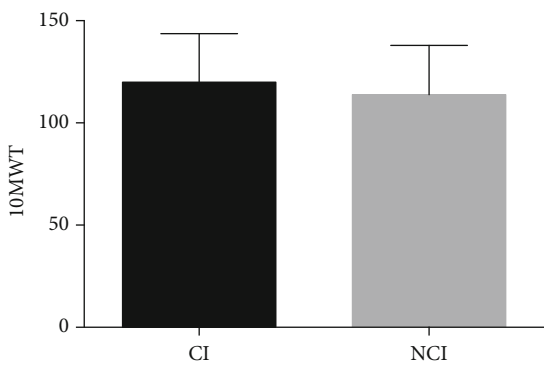

Figure 4: Differences in 10 m walking test between the observation and control groups. A P value > 0.05 was considered to not indicate statistical significance.

participation of expected posture adjustment ability), continuous walking (which requires dynamic control ability), and turning and sitting (which requires participation of spatial orientation ability) [22]. The present study showed significant differences in TUGT scores between the observation and control groups. The overall time was significantly longer in the observation group than in the control group. In TUGT, because different positions were timed separately, we could observe the time difference between the two groups in different postures. Further, ST and TT significantly differed between the two groups. The results indicated that sitting (walking to the chair, turning around, determining the height of the chair, and sitting down smoothly) and turning (stopping the walk, noticing the cone, and steering around the obstacle safely) required greater spatial orientation and attention ability based on the interpretation of convergent sensory information from the somatosensory, vestibular, and visual systems. There was no difference in WT and GT between the two groups. The results indicated that walking in a straight line and getting up required less cognitive resources.

Falls after stroke are common [23]. There are many factors that lead to fall in stroke patients, including impaired balance and damaged posture control. Postural control refers to the control of the body's position in space for the purpose of stability and orientation. Postural orientation is the ability to maintain appropriate relationships between the different body segments and the task environment, with the help of the vestibular system, the somatosensory system, and the visual system. Postural stability, also known as balance, is the ability to control the relationship between the center of mass and the base of support. Posture to adapt to the environment requires the perception, spatial orientation, and the ability to pay attention to environmental changes. Postural orientation determines the position of objects, actively aligns the trunk and head with respect to gravity, and considers surfaces, visual surroundings, and internal references. In ADL or community activity, patients need complex posture control abilities (including posture stability and orientation) for adaptation to the complex environments to avoid falling. A safe, smooth, and coordinated motion is regulated by the sensory-cognitive-motor system. The viewpoint is inaccurate that the motor system is sufficient in controlling effective motions. Every motion involves a highly complex skill-posture control in the process of cognition for adaption to the current environment [24]. While in walking, people generally prepare for the walk, stop, change the speed, turn, perform tasks, sit down, and so on. The two main functional goals of postural behavior are orientation and equilibrium.

An inappropriate preparation can cause a fall. However, studies are limited on accurate postural assessment, balance assessment, or resource allocation of cognitive function after stroke. Mechanisms mediating the preparation of coordinated motor function have not been clearly elucidated. It is important to understand the potential preparatory mechanisms for coordinated actions. Motor mechanisms in the brain are viewed as a slave system under the dictate of cognition. Accordingly, modality-specific sensory modules channel information to the central systems for attention, memory, language, concepts, and decisions, which, in turn, drive the motor output [25]. Previous studies have suggested that hemiplegic gait and poor balance function lead to falls. Recently, increasing evidence has suggested that cognitive function is involved in complex motor and posture control and that posture control during walking receives instructions from the cognitive brain regions. The prefrontal cortex is the central brain region for cognitive function. It is strongly associated with the primary motor cortex, motor area cortex (M1 area), subcortical structures, and cerebellum [26]. The regions, whether anatomical connections or functional network connections, related to gait posture control are uncertain. Some studies have focused on one or several regions, but a very few studies have assessed regions connected through structural tracts, which connect brain regions of posture control and cognition [18]. A study assessed the functional networks connecting the brain regions of cognition and gait posture control [27]. The basal ganglia region is

the most common site of stroke. Studies using neuroanatomy, neurophysiology, and functional magnetic resonance imaging have demonstrated that the cortical motor areas, basal ganglia, and cerebellum not only are associated with motor control but also play roles in cognition, language processing, perception, and learning [28]. The dorsolateral prefrontal cortex (the anatomical origin of cognitive function) connects with the striatum, basal ganglia, and thalamus through white matter tracts [29]. This frontal-subcortical circuit links cognitive and motor brain processes to adapt with environment. These impairments impact an individual's abilities to perform ADL and are associated with an increased risk of falls.

The simple view of a balance system that one or a few balance centers in the central nervous system were responsible to control balance is limiting and can partially account for our limited abilities to assess risks of falling accurately, to improve balance, or to reduce falls. Cognitive dysfunction, particularly executive dysfunction, is obscured by other sequelae after stroke. Mild CI may often be overlooked during evaluation in clinical settings [30]. With further studies on cognitive-motor functional brain networks, the new theory of balance and posture control could improve, and rehabilitation strategies could be more accurate. In our present study, based on the new cognitive-motor brain function network theory, we observed the important effect of cognitive function on postural control. Cognitive training may be a new therapeutic target to improve postural control after stroke.

Our study had some limitations. First, it was a retrospective study, which would provide a lower level of evidence than a randomized controlled trial. Second, we grouped patients only based on MoCA as the screening tool. In our subsequent studies, different cognitive domains were evaluated to understand the influence of different cognitive disorders on postural control. Finally, we did not collect the executive function, spatial orientation, and attention separately to clarify the effects of different cognitive functions on posture control and gait. We will continue to explore the characteristics of postural control disorders with CI after stroke. At the same time, in our further research (already ongoing), functional magnetic resonance imaging will be used to scan the brain of patients with or without CI after stoke. We will analyze the data, observe the activation of the regions of interest, and finally explore the cognitive-postural control brain network to find new therapeutic targets.

5. Conclusions

Patients with poststroke CI had poorer balance and a higher risk of falls. In daily activities, the risk of falls is significant during posture control, including turning and sitting. Our study suggested that posture control in turning around and sitting down required more cognitive resources in daily life. In physical therapy of balance and motor control after stroke, the assessment of cognitive function should not be neglected.

Data Availability

If you need our data, please contact the corresponding authors.

Conflicts of Interest

The authors declare that they have no conflicts of interest.

Acknowledgments

This work was supported by grants from the National Natural Science Foundation of China (Grant Numbers: 82072548, 81974357, and 81772438), the Science and Technology Planning Project of Guangdong Province, China (Grant Numbers: 2016A020213003), the Guangzhou Science and Technology Plan Project, China (grant numbers 201803010083), and the Fundamental Research Funds for the Central Universities (2018PY03).

References

[1] C. Dean and F. Mackey, "Motor assessment scale scores as a measure of rehabilitation outcome following stroke," *The Australian Journal of Physiotherapy*, vol. 38, no. 1, pp. 31–35, 1992.

[2] F. A. Batchelor, S. F. Mackintosh, C. M. Said, and K. D. Hill, "Falls after stroke," *International Journal of Stroke*, vol. 7, no. 6, pp. 482–490, 2012.

[3] Y. Watanabe, "Fear of falling among stroke survivors after discharge from inpatient rehabilitation," *International Journal of Rehabilitation Research*, vol. 28, no. 2, pp. 149–152, 2005.

[4] A. Forster and J. Young, "Incidence and consequences of falls due to stroke: a systematic inquiry," *BMJ*, vol. 311, no. 6997, pp. 83–86, 1995.

[5] S. Pouwels, A. Lalmohamed, B. Leufkens et al., "Risk of hip/femur fracture after stroke," *Stroke*, vol. 40, no. 10, pp. 3281–3285, 2009.

[6] M. Montero-Odasso, J. Verghese, O. Beauchet, and J. M. Hausdorff, "Gait and cognition: a complementary approach to understanding brain function and the risk of falling," *American Geriatrics Society*, vol. 60, no. 11, pp. 2127–2136, 2012.

[7] H. J. Park, N. G. Lee, and T. W. Kang, "Fall-related cognition, motor function, functional ability, and depression measures in older adults with dementia," *NeuroRehabilitation*, vol. 3, pp. 11–18, 2020.

[8] Q. Tian, S. A. Studenski, M. Montero-Odasso, C. Davatzikos, S. M. Resnick, and L. Ferrucci, "Cognitive and neuroimaging profiles of older adults with dual decline in memory and gait speed," *Neurobiology of Aging*, vol. 97, pp. 49–55, 2021.

[9] J. Yuan, H. M. Blumen, and J. Verghese, "Functional connectivity associated with gait velocity during walking and walking-while-talking in aging: a resting-state fMRI study," *Brain Mapp*, vol. 36, no. 4, pp. 1484–1493, 2015.

[10] R. Morris, S. Lord, J. Bunce, D. Burn, and L. Rochester, "Gait and cognition: mapping the global and discrete relationships in ageing and neurodegenerative disease," *Neuroscience and Biobehavioral Reviews*, vol. 64, pp. 326–345, 2016.

[11] K. E. Kobayashi-Cuya, R. Sakurai, N. Sakuma et al., "Hand dexterity, not handgrip strength, is associated with executive function in Japanese community-dwelling older adults: a

cross-sectional study," *BMC Geriatrics*, vol. 18, no. 1, p. 192, 2018.

[12] B. d. A. Almeida and A. C. Hamdan, "Impulsiveness and executive functions in Parkinson's disease," *Dementia & Neuropsychologia*, vol. 13, no. 4, pp. 410–414, 2019.

[13] Z. S. Nasreddine, N. A. Phillips, V. Bédirian et al., "The Montreal Cognitive Assessment, MoCA: a brief screening tool for mild cognitive impairment," *Journal of the American Geriatrics Society*, vol. 53, no. 4, pp. 695–699, 2005.

[14] H. Zhang, Y. Peng, C. Li et al., "Playing mahjong for 12 weeks improved executive function in elderly people with mild cognitive impairment: a study of implications for TBI-inducedcognitive deficits.," *Frontiers in Neurology*, vol. 11, p. 178, 2020.

[15] H. F. Mao, I. P. Hsueh, P. F. Tang, C. F. Sheu, and C. L. Hsieh, "Analysis and comparison of the psychometric properties of three balance measures for stroke patients," *Stroke*, vol. 33, no. 4, pp. 1022–1027, 2002.

[16] D. Podsiadlo and S. Richardson, "The timed "Up & Go": a test of basic functional mobility for frail elderly persons," *Journal of the American Geriatrics Society*, vol. 39, no. 2, pp. 142–148, 1991.

[17] B. T. Brice, H. Arshad, and S. Madhavan, "Concurrent validity of the GAITRite electronic walkway and the 10-m walk test for measurement of walking speed after stroke," *Gait & Posture*, vol. 68, pp. 458–460, 2019.

[18] U. Påhlman, C. Gutiérrez-pérez, M. Sävborg, E. Knopp, and E. Tarkowski, "Cognitive function and improvement of balance after stroke in elderly people: the Gothenburg cognitive stroke study in the elderly," *Disability and Rehabilitation*, vol. 33, no. 21-22, pp. 1952–1962, 2011.

[19] V. C. San Martín, L. D. Moscardó, and J. López-Pascual, "Effects of dual-task group training on gait, cognitive executive function, and quality of life in people with Parkinson disease: results of randomized controlled DUALGAIT trial," *Archives of Physical Medicine and Rehabilitation*, vol. 101, no. 11, pp. 1849–1856.e1, 2020.

[20] Y. Liao, I. Chen, Y. J. Lin, Y. Chen, and W. Hsu, "Effects of virtual reality-based physical and cognitive training on executive function and dual-task gait performance in older adults with mild cognitive impairment: a randomized control trial," *Frontiers in Aging Neuroence*, vol. 11, p. 62, 2019.

[21] J. Wilson and L. Allcock, "Ríona Mc Ardle,et al. The neural correlates of discrete gait characteristics in ageing: a structured review," *Neuroscience and Biobehavioral Reviews*, vol. 100, pp. 344–369, 2019.

[22] C. U. Persson, P. O. Hansson, and K. S. Sunnerhagen, "Clinical tests performed in acute stroke identify the risk of falling during the first year: postural stroke study in Gothenburg (POSTGOT)," *Journal of Rehabilitation Medicine*, vol. 43, no. 4, pp. 348–353, 2011.

[23] N. Kerse, V. Parag, V. L. Feigin et al., "Falls after stroke," *Stroke*, vol. 39, no. 6, pp. 1890–1893, 2008.

[24] S. Falbo, G. Condello, L. Capranica, R. Forte, and C. Pesce, "Effects of physical-cognitive dual task training on executive function and gait performance in older adults: a randomized controlled trial," *BioMed Research International*, vol. 2016, 12 pages, 2016.

[25] T. Hanakawa, "Rostral premotor cortex as a gateway between motor and cognitive networks," *Neuroscience Research*, vol. 70, no. 2, pp. 144–154, 2011.

[26] C. Blahak, H. Baezner, L. Pantoni et al., "Deep frontal and periventricular age related white matter changes but not basal ganglia and infratentorial hyperintensities are associated with falls: cross sectional results from the LADIS study," *Neurology, Neurosurgery & Psychiatry*, vol. 80, no. 6, pp. 608–613, 2009.

[27] V. J. Verlinden, M. de Groot, L. G. Cremers et al., "Tract-specific white matter microstructure and gait in humans," *Neurobiology of Aging*, vol. 43, pp. 164–173, 2016.

[28] T. Popa, L. S. Morris, R. Hunt et al., "Modulation of resting connectivity between the mesial frontal cortex and basal ganglia," *Frontiers in Neurology*, vol. 10, p. 587, 2019.

[29] I. Obeso, L. Wilkinson, J. T. Teo, P. Talelli, J. C. Rothwell, and M. Jahanshahi, "Theta burst magnetic stimulation over the pre-supplementary motor area improves motor inhibition," *Brain stimulation*, vol. 10, no. 5, pp. 944–951, 2017.

[30] A. Jaillard, B. Naegele, S. Trabucco-Miguel, J. F,. LeBas, and M. Hommel, "Hidden dysfunctioning in subacute stroke," *Stroke*, vol. 40, no. 7, pp. 2473–2479, 2009.

Hindawi
Neural Plasticity
Volume 2021, Article ID 6648004, 9 pages
https://doi.org/10.1155/2021/6648004

Review Article

The Mechanisms of Peripheral Nerve Preconditioning Injury on Promoting Axonal Regeneration

Xiaoyan Yang,[1,2] Ruixuan Liu,[1] Ying Xu,[1] XiangYu Ma,[1] and Bing Zhou[1,2]

[1]*Beijing Advanced Innovation Center for Big Data-Based Precision Medicine, Beihang University, Beijing 100191, China*
[2]*Interdisciplinary Innovation Institute of Medicine and Engineering Interdisciplinary, Beihang University, Beijing 100191, China*

Correspondence should be addressed to Bing Zhou; zhoub2@hotmail.com

Received 4 December 2020; Revised 18 December 2020; Accepted 22 December 2020; Published 6 January 2021

Academic Editor: Wei-Lin Liu

Two major factors contribute to the failure of axonal regrowth in the central nervous system (CNS), namely, the neuronal intrinsic regenerative capacity and the extrinsic local inhibitory microenvironments. However, a preconditioning peripheral nerve lesion could substantially enhance the regeneration of central axons following a subsequent spinal cord injury. In the present review, we summarize the molecular mechanisms of the preconditioning injury effect on promoting axonal regeneration. The injury signal transduction resulting from preconditioning peripheral nerve injury regulates the RAG expression to enhance axonal regeneration. Importantly, preconditioning peripheral nerve injury triggers interactions between neurons and nonneuronal cells to amplify and maintain their effects. Additionally, the preconditioning injury impacts mitochondria, protein, and lipid synthesis. All these coordinated changes endow axonal regeneration.

1. Introduction

The axons of neurons in the peripheral nervous system (PNS) retain considerable regenerative capacity following injury, while the axons of neurons in the adult central nervous system (CNS) fail to regrow spontaneously [1]. Two major factors contribute to the failure of axonal regrowth in the CNS: neurons losing their intrinsic regenerative capacity after maturation, and the inhibition of local microenvironments preventing axon growth [2, 3]. Studies have demonstrated that the elimination of external inhibitory molecules is not sufficient for promoting long distance axonal regeneration [4]. Thus, the low intrinsic regenerative capacity with aging is the main obstacle for central axonal regeneration [5–12].

The primary sensory neurons are pseudounipolar neurons that extend their axons into peripheral and central branches. The peripheral branches project to innervate sensory targets, and the central axonal branches enter into the dorsal column and relay sensory information back to the brain stem. Thus, the primary sensory neurons, with their cell bodies in the dorsal root ganglia, are ideal for investigating regeneration mechanisms following axotomy both in vivo and in vitro [13]. Interestingly, a prior injury of peripheral branches permits regeneration of axons in CNS following a subsequent injury, despite the existence of an inhibitory environment in the CNS, through the activation of intrinsic regeneration capacity, which is referred to as the preconditioning injury effect [14–17](Figure 1). The transection of DRG axons in the central nerve systems did not elicit the preconditioning injury effect similar to the peripheral axons axotomy [13].

The initial findings have driven the speculation that the distinct regenerating response is due to intrinsic differences in postinjury changes between the peripheral and central nerve axotomy [16], leading to significant concern and propelled molecular mechanism studies focused on the multiple genetic regulators of the axon regeneration capacity. Accordingly, many regeneration-associated genes (RAG) have been certified, such as ATF3 (activating transcription factor 3), Sprr1a, c-Jun, and Smad1 [18–20]. However, individual or combined axonal RAG regulation failed to induce the full axon regeneration in CNS, suggesting a permissive role of RAGs [18].

Recently, with technological advances in bioinformatics and high-throughput gene sequencing, an increasing body

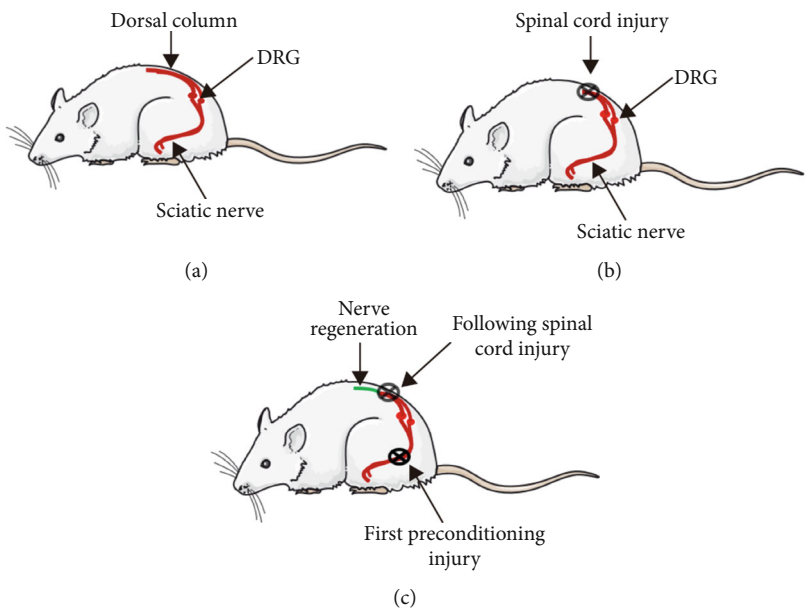

Figure 1: Preconditioning injury paradigm. (a) The DRGs are pseudounipolar neurons, dividing their axons into peripheral and central branches. The peripheral branches aggregate into the sciatic nerve to innervate sensory targets, and the central branches enter into the dorsal column and relay sensory information to the brain stem. (b) The central branch of DRG failed to regenerate after spinal cord injury. (c) A prior injury of the sciatic nerve could enhance the regrowth capacity of DRG to elicit regeneration of axons in the central nerve system following a subsequent spinal injury.

of evidence shows that epigenetic regulation for DNA accessibility and the transcriptional program are synergistic with PNS injury, while they are less affected by CNS injury [20, 21]. In addition to RAG dynamics, a significant concern of the damage response may also be related to the interaction between neurons and nonneuronal cells after axon axotomy [22]. Interestingly, the metabolic pathways and mitochondrial behavior regulation may also contribute to preconditioning injury effects, indicating enhanced cellular metabolism adaptation during axon regeneration, which caught extensive attention [23, 24]. Understanding the molecular mechanisms of preconditioning injury may ultimately benefit novel intervention to improve CNS recovery after injury. In the present review, we provide an overview of molecular and cellular mechanisms on preconditioning injury, including injury signal transduction, epigenetics modification, neuroinflammation, and immune response.

2. Injury Signal Transduction of the Preconditioning Injury Effect

With the preconditioning peripheral nerve injury induction, the adult DRG's axon growth capacity is revived, and the neurons are reprogramming into a proregenerative state, both in vivo and in vitro. Over the past decades, comprehensive studies indicate that peripheral nerve injury signals can retrograde back to the DRG cell bodies and initiate the neuronal genetic program responsible for enhancing axon growth. Injury signal transduction is encoded by rapid changes in Ca^{2+} fluxes in the injured neuron and some other slower signals that are conveyed by axoplasmic transport [25].

Studies of preconditioning injury have provided evidence that Ca^{2+} availability may regulate histone acetylation to enhance axon regrowth via HDAC5 and HDAC3. In the context of sciatic nerve injury, the peripheral axonal membrane breaks, and then ionic calcium flows into the cell. A back-propagating calcium wave to soma stimulates histone deacetylase 5 (HDAC5) export from the nucleus via protein kinase C-μ activation, which in turn boosts histone acetylation to reprogram the chromatin for subsequent transcription events [26]. As injury-regulated tubulin deacetylase, HDAC5 also plays an essential role in tubulin deacetylation at the injury site to regulate growth cone dynamics and axon regeneration [27]. Unlike PNS injury, the HDAC5 pathway cannot be activated in a model of CNS injury. The calcium increase induced by peripheral targeted nerve injury activates protein phosphatase 4 (PP4) to dephosphorylates HDAC3, resulting in inhibiting the HDAC3 activity and therefor promoting axonal regeneration through enhanced histone acetylation. PP4-dependent HDAC3 dephosphorylation is pivotal to regenerative success [28](Figure 2).

The cAMP was one of the major downstream effectors of calcium during axonal injury. Studies have shown that a preconditioning peripheral nerve injury activates the cAMP signaling pathway to improve growth capacity to overcome inhibition by myelin-associated glycoprotein (MAG) and myelin [29]. Endogenous cAMP levels in rat DRG are related to regenerative capacity [30]. The neurite outgrowth of young neurons is dramatically reduced by inhibiting protein kinase A (PKA, a downstream effector of cAMP), and increasing cAMP overcomes myelin-MAG inhibition for older neurons. Jin Qiu et al. [29] found that 1 day after peripheral nerve injury, cAMP levels were increased in DRG to overcome MAG/myelin's

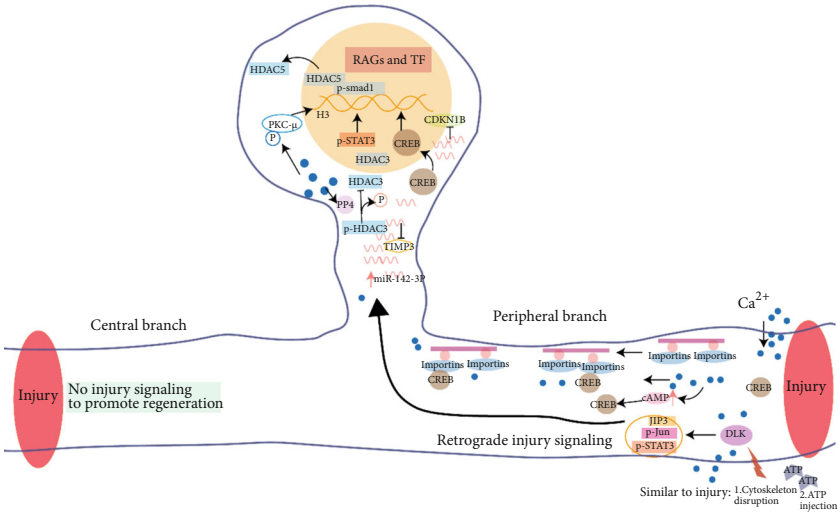

Figure 2: Signal transduction of peripheral nerve preconditioning injury regulates the RAG expression. Retrograded injury signaling after sciatic nerve injury includes calcium wave, a sensor of axon injury DLK, and axoplasmic importins. The injury signaling elicit genetic program to express RAGs and TFs responsible for enhancing axon growth. RAGs: regeneration-associated genes; TFs: transcription factors; CDKN1B: cyclin-dependent kinase inhibitor 1B; TIMP3: tissue inhibitor of metalloproteinase 3.

inhibitory effect on nerve regeneration dependent on PKA. Injection of db-cAMP can simulate a preconditioning injury effect. Elevated cAMP activated cAMP-responsive element-binding protein 1 (CREB1) to upregulate Arg I, leading to an increasing in polyamine synthesis [31].

A sensor of axon injury DLK (MAP3K, dual leucine zipper kinase), which is independent of calcium concentration changes, is responsible for the retrograde injury signal [32]. Lack of DLK reduces the upregulation of activated transcription factors such as phosphorylated JUN and STAT3 in sensory neuron cell bodies because DLK is required for retrograde transport of p-STAT3 at the site of axon injury to the cell body [32]. DLK and JNK are linked to the axon transport machinery by a scaffolding protein JIP3. Retrograde transport of JIP3 was also shown to be perturbed in DLK-knockout axons. A study has demonstrated that DLK is required for JNK-dependent retrograde injury signaling and also shows that it regulates other retrograde cargoes [32]. A recent study suggests that HSP90 is required for DLK functions in proregenerative axon injury signaling. As a chaperone protein, HSP90 binds DLK to inhibit rapid DLK protein degradation and stable it in the sciatic nerve [33]. Other groups had demonstrated that after sciatic nerve injury, STAT3 is phosphorylated rapidly and retrogradely transported to the nucleus and initiate transcription of target genes [34, 35], while STAT3 retrograde transport was attenuated in DLK-knockout axons [32]. Using a DLK-knockout mouse model that underwent DRG conditional injury, Shin's lab [36] also indicated that the gene expression changes on the DLK pathway according to the time course through gene ontology analysis. Su-Hyuk Ko and his colleague found DLK-1-mediated injury-triggered autophagy activation to promote axon regeneration [37].

Axoplasmic importins are DLK-independent signaling molecules sensing retrograde injury signaling in the injury nerve [38]. The importin β1 protein was presented and increased as a result of local translation of axonal mRNA after injury. This subsequently leads to the generation of high-affinity a NLS-binding complex that is transported retrogradely with the moto protein dynein to modulate the axonal regeneration (Figure 2). Furthermore, a study showed that axon-derived Luman/CREB3 also played an important role in transducing retrograde regeneration signal after axonal injury. Notably, CREB3 synthesis and releasing from the axonal endoplasmic reticulum was induced by axotomy and then transferred to the cell nucleus in an importin-mediated manner [39], which regulates the unfolded protein response (UPR^{ER}) and cholesterol biosynthesis that are crucially associating with the acute stress response in axonal growth [39, 40]. The authors also show that upregulation and nuclear localization of Luman coordinate with the increased transcriptional activity in injured neurons, achieving maximal outgrowth capacity at two-day injury-conditioned neurons relative to naïve [41].

In addition to sciatic nerve transection, Vera Valakh and colleges found that the perturbation of actin or cytoskeleton damaged by pharmacological agents also activated the DLK pathway (Figure 2). This activation of the DLK pathway may enhance axon regeneration akin to preconditioning [42]. Since the preconditioning injury can cause ATP release from axons and Schwann cells, some postulation suggested that ATP could also be the key injury signal to transmit injured neurons into a regeneration state [43]. One study shows that ATP injection or precondition injury increased the expression of phospho-STAT3 and GAP43, indicating that P2Y2 receptors are involved in the activation of STAT3 [44].In another study, through applying a cAMP agonist rolipram, the author elucidates that the mechanisms of low-frequency electrical stimulation are to upregulate neurotrophic factors and cAMP to accelerate nerve regeneration [45].

3. Preconditioning Injury Regulates the RAG Expression to Enhance Axon Regeneration

In contrast to transient signaling evoked by injury, epigenetic regulation, which refers to gene expression changes without altering underlying DNA sequences, is involved in the transcriptional profiling of the preconditioning injury effect [46]. Finelli MJ and coworkers established a correlation between histone acetylation and intrinsic axon growth capacity in adult DRG neurons [47]. They identified a transcriptional complex consisting of pSmad1 and other histone-modifying enzymes, which involved in the restoration of a subset of early RAG promoter histone acetylation and expression induction [47]. Consistently, when neurons are transmitted into a growth state with H4 acetylation, a set of target genes of Smad1 is restored in the preconditioning injury paradigm. Interestingly, Smad1, a conserved transcription factor (TF) downstream of bone morphogenetic protein (BMP) signaling, activated by peripheral nerve axotomy in adult sensory neurons, is correlated with neurotrophin-mediated axon regeneration in vitro and in vivo [48], while the central axotomy procedure of DRGs fails to activate the Smad1 pathway [49].

Histone acetylation and chromatin accessibility characterize injury discrepancy after PNS or CNS axonal injury. Specifically, the H3K9ac, H3K27ac, and H3K27me3 were modified differently in response to peripheral nerve axotomy and CNS axotomy. These modifications correlate with the various regenerative abilities of sensory neurons [21]. As mentioned above, the retrograde propagation of calcium wave from axotomy in DRG neurons elicits nuclear export of HDAC5, leading to elevated H3 acetylation and RAGs induction [26]. Interestingly, the expression of HIF1α in DRG neurons is necessary and sufficient for histone H3 acetylation to promote peripheral axon regeneration in a sciatic nerve injury model [50]. Moreover, systematic epigenetic studies showed that the histone acetyltransferase p300/CBP-associated factor (PCAF) promotes acetylation of histone 3 Lys 9 at the RAG promoters following a peripheral but not a central axonal injury [51]. Additionally, PCAF phosphorylation was required for retrograde transport of extracellular signal-regulated kinase (ERK) and nuclear localization after peripheral nerve axotomy, which provides a connection of the transduction pathway of injury signals from the site of axotomy to nuclear and chromatin modifications [51]. A recent study suggested that Creb-binding protein- (Cbp-) mediated histone acetylation increased the expression of RAGs [52]. Induction of Tet3 and elevated 5hmC levels in adult DRG after peripheral nerve axotomy is also correlated to induction of RAGs such as ATF3, Smad1, and STAT3 [53, 54].

Besides epigenetic alterations, various RNAs regulating translation after transcription have been found to play an important role in nerve regeneration. With the development of RNA sequencing, microRNAs (miRNAs), a novel class of small noncoding RNAs, were found to regulate posttranscription of the expression. Wu et al. identified the upregulation of miR-142-3p following sciatic nerve injury in rat DRG. miR-142-3p binds the 3′-UTR of cyclin-dependent kinase inhibitor 1B (CDKN1B, also as p27Kip1) and tissue inhibitor of metalloproteinase 3 (TIMP3), to regulate their expression for appropriate nerve regeneration [55]. The long noncoding RNA (LncRNAs) expression also changes markedly after nerve injury [56]. Circular RNAs (circRNAs), single-stranded regulatory RNAs participating in regulating transcription and splicing, were increased after sciatic nerve injury in rat via a quantitative real-time polymerase chain reaction. circ-Spidr, a kind of circular RNAs, partially modulated the PI3K-Akt pathway to control DRG axon regeneration in vitro and in vivo [57].

With the employing of system biology and bio-information approaches, Chandran et al. identified core networks that specifically change after PNS versus CNS injury. The major upregulated TFs after PNS injury include ATF3, EGR1, FOS, JUN, MYC, RELA, SMAD1, and STAT3. ATF3 and JUN are the top two hub TFs present in the core regeneration-associated gene network [20]. Another study suggested that peripheral axonal injury activated ATF3 to increase DRG neurite elongation in vitro. However, with the ATF3 transgenic mice, Seijffers et al. showed that ATF3 contributes to the intrinsic growth of injured neurons, while these neurons fail to overcome the environmental inhibitory effects [19].

Similarly, transcriptomic analysis suggested that sciatic nerve injury triggers the mRNA level change in the spinal cord [58]. Some of these regulated mRNAs are involved in cell growth and development. Combining axoplasmic proteomics with cell body RNA-seq, Guiping Kong and colleagues found that AMPKα1 is specifically downregulated and contributes to enhanced axonal regeneration following sciatic injury, different from injured central projecting of DRG [59].

4. Interactions between Neurons and Nonneurons from Preconditioning Injury

In consistent with the observed inflammation and immune response from the bioinformatic analysis [60], neuroimmunology regulation and the interaction between neurons and nonneurons were involved in the PNS preconditioning effect [22]. Inflammation-derived signals could also have an impaction on the intrinsic growth ability of DRG.

As a highly dynamic pathogenic process, the number of macrophages in DRGs and inflammatory mediators increased after sciatic nerve transection in rats. The preconditioning sciatic nerve injury may trigger neuron–macrophage interactions in the DRGs to drive macrophage activation toward a proregenerative phenotype [61], and macrophages tend to be closer proximity to small and large neurons in DRG [62] (Figure 3). Intriguing, the upregulation and release of miR-21 from DRG neurons after nerve injury contribute to sensory neuron–macrophage communication [63]. Minocycline, a macrophage inhibitor, could limit the number of macrophages and downregulate inflammatory mediators, coincide with abolished regenerative capacity enhancement by conditioning injury in vitro and in vivo [61]. The BDNF-cAMP pathway-dependent cell-cell interaction pathways have been identified as well. The upregulation of macrophage-derived neurotrophin BDNF is induced by preconditioning sciatic nerve injury [61]. Neutralization of endogenous BDNF impairs the

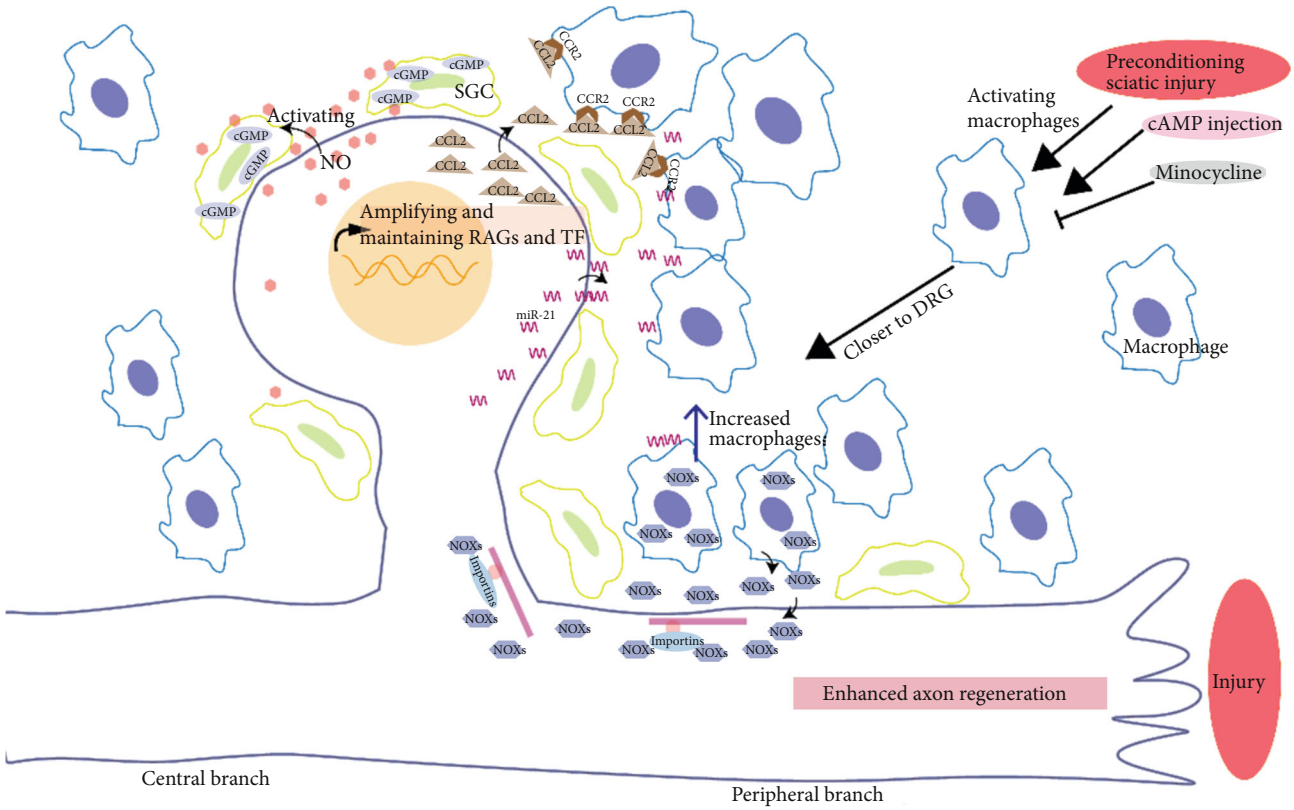

Figure 3: Interaction between neurons and nonneurons after PNS preconditioning injury. The preconditioning sciatic nerve injury increased the number of macrophages and inflammatory mediators and drives macrophage activation toward DRG. The interactions amplify and maintain RAGs and TF expression to enhance axon regeneration. SGC: satellite glial cells; CCL2:C-C motif chemokine ligand 2; CCR2: C-C motif chemokine receptor 2; NOXs: NADPH oxidase 2 complexes.

enhanced neurite growth and regeneration of DRG in vitro and in vivo [64], while the injection of cAMP also increases the macrophages. Besides, recent findings with RNA sequencing suggested that, after nerve injury, satellite glial cells (SGC) contain abundant genes involving in the immune system and cell-to-cell communication [62]. However, these genes changed at different time points, leading to the speculating that macrophages may result from the injury-induced proliferation of SGCs [62]. These studies indicated the importance of neuron-macrophage interactions, and that macrophages played a crucial role in maintaining regenerative capacity.

Wang et al. [65] reported that phospho-JUN is also involved in triggering the expression of Sarm1 and several chemokines in DRG neurons, including C-C motif chemokine ligand 2 (CCL2). CCL2 (also known as monocyte chemoattractant protein-1) was highly expressed in DRG 48 hours after nerve injury [66]. Upon preconditioning injury, CCL2 releasing from neurons activates CCR2 of macrophages to mediate neuron–macrophage interactions (Figure 3). Macrophage accumulation around axotomized cell bodies resulting from an injury of the sciatic nerve but not the dorsal root is necessary for a peripheral nerve preconditioning injury effect via a STAT3-dependent mechanism [67], since the CCL2 overexpression led to a selective increase in leukemia-inhibitory factor (LIF) mRNA and neuronal phosphorylated STAT3 (pSTAT3) in L5 DRGs. pSTAT3 is involved in DLK-dependent injury signal transduction [32]. However, how the injury of the sciatic nerve stimulates neurons to release CCL2 is unknown. Sigma-1 receptor (Sig-1R), expressed by DRG neurons, plays an important role in DRG neuron-macrophage/monocyte communication after sciatic nerve injury. Following the chemokine CCL2 produced by DRG neurons after nerve injury, macrophage/monocyte infiltration is mainly located around injured DRG with translocated Sig-1R in WT mice. In contrast, reducing levels of CCL2 and decreasing macrophage/monocyte infiltration were observed in DRG of Sig-1R knockout mice [68]. Cobos et al. [69] reported a number of chemokines increases, including CCL4, CCL7, and CCL9 after injury in the DRG with RNA seq study.

Additionally, preconditioning injury also has an impact on the remote DRG. Dubovy et al. found that 7 days after sciatic nerve injury, the ulnar nerve with subsequent crush regrows longer than with ulnar nerve crush only [70]. They speculated that DRG neurons in the cervical were *trans*-activated into the proregenerative state by preconditioning sciatic nerve injury through the IL-6 signaling pathway [71]. Highlighting the inflammatory cytokines IL-6 has also participated in preconditioning effects. After sciatic nerve injury, the IL-6 mRNA expression correlated with the increased macrophages in a similar time course [61]. Besides, a study shows that macrophages were the primary source of IL-6 by detecting IL-6 only in CD68-positive macrophages [61]. Cao et al. [72] have shown that cytokine interleukin-6

(IL-6) is upregulated in culture DRG neurons after cAMP treatment or a preconditioning injury. And this increase in IL-6 is sufficient to overcome the myelin-associated inhibitors and promote spinal axon regeneration in vivo, mimicking the preconditioning injury, although IL-6 is not an essential component of these responses [72]. IL-6 reactivates the expression of RAGs, such GAP-43, Sprr1a, and Arginase I and triggers the mTOR pathway in neurons surrounding the injury site to promote axonal regrowth [73]. The increased IL-6 is through the classic IL-6 trimeric receptor to activate the JAK signaling cascade. Together, the interaction between neurons and nonneurons mediated by chemokine signaling is necessary and sufficient for mimicking the preconditioning injury, which may coordinate with the retrograde signaling initiated from the injury site, to corroborate the successful axonal regeneration.

In addition to the regulated cytokines, reactive oxygen species (ROS) also play an important role in intraganglionic communications. Nitric oxide (NO), one of the reactive oxygen species, as a messenger released by sensory neurons after axotomy, activates satellite glial cells (SGCs) in DRG and induces cyclic GMP (cGMP) production in these SGCs [74]. Accordingly, NO also reinforced Ca^{2+} wave propagation in DRG cultures. Another study has shown that the sciatic nerve injury triggers NADPH oxidase 2 complexes (NOXs) releasing from macrophages, and then NOXs are endocytosed into injured axons [75]. Endosomal NOXs are transported to the cell body via importins and produced ROS to oxidize PTEN, which inhibited PTEN to promote axonal regeneration and functional recovery after spinal injury.

Other non-neuron cells are also involved in nerve regrowth, such as Schwann cells (SCs) and endothelial cells. The LDL receptor-related protein-1 (LRP1) is the cell-signaling receptor required for normal SC function. Comparing scLRP1-/- mice with wild-type littermates with and without peripheral nerve injury, Poplawski et al. provide evidence that SCs regulate the RAG expression in DRGs [76]. In addition, other cell type endothelial cells are also involved in nerve regrowth. Macrophages may selectively sense hypoxia and induced blood vessels via VEGF-A to alleviate the hypoxia in the process of reconnecting a severed nerve in PNS [77].

These interactions are essential for amplifying and maintaining the RAG expression and enhance regenerative capacity by preconditioning peripheral nerve injury [78]. Maintenance of the RAG expression is crucial for successful nerve regeneration [79].

5. The Effects of Preconditioning Injury on Mitochondria, Protein, and Lipid Synthesis

Kiryu-Seo et al. observed that mitochondrial fission increased in injured motor axons after sciatic nerve transection [80]. Simultaneously, the anterograde transport of mitochondrial increased in proximal segments of injured intercostal nerves with a vigorous growth response [81]. A preconditioning peripheral nerve injury also upregulated the levels of molecular motors, polyglutamylated, and tyrosinated tubulin to enhance mitochondria transport in both central and peripheral branches of DRG, which support a rapid and sustained central axon regeneration [82]. However, spinal cord injury cannot elicit increased mitochondrial transport [82]. Suggesting altered mitochondrial transport could be the potential intervention target. Zhou et al.'s previous studies suggest that enhancing mitochondrial transport might rescue energy deficits to promote axon regrowth [83], while the relationship between mitochondrial as a powerhouse and the preconditioning effect during nerve regrowth still needs to be investigated and answered.

In addition to the mitochondria, the preconditioning injury also impacts protein synthesis and lipid metabolism in injured neurons. The priming of peripheral nerve injury, not a central nerve lesion of rat DRGs, increases metabolic enzymes such as NADH dehydrogenase and catalase, which is detected by radiolabeling and mass spectrometry [82]. The preconditioning PNS injury promotes protein synthesis via enhancing the rapamycin-insensitive mTOR activity [84] and m6A signaling in adult DRGs [85]. The level of neuronal diglyceride acyltransferases (DGATs) was deceased during injury to switch from triglycerides to phospholipid synthesis, which facilitates axon regeneration [24]. Similarly, an upregulation of cAMP induced by sciatic transection initiated the expression of arginase 1 (Arg), a rate-limiting enzyme in the synthesis of the polyamines, in a cAMP response element-binding protein (CREB)-dependent manner [31, 86]. Activation of CREB is also required for cAMP to upregulate Arg I that increased polyamine synthesis and improves axonal regeneration on the inhibitory substrate.

6. Conclusion

Previous studies have advanced how preconditioning peripheral axon injury elicits widespread regulations, including injury signals transduction, gene expressions, epigenetic modification, and neuroinflammation to facilitate neuron regeneration. Considerable progress has been made in recent years. However, the coordination and integration of multifunctional pathways have prospected for the successful axon regeneration, and there are still many challenges for reconstructing a fully functional neural circuit. It is foreseeable that the key determinants will be identified to trigger central axon regeneration and functional recovery and mimics the preconditioning injury effect that has been applied clinically. Based on that understanding, novel pharmacological therapies recapitulating the preconditioning injury effect may be developed.

Conflicts of Interest

The authors declare that they have no conflicts of interest.

Acknowledgments

The authors thank all members of Zhou laboratory for their assistance. This work was supported by the National Natural Science Foundation of China [No. 81971198], Beijing Municipal Natural Science Foundation, China [No. 7192103], and Chinese Ministry of Science and Technology, China [No. 2019YFA0508603].

References

[1] M. Mahar and V. Cavalli, "Intrinsic mechanisms of neuronal axon regeneration," *Nature Reviews. Neuroscience*, vol. 19, no. 6, pp. 323–337, 2018.

[2] P. Nix and M. Bastiani, "DLK: the "preconditioning" signal for axon regeneration?," *Neuron*, vol. 74, no. 6, pp. 961–963, 2012.

[3] A. Tedeschi and F. Bradke, "Spatial and temporal arrangement of neuronal intrinsic and extrinsic mechanisms controlling axon regeneration," *Current Opinion in Neurobiology*, vol. 42, pp. 118–127, 2017.

[4] K. Liu, A. Tedeschi, K. K. Park, and Z. He, "Neuronal intrinsic mechanisms of axon regeneration," *Annual Review of Neuroscience*, vol. 34, no. 1, pp. 131–152, 2011.

[5] T. Spencer, M. Domeniconi, Z. Cao, and M. T. Filbin, "New roles for old proteins in adult CNS axonal regeneration," *Current Opinion in Neurobiology*, vol. 13, no. 1, pp. 133–139, 2003.

[6] G. Yiu and Z. He, "Glial inhibition of CNS axon regeneration," *Nature Reviews. Neuroscience*, vol. 7, no. 8, pp. 617–627, 2006.

[7] F. Q. Zhou and W. D. Snider, "Intracellular control of developmental and regenerative axon growth," *Philosophical Transactions of the Royal Society of London. Series B, Biological Sciences*, vol. 361, no. 1473, pp. 1575–1592, 2006.

[8] K. K. Park, K. Liu, Y. Hu et al., "Promoting axon regeneration in the adult CNS by modulation of the PTEN/mTOR pathway," *Science*, vol. 322, no. 5903, pp. 963–966, 2008.

[9] D. L. Moore, M. G. Blackmore, Y. Hu et al., "KLF family members regulate intrinsic axon regeneration ability," *Science*, vol. 326, no. 5950, pp. 298–301, 2009.

[10] F. Bradke, J. W. Fawcett, and M. E. Spira, "Assembly of a new growth cone after axotomy: the precursor to axon regeneration," *Nature Reviews. Neuroscience*, vol. 13, no. 3, pp. 183–193, 2012.

[11] M. M. Farley and T. A. Watkins, "Intrinsic neuronal stress response pathways in injury and disease," *Annual Review of Pathology*, vol. 13, no. 1, pp. 93–116, 2018.

[12] S. David and A. J. Aguayo, "Axonal elongation into peripheral nervous system "bridges" after central nervous system injury in adult rats," *Science*, vol. 214, no. 4523, pp. 931–933, 1981.

[13] C. L. Attwell, M. van Zwieten, J. Verhaagen, and M. Mason, "The dorsal column lesion model of spinal cord injury and its use in deciphering the neuron-intrinsic injury response," *Developmental Neurobiology*, vol. 78, no. 10, pp. 926–951, 2018.

[14] P. M. Richardson and V. M. Issa, "Peripheral injury enhances central regeneration of primary sensory neurones," *Nature*, vol. 309, no. 5971, pp. 791–793, 1984.

[15] S. Neumann and C. J. Woolf, "Regeneration of dorsal column fibers into and beyond the lesion site following adult spinal cord injury," *Neuron*, vol. 23, no. 1, pp. 83–91, 1999.

[16] J. B. Senger, V. Verge, K. M. Chan, and C. A. Webber, "The nerve conditioning lesion: a strategy to enhance nerve regeneration," *Annals of Neurology*, vol. 83, no. 4, pp. 691–702, 2018.

[17] I. G. McQuarrie and B. Grafstein, "Axon outgrowth enhanced by a previous nerve injury," *Archives of Neurology*, vol. 29, no. 1, pp. 53–55, 1973.

[18] N. D. Fagoe, C. L. Attwell, D. Kouwenhoven, J. Verhaagen, and M. R. Mason, "Overexpression of ATF3 or the combination of ATF3, c-Jun, STAT3 and Smad1 promotes regeneration of the central axon branch of sensory neurons but without synergistic effects," *Human Molecular Genetics*, vol. 24, no. 23, pp. 6788–6800, 2015.

[19] R. Seijffers, C. D. Mills, and C. J. Woolf, "ATF3 increases the intrinsic growth state of DRG neurons to enhance peripheral nerve regeneration," *The Journal of Neuroscience*, vol. 27, no. 30, pp. 7911–7920, 2007.

[20] V. Chandran, G. Coppola, H. Nawabi et al., "A systems-level analysis of the peripheral nerve intrinsic axonal growth program," *Neuron*, vol. 89, no. 5, pp. 956–970, 2016.

[21] I. Palmisano, M. C. Danzi, T. H. Hutson et al., "Epigenomic signatures underpin the axonal regenerative ability of dorsal root ganglia sensory neurons," *Nature Neuroscience*, vol. 22, no. 11, pp. 1913–1924, 2019.

[22] R. E. Zigmond and F. D. Echevarria, "Macrophage biology in the peripheral nervous system after injury," *Progress in Neurobiology*, vol. 173, pp. 102–121, 2019.

[23] J. J. Ma, X. Ju, R. J. Xu et al., "Telomerase reverse transcriptase and p53 regulate mammalian peripheral nervous system and CNS axon regeneration downstream of c-Myc," *The Journal of Neuroscience*, vol. 39, no. 46, pp. 9107–9118, 2019.

[24] C. Yang, X. Wang, J. Wang et al., "Rewiring neuronal glycerolipid metabolism determines the extent of axon regeneration," *Neuron*, vol. 105, no. 2, pp. 276–292.e5, 2020.

[25] I. Rishal and M. Fainzilber, "Axon-soma communication in neuronal injury," *Nature Reviews. Neuroscience*, vol. 15, no. 1, pp. 32–42, 2014.

[26] Y. Cho, R. Sloutsky, K. M. Naegle, and V. Cavalli, "Injury-induced HDAC5 nuclear export is essential for axon regeneration," *Cell*, vol. 155, no. 4, pp. 894–908, 2013.

[27] Y. Cho and V. Cavalli, "HDAC5 is a novel injury-regulated tubulin deacetylase controlling axon regeneration," *The EMBO Journal*, vol. 31, no. 14, pp. 3063–3078, 2012.

[28] A. Hervera, L. Zhou, I. Palmisano et al., "PP4-dependent HDAC3 dephosphorylation discriminates between axonal regeneration and regenerative failure," *The EMBO Journal*, vol. 38, no. 13, article e101032, 2019.

[29] J. Qiu, D. Cai, H. Dai et al., "Spinal axon regeneration induced by elevation of cyclic AMP," *Neuron*, vol. 34, no. 6, pp. 895–903, 2002.

[30] D. Cai, J. Qiu, Z. Cao, M. McAtee, B. S. Bregman, and M. T. Filbin, "Neuronal cyclic AMP controls the developmental loss in ability of axons to regenerate," *The Journal of Neuroscience*, vol. 21, no. 13, pp. 4731–4739, 2001.

[31] Y. Gao, K. Deng, J. Hou et al., "Activated CREB is sufficient to overcome inhibitors in myelin and promote spinal axon regeneration in vivo," *Neuron*, vol. 44, no. 4, pp. 609–621, 2004.

[32] J. E. Shin, Y. Cho, B. Beirowski, J. Milbrandt, V. Cavalli, and A. DiAntonio, "Dual leucine zipper kinase is required for retrograde injury signaling and axonal regeneration," *Neuron*, vol. 74, no. 6, pp. 1015–1022, 2012.

[33] S. Karney-Grobe, A. Russo, E. Frey, J. Milbrandt, and A. DiAntonio, "HSP90 is a chaperone for DLK and is required for axon injury signaling," *Proceedings of the National Academy of Sciences of the United States of America*, vol. 115, no. 42, pp. E9899–E9908, 2018.

[34] J. Qiu, W. B. Cafferty, S. B. McMahon, and S. W. Thompson, "Conditioning injury-induced spinal axon regeneration requires signal transducer and activator of transcription 3 activation," *The Journal of Neuroscience*, vol. 25, no. 7, pp. 1645–1653, 2005.

[35] R. Eulenfeld, A. Dittrich, C. Khouri et al., "Interleukin-6 signalling: more than Jaks and STATs," *European Journal of Cell Biology*, vol. 91, no. 6-7, pp. 486–495, 2012.

[36] J. E. Shin, H. Ha, Y. K. Kim, Y. Cho, and A. DiAntonio, "DLK regulates a distinctive transcriptional regeneration program after peripheral nerve injury," *Neurobiology of Disease*, vol. 127, pp. 178–192, 2019.

[37] S. H. Ko, J. Y. Yun, I. J. Baek et al., "Mitophagy deficiency increases NLRP3 to induce brown fat dysfunction in mice," *Autophagy*, pp. 1–17, 2020.

[38] S. Hanz, E. Perlson, D. Willis et al., "Axoplasmic importins enable retrograde injury signaling in lesioned nerve," *Neuron*, vol. 40, no. 6, pp. 1095–1104, 2003.

[39] Z. Ying, V. Misra, and V. M. Verge, "Sensing nerve injury at the axonal ER: activated Luman/CREB3 serves as a novel axonally synthesized retrograde regeneration signal," *Proceedings of the National Academy of Sciences of the United States of America*, vol. 111, no. 45, pp. 16142–16147, 2014.

[40] Z. Ying, R. Zhai, N. A. McLean, J. M. Johnston, V. Misra, and V. M. Verge, "The unfolded protein response and cholesterol biosynthesis link Luman/CREB3 to regenerative axon growth in sensory neurons," *The Journal of Neuroscience*, vol. 35, no. 43, pp. 14557–14570, 2015.

[41] J. Hasmatali, J. de Guzman, R. Zhai et al., "Axotomy induces phasic alterations in Luman/CREB3 expression and nuclear localization in injured and contralateral uninjured sensory neurons: correlation with intrinsic axon growth capacity," *Journal of Neuropathology and Experimental Neurology*, vol. 78, no. 4, pp. 348–364, 2019.

[42] V. Valakh, E. Frey, E. Babetto, L. J. Walker, and A. DiAntonio, "Cytoskeletal disruption activates the DLK/JNK pathway, which promotes axonal regeneration and mimics a preconditioning injury," *Neurobiology of Disease*, vol. 77, pp. 13–25, 2015.

[43] X. Bo, "Is ATP a key player in conditioning neurons to support axonal regeneration?," *Neural Regeneration Research*, vol. 13, no. 12, pp. 2077–2079, 2018.

[44] D. Wu, S. Lee, J. Luo et al., "Intraneural injection of ATP stimulates regeneration of primary sensory axons in the spinal cord," *The Journal of Neuroscience*, vol. 38, no. 6, pp. 1351–1365, 2018.

[45] T. Gordon, K. M. Chan, O. A. Sulaiman, E. Udina, N. Amirjani, and T. M. Brushart, "Accelerating axon growth to overcome limitations in functional recovery after peripheral nerve injury," *Neurosurgery*, vol. 65, suppl_4, pp. A132–A144, 2009.

[46] S. Wahane, D. Halawani, X. Zhou, and H. Zou, "Epigenetic regulation of axon regeneration and glial activation in injury responses," *Frontiers in Genetics*, vol. 10, p. 640, 2019.

[47] M. J. Finelli, J. K. Wong, and H. Zou, "Epigenetic regulation of sensory axon regeneration after spinal cord injury," *The Journal of Neuroscience*, vol. 33, no. 50, pp. 19664–19676, 2013.

[48] P. Parikh, Y. Hao, M. Hosseinkhani et al., "Regeneration of axons in injured spinal cord by activation of bone morphogenetic protein/Smad1 signaling pathway in adult neurons," *Proceedings of the National Academy of Sciences of the United States of America*, vol. 108, no. 19, pp. E99–107, 2011.

[49] H. Zou, C. Ho, K. Wong, and M. Tessier-Lavigne, "Axotomy-induced Smad1 activation promotes axonal growth in adult sensory neurons," *The Journal of Neuroscience*, vol. 29, no. 22, pp. 7116–7123, 2009.

[50] Y. Cho, J. E. Shin, E. E. Ewan, Y. M. Oh, W. Pita-Thomas, and V. Cavalli, "Activating injury-responsive genes with hypoxia enhances axon regeneration through neuronal HIF-1α," *Neuron*, vol. 88, no. 4, pp. 720–734, 2015.

[51] R. Puttagunta, A. Tedeschi, M. G. Sória et al., "PCAF-dependent epigenetic changes promote axonal regeneration in the central nervous system," *Nature Communications*, vol. 5, no. 1, p. 3527, 2014.

[52] T. H. Hutson, C. Kathe, I. Palmisano et al., "Cbp-dependent histone acetylation mediates axon regeneration induced by environmental enrichment in rodent spinal cord injury models," *Science Translational Medicine*, vol. 11, no. 487, article eaaw2064, 2019.

[53] Y. E. Loh, A. Koemeter-Cox, M. J. Finelli, L. Shen, R. H. Friedel, and H. Zou, "Comprehensive mapping of 5-hydroxymethylcytosine epigenetic dynamics in axon regeneration," *Epigenetics*, vol. 12, no. 2, pp. 77–92, 2017.

[54] Y. L. Weng, R. An, J. Cassin et al., "An intrinsic epigenetic barrier for functional axon regeneration," *Neuron*, vol. 94, no. 2, pp. 337–346.e6, 2017.

[55] D. M. Wu, X. Wen, X. R. Han et al., "MiR-142-3p enhances cell viability and inhibits apoptosis by targeting CDKN1B and TIMP3 following sciatic nerve injury," *Cellular Physiology and Biochemistry*, vol. 46, no. 6, pp. 2347–2357, 2018.

[56] G. Baskozos, J. M. Dawes, J. S. Austin et al., "Comprehensive analysis of long noncoding RNA expression in dorsal root ganglion reveals cell-type specificity and dysregulation after nerve injury," *Pain*, vol. 160, no. 2, pp. 463–485, 2019.

[57] S. Mao, T. Huang, Y. Chen et al., "Circ-Spidr enhances axon regeneration after peripheral nerve injury," *Cell Death & Disease*, vol. 10, no. 11, p. 787, 2019.

[58] J. Weng, D. D. Li, B. G. Jiang, and X. F. Yin, "Temporal changes in the spinal cord transcriptome after peripheral nerve injury," *Neural Regeneration Research*, vol. 15, no. 7, pp. 1360–1367, 2020.

[59] G. Kong, L. Zhou, E. Serger et al., "AMPK controls the axonal regenerative ability of dorsal root ganglia sensory neurons after spinal cord injury," *Nature Metabolism*, vol. 2, no. 9, article 252, pp. 918–933, 2020.

[60] S. Yi, H. Zhang, L. Gong et al., "Deep sequencing and bioinformatic analysis of lesioned sciatic nerves after crush injury," *PLoS One*, vol. 10, no. 12, article e0143491, 2015.

[61] M. J. Kwon, J. Kim, H. Shin et al., "Contribution of macrophages to enhanced regenerative capacity of dorsal root ganglia sensory neurons by conditioning injury," *The Journal of Neuroscience*, vol. 33, no. 38, pp. 15095–15108, 2013.

[62] S. E. Jager, L. T. Pallesen, M. Richner et al., "Changes in the transcriptional fingerprint of satellite glial cells following peripheral nerve injury," *Glia*, vol. 68, no. 7, pp. 1375–1395, 2020.

[63] R. Simeoli, K. Montague, H. R. Jones et al., "Exosomal cargo including microRNA regulates sensory neuron to macrophage communication after nerve trauma," *Nature Communications*, vol. 8, no. 1, p. 1778, 2017.

[64] X. Y. Song, F. Li, F. H. Zhang, J. H. Zhong, and X. F. Zhou, "Peripherally-derived BDNF promotes regeneration of ascending sensory neurons after spinal cord injury," *PLoS One*, vol. 3, no. 3, article e1707, 2008.

[65] Q. Wang, S. Zhang, T. Liu et al., "Sarm1/Myd88-5 regulates neuronal intrinsic immune response to traumatic axonal injuries," *Cell Reports*, vol. 23, no. 3, pp. 716–724, 2018.

[66] J. A. Lindborg, J. P. Niemi, M. A. Howarth et al., "Molecular and cellular identification of the immune response in peripheral ganglia following nerve injury," *Journal of Neuroinflammation*, vol. 15, no. 1, p. 192, 2018.

[67] J. P. Niemi, A. DeFrancesco-Lisowitz, J. M. Cregg, M. Howarth, and R. E. Zigmond, "Overexpression of the monocyte chemokine CCL2 in dorsal root ganglion neurons causes a conditioning-like increase in neurite outgrowth and does so _via_ a STAT3 dependent mechanism," *Experimental Neurology*, vol. 275, no. 1, pp. 25–37, 2016.

[68] I. Bravo-Caparrós, M. C. Ruiz-Cantero, G. Perazzoli et al., "Sigma-1 receptors control neuropathic pain and macrophage infiltration into the dorsal root ganglion after peripheral nerve injury," *The FASEB Journal*, vol. 34, no. 4, pp. 5951–5966, 2020.

[69] E. J. Cobos, C. A. Nickerson, F. Gao et al., "Mechanistic differences in neuropathic pain modalities revealed by correlating behavior with global expression profiling," *Cell Reports*, vol. 22, no. 5, pp. 1301–1312, 2018.

[70] P. Dubový, I. Klusáková, I. Hradilová-Svíženská, V. Brázda, M. Kohoutková, and M. Joukal, "A conditioning sciatic nerve lesion triggers a pro-regenerative state in primary sensory neurons also of dorsal root ganglia non-associated with the damaged nerve," *Frontiers in Cellular Neuroscience*, vol. 13, p. 11, 2019.

[71] P. Dubový, I. Hradilová-Svíženská, I. Klusáková, V. Brázda, and M. Joukal, "Interleukin-6 contributes to initiation of neuronal regeneration program in the remote dorsal root ganglia neurons after sciatic nerve injury," *Histochemistry and Cell Biology*, vol. 152, no. 2, pp. 109–117, 2019.

[72] Z. Cao, Y. Gao, J. B. Bryson et al., "The cytokine interleukin-6 is sufficient but not necessary to mimic the peripheral conditioning lesion effect on axonal growth," *The Journal of Neuroscience*, vol. 26, no. 20, pp. 5565–5573, 2006.

[73] P. Yang, H. Wen, S. Ou, J. Cui, and D. Fan, "IL-6 promotes regeneration and functional recovery after cortical spinal tract injury by reactivating intrinsic growth program of neurons and enhancing synapse formation," *Experimental Neurology*, vol. 236, no. 1, pp. 19–27, 2012.

[74] V. Belzer and M. Hanani, "Nitric oxide as a messenger between neurons and satellite glial cells in dorsal root ganglia," *Glia*, vol. 67, no. 7, pp. 1296–1307, 2019.

[75] A. Hervera, F. de Virgiliis, I. Palmisano et al., "Reactive oxygen species regulate axonal regeneration through the release of exosomal NADPH oxidase 2 complexes into injured axons," *Nature Cell Biology*, vol. 20, no. 3, pp. 307–319, 2018.

[76] G. Poplawski, T. Ishikawa, C. Brifault et al., "Schwann cells regulate sensory neuron gene expression before and after peripheral nerve injury," *Glia*, vol. 66, no. 8, pp. 1577–1590, 2018.

[77] A. L. Cattin, J. J. Burden, L. van Emmenis et al., "Macrophage-induced blood vessels guide Schwann cell-mediated regeneration of peripheral nerves," *Cell*, vol. 162, no. 5, pp. 1127–1139, 2015.

[78] M. J. Kwon, H. Y. Shin, Y. Cui et al., "CCL2 mediates neuron-macrophage interactions to drive proregenerative macrophage activation following preconditioning injury," *The Journal of Neuroscience*, vol. 35, no. 48, pp. 15934–15947, 2015.

[79] G. H. D. Poplawski, R. Kawaguchi, E. van Niekerk et al., "Injured adult neurons regress to an embryonic transcriptional growth state," *Nature*, vol. 581, no. 7806, pp. 77–82, 2020.

[80] S. Kiryu-Seo, H. Tamada, Y. Kato et al., "Mitochondrial fission is an acute and adaptive response in injured motor neurons," *Scientific Reports*, vol. 6, no. 1, article 28331, 2016.

[81] T. Misgeld, M. Kerschensteiner, F. M. Bareyre, R. W. Burgess, and J. W. Lichtman, "Imaging axonal transport of mitochondria in vivo," *Nature Methods*, vol. 4, no. 7, pp. 559–561, 2007.

[82] F. M. Mar, A. R. Simoes, S. Leite et al., "CNS axons globally increase axonal transport after peripheral conditioning," *The Journal of Neuroscience*, vol. 34, no. 17, pp. 5965–5970, 2014.

[83] B. Zhou, P. Yu, M. Y. Lin, T. Sun, Y. Chen, and Z. H. Sheng, "Facilitation of axon regeneration by enhancing mitochondrial transport and rescuing energy deficits," *The Journal of Cell Biology*, vol. 214, no. 1, pp. 103–119, 2016.

[84] W. Chen, N. Lu, Y. Ding et al., "Rapamycin-resistant mTOR activity is required for sensory axon regeneration induced by a conditioning lesion," *eNeuro*, vol. 3, no. 6, pp. -ENEURO.0358–ENEU16.2016, 2016.

[85] Y. L. Weng, X. Wang, R. An et al., "Epitranscriptomic m6A regulation of axon regeneration in the adult mammalian nervous system," *Neuron*, vol. 97, no. 2, pp. 313–325.e6, 2018.

[86] D. Cai, K. Deng, W. Mellado, J. Lee, R. R. Ratan, and M. T. Filbin, "Arginase I and polyamines act downstream from cyclic AMP in overcoming inhibition of axonal growth MAG and myelin in vitro," *Neuron*, vol. 35, no. 4, pp. 711–719, 2002.

Hindawi
Neural Plasticity
Volume 2020, Article ID 8828826, 11 pages
https://doi.org/10.1155/2020/8828826

Research Article

Chinese Tuina Protects against Neonatal Hypoxia-Ischemia through Inhibiting the Neuroinflammatory Reaction

Pengyue Zhang,[1] Qian Zhang,[1] Bowen Zhu,[2] Shijin Xia,[3] Xianyan Tai,[4] Xiantao Tai,[1] and Bing Li[5]

[1]*Key Laboratory of Acupuncture and Tuina for Treatment of Encephalopathy, College of Acupuncture, Tuina and Rehabilitation, Yunnan University of Traditional Chinese Medicine, Kunming 650500, China*
[2]*Zhejiang Provincial Hospital of TCM, Zhejiang Hangzhou 310006, China*
[3]*Department of Geriatrics, Shanghai Institute of Geriatrics, Huadong Hospital, Fudan University, Shanghai 200040, China*
[4]*Department of Prevention and Health Care, The First Hospital Affiliated to Kunming Medical University, Kunming 650032, China*
[5]*Jinshan Hospital of Fudan University, Shanghai 200054, China*

Correspondence should be addressed to Xiantao Tai; taixiantao@163.com and Bing Li; 13788998975@126.com

Pengyue Zhang, Qian Zhang, and Bowen Zhu contributed equally to this work.

Received 28 September 2020; Revised 30 November 2020; Accepted 17 December 2020; Published 31 December 2020

Academic Editor: Feng Zhang

Aim. Neonatal hypoxic-ischemic encephalopathy (HIE) is a significant cause of perinatal morbidity and mortality. Chinese Tuina is an effective treatment for HIE, but the molecular mechanisms are yet unknown. This study investigated the effect and mechanisms of Chinese Tuina on the inflammatory response in neonatal HIE rats. *Main Methods*. 30 male neonatal rats were divided randomly into 3 groups: sham, HIE, and HIE with Chinese Tuina (CHT) groups. The HIE and CHT groups were subjected to left common carotid occlusion and hypoxia at 3 days postnatal (P3). The pups in the CHT group received Chinese Tuina treatment on the next day for 28 days. The weight was measured at P4, P9, P13, P21, and P31. The behavioral functions were determined at P21. The protein expression and the methylation level in promoter regions of TNF-α and IL-10 were determined by Western blotting, immunohistochemistry, and pyrosequencing, respectively, at P33. *Key Findings*. The weight gain in the HIE group was slow compared with that of the CHT group. The rats in the CHT group performed better both in the balance beam and hang plate experiment. Chinese Tuina inhibited the expression of TNF-α and upregulated the expression of IL-10. Neonatal hypoxic-ischemic injury downregulated the methylation level in promoter regions of TNF-α at all CpG points but not IL-10. However, Chinese Tuina did not change the methylation level in promoter regions of TNF-α and IL-10. *Significance*. Chinese Tuina protected against HIE through inhibiting the neuroinflammatory reaction. While HIE markedly downregulated the methylation level of TNF-α, the protective effects of Chinese Tuina were independent of the regulation of the methylation level of TNF-α and IL-10.

1. Introduction

Neonatal hypoxic-ischemic encephalopathy (HIE) is a significant cause of perinatal morbidity and mortality. HIE damages the gray matter, including the sensorimotor cortex, basal ganglia, and thalamus, and results in abnormal white matter development [1, 2]. This leads to severe neurological deficits, such as cerebral palsy, mental retardation, seizures, learning disabilities, and other neurological disorders [3–5]. Although there is an increased understanding of the mechanisms underlying the pathophysiology of HIE, there are no current well-established treatments for HIE [6, 7]. Thus, it is essential to further study the pathophysiology of HIE and discover new treatment strategies and effective interventions.

Massage has significant effects on child development, especially for motor function disorders of children affected by cerebral palsy. The more early the treatment, the more effective is the massage therapy [8, 9]. Massage can increase

the distribution of blood and warmth to distal regions by pressing the major signal point [10, 11]. Chinese Tuina is a branch of massage technology that is widely used for spinal joint diseases or visceral diseases and involves manipulating spinal tissue, bone, joint, and meridians [12]. In Western countries, the corresponding treatment technology is called chiropractic or spinal manipulation, which refers to the dysfunction caused by spinal and adjacent subluxation, and is treated with specific treatment techniques [13]. These techniques can relieve skeletal muscle pain, shorten the recovery time of pain, improve the range of activity, correct the pathological deformity, and improve the physiological response in the central nervous system [14, 15]. Our previous clinical trial found that a three-month Chinese Tuina treatment alleviated muscle cramps and improved joint activity in cerebral palsy-affected children [16]. Furthermore, our animal experiments showed that Chinese Tuina therapy promoted growth and movement function recovery of hypoxia-ischemia injured SD rats [17]. However, the underlying molecular mechanism responsible for the neuroprotection of Chinese Tuina remains poorly understood.

The neuroinflammatory reaction is considered to be a critical pathophysiological factor in the development of an immature brain. The initial inflammatory response to hypoxic-ischemic injury results in secondary neuronal injury [18, 19]. Hypoxia-ischemia initially activates microglia, the resident immune cells in the brain, and then disrupts the blood-brain barrier (BBB), leading to peripheral leukocyte infiltration, which further intensifies inflammation and brain damage [20, 21]. Thereafter, a multitude of inflammatory cytokines are secreted by immune cells and activated astrocytes, which induces neuronal apoptosis, inhibits neurogenesis, and hampers repair of the brain [22]. Our previous research provided evidence that expression of proinflammatory cytokines including TNF-α was upregulated and expression of anti-inflammatory cytokines such as IL-10 was downregulated in patients [23, 24]. Evidence from neonatal animals demonstrated that inhibition of the inflammatory reaction is beneficial to recovery from the hypoxic-ischemic insult [25–27]. Thus, the neuroinflammatory reaction is a key therapeutic target for the treatment of neonatal ischemic brain damage.

DNA methylation is an epigenetic mechanism connected with somatopsychic fitness and disease [28]. It is also a crucial cellular mechanism for regulating gene expression associated with inflammatory processes [29]. DNA methylation can be modified and subsequently influence behavior and gene expression through early life experiences, as shown by studies in humans and animals [30–32]. In this study, we used an experimental neonatal hypoxic-ischemic rat model to investigate the effects of Chinese Tuina on the neuroinflammatory reaction, as well as the underlying mechanism.

2. Materials and Methods

2.1. Animals and Grouping. Animal experiments were carried out according to the regulations of Shanghai health clinical center laboratory animal welfare and ethics committee: N0.2019-A018-02 in Shanghai, China. Pregnant Sprague-Dawley (SD) rats (gestation age: 14-18 d) weighing 340-380 g were purchased from Shanghai Slac Laboratory Animal Co. Ltd. Before natural birth, the rats were reared at 24 ± 2°C with a 12-hour day and night cycle, in the animal laboratory of the Jinshan Hospital, which is affiliated with Fudan University, Shanghai. Relative conditions of humidity were 40%~70%. Water and food intake was available ad libitum. To avoid fighting, pregnant rats were housed separately. A total of 30 male pups were included in this study, which were randomly assigned to the hypoxic-ischemic model. The groups were the Chinese Tuina group (CHT group), sham control group (sham group), and hypoxic-ischemic model group (HIE group) with 10 rats in each group. The cortex tissue of 5 rats was used for WB and methylation detection experiment; limited by fund, the rats in the methylation detection experiment were 3. And 5 rats were used for the immunohistochemistry experiment.

2.2. Hypoxic-Ischemic Model and Testing. Three-day-old rats were used to prepare the hypoxic-ischemic model after their natural delivery by pregnant rats, as previously described [33]. The rats lying on their back on the operating table were anesthetized with isoflurane, and then, the neck skin was opened under a dissection microscope. After separating and ligating the left carotid artery, the wound was sutured, and then, they were placed in an airtight hypoxic box for 2 hours at 37°C temperature, 8% oxygen, and 92% nitrogen gas mixture.

The righting reflex experiment was used to detect whether the model was successful or not. The experiment was performed before weighing at P4 (4 days postnatal). The operation was initially to lift the tail of the rat pup and place its back on a horizontal board at first. Then, the operator placed their right index finger against the mandible of the rat pup and the right thumb on the hind legs. The two fingers of the right hand were then released while the left hand used a stopwatch to start the time. Each of the rat pups was tested twice, and rat pups that could not return to the normal position from an abnormal position in 20 seconds were placed into the hypoxic-ischemic group of pups.

2.3. Manipulation Method. A professional, certified physician was responsible for the Chinese Tuina intervention. On the first day after the HIE operation, the rats in the CHT group were given the Chinese Tuina intervention for 28 days with a frequency of Chinese Tuina manipulations of 120 per minute, which continued for 15 minutes. While the CHT group carried out the Chinese Tuina intervention, the sham group and the HIE group of pups were kept in their cages with no intervention. The Chinese Tuina intervention consisted of putting the pups with the face down on a slightly bent palm of the left hand, which provided balance and allowed pups to adapt to the environment. Thereafter, the middle finger of the right hand was used to do gentle Chinese Tuina from the back of the neck of the pup to the tail two or three times to relax the muscles. The dorsal and bilateral ligaments and muscles (called the Du meridian and bladder meridian, in traditional Chinese medicine (TCM)) of the pups were subjected to rubbing manipulation and pushing manipulation

Table 1: The gene sequence information of IL-10 and TNF-α.

Gene	Sequence and CpG loci information
TNF-α	TCCCAGAGCCCATACACACTCCCAGCTCTCAAGCCACTCTGCCTTCAGCCACTTCCTCTAAGAACTCAGACAAGGG GGCTTTCCCTCCTCAA**CG**TTGAGTCTCCCCCCTTATGCAGCCAGCTGTCAGAAGCACTCCCAATGCTAAGTTCTCCC CCATGGAAGTCCTGTTTAGAAATCAAAGGGGAA**CG**GACATAGGCATGGTGTCTCTGCAGAGAAACAATGGAAGACA GAGAGGAAATGGGTTTCAGTTCCCAGGGTTCTATACATCACACACACACACACACACACACACACACACACACAC ACACACA**CG**TTCCTGATTGGCCC**CG**GATTGCCACAGAATCCTGGTGAGGA**CG**GAGAGGAGATTCCTTGATGCCTGG GTGTCCCCAACTTTCCAAACCTCTGCCCC**CG**CATTGGAGAAGAAACTGAGAGAGGTGCAGGGCCACTAC**CG**CTTCCT CCACATGAGATCATGGTTTTCTCCACCAAGGAAGTTTTC**CGCG**GGTTGAATGAGAGCTTTTCCC**CG**CCCTCTTCCCC AAGGGCTATAAAGGCAGC**CG**GTACACAGCCAGC**CG**GCAGAACTCAG**CG**AGGACACCAAGGGACCAGCCAGGAGG GAGAACAGCAACTCCAGAACACCCTGGTACTAACTCCCAGAAAAGCAAGCAACCAGCCAGGCAGGTTC**CG**TCCCTC TCATACACTGGCC**CG**(**CpG1**)AGGCAACACATCTCCCTC**CG**(**CpG2**)GAAAGGACACCATGAGCA**CG**GAAAGCATGAT CCGAGATGTGGAACTGGCAGAGGAGG**CG**(**CpG3**)CTCCCCAAAAAGATGGGGGGCCTCCAGAACTCCA GG**CG**(**CpG4**)GTGTCTGTGCCTCAGCCTCTTCTCATTCCTGCT**CG**TGG**CG**(**CpG5**)GGGGCCACCA**CG**(**CpG6**)CTCTTC TGTCTACTGAACTT**CG**GGGTGAT**CG**(**CpG7**)GTCCCAACAAGGAGGAGGTGAGTGCCTGGGCAG**CG**TTTATTCTCAC TCACAAGCAAAGTAGGGTGGGAGGGCAAGAAAGGCAGGAGGGTAAGGGAAAGAGGT**CG**(**CpG8**)GCTGGTGGGCA CAGTAATGTGGAGGAGAGTTGGGGAGGGAGACCT**CG**GACC**CG**TGCAGCCAGTTGTCTAAACATCCTTGGGTGGATG CA**CG**GAGGGG**CG**AATGAA**CG**AACAAG**CG**TG**CG**TACA**CG**TGCAGAGATGTGCAGAGA**CG**TGGCCAGGGGAACAGG GAAGAAGCAAGAGATAAAAATT**CG**AGA**CG**GAGATGGGAGA**CG**AGGGAGATAAGGAGATATGAGAGATAAGGAG GGAGATGGAGGGGAAACAACAGATCAAGC
IL-10	AAGACCAAATAAGCTGAAGTTCCTGGTCCAC**CG**(**CpG1**)GCTCCAGTATGGTAACCCTCTCCAATGGGACAGGCTTGG AACCCTGTACCAAAAGAGATTCTCCTC**CG**(**CpG2**)TGCTGATGTGGGAAGGAGAACCCTGGGGTGTGCTCTCCACA TGGGTCAACTTTTATTTAAGCAAACAGTCCCTGGCCAACAGGACATGTAGTATTGCCCTGCTTGGGTCACACAGA AAACAGGTACCAGGAGGACAAGTGGCTTGCCCAGAGCACAGAGGGAAAAGCAGTGGAGGACTCTAGGTGAATGTT CTCCCCATCCAAACTAGAAGTAGGAGAAGTCC**CG**(**CpG3**)GTTGAAGGGAAGAACTAGCAGAGACTTCTGAGGACT CTGTAGAAATAATGACATCATCTCCATCCCTCCATCCTTCAACAGCCACAGGTCACACTTCTCCAAGCCT GGGA**CG**(**CpG4**)TTATAAAA**CG**GGGCCATGGTGAGGACTACCTAACAGCACAGAGCAAGCTTCCTGGAAGTCTGAGCT CCTTCTCCTAACTTTCCA**CG**CTGGAATCTGAGAACCTTTACAAAACACAGGCCAGAGAAGGCACCAGAACCCTCCT CTGAT**CG**TCTGTCACACAGCCAACAAACCTTTCAAGGAAGAGTCTTGAACACACAATGGAAGAATCAAAGAGAGTG AGTTTTGAGGGTAATCAGCCCTCTCCTGTTTCCTTTGGGTAACTGAGTGCTAAGGTGACCTCCTGGTCAGCAAGAAA TAG**CG**GACATTCAACCCAGGTTGAGTGGAGGAAATAATTATTTCTCAATCCTAATGTGCTCTGGAATAGCCCATTT ATGCA**CG**TCATTGTGACTTA**CG**AGTG**CG**TGAATGGAACCCACAGTTGTAGATTCTCTGTACATAGAACAGCTGTCTG CCTCAGGAAATACAACTTTTAGTATTGAGAAGCTAAAAAG

with one finger and a kneading manipulation from top to bottom, center to side [17].

2.4. Weight. To observe the growth and development of young rats, their weights were measured at P4, P9, P13, P21, and P31. The behavioral assessment including weight, balance beam experiment, and tilting plate experiment was performed by a laboratory assistant blinded to experiment design.

2.5. Balance Beam Experiment. The balance during movement was measured using a balance beam (35 cm long, 1.5 cm wide, and 100 cm high). Each rat starting from P21 was trained once a day for 3 consecutive days, and the height was gradually increased in preparation for the balance beam test. The test was conducted three times, and the mean of measurements was determined. Dates were recorded, as was the time of the initial setting, the time when the rat first entered the dark box (safety area), and the number of times when the rat's hind legs slipped on the balance beam.

2.6. Tilting Plate Experiment. The experiment was based on Rivlin's method to carry out a tilting plate experiment, which measured the recovery of motion function at P21 [34]. We placed the rat head forward, and the body longitudinal axis paralleled to the longitudinal axis of the inclined plate. The angle of the plate was increased gradually from small to large, until the maximum angle was achieved where the rat stayed on the plate for 5 s without dropping. This maximum angle was the behavior score of the slanting experiment. Each rat was tested 3 times, and the results were averaged.

2.7. Western Blot. These rats from each group were euthanized on the 33rd day after birth with 5% isoflurane. And the brains were obtained; the total proteins from the cerebral cortex of rats ($n = 5$) were extracted, and the protein concentration was measured by a BCA kit (Thermo). Then, the total protein was separated on 10% SDS-PAGE gels (Beyotime Biotechnology). Proteins on SDS-PAGE were transferred to a PVDF membrane, which was immersed in TBST blocking solution containing 5% skim milk powder and blocked at room temperature for 2 h. After removing the blocking solution, the PVDF membrane was cut according to the prestained protein standards and incubated in primary antibody against TNF-α and IL-10 rabbit polyclonal antibodies (Abcam) for 24 h at 4°C. An internal reference protein (β-actin) was applied in this study. After that, the membranes were washed three times by TBST (PBS containing 0.1% tween-20) and incubated in HRP-conjugated anti-rabbit IgG (Jackson ImmunoResearch Laboratories) for 1 h

Table 2: PCR primers and sequencing primers for CpG loci in the promoter region.

Primer	Base sequence (5′ to 3′)	Primer	Base sequence (5′ to 3′)
IL-10-1	F: AGATTAAATAAGTTGAAGTTTTTGGTTTA R: 5′biotin-CCAAAATTCTCCTTCCCACATCAA S: AGTTGAAGTTTTTGGTTTAT	TNF-α3	F: GAGATGTGGAATTGGTAGAGG R: 5′biotin-ATTCTAAAAACCCCCCATCTT S: GGAATTGGTAGAGGAG
IL-10-2	F: GGGATAGGTTTGGAATTTTGTATTAAAAGA R: 5′biotin-CCAAAATTCTCCTTCCCACATC S: GGAATTTTGTATTAAAAGAGATTT	TNF-α4	F: GAGATGTGGAATTGGTAGAGG R: 5′biotin-ACACTCACCTCCTCCTTAT S: GGGGGGTTTTTAGAAT
IL-10-3	F: TAGTGGAGGATTTTAGGTGAATGT R: 5′biotin-TTCTACAAAATCCTCAAAAATCTCTAC S: ATTAGAAGTAGGAGAAGTT	TNF-α5	F: AGAATTTTAGGAGGTGTTTGTGTTTTAGT R: 5′biotin-CCTCCCACCCTACTTTACTTATAAAT S: ATTAAGTTTTTTTGTTTATTGAAT
IL-10-4	F: AGATTTTTGAGGATTTTGTAGAAATAATG R: 5′biotin-AACTCAAACTTCCAAAAAACTTACTC TAT S: TCCTCACCATAACCC	TNF-α6	F: AGAATTTTAGGAGGTGTTTGTGTTTTAGTT R: 5′biotin-ACCCTCCCACCCTACTTTACTTATAAAT S: GTGAGTGTTTGGGTAG
TNF-α1	F: GGGATTAGTTAGGAGGGAGAATAGTA R: 5′biotin-TAAAATTCTAAAAACCCCCCATCTT S: AGTAATTAGTTAGGTAGGTT	TNF-α7	F: GGTAGGAGGGTAAGGGAAAGA R: 5′biotin-ATCCCAAATCTCCCTCCCCAACTC S: GGTAAGGGAAAGAGGT
TNF-α2	F: GGGATTAGTTAGGAGGGAGAATAGTA R: 5′biotin-CTAAAATTCTAAAAACCCCCCATC S: ATTTTTTTTAGGAAAGGATATTAT	TNF-α8	F: ATAGTAATGTGGAGGAGAGTTGG R: 5′biotin-ACCCAAAAATATTTAAACAACTAACT ACA S: TTGGGGAGGGAGATT

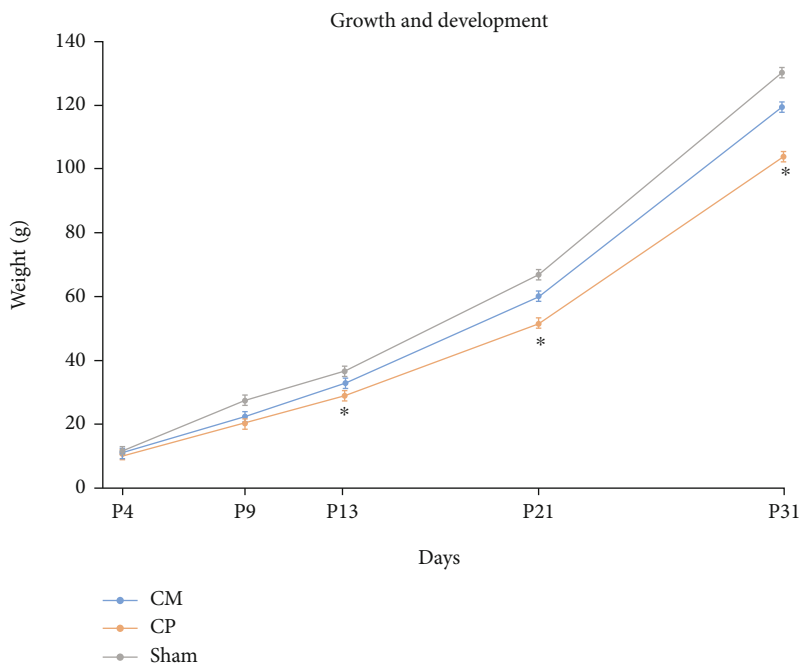

Figure 1: Chinese Tuina promoted growth and development in rats with HIE. $^{*}P < 0.05$, comparison with the HIE group, $n = 10$.

at room temperature. After three washes, the protein signals were determined by the gel imager and image analysis system (Tanon Technology Co., Ltd., Shanghai).

2.8. Immunohistochemistry Staining. Rat pups were deeply anesthetized with 5% isoflurane on the 33rd day after birth and transcardially perfused with physiological saline and

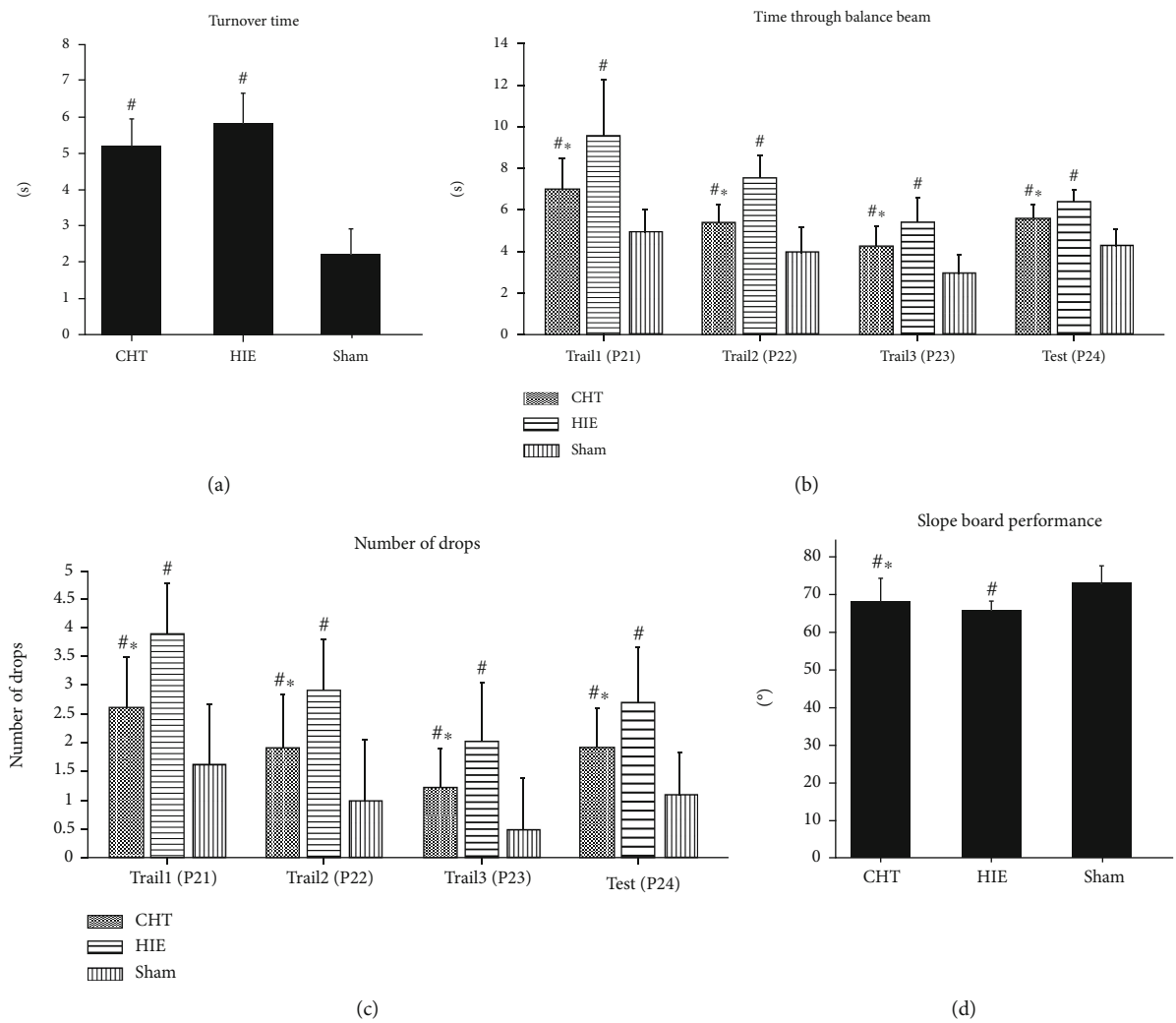

Figure 2: Chinese Tuina improved behavioral recovery in rats with HIE. $^{*}P < 0.05$, comparison with the HIE group, $^{\#}P < 0.05$: comparison with the sham group, $n = 10$.

4% paraformaldehyde. The brains were gained and dehydrated in 20% sucrose solution overnight. Then, these brains were cut into slices of 30 μm thick on the freezing microtome (SLEE, Germany). These slices were permeabilized with 0.2% Triton X-100 for 15 min and were then blocked with 10% normal goat serum for 1 h at room temperature. After that, they were incubated with primary antibody against TNF-α and IL-10 rabbit polyclonal antibodies (Abcam) for 1 hour at room temperature and then at 4°C overnight. On the next day, they were washed with PBS and incubated with biotinylated goat anti-rabbit IgG for one hour at room temperature. And then, they were treated in an avidin-horseradish peroxidase complex (Vectastain Elite ABC-Reagent, Vector) for 30 min and colored with diaminobenzidine (Sigma-Aldrich). The positive signals were digitized with a microscope (Nikon, Japan).

2.9. The Detection of Level in Methylation by Pyrosequencing. Genomic DNA extraction kits (Qiagen Co., Ltd., No. 51306) and methylation modification kits (Qiagen Co., Ltd., No. 59104) were used. The DNA methylation analysis by Sequenom mass spectra was carried out by Shanghai Benegene Biotechnology Co., Ltd. The gene sequence information of IL-10 and TNF-α in rats was obtained through the NCBI (National Center of Biotechnology Information) website. Primers for these genes were designed by PyroMark Assay Design 2.0 and synthesized by BGI Genomics (Tables 1 and 2). Rats ($n = 3$) were sacrificed to extract DNA with a genomic DNA extraction kit (Qiagen Co., Ltd., No. 51306) on the 33rd day. The DNA was modified with a bisulfate reagent with a methylation modification kit (Qiagen Co., Ltd, No. 59104). PCR amplification of the pyrosequencing template was performed using primers in Table 2. PCR amplification conditions were 95°C for 3 min, 94°C for 30 s, 56°C for 30 s, and 72°C for 1 min, 40 cycles. Pyrosequencing and the frequency of methylation were determined by PyroMark Q96 ID (Qiagen) [35]. Pyro Q-CpG software automatically analyzed the methylation state of each site.

F: upstream primer; R: downstream primers; S: sequencing primers; biotin: labeled biotin.

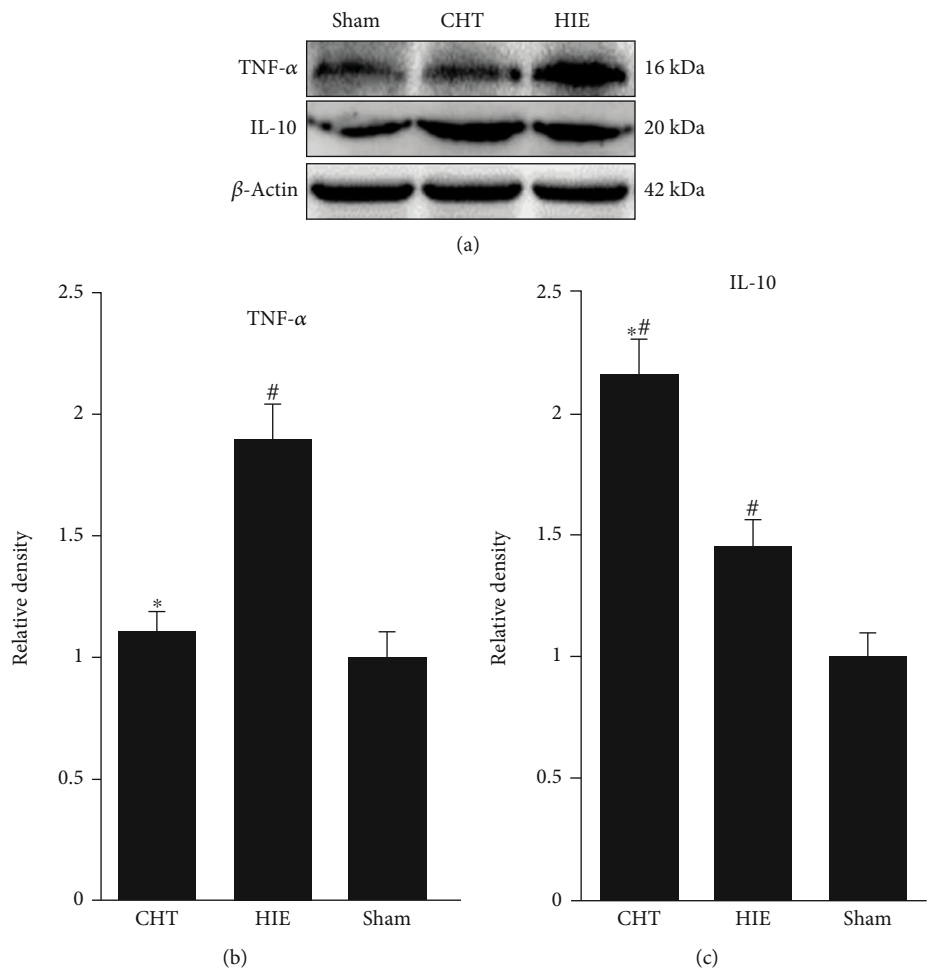

Figure 3: Chinese Tuina improved the neuroinflammatory reaction in rats with HIE. (a) Representative images of Western blotting for TNF-α and IL-10. (b, c) Quantification of the optical density for TNF-α and IL-10, normalized to β-actin. $^{*}P < 0.05$, comparison with the HIE group; $^{\#}P < 0.05$, comparison with the sham group, $n = 5$.

2.10. Statistical Analysis. The data were presented as means ± standard deviation (SD). The test standard was $\alpha = 0.05$. Single factor analysis of variance (one-way ANOVA) was used to compare the differences among groups of measurement data. The LSD t-test (Fisher's least significant difference t-test) was used for pairwise comparison of multiple measurement data. A value of $P < 0.05$ was considered to be statistically significant.

3. Results

3.1. Chinese Tuina Promoted the Growth and Development in Neonatal Hypoxic-Ischemic Rats. The results from weight gain showed that the hypoxic-ischemic model led to delayed growth and development. Chinese Tuina promoted the growth and development in rats with HIE at postnatal days 13, 21, and 31 (the days 9, 17, and 27 of operation) compared with the CHT group ($P < 0.05$, Figure 1). Notably, there was no difference in the weight gain between the CHT group and the sham group ($P > 0.05$ for all test points). These results indicated that rats in the HIE group were slow to gain and grow, whereas Chinese Tuina promoted the growth and development in neonatal hypoxic-ischemic rats.

3.2. Chinese Tuina Improved Behavioral Recovery in Neonatal Hypoxic-Ischemic Rats. The hypoxic-ischemic treatment led to significant impairment in righting reflex in both the CHT and HIE groups compared with the sham group on day 4 postnatal ($P < 0.05$, Figure 2), whereas there were no statistical differences between the CHT group and the HIE group ($P = 0.293 > 0.05$). This result showed that the hypoxic-ischemic model was successful. The motor and balance function recovery in the balance beam test showed that Chinese Tuina improved the time taken to pass through the balance beam and reduced the number of drops from the balance beam ($P < 0.05$, Figures 2(b) and 2(c)). However, these beneficial effects induced by Chinese Tuina did not reach the level of the sham group ($P < 0.05$, compared with the sham group, Figures 2(b) and 2(c)). Similarly, the rats in the CHT group had a steeper slope than rats in the HIE group ($P < 0.05$, Figure 2(d)), while the rats in the sham group had the steepest slope among the three groups. These results indicated that Chinese Tuina promoted the motor

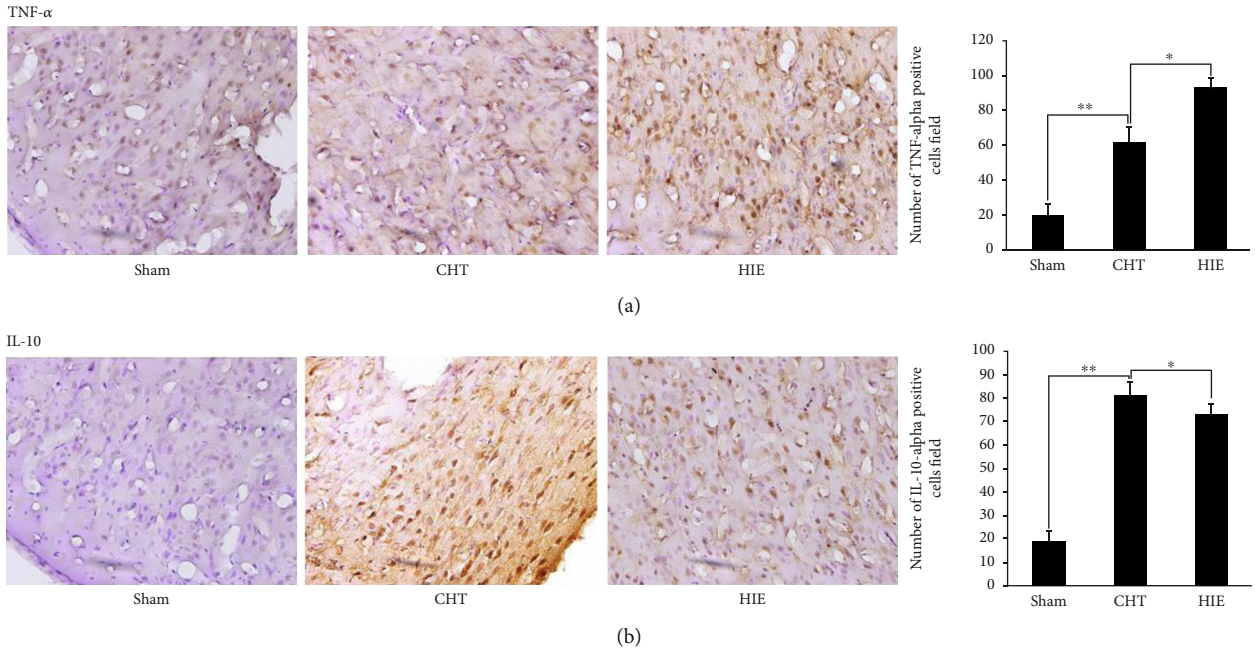

Figure 4: Chinese Tuina improved the neuroinflammatory reaction in rats with HIE. (a) Representative photomicrographs of TNF-α-positive cells (40x) and the quantitative results of the number of positive cells; (b) representative photomicrographs of IL-10-positive cells (40x) and the quantitative results of the number of positive cells.

and balance function recovery in neonatal hypoxic-ischemic, rats but the recovery was not complete.

3.3. Chinese Tuina Improved the Neuroinflammatory Reaction in Neonatal Hypoxic-Ischemic Rats. TNF-α is a key proinflammatory cytokine in neonatal hypoxic-ischemic encephalopathy and prevents nerve growth and repair. Western blot analysis showed that 4 weeks of Chinese Tuina inhibited the expression of TNF-α, which attained the level of the sham group (Figures 3(a) and 3(b)).

IL-10 has an important anti-inflammatory action, and its upregulated expression is beneficial to the neuroplastic niche in brain disease. We measured the expression of IL-10 by Western blot, and the results showed that neonatal hypoxia-ischemia upregulated the expression of IL-10 compared to the sham group and that Chinese Tuina increased the expression of IL-10 compared to the HIE group.

These findings suggest that Chinese Tuina improves the neuroplastic niche in neonatal hypoxic-ischemic rats through the decreased expression of proinflammatory cytokine TNF-α and increased expression of anti-inflammatory cytokine IL-10.

3.4. Evaluation of Neuroinflammatory Reaction by Immunohistochemistry. To further investigate the effects of Chinese Tuina on the neuroinflammatory reaction, we detected the expressions of TNF-α and IL-10 by immunohistochemistry. Similar to the results of Western blot, Chinese Tuina significantly decreased the positive cells of TNF-α and increased the positive cells of IL-10 in the cortex of neonatal hypoxic-ischemic rats (Figures 4(a) and 4(b)).

3.5. The Effects of Chinese Tuina on the Methylation Level of Cytokines TNF-α and IL-10 in Neonatal Hypoxic-Ischemic Rats. Through sequence analysis, we chose 8 and 4 CpG islands in the promoter regions of the TNF-α and the IL-10 gene, respectively. While the results showed that the hypoxic-ischemic injury markedly changed the methylation status in the promoter region of TNF-α at all of the tested CpG islands, the Chinese Tuina intervention did not change the methylation status in the promoter region of TNF-α compared to the HIE group (Figure 5(a)). Interestingly, the neonatal hypoxic-ischemic model led to reduced methylation levels at CpG islands 1-7 in the TNF-α promoter region but increased the methylation level at the 8th CpG island. The results indicated that the neonatal hypoxic-ischemic model resulted in changes in the methylation status in the promoter region of TNF-α. However, the neonatal hypoxic-ischemic model did not change the methylation status in the promoter region of IL-10, and Chinese Tuina did not change the methylation status in the promoter region of IL-10 compared to the HIE group (Figure 5(b)).

4. Discussion

The neuroinflammatory reaction is the major detrimental factor within the neuroplastic niche in nervous system disease. The improved neuroinflammatory reaction is critical for renewal and repair. In the present study, we found that neonatal hypoxia-ischemia markedly downregulated the methylation level of TNF-α but did not change the methylation level of IL-10. Chinese Tuina may improve the neuroplastic niche in neonatal hypoxic-ischemic rats through inhibition of the expression of the proinflammatory cytokine

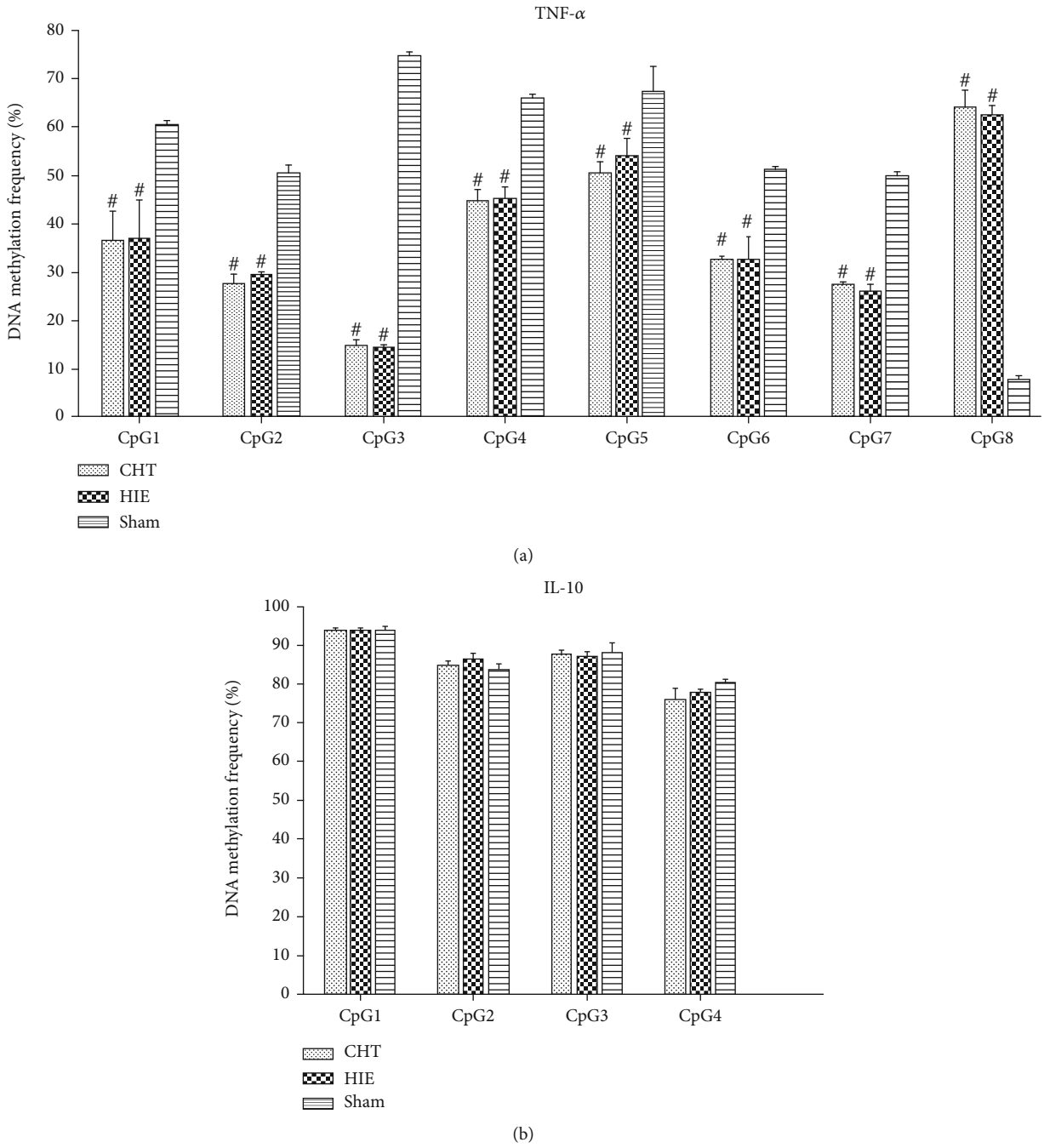

Figure 5: DNA methylation level in the promoter region of cytokines TNF-α and IL-10. $^{\#}P < 0.05$: comparison with the sham group, $n = 3$.

TNF-α and increasing the expression of the anti-inflammatory cytokine IL-10. However, the beneficial effects of Chinese Tuina were independent of the regulation of methylation levels in the TNF-α and IL-10 promoter regions.

Chinese Tuina, massage, and touch therapy was widely applied to the prevention and treatment of pediatric diseases. Touch therapy promoted the maturation of the autonomic system, heart rate, and respiration and circadian systems through skin-to-skin contact between a mother or physiotherapists and an infant [36]. And massage enhanced vagal activity and reduced cortisol levels through the stimulation of pressure receptors [37]. Chinese Tuina regulated the circulation of Qi and blood, unblocked the impaired meridians, and promoted the recovery of function. The therapy method of Chinese Tuina was a series of orderly manual techniques on the surface of the body. These manual techniques included press, knead, knock, and friction. Although Chinese Tuina, massage, and touch therapy belonged to noninvasive therapy through using various manual techniques, the choice of locations on the body and the specified manual techniques of Chinese Tuina were based on Traditional Chinese Medicine (TCM) zang-fu organs and meridian theory. Chinese Tuina paid more attention to unblocking meridians and the balance of Yin and Yang [38]. Previous studies showed that

Chinese Tuina improved learning ability and memory in rat pups with hypoxic ischemia. The mechanism may involve the regulation of monoamine neurotransmitters such as 5-HT, norepinephrine (NE), adrenaline (E), and dopamine (DA) in the hippocampus [39].

The cerebral cortex and hippocampus show obvious abnormal inflammatory responses and are involved in the development of neonatal hypoxic-ischemic injury [40, 41]. The most important neuropathological changes in the brains of children with hypoxic ischemia are in the area of cerebral white matter injury accompanied by periventricular leukomalacia (PVL) [42]. This injury is due to the high sensitivity of some nerve cells to ischemia and hypoxia. Chronic cerebral ischemia and hypoxia increase the release of proinflammatory cytokines and promote the apoptosis of oligodendrocytes, which are the main cells that make up the white matter of the brain [41, 43, 44]. Therefore, we suspect that abnormal regulation of neurotransmitters is closely related to the occurrence and progression of hypoxic ischemia, and this is mediated by inflammatory factors. Variations in DNA methylation are an important inflammatory regulatory mechanism in hypoxia-ischemia [45, 46]. Our results confirmed that neonatal hypoxia-ischemia markedly decreased the methylation level at CpG islands 1-7 in the TNF-α promoter region, which is a critical proinflammatory factor in neonatal hypoxic-ischemic encephalopathy. Although the methylation position at the 8th CpG island was increased in the CHT group, the methylation level in the whole methylated region was decreased. Thus, the transcription and the protein expression of the TNF-α were increased. This result had been confirmed by Western blot detection which showed that the protein expression of TNF-α was significantly upregulated in the HIE group compared with the sham group. However, Chinese Tuina inhibited the upregulation of TNF-α which was detected by Western blot. The possible reason was posttranscriptional regulation. The undergoing mechanisms need further study.

In this study, to compensate for the known effect of estrogen [47], we only included male rat pups in the study and we carried out the righting reflex experiment to substantiate the hypoxic-ischemic model [48]. Further support for the model was obtained at the behavior and molecular levels. This study has several novel findings: (i) Chinese Tuina promoted weight gain of hypoxic-ischemic rats, shortened the time taken to pass through the balance beam, and increased the angle at which the rat pups stayed on the inclined plate. These data suggested that Chinese Tuina was beneficial to the development of motor and balance function in the hypoxic-ischemic rats. (ii) The cerebral cortex of hypoxic-ischemic rat pups had an inflammatory response, which involved the pro- and anti-inflammatory factors TNF-α and IL-10, respectively. Chinese Tuina improved the neural inflammatory response through reduced protein expression of TNF-α and increased protein expression of IL-10. These results suggest that Chinese Tuina therapy may confer neuroprotection by restoring the equilibrium in the inflammatory response niche in neonatal hypoxic-ischemic rats. (iii) The results indicated that the hypoxic-ischemic model changed the methylation status in the promoter region of TNF-α. However, the hypoxic-ischemic model did not change the methylation status in the promoter region of IL-10, and Chinese Tuina did not change the methylation status in the promoter region of IL-10 and TNF-α compared to the HIE group.

Methylation is an important epigenetic modification that regulates the expression of many genes, including those that encode inflammatory cytokines [49]. In the present study, we found that neonatal hypoxia-ischemia changed the methylation level in the promoter regions of inflammation-related genes. Thus, the regulation of methylation levels is a potential therapeutic target for the treatment of neonatal hypoxic-ischemic encephalopathy. However, the mechanism by which Chinese Tuina improved the inflammatory response in neonatal hypoxic-ischemic encephalopathy was independent of the regulation of methylation levels in IL-10 and TNF-α.

5. Conclusion

In this study, we found that neonatal hypoxic-ischemic injury markedly downregulated the methylation level in the promoter regions of the TNF-α gene and increased its protein expression. Meanwhile, neonatal hypoxic-ischemic injury upregulated the expression of IL-10 but did not change the methylation level in the promoter regions of IL-10. We concluded that Chinese Tuina was beneficial for improving the growth and the ability to balance in rats with neonatal HIE. The possible mechanism could be that Chinese Tuina inhibited the neuroinflammatory reaction and improved the neuroplastic niche in neonatal hypoxic-ischemic rats. But the protective effects of Chinese Tuina were independent of the regulation of methylation levels of TNF-α and IL-10. The undergoing mechanism needs further study.

Data Availability

The data used to support the findings of this study are included within the article.

Conflicts of Interest

The authors declare that there are no conflicts of interest.

Authors' Contributions

Pengyue Zhang, Qian Zhang, and Bowen Zhu contributed equally to this work.

Acknowledgments

This study was funded by the National Natural Science Foundation of China (grant numbers: 81860886, 81460748 and 81660384), Yunnan Applied Basic Research Projects (2017FB119), and Yunnan Province University Innovation Team Projects (Acupuncture prevents Mental disease). Thanks are due to all the instructors and colleagues in this study for their work in data collection and entry, especially Yunpeng Zhang and Qiong Luo in Shanghai and Yongli

Song in Kunming Medical University. We also thank the staff in the central laboratories of Jinshan Hospital, Fudan University. We also acknowledge Dr. Bill Kalionis for his assistance with editing this manuscript.

References

[1] R. D. Folkerth, "Neuropathologic substrate of cerebral palsy," *Journal of Child Neurology*, vol. 20, pp. 940–949, 2005.

[2] K. R. Gopagondanahalli, J. Li, M. C. Fahey et al., "Preterm hypoxic–ischemic encephalopathy," *Frontiers in Pediatrics*, vol. 4, p. 114, 2016.

[3] F. J. Northington, R. Chavez-Valdez, and L. J. Martin, "Neuronal cell death in neonatal hypoxia-ischemia," *Annals of Neurology*, vol. 69, no. 5, pp. 743–758, 2011.

[4] J. Shetty, "Neonatal seizures in hypoxic-ischaemic encephalopathy-risks and benefits of anticonvulsant therapy," *Developmental Medicine and Child Neurology*, vol. 57, pp. 40–43, 2015.

[5] M. Douglas-Escobar and M. D. Weiss, "Hypoxic-ischemic encephalopathy," *JAMA Pediatrics*, vol. 169, no. 4, pp. 397–403, 2015.

[6] S. Shankaran, "Hypoxic-ischemic encephalopathy and novel strategies for neuroprotection," *Clinics in Perinatology*, vol. 39, no. 4, pp. 919–929, 2012.

[7] B. Dixon, C. Reis, W. Ho, J. Tang, and J. Zhang, "Neuroprotective strategies after neonatal hypoxic ischemic encephalopathy," *International Journal of Molecular Sciences*, vol. 16, pp. 22368–22401, 2015.

[8] M. A. Diego, T. Field, and M. Hernandez-Reif, "Vagal activity, gastric motility, and weight gain in massaged preterm neonates," *The Journal of Pediatrics*, vol. 147, no. 1, pp. 50–55, 2005.

[9] W. Shi, H. Yang, B. Shi et al., "Effects of motor-development massage therapy on gross motor function in children with cerebral palsy," *Chinese Journal of Evidence-based Pediatrics*, vol. 2, pp. 354–363, 2007.

[10] Y. Viravud, A. Apichartvorakit, P. Mutirangura et al., "The anatomical study of the major signal points of the court-type Thai traditional massage on legs and their effects on blood flow and skin temperature," *Journal of Integrative Medicine*, vol. 15, no. 2, pp. 142–150, 2017.

[11] G. Seifert, J. L. Kanitz, C. Rihs, I. Krause, K. Witt, and A. Voss, "Rhythmical massage improves autonomic nervous system function: a single-blind randomised controlled trial," *Journal of Integrative Medicine*, vol. 16, no. 3, pp. 172–177, 2018.

[12] P. D. Liao, *Pediatric Tuina*, People's Medical Publishing House, Beijing, 2016.

[13] G. Gyer, J. Michael, J. Inklebarger, and J. S. Tedla, "Spinal manipulation therapy: is it all about the brain? A current review of the neurophysiological effects of manipulation," *Journal of Integrative Medicine*, vol. 17, no. 5, pp. 328–337, 2019.

[14] L. Yikai, "The history of spinal manipulation," *The Journal of Cervicodynia and Lumbodynia*, vol. 22, no. 2, pp. 169–171, 2001.

[15] L. Xie and L. Yikai, "Advances in research on the therapeutic effect of spinal massage on low back pain," *Journal of External Therapy of TCM*, vol. 23, no. 4, pp. 49–52, 2014.

[16] L. Hu, X. Tai, and C. Wang, "Clinical trial of selective spinal massage therapy in the treatment for child spastic cerebral palsy," *Journal of Yunnan University of Traditional Chinese Medicine*, vol. 32, no. 1, pp. 1000–2723, 2009.

[17] B. Zhu, G. Xiong, Q. Zhang, X. Hua, and X. Tai, "The experimental study of time effects of spinal massage intervention on hypoxic ischemic cerebral palsy rats growth and function of movement," *Lishizhen Medicine And Materia Research*, vol. 28, no. 9, pp. 2274–2277, 2017.

[18] U. S. Bhalala, R. C. Koehler, and S. Kannan, "Neuroinflammation and neuroimmune dysregulation after acute hypoxic-ischemic injury of developing brain," *Frontiers in Pediatrics*, vol. 2, p. 144, 2014.

[19] H. Hagberg, C. Mallard, D. M. Ferriero et al., "The role of inflammation in perinatal brain injury," *Nature Reviews Neurology*, vol. 11, no. 4, pp. 192–208, 2015.

[20] F. Liu and L. D. Mccullough, "Inflammatory responses in hypoxic ischemic encephalopathy," *Acta PharmacologicaSinica*, vol. 34, pp. 1121–1130, 2013.

[21] B. Li, K. Concepcion, X. Meng, and L. Zhang, "Brain-immune interactions in perinatal hypoxic-ischemic brain injury," *Progress in Neurobiology*, vol. 159, pp. 50–68, 2017.

[22] R. K. Jellema, P. V. Lima, D. R. Ophelders, T. G. Wolfs, A. Zwanenburg, and S. De Munter, "Systemic G-CSF attenuates cerebral inflammation and hypomyelination but does not reduce seizure burden in preterm sheep exposed to global hypoxia-ischemia," *Experimental Neurology*, vol. 250, pp. 293–303, 2013.

[23] D. Jianwei, T. Xiantao, X. Lei, J. J. YangXiaojiao, W. J. LiaoYingye, and P. Zhengyu, "Characteristics of inflammatory cytokine gene expression profiles of cerebral cortex and white matter of rats with hypoxic-ischemic cerebral palsy," *Journal of Chengdu Medical College*, vol. 7, no. 4, pp. 508–511, 2012.

[24] X. Tai, J. Ding, X. Yang et al., "Regulation of inflammatory cytokine genes in the therapy of massage rehabilitation for cerebral palsy," *Journal of Chengdu Medical College.*, vol. 4, pp. 527–532, 2012.

[25] M. Hedtjärn, A.-L. Leverin, K. Eriksson, K. Blomgren, C. Mallard, and H. Hagberg, "Interleukin-18 involvement in hypoxic-ischemic brain injury," *The Journal of Neuroscience*, vol. 22, no. 14, pp. 5910–5919, 2002.

[26] N. Fathali, N. H. Khatibi, R. P. Ostrowski, and J. H. Zhang, "The evolving landscape of neuroinflammation after neonatal hypoxia-ischemia," in *Intracerebral Hemorrhage Research*, J. Zhang and A. Colohan, Eds., vol. 111 of Acta Neurochirurgica Supplementum, pp. 93–100, Springer, Vienna, 2011.

[27] C. H. Nijboer, H. J. Bonestroo, J. Zijlstra, A. Kavelaars, and C. J. Heijnen, "Mitochondrial jnk phosphorylation as a novel therapeutic target to inhibit neuroinflammation and apoptosis after neonatal ischemic brain damage," *Neurobiology of Disease*, vol. 54, pp. 432–444, 2013.

[28] S. Docherty and J. Mill, "Epigenetic mechanisms as mediators of environmental risks for psychiatric disorders," *Psychiatry*, vol. 7, no. 12, pp. 500–506, 2008.

[29] P. Stenvinkel, M. Karimi, S. Johansson, and J. Axelsson, "Impact of inflammation on epigenetic DNA methylation ? A novel risk factor for cardiovascular disease?," *Internal Medicine*, vol. 261, no. 5, pp. 488–499, 2007.

[30] I. C. G. Weaver, N. Cervoni, F. A. Champagne et al., "Epigenetic programming by maternal behavior," *Nature Neuroscience*, vol. 7, no. 8, pp. 847–854, 2004.

[31] T. F. Oberlander, J. Weinberg, M. Papsdorf, R. Grunau, S. Misri, and A. M. Devlin, "Prenatal exposure to maternal

depression, neonatal methylation of human glucocorticoid receptor gene (NR3C1) and infant cortisol stress responses," *Epigenetics*, vol. 3, pp. 97–106, 2008.

[32] D. Spengler, C. Murgatroyd, A. V. Patchev et al., "Dynamic DNA methylation programs persistent adverse effects of early-life stress," *Nature Neuroscience*, vol. 12, pp. 1559–1566, 2009.

[33] J. E. Rice 3rd, R. C. Vannucci, and J. B. Brierley, "The influence of immaturity on hypoxic-ischemic brain damage in the rat," *Annals of Neurology*, vol. 9, no. 2, pp. 131–141, 1981.

[34] A. S. Rivlin and C. H. Talor, "Objective clinical assessment of motor function after experimental spinal cord injury in the rat," *Journal of Neurosurgery*, vol. 47, no. 4, pp. 577–581, 1977.

[35] Z. Yan and Z. Gang, "Comparative study of EGFR mutations in non-small cell cancer patients by Sanger sequencing and pyrosequencing," *Modern Preventive Medicine*, vol. 44, no. 8, pp. 1494–1498, 2017.

[36] R. Feldman and A. I. Eidelman, "Skin-to-skin contact (kangaroo care) accelerates autonomic and neurobehavioural maturation in preterm infants," *Developmental Medicine and Child Neurology*, vol. 45, no. 4, pp. 274–281, 2003.

[37] T. Field, "Massage therapy research review," *Complementary Therapies in Clinical Practice*, vol. 24, pp. 19–31, 2016.

[38] World Health Organization, *Benchmarks for training in traditional/complementary and alternative medicine: benchmarks for training in tuina*, World Health Organization, Geneva, 2010.

[39] Q. He, Q. Zhang, X. Tai et al., "Influence and mechanism of spinal massage on learning and memory in juvenile rat with cerebralpalsy," *Guiding Journal of Traditional Chinese Medicine and Pharmacology*, vol. 24, no. 11, pp. 36–39, 2018.

[40] H. Kadhim, B. Tabarki, C. De Prez, and G. Sébire, "Cytokine immunoreactivity in cortical and subcortical neurons in periventricular leukomalacia:are cytokines implicated in neuronal dysfunction in cerebral palsy," *Acta Neuropathologica*, vol. 105, no. 3, pp. 209–216, 2003.

[41] C. Y. Lin, Y. C. Chang, S. T. Wang, T. Y. Lee, C. F. Lin, and C. C. Huang, "Altered inflammatory responses in preterm children with cerebral palsy," *Annals of Neurology*, vol. 68, no. 2, pp. 204–212, 2010.

[42] L. W. Fan, A. Kaizaki, L. T. Tien et al., "Celecoxib attenuates systemic lipopolysaccharide-induced brain inflammation and white matter injury in the neonatal rats," *Neuroscience*, vol. 240, pp. 27–38, 2013.

[43] J. R. Buser, K. N. Segovia, J. M. Dean et al., "Timing of appearance of late oligodendrocyte progenitors coincides with enhanced susceptibility of preterm rabbit cerebral white matter to hypoxia-ischemia," *Journal of Cerebral Blood Flow and Metabolism*, vol. 30, no. 5, pp. 1053–1065, 2010.

[44] C. Sterling, E. Taub, D. Davis et al., "Structural neuroplastic change after constraint-induced movement therapy in children with cerebral palsy," *Pediatrics*, vol. 131, no. 5, pp. e1664–e1669, 2013.

[45] J. Vanselow, W. Yang, J. Herrmann et al., "DNA-remethylation around a STAT5-binding enhancer in the αS1-casein promoteris associated with abrupt shutdown of αS1-casein synthesis during acute mastitis," *Journal of Molecular Endocrinology*, vol. 37, no. 3, pp. 463–477, 2006.

[46] B. Tycko, "Epigenetic gene silencing in cancer," *Journal of Clinical Investigation*, vol. 105, no. 4, pp. 40l–407, 2000.

[47] M. A. Mirza, R. Ritzel, Y. Xu, L. D. McCullough, and F. Liu, "Sexually dimorphic outcomes and inflammatory responses in hypoxic-ischemic encephalopathy," *Journal of Neuroinflammation*, vol. 12, no. 1, p. 32, 2015.

[48] T. Zeng, L. H. Yang, J. J. Huang et al., "Effects of hypoxic-ischemic brain damage on study and memory and emotional behavior in 3-day-old neonatal rats," *China Journal of Modern Medicine*, vol. 20, no. 23, pp. 3530–3538, 2010.

[49] R. Myte, B. V. G. AnneliSundkvist, and S. Harlid, "Circulating levels of inflammatory markers and DNA methylation, an analysis of repeated samples from a population based cohort," *Epigenetics*, vol. 14, no. 7, pp. 649–659, 2019.

Hindawi
Neural Plasticity
Volume 2020, Article ID 8830005, 8 pages
https://doi.org/10.1155/2020/8830005

Research Article

Brief Mindfulness Meditation Induces Gray Matter Changes in a Brain Hub

Rongxiang Tang,[1] Karl J. Friston,[2] and Yi-Yuan Tang[3]

[1]*Department of Psychological and Brain Sciences, Washington University in St. Louis, St. Louis, MO 63105, USA*
[2]*Wellcome Centre for Human Neuroimaging, UCL Queen Square Institute of Neurology, University College London, London WC1N 3AR, UK*
[3]*Department of Psychological Sciences, Texas Tech University, Lubbock, TX 79409, USA*

Correspondence should be addressed to Yi-Yuan Tang; yiyuan.tang@ttu.edu

Received 6 September 2020; Revised 11 October 2020; Accepted 30 October 2020; Published 16 November 2020

Academic Editor: Wei-Lin Liu

Previous studies suggest that the practice of long-term (months to years) mindfulness meditation induces structural plasticity in gray matter. However, it remains unknown whether short-term (<30 days) mindfulness meditation in novices could induce similar structural changes. Our previous randomized controlled trials (RCTs) identified white matter changes surrounding the anterior cingulate cortex (ACC) and the posterior cingulate cortex (PCC) within 2 to 4 weeks, following 5-10 h of mindfulness training. Furthermore, these changes were correlated with emotional states in healthy adults. The PCC is a key hub in the functional anatomy implicated in meditation and other perspectival processes. In this longitudinal study using a randomized design, we therefore examined the effect of a 10 h of mindfulness training, the Integrative Body-Mind Training (IBMT) on gray matter volume of the PCC compared to an active control—relaxation training (RT). We found that brief IBMT increased ventral PCC volume and that baseline temperamental trait—an index of individual differences was associated with a reduction in training-induced gray matter increases. Our findings indicate that brief mindfulness meditation induces gray matter plasticity, suggesting that structural changes in ventral PCC—a key hub associated with self-awareness, emotion, cognition, and aging—may have important implications for protecting against mood-related disorders and aging-related cognitive declines.

1. Introduction

Decades of scientific research on mindfulness meditation has demonstrated a wide range of positive effects on psychological well-being and related aspects of cognitive function in healthy and clinical populations [1, 2]. Neuroimaging studies speak to the correlates of mindfulness meditation in terms of brain functional and structural plasticity; especially, key brain hubs involved in self-awareness, emotion regulation, and attentional control [1, 3, 4]. Although prior work suggests *functional* changes in both novices with short-term training and experienced meditators with long-term practice, *structural* changes in gray matter have been found mainly in experienced meditators [1, 5]. One preliminary finding indicated changes in gray matter after 2 months of mindfulness-based stress reduction, compared to a waitlist control [6]. However, it remains to be established whether such structural effects of mindfulness training are evident when compared to an active control, using a rigorous randomized design [7–9].

A meta-analysis has identified several brain structures altered by meditation, such as the anterior cingulate cortex (ACC), insula, and hippocampus [5]. However, while both the ACC and insula are important constituents of the salience network implicated in self-awareness and mindfulness meditation [1], the default mode network (DMN) has received less attention in structural studies. The DMN includes the medial prefrontal cortex and posterior cingulate cortex (PCC) and is actively engaged (and affected) in mindfulness as evidenced by functional neuroimaging studies [1, 10, 11].

Prior literature regarding the effect of meditation on the PCC has shown a reduction in its activation during meditation [11], but an increase in its functional connectivity with "task-positive" regions in the executive control network and salience network (e.g., ACC and prefrontal cortex), both at rest and during meditation [11–13]. Because the PCC is commonly implicated in self-referential processing and mind-wandering [14], decreased activation during meditation could be interpreted as reduced mind-wandering, whereas increased coupling with other control-related networks may suggest better self-regulatory function as a result of meditation experiences [11–13]. Therefore, it is plausible that brief or short-term mindfulness could induce not only functional changes in the DMN but also structural plasticity in key nodes or integrative hubs.

Our randomized studies—using a form of mindfulness meditation, the integrative body–mind training (IBMT)—have shown that 5 sessions of IBMT (30 min/session) improved self-control abilities in domains of attention and emotion, as well as increased functional changes in neuronal activity and metabolism in the ACC and PCC [15, 16]. Moreover, 10-20 sessions of IBMT (5-10 h in total) induced white matter plasticity, mainly in white-matter tracts surrounding the ACC and PCC, and the improved mood/affect states were correlated with increased white matter changes surrounding the PCC and other areas [17–20]. These convergent findings suggest that the PCC—a key hub of the DMN [21, 22]—may also undergo structural changes in grey matter following mindfulness.

However, evidence regarding the relationship between mindfulness and the PCC volume has so far been inconclusive. In a study examining trait mindfulness and brain structures, the PCC grey matter volume was found to be negatively related to this tendency to be attentive to and aware of present-moment experiences in everyday life [23]. Conversely, individuals who underwent two months of MBSR showed increased grey matter density in the PCC [6]. Moreover, greater PCC volume in expert meditators was detected compared to controls [24]. Based on the theoretical model regarding the role of PCC [14], as well as preliminary study suggesting mindfulness meditation can induce grey matter improvement [6, 24], we hypothesized that brief IBMT would increase grey matter volume in the ventral PCC, as it is hypothesized to be related to narrow attentional focus both internally and externally, and has also shown greater connectivity with control-related regions in meditation literature [1, 11].

Finally, people differ in their attitudes toward the practice of mindfulness, and that short-term mindfulness practice induces changes in mental state, while long-term practice changes personality or temperamental traits [1, 4, 25]. However, little is known about the role of individual differences (e.g., preexisting differences and traits of temperament) in predisposing to structural plasticity following brief mindfulness. We therefore used the adult temperament questionnaire (ATQ) to assess baseline individual differences [26, 27]. Given that our prior work showed behavioral improvement in emotion or affect was related to increased white matter plasticity surrounding the PCC, we focused on affect-related temperamental traits within the ATQ to examine their relationships with the magnitude of gray matter changes in PCC. We hypothesized that preexisting individual differences in affectivity would predict the degree of gray matter plasticity in PCC following brief IBMT. A significant correlation between baseline temperamental trait and gray matter change would provide important evidence for a role of individual differences in influencing brain structural plasticity following mindfulness.

2. Materials and Methods

2.1. Participants. Forty-four healthy and meditation-naive college students ($M = 20.28$ years, SD = 1.47 years) were recruited and randomly assigned to either the IBMT group (22 participants, 13 males) or the relaxation group (RT) (22 participants, 14 males). The randomized controlled trial (RCT) was approved by the University of Oregon Institutional Review Board, and informed consent was obtained from each participant. Behavioral and brain measurements included Adult Temperament Questionnaire (ATQ) and functional magnetic resonance imaging (fMRI).

2.2. Experiment Design. We used a longitudinal randomized design with an active control RT group and an intervention IBMT group in this study.

2.3. Behavioral Measurement. Our previous studies have shown that brief IBMT increases cognition, emotion, and behavior [4, 15, 18, 28–30]. Therefore, we did not conduct these measurements in this study but chose the widely used short form of ATQ with 77 items [26, 27] to examine individual differences in temperament. The ATQ assesses four general constructs (also known as factor scales), including effortful control, negative affect, extraversion/surgency, and orienting sensitivity, developed based on a self-report model of temperament [26, 27]. Our previous randomized studies have shown that the mood/affect states correlate with white matter plasticity following short-term IBMT [18], but a relationship between mood/affect trait of temperament and gray matter plasticity has not been established. Given our hypothesis, we were particularly interested in the positive affect subconstruct of extraversion and nonaggressive subconstructs of negative affect including fear, sadness, and discomfort, which tend to relate more closely to emotion dysregulation and symptoms of mood-related disorders such as depression. Two participants were excluded from further analysis due to incomplete ATQ data.

2.4. Structural MRI Data Acquisition. All brain imaging data were collected via a 3 Tesla Siemens scanner. A high resolution ($1 \times 1 \times 1$ mm) T1-weighted whole-brain image (with TR = 2500 msec, TE = 4.38 msec, TI = 1100 msec, flip angle = 8°) was acquired for every participant, using a standard magnetization prepared rapid gradient-echo (MPRAGE) sequence. After visual inspection, structural data from four participants were excluded due to structural abnormality or poor data quality from excessive motion.

2.5. Statistical Analysis. Statistical analyses were performed by the use of IBM SPSS Statistics 20.0 and Free-Surfer 5.3 (http://surfer.nmr.mgh.harvard.edu/). Structural data were automatically processed using FreeSurfer for cortical reconstruction and segmentation. A standard longitudinal processing pipeline was employed to extract reliable volume estimates [31]. Specifically, an unbiased within-subject template space and image [32] was created using robust, inverse consistent registration [33]. Several processing steps, such as skull stripping, Talairach transforms, atlas registration, and spherical surface maps and parcellations, were then initialized with common information from the within-subject template, significantly increasing reliability and statistical power [31]. The white and pial surfaces were visually inspected and were manually edited to correct for errors when necessary.

The index of symmetrized percent change (spc) is a standard measure for examining longitudinal structural changes in volume and cortical thickness and is sensitive to intervention effects. The spc is the rate of change with respect to the average volume of time point 1 and time point 2: spc = 100 ∗ rate/avg. For longitudinal design, this is also a more robust measure (more statistical power) than the rate of change from time point 1 to time point 2 [31]. The spc has been used widely in studies of mental training, Alzheimer's disease, aging, mood disorders, traumatic brain injury, and other neuropsychiatric disorders [31, 34–40]. To examine whether IBMT and RT groups exhibit differences after 10 h of training, we calculated the spc of bilateral ventral posterior cingulate cortex/isthmus of cingulate (ventral PCC/ISC). The PCC was subdivided into dorsal and ventral portions by the Destrieux cortical parcellation scheme [41]. We are specifically interested in the ventral PCC, defined as the "G_cingul-Post-ventral" in the Destrieux cortial atlas. The spc of bilateral ventral PCC volumes was examined separately for left and right hemispheres. We calculated spc using long_stats_slopes command lines in Free-Surfer, part of the longitudinal processing pipelines. The calculation of spc yielded a single measure for each participant, where positive values indicate increases in volume, and *vice versa* for negative values.

2.6. Training Methods. Integrative Body-Mind Training (IBMT) is an open-monitoring mindfulness meditation that mainly involves bodifulness and mindfulness techniques. Bodifulness refers to the gentle adjustment and exercise of body postures with a full awareness, in order to achieve a presence, balance, and integration in our bodies [1, 4, 42, 43]. In each session, guided by an experienced IBMT coach, participants start from bodifulness—the body is naturally relaxed and extended, the mind is calm but alert, and the balanced body postures flow from one to another to promote concentration and mindfulness. IBMT emphasizes the cooperation between body and mind in facilitating and achieving a mindfulness state ecologically. The interaction between mind and body involves both the central nervous system and autonomic nervous system [4, 42]. IBMT stresses no effort to control thoughts but instead encourages a natural state of restful alertness and accepts whatever arises in one's awareness at each moment that facilitates a high degree of awareness of body, mind, and environment [3, 4].

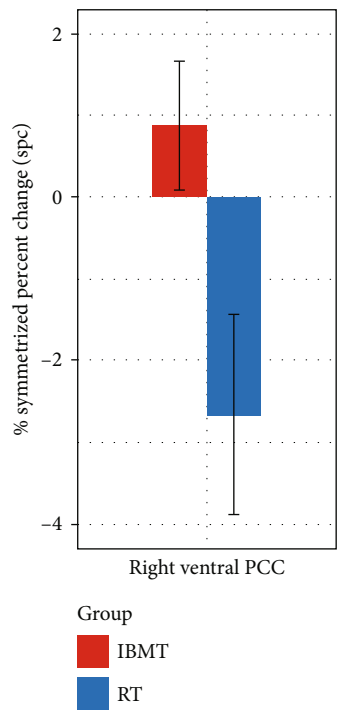

Figure 1: Symmetrized percent change (SPC) of right ventral PCC/ISC. Compared to RT, IBMT induced a significantly higher spc of right ventral PCC/ISC volume.

Relaxation training (RT) involves the relaxing of different muscle groups over the face, head, shoulders, arms, legs, chest, back, abdomen, and so on. With eyes closed and in a sequential fashion, one concentrates on the sensation of relaxation, such as the feelings of warmth and heaviness. This progressive training helps the participant achieve physical and mental relaxation and calmness [15]. The participants received 30 min of IBMT, or RT group practice every night for 20 consecutive sessions in lab, for a total of 10 h of training. The participants were not instructed to practice outside of IBMT or RT training.

3. Results

3.1. Brain Imaging. Before training, the two groups did not differ significantly in terms of bilateral ventral PCC/ISC volumes (independent-samples t-tests, $p > 0.05$). To detect longitudinal structural changes using spc, an index sensitive to intervention effects, analysis of covariance (ANCOVA) was conducted between the two groups, with group assignment as the independent variable, while controlling for age and gender as covariates. As hypothesized, we found a significant effect of group on the spc of right ventral PCC/ISC volume $F(1, 36) = 5.08$, $p = 0.03$, such that the IBMT group had a significantly higher spc ($M = 0.88$, SD = 3.50) relative to the RT group ($M = -2.66$, SD = 5.47), shown in Figure 1. The parcellation of bilateral ventral PCC/ISC is shown in Figure 2. A large effect size 0.124 (partial eta-squared) was detected. However, no significant difference was detected for the spc of left ventral PCC/RSC volume between the IBMT and RT group ($p > 0.05$). Additionally, age and gender

Figure 2: Increased volume of right ventral PCC/ISC. Display of increased volume of ventral PCC/ISC following IBMT.

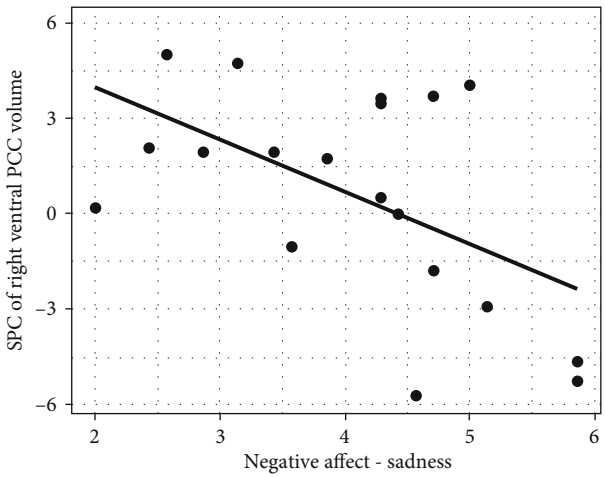

Figure 3: Relationship of negative affect and SPC of right ventral PCC/ISC. Sadness negatively correlated with the spc of right ventral PCC/ISC.

did not have any significant effect on the spc of bilateral ventral PCC/ISC volumes. We also explored the spc of bilateral dorsal PCC volumes following IBMT but did not find any significant group effects ($p > 0.05$).

3.2. Temperamental Traits and Structural Plasticity. To examine whether temperamental traits are associated with the degree of structural plasticity in ventral PCC/ISC, Pearson's correlations were computed between the spc of right ventral PCC/ISC volume and the four temperamental traits. Sadness was the only subconstruct that showed a significantly negative correlation with the right ventral PCC/ISC spc ($r = -0.535$, $p < 0.018$). Figure 3 illustrates this negative relationship, such that lower level of unpleasant affect, mood, and energy—related to object or person loss, disappointment, and exposure to suffering—was associated with a greater spc in the right ventral PCC/ISC volume.

4. Discussion

Our RCT results demonstrate that 10 h of IBMT induced gray matter changes in ventral PCC/ISC—a brain hub associated with cognition, emotion, and self-related processes (e.g., self-awareness). Moreover, temperamental traits reflecting negative affect predicted the extent of training-induced gray matter volumetric increases in ventral PCC/ISC, suggesting a predisposing role of individual differences in influencing training-induced gray matter plasticity. These findings may have important implications for understanding the pathophysiology of—and monitoring—therapeutic interventions in mood-related disorders and aging-related cognitive decline that often manifest functional and structural abnormalities within these brain regions [1, 14].

Mental training studies such as working memory training, meditation, and yoga have shown both increased and decreased grey matter volume and/or density in different regions throughout the brain [5, 6, 24, 44–46]. In most meditation studies, increases were often detected in areas involving interoceptive awareness and self-regulation, such as the ACC, insular cortex, prefrontal cortex, and sensory cortices [1, 5]. Additionally, hippocampus, a structure critical for memory, has also been shown to increase in volume in long-term meditators [1, 5]. Conversely, reduction in volume was often detected in the amygdala in meditation studies [44, 46], suggesting that this subcortical structure associated with emotion and stress may manifest a different trend of structural plasticity, and may underlie the behavioral reduction of stress reactivity commonly observed in meditators. In the present study, we focused on a brain hub within the default mode network and detected an increase in ventral PCC/ISC volume in the meditation group, which is consistent with the two studies that, respectively, showed greater grey matter density in PCC for novices who underwent meditation training and greater PCC volume in expert meditators relative to controls [6, 24]. According to a theoretical account of the PCC function, the ventral PCC may play a key role in narrow attentional focus [14], which suggests that the increased volume of the ventral PCC may reflect enhanced attentional control following meditation training.

Interestingly, for the relaxation training group, we detected a reduction of grey matter volume in bilateral ventral PCC/ISC. It is important to recognize that the relaxation training has a very different emphasis from the mindfulness training; thus, it is possible that these two forms of training work through different neural mechanisms that led to structural changes in completely different directions. On the other hand, reduction in grey matter volume and density is not uncommon in training studies [44–46], and one possible mechanism of the observed reduction in the relaxation group might be the usage-dependent selective elimination of synapses which helps to sculpt neural circuitry [45]. However, further investigations are needed to fully examine the impact of relaxation training on brain plasticity of the PCC, as well as that of other brain regions. Overall, our finding concerning the meditation group was in line with prior literature that showed structural improvement in the PCC either following short-term or long-term meditation experiences.

Looking more closely at our target region, ventral PCC (vPCC), it includes the ventral subdivision of PCC and isthmus of cingulate (ISC) as defined by the Destrieux cortical atlas. The ISC lies within Brodmann areas 29/30, overlapping the same BA 29/30 with adjacent retrosplenial cortex (RSC). The anatomical location of RSC (BA 29/30) is behind the

splenium of the corpus callosum, where RSC directly connects to the vPCC (BA 23) [41, 47–49]. Our previous work showed enhanced white matter connectivity in the vPCC and adjacent ISC/RSC following 5-10 h of IBMT, suggesting a putative relationship between the concurrent structural plasticity of white and grey matter in vPCC and adjacent ISC/RSC following brief mindfulness [4]. A closer examination of these brain regions reveals two important functions: emotion- and cognition-related processes [34, 50–65].

Emotion-related problems and disorders—such as clinical depression and subthreshold depressive symptoms in adults—are related to structural changes in cingulate cortex [34, 53–55]. In a nonclinical sample, one study examined the relationship between depressive symptoms and gray matter volumes in the ACC, PCC, and ISC/RSC and showed that higher scores on the somatic symptoms were related to smaller volume in the PCC and that higher scores on the depressed mood were associated with smaller volume in the ISC/RSC [53]. A further study indicated that unipolar depressed patients had smaller ACC and PCC volumes compared to healthy subjects. Additionally, when patients were divided into currently depressed and remitted subgroups, currently depressed patients had smaller ACC and PCC volumes than the healthy controls [54]. Similarly, one study suggests that the gray matter volumes of PCC and hippocampus are key regions that disambiguate MDD and BD patients from healthy controls [55]. Together, these findings suggest that the PCC and ISC/RSC actively engage in emotional processing and regulation, which may explain why enhanced mood and reduced negative affect are often reported after mindfulness [1]. Increased volume in vPCC and ISC/RSC may be associated with better psychological well-being, which could be one of the mechanisms that underwrites the commonly observed improvement in mood and psychological health following mindfulness [42]. Our findings also provide support for the notion that increasing structural plasticity of vPCC and ISC/RSC may protect individuals against mood-related symptoms, making them less susceptible to emotion-related disorders.

The vPCC and RSC have dense connections to medial temporal lobe, hippocampus, and parahippocampal cortex, which are important areas for memory [47–51]. Growing evidence suggests that decreased PCC activity (e.g., resting-state or task) and metabolism (e.g., glucose metabolic rate) are associated with cognitive decline, mild cognitive impairment (MCI), and Alzheimer's disease (AD) [56–62], which often severely impact memory-related functions. In addition, vPCC also showed associations with MCI/AD, consistent with previous reports concerning the importance of PCC in amyloid deposition with AD—and performance on an episodic memory retrieval task in MCI [63, 64]. Moreover, the locations of amyloid deposition and fMRI activity in both studies were centered on vPCC. Relatedly, greater cortical thickness in PCC is found in high-performing elderly, indicating that greater gray matter in PCC may be a putative signature of optimal aging [65]. This is consistent with the evidence that the PCC may play a direct role in regulating the focus of attention and thus facilitating cognitive performance [4, 14]. There is also support for the roles of vPCC and RSC in internally directed thoughts and cognition such as the retrieval of episodic and semantic memories, imagining, and planning [14, 52]. Lastly, RSC is associated with perspective taking and switching between different frames of reference, which is a capacity that mindfulness practices seek to promote [4, 48].

Previous work showed that five sessions of IBMT improves PCC activity and metabolism, and cognitive function such as attention, creativity, working memory, problem-solving, learning, and self-control capacities [1, 4, 15–18, 28–30]. The present structural finding endorses our functional and behavioral findings, implicating the same brain hub—vPCC and suggests that increased functional and structural plasticity in the PCC may play a key role in the preservation of cognitive capacity and performance in aging population [13, 65]. Increased gray matter in the PCC following 10 h of IBMT in healthy adults may suggest some protection against aging-related processes, such as cognitive decline and MCI [4, 66]. It is worth pointing out that only right vPCC/ISC/RSC was significantly affected by brief IBMT, which is consistent with prior work showing the lateralized function of RSC—the right RSC is more associated with MCI/AD and memory-related impairment than left RSC [52].

Network neuroscience on large-scale (intrinsic) brain networks has indicated an architectural core (i.e., brain hub) in the PCC and parietal cortex, regions with high degree, strength and betweenness centrality, and constitute connector hubs that link major structural modules [22], suggesting that PCC is a key brain hub for efficient information processing—which is implicated in diverse cognitive processes and emotion regulation. Prior work has shown that mindfulness directly changes these mental processes [3, 4]. One emotion regulation strategy, distancing (e.g., reformulating aversive stimuli in a neutral and objective way), is one of mindfulness skills that emphasizes the experience of presence without judgment. Indeed, increased PCC activity and decreased amygdala activity are related to distancing [67], consistent with recent meta-analyses showing that the PCC is one of the main regions implicated in the upregulation and downregulation of emotion [68, 69]. Studies also indicate a role of PCC in conscious awareness, which may explain why enhanced interoceptive awareness is typically observed following mindfulness [1, 3, 70]. Furthermore, PCC has been thought to underpin consciousness, further supporting a role in self-awareness and self-related processing [71–73].

Individual differences in mindfulness training-induced brain structural plasticity are rarely explored [1, 4]. We provide preliminary evidence that temperament traits may play a role in underwriting structural volumetric responses to brief mindfulness. Sadness is one of the negative affects in the ATQ and defined as unpleasant affect/mood, energy related to object/person loss, disappointment, and exposure to suffering. Studies showed that sadness is associated with depressive symptoms [73]. Given the strong functional relevance of vPCC/ISC/RSC in the pathophysiology of depression, it is not surprising that preexisting individual differences in this particular trait could influence subsequent volumetric change. We found that individuals with higher level of

sadness either showed less improvement (or indeed reduction) in gray matter volume following mindfulness, suggesting that they were not sensitive to such training and that alternative interventions may be more effective. Crucially, the fact that preexisting temperamental traits were able to predict subsequent gray matter changes suggests that individual differences may play an important role in underlying mechanisms of brain structural plasticity.

Taken together, our results to date suggest it is possible to induce gray matter plasticity in the vPCC and adjacent ISC/RSC following brief mindfulness in novices. However, we do not yet know how long the plasticity will last; this warrants further investigation. Given the relatively small sample size and exploratory nature of the study, the findings need to be validated by future studies. Nevertheless, the present findings may have important implications for protecting individuals against mood-related disorders and aging-related cognitive declines, which exhibit brain functional and structural abnormalities in the vPCC.

Data Availability

The datasets used to support the findings of this study are available from the corresponding author upon reasonable request.

Ethical Approval

All procedures performed in studies involving human participants were in accordance with the ethical standards of the institutional and/or national research committee and with the 1964 Helsinki declaration and its later amendments or comparable ethical standards.

Conflicts of Interest

The authors declare that they have no conflict of interest.

Authors' Contributions

R.T. and Y.Y.T. conducted the investigation. R.T. and Y.Y.T. contributed to the methodology and conducted formal analyses. R.T. visualized the results. R.T. prepared the original draft. R.T., K.J.F, and Y.Y.T. contributed to writing the manuscript and interpretation of data.

Acknowledgments

YYT was partly supported by the Office of Naval Research (ONR) N000141512148 and National Institutes of Health (NIH) research grant AT010138. KJF is funded by a Wellcome Trust Principal Research Fellowship (Ref: 088130/Z/09/Z). RT was supported by NIH F31 AT010422. We thank Michael Posner for his valuable comments.

References

[1] Y. Y. Tang, B. K. Holzel, and M. I. Posner, "The neuroscience of mindfulness meditation," *Nature Reviews Neuroscience*, vol. 16, no. 4, pp. 213–225, 2015.

[2] M. Goyal, S. Singh, E. M. S. Sibinga et al., "Meditation programs for psychological stress and well-being: a systematic review and meta-analysis," *JAMA Internal Medicine*, vol. 174, no. 3, pp. 357–368, 2014.

[3] B. K. Hölzel, S. W. Lazar, T. Gard, Z. Schuman-Olivier, D. R. Vago, and U. Ott, "How does mindfulness meditation work? Proposing mechanisms of action from a conceptual and neural perspective," *Perspectives on Psychological Science*, vol. 6, no. 6, pp. 537–559, 2011.

[4] Y. Y. Tang, *The Neuroscience of Mindfulness Meditation: How the Body and Mind Work Together to Change our Behavior?*, Springer Nature, London, 2017.

[5] K. C. R. Fox, S. Nijeboer, M. L. Dixon et al., "Is meditation associated with altered brain structure? A systematic review and meta-analysis of morphometric neuroimaging in meditation practitioners," *Neuroscience and Biobehavioral Reviews*, vol. 43, pp. 48–73, 2014.

[6] B. K. Hölzel, J. Carmody, M. Vangel et al., "Mindfulness practice leads to increases in regional brain gray matter density," *Psychiatry Research: Neuroimaging*, vol. 191, no. 1, pp. 36–43, 2011.

[7] D. G. MacCoon, Z. E. Imel, M. A. Rosenkranz et al., "The validation of an active control intervention for Mindfulness Based Stress Reduction (MBSR)," *Behaviour Research and Therapy*, vol. 50, no. 1, pp. 3–12, 2012.

[8] M. A. Rosenkranz, R. J. Davidson, D. G. MacCoon, J. F. Sheridan, N. H. Kalin, and A. Lutz, "A comparison of mindfulness based stress reduction and an active control in modulation of neurogenic inflammation," *Brain, Behavior, and Immunity*, vol. 27, no. 1, pp. 174–184, 2013.

[9] D. G. MacCoon, K. A. MacLean, R. J. Davidson, C. D. Saron, and A. Lutz, "No sustained attention differences in a longitudinal randomized trial comparing mindfulness based stress reduction versus active control," *PLoS One*, vol. 9, no. 6, article e97551, 2014.

[10] A. Doll, B. K. Hölzel, C. C. Boucard, A. M. Wohlschläger, and C. Sorg, "Mindfulness is associated with intrinsic functional connectivity between default mode and salience networks," *Frontiers in Human Neuroscience*, vol. 9, p. 461, 2015.

[11] J. A. Brewer, P. D. Worhunsky, J. R. Gray, Y. Y. Tang, J. Weber, and H. Kober, "Meditation experience is associated with differences in default mode network activity and connectivity," *Proceedings of the National Academy of Sciences of the United States of America*, vol. 108, no. 50, pp. 20254–20259, 2011.

[12] J. D. Creswell, A. A. Taren, E. K. Lindsay et al., "Alterations in resting-state functional connectivity link mindfulness meditation with reduced interleukin-6: a randomized controlled trial," *Biological Psychiatry*, vol. 80, no. 1, pp. 53–61, 2016.

[13] R. E. Wells, G. Y. Yeh, C. E. Kerr et al., "Meditation's impact on default mode network and hippocampus in mild cognitive impairment: a pilot study," *Neuroscience Letters*, vol. 556, pp. 15–19, 2013.

[14] R. Leech and D. J. Sharp, "The role of the posterior cingulate cortex in cognition and disease," *Brain*, vol. 137, no. 1, pp. 12–32, 2014.

[15] Y. Y. Tang, Y. Ma, J. Wang et al., "Short-term meditation training improves attention and self-regulation," *Proceedings of the National Academy of Sciences of the United States of America*, vol. 104, no. 43, pp. 17152–17156, 2007.

[16] Y. Y. Tang, Y. Ma, Y. Fan et al., "Central and autonomic nervous system interaction is altered by short-term meditation,"

Proceedings of the National Academy of Sciences of the United States of America, vol. 106, no. 22, pp. 8865–8870, 2009.

[17] Y. Y. Tang, Q. Lu, X. Geng, E. A. Stein, Y. Yang, and M. I. Posner, "Short-term meditation induces white matter changes in the anterior cingulate," *Proceedings of the National Academy of Sciences of the United States of America*, vol. 107, no. 35, pp. 15649–15652, 2010.

[18] Y. Y. Tang, Q. Lu, M. Fan, Y. Yang, and M. I. Posner, "Mechanisms of white matter changes induced by meditation," *Proceedings of the National Academy of Sciences of the United States of America*, vol. 109, no. 26, pp. 10570–10574, 2012.

[19] S. Mori, S. Wakana, P. C. van Zijl et al., *MRI Atlas of Human White Matter*, Elsevier Science, New York, 2005.

[20] S. Wakana, H. Jiang, L. M. Nagae-Poetscher, P. C. M. van Zijl, and S. Mori, "Fiber tract-based atlas of human white matter anatomy," *Radiology*, vol. 230, no. 1, pp. 77–87, 2004.

[21] M. E. Raichle, A. M. MacLeod, A. Z. Snyder, W. J. Powers, D. A. Gusnard, and G. L. Shulman, "A default mode of brain function," *Proceedings of the National Academy of Sciences of the United States of America*, vol. 98, no. 2, pp. 676–682, 2001.

[22] P. Hagmann, L. Cammoun, X. Gigandet et al., "Mapping the structural core of human cerebral cortex," *PLoS Biology*, vol. 6, no. 7, article e159, 2008.

[23] H. Lu, Y. Song, M. Xu, X. Wang, X. Li, and J. Liu, "The brain structure correlates of individual differences in trait mindfulness: a voxel-based morphometry study," *Neuroscience*, vol. 272, pp. 21–28, 2014.

[24] G. Chételat, F. Mézenge, C. Tomadesso et al., "Reduced age-associated brain changes in expert meditators: a multimodal neuroimaging pilot study," *Scientific Reports*, vol. 7, no. 1, article 10160, 2017.

[25] Y. Y. Tang, B. K. Hölzel, and M. I. Posner, "Traits and states in mindfulness meditation," *Nature Reviews Neuroscience*, vol. 17, no. 1, p. 59, 2016.

[26] M. K. Rothbart, S. A. Ahadi, and D. E. Evans, "Temperament and personality: origins and outcomes," *Journal of Personality and Social Psychology*, vol. 78, no. 1, pp. 122–135, 2000.

[27] D. E. Evans and M. K. Rothbart, "Developing a model for adult temperament," *Journal of Research in Personality*, vol. 41, no. 4, pp. 868–888, 2007.

[28] Y.-Y. Tang, R. Tang, C. Jiang, and M. I. Posner, "Short-term meditation intervention improves self-regulation and academic performance," *Journal of Child and Adolescent Behaviour*, vol. 2, no. 4, p. 154, 2014.

[29] X. Ding, Y. Y. Tang, R. Tang, and M. I. Posner, "Improving creativity performance by short-term meditation," *Behavioral and Brain Functions*, vol. 10, no. 1, p. 9, 2014.

[30] Y. Fan, Y. Y. Tang, R. Tang, and M. I. Posner, "Time course of conflict processing modulated by brief meditation training," *Frontiers in Psychology*, vol. 6, p. 911, 2015.

[31] M. Reuter, N. J. Schmansky, H. D. Rosas, and B. Fischl, "Within-subject template estimation for unbiased longitudinal image analysis," *NeuroImage*, vol. 61, no. 4, pp. 1402–1418, 2012.

[32] M. Reuter and B. Fischl, "Avoiding asymmetry-induced bias in longitudinal image processing," *NeuroImage*, vol. 57, no. 1, pp. 19–21, 2011.

[33] M. Reuter, H. D. Rosas, and B. Fischl, "Highly accurate inverse consistent registration: a robust approach," *NeuroImage*, vol. 53, no. 4, pp. 1181–1196, 2010.

[34] H. K. Lim, W. S. Jung, K. J. Ahn et al., "Regional cortical thickness and subcortical volume changes are associated with cognitive impairments in the drug-naive patients with late-onset depression," *Neuropsychopharmacology*, vol. 37, no. 3, pp. 838–849, 2012.

[35] A. Hervais-Adelman, B. Moser-Mercer, M. M. Murray, and N. Golestani, "Cortical thickness increases after simultaneous interpretation training," *Neuropsychologia*, vol. 98, pp. 212–219, 2017.

[36] J. Pegueroles, E. Vilaplana, V. Montal et al., "Longitudinal brain structural changes in preclinical Alzheimer's disease," *Alzheimer's & Dementia*, vol. 13, no. 5, pp. 499–509, 2017.

[37] E. L. Bercaw, R. A. Hanks, S. R. Millis, and T. J. Gola, "Changes in neuropsychological performance after traumatic brain injury from inpatient rehabilitation to 1-year follow-up in predicting 2-year functional outcomes," *The Clinical Neuropsychologist*, vol. 25, no. 1, pp. 72–89, 2010.

[38] R. Nesvåg, Ø. Bergmann, L. M. Rimol et al., "A 5-year follow-up study of brain cortical and subcortical abnormalities in a schizophrenia cohort," *Schizophrenia Research*, vol. 142, no. 1-3, pp. 209–216, 2012.

[39] A. B. Storsve, A. M. Fjell, C. K. Tamnes et al., "Differential longitudinal changes in cortical thickness, surface area and volume across the adult life span: regions of accelerating and decelerating change," *The Journal of Neuroscience*, vol. 34, no. 25, pp. 8488–8498, 2014.

[40] J. Greenberg, V. L. Romero, S. Elkin-Frankston, M. A. Bezdek, E. H. Schumacher, and S. W. Lazar, "Reduced interference in working memory following mindfulness training is associated with increases in hippocampal volume," *Brain Imaging and Behavior*, vol. 13, no. 2, pp. 366–376, 2019.

[41] C. Destrieux, B. Fischl, A. Dale, and E. Halgren, "Automatic parcellation of human cortical gyri and sulci using standard anatomical nomenclature," *NeuroImage*, vol. 53, no. 1, pp. 1–15, 2010.

[42] Y. Y. Tang, R. Tang, and J. J. Gross, "Promoting psychological well-being through an evidence-based mindfulness training program," *Frontiers in Human Neuroscience*, vol. 13, p. 237, 2019.

[43] A. Lutz, H. A. Slagter, J. D. Dunne, and R. J. Davidson, "Attention regulation and monitoring in meditation," *Trends in Cognitive Sciences*, vol. 12, no. 4, pp. 163–169, 2008.

[44] B. K. Hölzel, J. Carmody, K. C. Evans et al., "Stress reduction correlates with structural changes in the amygdala," *Social Cognitive and Affective Neuroscience*, vol. 5, no. 1, pp. 11–17, 2010.

[45] H. Takeuchi, Y. Taki, Y. Sassa et al., "Working memory training using mental calculation impacts regional gray matter of the frontal and parietal regions," *PLoS One*, vol. 6, no. 8, article e23175, 2011.

[46] R. A. Gotink, M. W. Vernooij, M. A. Ikram et al., "Meditation and yoga practice are associated with smaller right amygdala volume: the Rotterdam study," *Brain Imaging and Behavior*, vol. 12, no. 6, pp. 1631–1639, 2018.

[47] K. Brodmann, *Vergleichende Lokalisationslehre der Grosshirnrinde inihren Prinzipien dargestellt auf Grund des Zellenbaues*, Barth, Berlin, 1909.

[48] S. D. Vann, J. P. Aggleton, and E. A. Maguire, "What does the retrosplenial cortex do?," *Nature Reviews Neuroscience*, vol. 10, no. 11, pp. 792–802, 2009.

[49] https://en.wikipedia.org/wiki/Isthmus_of_cingulate_gyrus.

[50] E. R. Chrastil, "Heterogeneity in human retrosplenial cortex: a review of function and connectivity," *Behavioral Neuroscience*, vol. 132, no. 5, pp. 317–338, 2018.

[51] K. A. Corcoran, N. Yamawaki, K. Leaderbrand, and J. Radulovic, "Role of retrosplenial cortex in processing stress-related context memories," *Behavioral Neuroscience*, vol. 132, no. 5, pp. 388–395, 2018.

[52] Y. Huang, J. Hullfish, D. de Ridder, and S. Vanneste, "Meta-analysis of functional subdivisions within human posteromedial cortex," *Brain Structure & Function*, vol. 224, no. 1, pp. 435–452, 2019.

[53] M. E. McLaren, S. M. Szymkowicz, A. O'Shea, A. J. Woods, S. D. Anton, and V. M. Dotson, "Dimensions of depressive symptoms and cingulate volumes in older adults," *Translational Psychiatry*, vol. 6, no. 4, article e788, 2016.

[54] S. C. Caetano, S. Kaur, P. Brambilla et al., "Smaller cingulate volumes in unipolar depressed patients," *Biological Psychiatry*, vol. 59, no. 8, pp. 702–706, 2006.

[55] P. H. Yeh, H. Zhu, M. A. Nicoletti, J. P. Hatch, P. Brambilla, and J. C. Soares, "Structural equation modeling and principal component analysis of gray matter volumes in major depressive and bipolar disorders: differences in latent volumetric structure," *Psychiatry Research*, vol. 184, no. 3, pp. 177–185, 2010.

[56] P. Pan, L. Zhu, T. T. Yu et al., "Aberrant spontaneous low-frequency brain activity in amnestic mild cognitive impairment: a meta-analysis of resting-state fMRI studies," *Ageing Research Reviews*, vol. 35, pp. 12–21, 2017.

[57] H. Wang, L. Tan, H. F. Wang et al., "Magnetic resonance spectroscopy in Alzheimer's disease: systematic review and meta-analysis," *Journal of Alzheimer's Disease*, vol. 46, no. 4, pp. 1049–1070, 2015.

[58] S. Tumati, S. Martens, and A. Aleman, "Magnetic resonance spectroscopy in mild cognitive impairment: systematic review and meta-analysis," *Neuroscience and Biobehavioral Reviews*, vol. 37, no. 10, pp. 2571–2586, 2013.

[59] E. M. Reiman, R. J. Caselli, K. Chen, G. E. Alexander, D. Bandy, and J. Frost, "Declining brain activity in cognitively normal apolipoprotein E epsilon 4 heterozygotes: a foundation for using positron emission tomography to efficiently test treatments to prevent Alzheimer's disease," *Proceedings of the National Academy of Sciences of the United States of America*, vol. 98, no. 6, pp. 3334–3339, 2001.

[60] E. M. Reiman, K. Chen, G. E. Alexander et al., "Functional brain abnormalities in young adults at genetic risk for late-onset Alzheimer's dementia," *Proceedings of the National Academy of Sciences of the United States of America*, vol. 101, no. 1, pp. 284–289, 2004.

[61] C. L. Maarouf, T. A. Kokjohn, D. G. Walker et al., "Biochemical assessment of precuneus and posterior cingulate gyrus in the context of brain aging and Alzheimer's disease," *PLoS One*, vol. 9, no. 8, article e105784, 2014.

[62] Y. He, L. Wang, Y. Zang et al., "Regional coherence changes in the early stages of Alzheimer's disease: a combined structural and resting-state functional MRI study," *NeuroImage*, vol. 35, no. 2, pp. 488–500, 2007.

[63] R. A. Sperling, P. S. LaViolette, K. O'Keefe et al., "Amyloid deposition is associated with impaired default network function in older persons without dementia," *Neuron*, vol. 63, no. 2, pp. 178–188, 2009.

[64] M. L. Ries, T. W. Schmitz, T. N. Kawahara, B. M. Torgerson, M. A. Trivedi, and S. C. Johnson, "Task-dependent posterior cingulate activation in mild cognitive impairment," *NeuroImage*, vol. 29, no. 2, pp. 485–492, 2006.

[65] A. M. Fjell, K. B. Walhovd, I. Reinvang et al., "Selective increase of cortical thickness in high-performing elderly–structural indices of optimal cognitive aging," *NeuroImage*, vol. 29, no. 3, pp. 984–994, 2006.

[66] T. Gard, B. K. Hölzel, and S. W. Lazar, "The potential effects of meditation on age-related cognitive decline: a systematic review," *Annals of the New York Academy of Sciences*, vol. 1307, no. 1, pp. 89–103, 2014.

[67] H. W. Koenigsberg, J. Fan, K. N. Ochsner et al., "Neural correlates of using distancing to regulate emotional responses to social situations," *Neuropsychologia*, vol. 48, no. 6, pp. 1813–1822, 2010.

[68] C. Morawetz, S. Bode, B. Derntl, and H. R. Heekeren, "The effect of strategies, goals and stimulus material on the neural mechanisms of emotion regulation: a meta-analysis of fMRI studies," *Neuroscience and Biobehavioral Reviews*, vol. 72, pp. 111–128, 2017.

[69] J. P. Powers and K. S. LaBar, "Regulating emotion through distancing: a taxonomy, neurocognitive model, and supporting meta-analysis," *Neuroscience and Biobehavioral Reviews*, vol. 96, pp. 155–173, 2019.

[70] R. M. Adapa, M. H. Davis, E. A. Stamatakis, A. R. Absalom, and D. K. Menon, "Neural correlates of successful semantic processing during propofol sedation," *Human Brain Mapping*, vol. 35, no. 7, pp. 2935–2949, 2014.

[71] C. Koch, M. Massimini, M. Boly, and G. Tononi, "Neural correlates of consciousness: progress and problems," *Nature Reviews Neuroscience*, vol. 17, no. 5, pp. 307–321, 2016.

[72] C. Koch, M. Massimini, M. Boly, and G. Tononi, "Posterior and anterior cortex – where is the difference that makes the difference?," *Nature Reviews Neuroscience*, vol. 17, no. 10, p. 666, 2016.

[73] M. W. Vasey, C. N. Harbaugh, C. J. Lonigan et al., "Dimensions of temperament and depressive symptoms: replicating a three-way interaction," *Journal of Research in Personality*, vol. 47, no. 6, pp. 908–921, 2013.